Filling a Critical Knowledge Gap in Androgen Receptor Variant Splicing to Enable Development of New Prostate Cancer Therapies.

Thesis submitted in partial fulfilment of the requirement of the degree of Doctor of Philosophy

Ryan Nelson
200707129
Institute of Translational and Clinical Research
Faculty of Medicinal Sciences
Newcastle University
September 2024

Abstract

Androgen receptor (AR) signalling has long been recognised as critical in the initiation and progression of prostate cancer (PC). Therapeutic interventions therefore focus on interrupting AR signalling through suppression of circulating testosterone with androgen deprivation therapy (ADT) or direct inhibition of the AR with anti-androgens, such as enzalutamide. Whilst initially effective, a significant proportion of patients will see progression of their disease despite castrate levels of androgens.

Castrate-resistant prostate cancer (CRPC) arises through several mechanisms including alternative splicing of the androgen receptor leading to the generation of androgen receptor spliced variants (AR-Vs). Cryptic exons (CEs) of AR-Vs replace the ligand-bind domain (LBD) of the AR consequently rendering them constitutively activated and able to drive disease progression. AR-Vs are currently resistant to all therapeutic interventions and themselves are complex targets due to their high level of structural disorder.

Histone demethylase (HDMs) can influence splicing decisions and may offer an alternative therapeutic option to direct targeting of splicing factors (SFs) which often lack specificity to pathophysiological splicing events. KDM6A is one such HDM which is known to be highly mutated in CRPC. However, its role in disease progression is relatively unknown.

Data obtained during this PhD reveals that KMD6A contributes to PC progression to CRPC through both catalytic-dependent and independent mechanisms. The influence of KDM6A on splicing appeared to be through the chromatin-adapter model, recruiting SFs to CE3 driving the generation of AR-V7. Critically, this work revealed that in models of enzalutamide resistance, KDM6A inhibition can lead to enzalutamide re-sensitisation by affecting both genes and pathways essential for the emergence of resistance.

Results from this work show KDM6A to be an attractive target in CRPC for which there are currently no curative treatment options.

Acknowledgements

I would firstly like to thank my supervisor Luke Gaughan for providing me with the opportunity to work on this exciting project and the scientific guidance along the way. I am grateful for the support Luke has always provided during my PhD and for allowing me the freedom to develop my ideas and drive my project. Additionally, I would like to thank my previous PI Olaf Heidenreich who, as a research technician, gave me autonomy and self-belief that I could complete a PhD. I am grateful for his support in wanting to pursue a PhD. I would like to thank both Derek Mann and Jon Higgins who have been my panel members throughout my PhD. Whilst initially providing thought-provoking ideas and suggestions which helped shape this PhD, they later offered excellent career development advice. This PhD would not have been possible without the rest of the Solid Tumour Targeted Discovery group, especially those who directly contributed to some of the work in this thesis. I have built lifelong friendships during this time which has been one of the greatest gifts of this PhD. I would like to thank Nick for his scientific discussion but more importantly joint passion for 'the office' and Alan, whose Monday morning football debriefs were always a welcome break from scientific thoughts.

Outside of the lab, I am forever indebted to Flavia, my amazing partner, who supported me in pursuing a PhD despite this meaning that we spent three years and one global pandemic in two different countries. I am delighted that as I write this now, we are reaping the rewards of our hard work and enjoying our lives together in the UK. And of course, to my friends and family, despite most of them thinking I have been the world's longest 'Tax dodger', their laughter and love have been an important part of this journey. They are now happy I have a 'proper' job.

Table of Contents

Abbreviation list

°C – Degrees Celsius
µg – micro grammes
µl – _micro litre
ADT - Androgen Deprivation Therapy
AF-1 – Activation Function 1
AF-2 – Activation Function 2
AR – Androgen Receptor
ARE – Androgen Response Elements
AR-FL – Androgen Receptor Full length
AR-V – Androgen Receptor Variants
AR-V7 – Androgen Receptor Variant 7
ATCH - Adrenocorticotrophic Hormone
CE3 – Cryptic Exon 3
ChIP – _Chromatin Immunoprecipitation
CRPC – _Castrate Resistant Prostate Cancer
CSPC- Castrate Sensitive Prostate Cancer
DBD – _DNA Binding Domain
DEG- Differential Gene Expression
DHT – _Dihydrotestosterone
DMSO – _Dimethyl Sulfoxide
DNA – _Deoxyribose Nucleic Acid
DRB - 5,6-dichlorobenzimidazole (DRB) assay
ENZ - Enzalutamide
EnzaR- Enzalutamide Resistant
FBS- Foetal Bovine Serum
FPKM- Fragments per Kilobase million
GnRH - Gonadotropin Releasing Hormone
GR – Glucocorticoid Receptor
GWAS – Genome Wide Association Study
hnRNP Heterogeneous nuclear ribonucleoproteins
HPG-Axis – Hypothalamic Pituitary Gonadal axis
HSP – Heat shock proteins
KD – Knockdown
KDM – Lysine Demethylase
KEGG– Kyoto Encyclopaedia of Genes and Genomes
LBD – Ligand Binding Domain
LH – Luteinizing Hormone
mCRPC – Metastatic Castrate resistant Prostate Cancer
mM – Milli molar

Mt - Mutant
mRNA – Messenger RNA
NEPC – Neuroendocrine Prostate Cancer
NICE – National Institute for Health and Care Excellence
ng – Nano gram
NT- Non-targeting
NTD – N-terminal Domain
PBS – Phosphate Buffer Saline
PC – Prostate Cancer
PCR – Polymerase Chain Reaction
PSA – Prostate Specific Antigen
RNA - Ribonucleic Acid
RNASeq – RNA sequencing
RT-PCR – Reverse Transcription Polymerase Chain Reaction
Scrm- Scrambled
SDM – Steroid-depleted media
SNP – Single Nucleotide Polymorphisms
siRNA – small interfering RNA
snRNP - Small nuclear ribonuclear protein
SR Protein – Serine-arginine rich protein
SU2C – Stand Up to Cancer
TCGA – The Cancer Genoe Atlas
Wt – Wild-Type

Table of Figures

List of Tables

Chapter 1. Introduction

1.1 Prostate Cancer

1.1.1 The function and anatomy of the prostate

The prostate is a walnut-sized gland that surrounds the urethra at the base of the penis and bladder. The role of the prostatic gland is to secrete a multi-component alkaline fluid which protects and nourishes the spermatozoa (Sharma et al., 2017). The prostate constitutes four distinct anatomical regions **(Figure 1.1A)**, first described by John McNeal utilising hundreds of cadavers (McNeal, 1981). The zones described are; the peripheral (PZ), transition (TZ) and central zones (CZ) as well as the anterior fibromuscular stroma (AFS) (Czarniecki and Yacoub, 2020). Interestingly, the volume of the zones can alter during natural ageing because of clinical, but non-cancerous, pathologies such as benign prostatic hyperplasia (BPH) (Garvey et al., 2014). The PZ encompasses all the prostate glandular tissue and accounts for 70% of the gland by volume. Perhaps unsurprising due to its mass, the PZ is the most common site in the prostate for developing prostate carcinomas, as well as other clinical pathologies such as prostatitis and proinflammatory atrophy (Hricak & Scardino, 2009). The CZ surrounds the ejaculatory duct and makes up most of the prostatic base and generally, the volume of it naturally reduces with age. As shown in Figure 1A, the TZ constitutes two sections which surround the prostatic urethra and is the region where BPH most commonly originates. The AFS consists of both muscle cells as connective tissue, without glandular tissue, forming the outmost part of the prostate (Zurowska et al., 2023).

Histologically, prostate glandular tissue comprises two distinct layers of epithelial cells **(Figure 1.1B)**: a columnar luminal cell layer responsible for the secretion of proteins such as prostate-specific antigen (PSA); and underlying this, a layer of basal cells, for which there is little known about their function other than they contain the pool of prostate stem cells, highlighted by their high expression of stem cell transcript factor p63(D. Zhang et al., 2018). Within these layers are also additional epithelial cells; neuroendocrine (~1%) and more recently with the advances in single-cell sequencing, hillock and club cells have also been identified; however their role and significance are currently poorly understood (Song et al., 2022). Most prostate cancers (PC) present as adenocarcinoma of malignant cells from the luminal compartment demonstrated through a clear phenotype of strong androgen receptor (AR) signalling and absence of basal cell markers **(Figure 1.1C)** (Park et al., 2016).

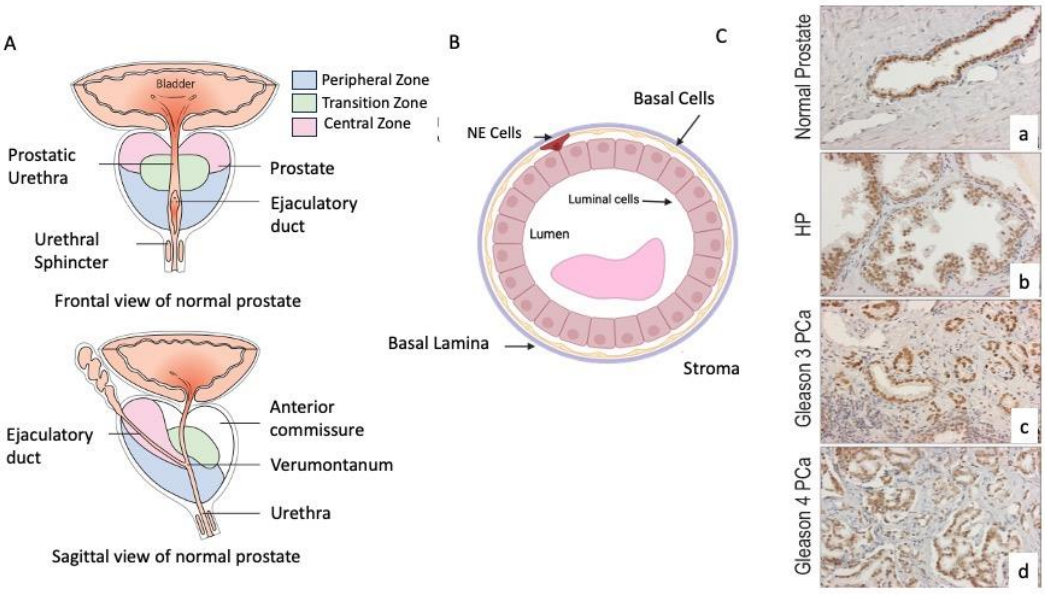

Figure 1.1 Anatomy and Structure of the Prostate*. Location of the peripheral, transition, and central zones in a frontal and sagittal view, in relation to the bladder and urethra (Picture taken from Cheng et al., 2017) B. Luminal epithelium cells of the prostatic ducts which secrete prostatic fluid. Basal cells surround the luminal layers and within this are a rare few neuroendocrine cell (BioRender). C. Androgen Receptor staining showing luminal cells of a) normal prostate tissue b) benign hypoplasia c) low-grade primary cancer d) higher-grade primary cancer. (Picture adapted from Zheng et al., 2011)*

1.1.2 Epidemiology

The latest figures from Cancer Research UK reveal that annually there are approximately 52,000 new cases of PC in the UK alone and from this there is annually over 12,000 deaths (Cancer Research UK, 2019). In the UK, along with most other countries, there are more cases of PC being diagnosed, likely due to the ageing population and more testing, but importantly the mortality rate is slightly decreasing (L. Wang et al., 2022).

Age, race, family history and germline mutations are established risk factors for PC (Bergengren et al., 2023) . Generally, men under 50 have a very low risk of PC, and the UK has a peak age of diagnosis between 75-79 years (Prostate Cancer UK, 2019).

A startling statistic for PC regards race discrepancy. PC incidence in black men is significantly higher than in white men with reports suggesting that the incidence rate is between 1.6 to 3.0-fold higher in the black community (Ben-Shlomo et al., 2008; Conti et al., 2017). This discrepancy is likely multifactorial; with genetic alterations that predisposes certain races to a higher chance of cancer (Conti et al., 2021) and social issues, such as reduced awareness or poor experience with healthcare professionals amongst certain communities (Martins et al., 2015; Thompson, 2013).

Men whose father or brother (first-degree relative) have had PC have around a 2.5-fold increased chance of also getting the disease. Worryingly this can increase to 5-fold if the relative was diagnosed with PC at younger than 55 years old (Brook et al., 2023). In addition, if the family member has had an aggressive/metastatic prostate cancer this is likely to also cause a more aggressive disease in their offspring; emphasising the need for men with a family history of PC to be screened early (Barber et al., 2018; Bratt et al., 2016). The cause of this is likely down to the inheritance of germline mutations in mismatch repair and homologous recombination genes such as *BRCA1/2*. Mutations in either *BRCA1* or *BRCA2* occur in approximately 2% of hereditary PC and cause an increased risk of PC by the age of 65 of 4-fold and 8.5-fold, respectively (Marino et al., 2023; Vietri et al., 2021). Genetic mutations are discussed in more detail below in section 1.1.3.

In addition to the above, Bergengren et al., also describe modifiable risk factors which could be changed through lifestyle changes, such as weight, smoking status and metabolic syndromes (Bergengren et al., 2023). Generally, a higher BMI has been shown in multiple studies to increase the risk of PC, likely due to obesity causing metabolic and hormonal changes that can promote the development of cancer (Perez-Cornago et al., 2017; Rivera-Izquierdo et al., 2021; Vidal et al., 2020). Smoking is a well-documented risk factor for many cancer types and has been discussed in numerous publications (Gandaglia et al., 2021; Riviere et al., 2020).

1.1.3 Genetic mutations in prostate cancer

As mentioned previously germline mutations in certain genes are a prevalent area of research in prostate cancer, with the hope of opening new treatment options. *HOXB13* and *BRCA2* are two of the most mutated loci in PC patients with a prevalence of 0.2-4.5% and 7-33% respectively (Beebe-Dimmer et al., 2015; Mateo, Seed, et al., 2020; Nicolosi et al., 2019).

BRCA genes are part of the DNA Damage Response (DDR) which is essential for genomic stability and repairing DNA defects which occur during the cell cycle. Loss of function mutations in these genes renders them inactive, and consequently cells of the prostate can transform into oncogenic cells because of DNA damage accumulation (Gorodetska et al., 2019).

HOXB13 is a transcript factor that plays a critical role in the differentiation and thus development of the prostate gland (Marino et al., 2023; Patel et al., 2024). Interestingly HOXB13 has been identified as an AR coregulator that can positively or negatively regulate the recruitment of AR to target genes which in turn affects their expression (Norris et al., 2009). The *HOXB13(G84E)* missense mutation commonly found in PC tumours was first described by Ewing et al., where they demonstrated the amino acids change in the MEIS domain of HOXB13 leads to a significantly higher chance of developing PC, although exactly how this occurs is still under debate (Ewing et al., 2012).

Other frequent germline mutations in PC involve other components of both the DNA damage response (*CHEK2, ATM* and *PALB2*) as well as the DNA mismatch repair genes (*MLH1, MSH2, MSH6* and *PMS2*) (Bancroft et al., 2021; Khan & Cheng, 2022; Vietri et al., 2021).

As well as these germline mutations, it is imperative to highlight common somatic mutations found in PC tumours. The Cancer Genome Atlas (TCGA) was a landmark study in characterising common mutations in primary PC tumours, many of the findings have been validated in subsequent studies. While the TCGA contains over 300 primary PC samples with a range of aggressiveness, all samples were treatment naïve which limits its use if interested in more longitudinal treatment-related studies. The most mutated genes from this data-set are *TP53* (11.5%), *SPOP* (11.1%) and *TTN* (10.9%). In addition to this, a key finding from the data identified, in over 50% of the samples, a translocation event whereby the androgen-responsive gene *TMPRSS2* promoter is fused to the coding sequence of proto-oncogene and ETS family member *ERG* (fusion can include other ETS family members although much less frequently). The resultant fusions, *TMPRSS2:ERG*, is constitutively activated by androgen receptor signalling and because of this, elevated *ERG* expression drives the proliferation of PC cells (Boysen et al., 2015; Cancer Genome Atlas Research, 2015; X. Wang et al., 2017).

1.2 The Androgen Receptor

The androgen receptor (AR) pathway is essential for normal prostate development and homeostasis. However, it is widely accepted that the AR signalling pathway is crucial in early and advanced stages of PC being linked to several key cellular processes, such as proliferation, cell cycle progression, migration and epithelial to mesenchymal transition

(Culig & Santer, 2014; Eisermann & Fraizer, 2017; Ko et al., 2020; M. L. Zhu et al., 2010). The AR **(figure 1.2A)** is located on chromosome Xq-12 and encodes a 110kDa, 920 amino acid protein which, like all steroid receptors, has distinct functional domains; an N-terminal transactivation domain (NTD), a DNA-binding domain (DBD), a hinge region (HR) and a C-terminal domain ligand binding domain (LBD) (D. K. Lee & Chang, 2003; Messner et al., 2020). The 8 exons which encode for the distinct regions of the full-length AR are shown in Figure 2.

The NTD is exclusively encoded by exon 1 and as the name suggests, it is crucial for mediating AR-mediated transcription and this is possible through the three transcriptional activation units it contains; AF1, Tau1 and Tau-5 (J. Li & Al-Azzawi, 2009; Messner et al., 2020). Due to the structural plasticity of the NTD, it can bind many co-regulators which control AR localization, ARE binding and transcriptional activity (Davey & Grossmann, 2016; Tan et al., 2015).

The DBD is a cysteine-rich region encoded by exons 2 and 3 (Messner et al., 2020). The DBD contains two zinc finger motifs; one which facilitates the binding to androgen response elements of the DNA and a second that stabilizes the AR on AREs by mediating 'head-to-head' dimerization of the AR and interactions with the sugar-phosphate backbone of DNA (Davey & Grossmann, 2016; J. Li & Al-Azzawi, 2009). The nuclear localization signal (NLS), which is essential for the translocation of the AR from the cytoplasm to the nucleus upon ligand binding, is located at the junction between the DBD and the hinge region (Claessens et al., 2008; Dehm & Tindall, 2007)

The C-terminal LBD, encoded by exons 5 to 8, mediates binding to androgenic ligands, such as testosterone and dihydrotestosterone (DHT), the more active metabolite of testosterone (J. Li & Al-Azzawi, 2009). The LBD contains an 11 α-helices ligand binding pocket which, upon androgen binding, undergoes a conformational change by which helix 12 of the binding pocket repositions so the LBD is closed (Claessens et al., 2008; Dehm & Tindall, 2007). This change stabilizes ligand-AR interaction and leads to the formation of the activation function 2 domain (AF2) which can form an intra-AR-interaction with the AF1 of the DBD, termed the N/C-terminal interaction, which is essential for the proper function of the AR (Davey & Grossmann, 2016; Messner et al., 2020).

It is noteworthy that post translational modifications (PTMs) seem to occur non-randomly across the AR protein. As shown in **Figure 1.2B** most PTMs occur in the N-

terminal domain of the AR but clearly there is a cluster of PTMs to the NLS region also. The PTM modify the receptor and modulate its activity through regulation of protein stability, interactions with other proteins, cellular localisation and the structure of the protein itself (Coffey & Robson, 2012). The cluster of modifications in the NLS region constitute acetylation and methylation of lysine 630/32 (K630/632). Acetylation regulates affinity of AR for co-factors and enhances transcription of genes and cell growth. Acetylation mutation at this residue result in reduced co-activation by SRC1, Ubc9, TIP60 and p300 of the AR causing reduced transactivation (Gioeli & Paschal, 2012). Mechanistically it has been shown that DHT binding to the AR causes it to become demethylated (by members of the lysine demethylase family) which allows of the K630 and K632 residues to become acetylated. This acetylation allows for transcriptional activity of the AR (Van der Steen et al., 2013).

Testosterone and its potent metabolite DHT are the most significant cognate ligands of the AR. The hypothalamus-pituitary axis **(Figure 1.2C)** controls most of the androgen synthesis, and it is important to briefly highlight this to understand the treatment options in PC which are discussed later. Gonadotropin-releasing hormone (GnRH) is released from the hypothalamus which stimulates luteinizing hormone (LH) release by the anterior pituitary. LH binds to the LH receptor on Leydig cells of the testes to activate the enzyme P450scc, which begins testosterone production. Testosterone is released from the Leydig cells into the circulation where it acts in a negative feedback loop to inhibit the further release of GnRH and LH (Kluth et al., 2014; Messner et al., 2020; Oyola & Handa, 2017).

In the absence of androgens, the AR is located predominantly in the cytoplasm of the cell, where it is associated with chaperones, such as heat shock protein 70 (HSP70) and HSP90 (Lonergan & Tindall, 2011). Upon ligand binding to the LBD, the AR undergoes a conformational change involving an intra-AR interaction between the N- and the C-termini which is essential for full AR activity (X. Yu et al., 2020). This conformational change occurs concurrently with exposure of the nuclear localisation signal (NLS) within the hinge region of the receptor, which enables translocation of the AR into the nucleus. Once in the nucleus, the AR dimerises and binds to androgen response elements (AREs) in the promoter and enhancer regions of target genes such as *KLK3* (that encodes prostate-

specific antigen (PSA)) thus modulating gene expression **(Figure 1.2D)** (Bennett et al., 2010; Estebanez-Perpina et al., 2021).

Hormonal involvement is well established as a driver of PC. Some of the earliest work demonstrating this was by Huggins and Hodges in the 1940s in which they showed that either orchiectomy (removal of the testes) or injection of androgen/oestrogen could reduce progression and metastatic disease burden (Huggins & Hodges, 1941). Since then, there has been great interest in developing treatments that interfere with the AR signalling cascade, and it has led to numerous treatments being available to men with advanced and/or metastatic disease (Ritch & Cookson, 2018; Teo et al., 2019).

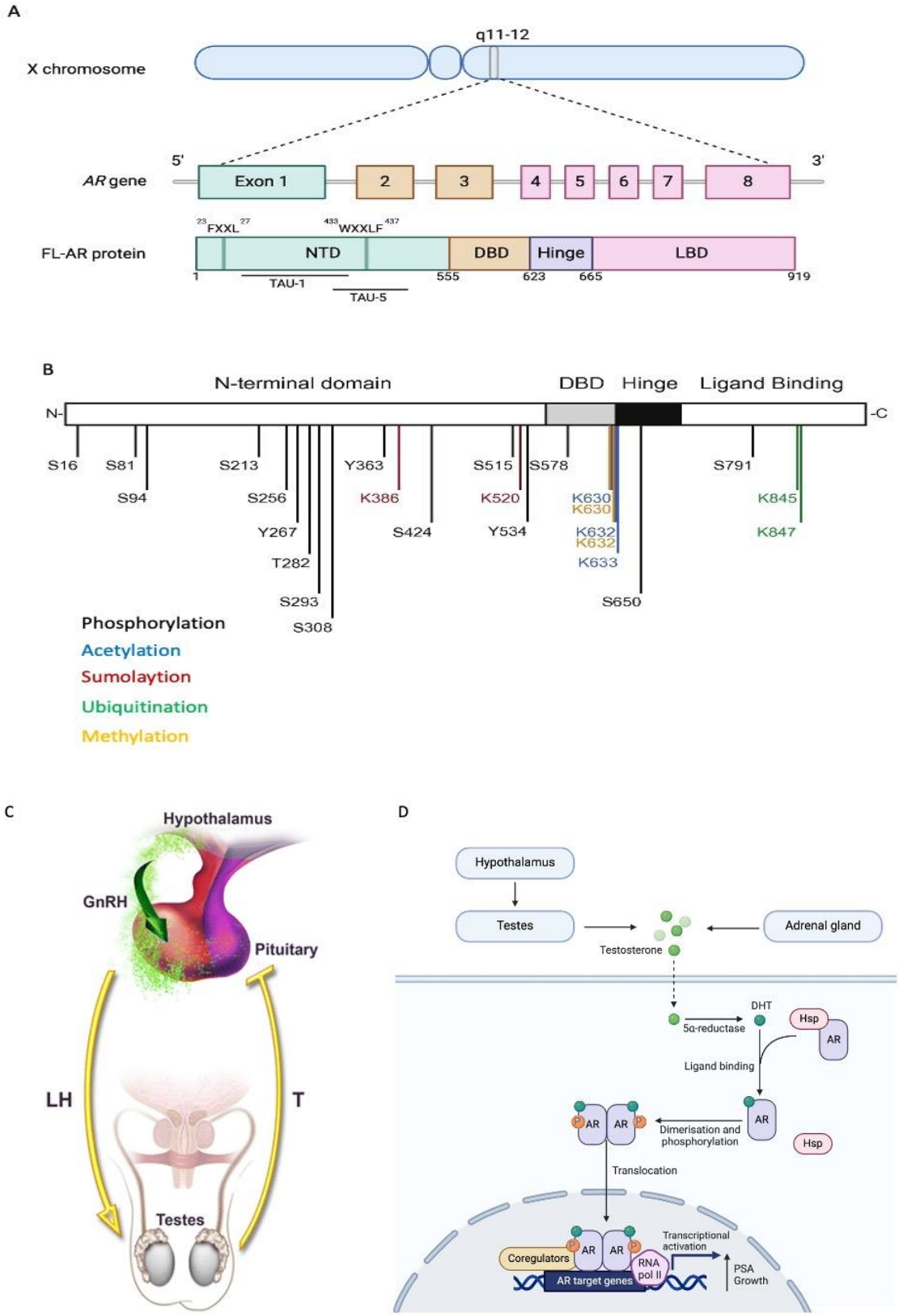
A
X chromosome
q11-12
5'
3'
AR gene
Exon 1
2
3
4
5
6
7
8
FL-AR protein
23 FXXL 27
433 WXXLF 437
NTD
DBD
Hinge
LBD
1
555
623
665
919
TAU-1
TAU-5
B
N-terminal domain
DBD
Hinge
Ligand Binding
N-
-C
S16
S81
S94
S213
S256
Y267
T282
S293
S308
Y363
K386
S424
S515
K520
Y534
S578
K630
K630
K632
K632
K633
S650
S791
K845
K847
Phosphorylation
Acetylation
Sumolaytion
Ubiquitination
Methylation
C
Hypothalamus
GnRH
Pituitary
LH
T
Testes
D
Hypothalamus
Testes
Adrenal gland
Testosterone
DHT
5α-reductase
Hsp
AR
Ligand binding
AR
AR
AR
Dimerisation and phosphorylation
Hsp
Translocation
Transcriptional activation
Coregulators
AR
AR
RNA pol II
AR target genes
PSA
Growth

Figure 1.2 The androgen receptor structure, synthesis, and signalling cascade. A *The androgen receptor gene and the protein it is translated into with its major domains; N-terminal, DNA binding and C-terminal domain which functions are discussed in section 1.2* ***B*** *PTMs found across the AR protein (Picture taken from Gioeli and Paschal, 2012).* ***C*** *The hypothalamic-piturity-axis which regulates the release of testosterone (ligand of AR signalling) from both the testes and adrenal glands. Negative feedback loop whereby increased testosterone suppress GnRH and LH production (Picture takend from Kluth et al, 2013)* ***D.*** *The AR signalling cascade is clinically significant to prostate cancer initiation and progression. Testosterone enters the cells and is metabolised to DHT which can bind to the AR LBD. DHT-bound AR is phosphorylated causing it to homodimerize and translocate to the nucleus where it binds to androgen response elements (AREs). This drives the expression of AR target genes aided by coregulators such as FOXA1. (BioRender)*

1.3 Diagnosis and Treatment for Prostate Cancer

1.3.1 Diagnosis of PC

In the UK, there is currently no dedicated screening programme for PC, this is due to NICE recommendations. However, this may change in the future due to the launch of the TRANSFORM trial (opening Spring 2024) which will use a combination of screening methods to diagnose PC earlier. Figures from Cancer Research UK indicate that currently there is an equal split between men diagnose with early and late-stage PC, which poses a significant clinical problem given that there are limited curative options for late stage PC (Cancer Research UK, 2019; Carlsson & Vickers, 2020).

For men in the UK being tested for PC, the initial clinical examination involves a routine blood test for PSA, a marker used in the diagnosis of prostate cancer since the 1990s (Lomas & Ahmed, 2020). In healthy patients, there are very low amounts of PSA in serum (typically <4ng/mL) as it is secreted into the seminal fluid and exits the body. However, in PC, where there is an expansion of PSA-secreting cells, levels of PSA can rise in the serum allowing for detection via a simple blood test. If men have elevated levels of serum PSA they would then routinely undergo transrectal ultra-sound biopsies (TRUS-Biopsy) to allow for a histopathological diagnosis of PC (Moe & Hayne, 2020). A TRUS-biopsy involves the insertion of a fine needle into the prostate to extract a small ‘puncture’ of tissue which can be examined microscopically. The issues with TRUS-biopsies are they: i) regularly miss disease that is there; ii) may lead to the diagnosis of clinically insignificant PC; iii) cause rare but important complications such as sepsis from the procedure (NICE, 2019). More commonly now, magnetic resonance imaging (MRI) is being used as an additional

diagnostic tool to improve detection of PC. Large-scale trials comparing the use of multi-parametric magnetic resonance imaging (MP-MRI) before TRUS biopsies demonstrate that MP-MRI can reduce biopsies by over 25% and, importantly, can lead to improved detection of clinically significant PC (Ahmed et al., 2017).

From these clinical tests, a patient's PC will be scored and graded to indicate the severity of the disease and guide treatment options. In the UK, clinicals follow The Cambridge Prognostic Group (CGP) System which evaluates the Gleason Score, PSA serum levels and tumour stage (whether the tumour localise to the prostate or spread)(Gnanapragasam et al., 2018). **Table 1** gives a summary of the scoring system. It should be noted that this system does not apply if the cancer has already spread to another part of the body or to patients who have not responded to treatment.

Table 1*. Patient characteristics of men diagnosed with non-metastatic, treatment-naive, PC according to the NICE three-tiered risk stratification and the Cambridge Prognostic Group classification (CPG) (Adapted from NICE)*

NICE risk group	Criteria	CGP Category	Criteria
Low-risk disease	Gleason Score ≤ 6 AND PSA <10ng/ml AND stage T1-T2a	**1**	Gleason Score 6 AND PSA <10ng/ml AND stage T1-T2
Intermediate-risk disease	Gleason score 7 **Or** PSA 10-20ng/ml **Or** Stage T2b	**2**	Gleason Score 3 + 4 = 7 (Grade Group 2) **Or** PSA 10-20 ng/ml AND stage T1-T2
		3	Gleason Score 3 + 4 = 7 (Grade Group 2) AND PSA 10-20 ng/ml

			AND stage T1-T2 **Or** Gleason score 4 + 3 =7 (Grade group 3) AND stage T1-T2
High-risk or locally advanced disease	Gleason Score 8-10 **Or** PSA > 20ng/ml **Or** Stage ≥T2c	**4**	***One of:*** Gleason score 8 **Or** PSA .20 ng/ml **Or** Stage T3
		5	Any combination of: Gleason score 8, PSA >20ng/ml or stage T3 **Or** Gleason score 9-10 **Or** Stage T4
Footnote: PSA= Prostate specific antigen; T=Tumour stage			

1.3.2 Treatment of localised Prostate cancer

In the UK, for patients with a CPG score of 1,2 or 3, there are three treatment options: i) active surveillance ii) radical prostatectomy iii) radical radiotherapy. There is almost no difference in 10-year survival between treatment options as most patients with low-grade, localised PC have almost a 100% 10-year survival. There is some variation in disease progression over 10 years based on therapy; radical prostatectomy and radical radiotherapy have an 8% incidence of progression whilst for patients who underwent active surveillance this figure is 21% (Hamdy et al., 2023) . For patients who have a CPG score of 4 or 5, NICE recommendations for patients undergoing radical prostatectomy or radical radiotherapy, literature suggests that both procedures have equally favourable outcomes (X.-X. Guo et al., 2021; Hayashi et al., 2020; Y.-C. Lu et al., 2022).

1.3.3 Biochemical reoccurrence and treatments for advanced prostate cancer

Following the radical treatment options mentioned above, patients will receive regular check-ups, namely in the form of PSA testing, to assess for biochemical relapse. If PSA levels begin to rise, patients will be offered hormone therapy with the aim of reducing circulating androgen levels in the body. Hormonal therapies fall into one of two categories: androgen deprivation therapy (ADT), which involves starving the AR of its ligand by inhibiting the hormonal signalling cascades or metabolic pathways which synthesise AR; or antiandrogens which are direct antagonists of the AR proteins and thus prevent nuclear translocation and transactivation **(Figure 1.3).**

1.3.4 Androgen Depravation Therapy

In healthy adult males, the normal concentration range for circulating testosterone is between 260-920 ng/dl (Travison et al., 2017). ADT treatment aims to reduce testosterone levels to <20ng/dl thus starving the cancer cells of androgens which they require (Karantanos et al., 2013). Whilst an orchiectomy used to be the route clinicians took to reduce serum testosterone, this clearly harboured severe physical and psychological morbidities and therefore chemical castration is the mainstay in treatment- this is also significantly cheaper than orchiectomy surgery (Garje et al., 2020; M. Sun et al., 2016). ADT treatments consist of either LHRH agonists or GnRH antagonists. Briefly, LHRH agonists such as leuprorelin, work by continually stimulating the pituitary gonadotroph cells which activates a negative feedback loop to reduce the secretion of gonadotropins thus preventing testosterone production (Rick et al., 2013; Shim et al., 2019). With LHRH agonists, there is an initial spike in testosterone levels as the drugs overstimulate the release of testosterone by the testes however this only lasts around 2-3 weeks and can be controlled by co-administration with a direct AR antagonist. GnRH antagonists, with Degarelix being the most common in the UK, reduce serum testosterone levels more rapidly than LHRH agonists with the added benefit of not causing an initial spike in testosterone (Y. F. Liu et al., 2021; Shore et al., 2013). Mechanistically, these compounds antagonise the GnRH receptor of the picturality gland which consequently reduces the release of LH thus halting testosterone production immediately (Steinberg, 2009).

Comparing the use of LHRH agonists and GnRH antagonists by clinicians in the UK, LNRH agonists are more readily prescribed due to the high costs associated with Degarelix.

NICE recommends that Degarelix should only be used in patients with spinal metastases as the initial testosterone flair is of a bigger concern (Uttley et al., 2017) .

Abiraterone is a potent androgen biosynthesis inhibitor, it does this by blocking cytochrome P450 c17 (CYP17), a critical enzyme in testosterone synthesis, thereby blocking androgen synthesis by the adrenal glands and testes as well as within the prostate tumour **(Figure 1.3)** (de Bono et al., 2011; Schweizer & Antonarakis, 2012). The metabolite, abiraterone acetate, also acts as a partial antagonist of the AR with studies suggesting this metabolite is as potent at blocking the AR as second-generation anti-androgen enzalutamide (Z. Li et al., 2015). Essentially this means Abiraterone has both androgen deprivation and anti-androgen mechanisms of action.

1.3.6 Anti-androgen treatments

Anti-androgens act directly within PC cells and prevents AR signalling. Numerous non-steroidal anti-androgens (NSAA) have been developed over the years. Flutamide and bicalutamide compete with testosterone and DHT for AR binding, thereby inhibiting receptor-dependent gene regulation and prostate tumour growth (Estebanez-Perpina et al., 2021). Studies have shown that when NSAAa are combined with GnRH agonists there can be an, albeit small (>5%), increase in survival over monotherapy (Akaza et al., 2009). These compounds are often used early in the disease, along with GnRH inhibitors to complete reduced levels of testosterone in the body and to inhibit the testosterone flux which occurs early in the treatment with GnRH agonists.

Enzalutamide, a second-generation anti-androgen, was approved by the FDA in 2012. It was shown to increase overall survival in men when compared to flutamide or bicalutamide in two separate clinical trials (Davis et al., 2019). Enzalutamide has a five times greater affinity for the AR compared to first-generation anti-androgens, such as bicalutamide, making it a much more potent anti-androgen. It has been shown to impact several steps in AR signalling, including: (i) inhibition of androgen binding to the AR; (ii) blocks androgen-receptor nuclear translocation; and (iii) attenuates AR-DNA binding (Iguchi et al., 2019; Ito & Sadar, 2018). It is currently being used in men with CRPC who fail first-line therapy. However, there is ongoing debate as to whether it should be included as first-line treatment. Clinical trials have proven that utilising enzalutamide as a first-line treatment can significantly increase overall survival (Davis et al., 2019).

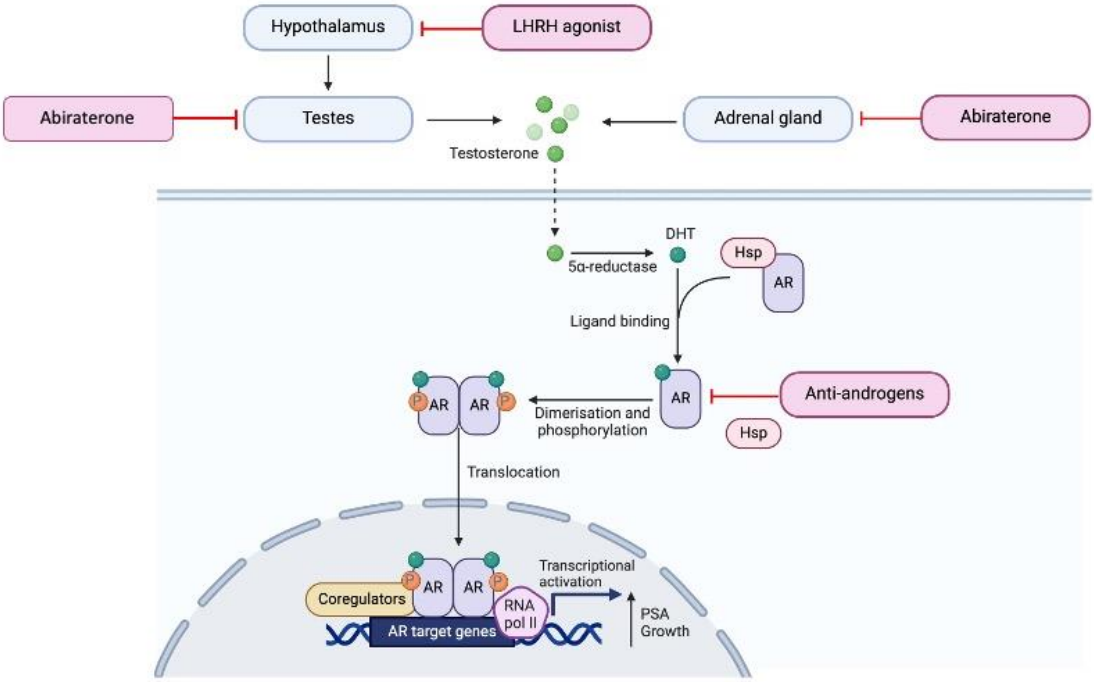

Figure 1.3 Anti-androgen and Androgen Deprivation Therapy Treatments*. Antiandrogen treatments, normally in the form of LHRH agonists, which bind and overstimulate the GRH receptor in the anterior pituitary gland. Whilst this may cause an initial "spike" in testosterone release it quickly shuts down due to a negative feedback loop. This feedback downregulated the GnRH receptor, blocking LH production and thus preventing the testes from releasing testosterone. Abiraterone is regarded as an ADT as it inhibits an enzyme essential for testosterone production. However, it also demonstrates AA effects by also antagonising the AR. Antiandrogens, Enzalutamide being the most recently developed and most effective, are AR antagonists which block AR translocation and transaction capabilities.*

1.3.7 Future perspectives on treatment

Whilst there appears to be an expansive repertoire of treatments for men, unfortunately, around 10-20% of men progress to a disease state termed castrate resistant PC (CRPC). Crucially, despite castrate levels of androgens, the tumour still progresses in an AR-dependent manner (Karantanos et al., 2013; Vellky & Ricke, 2020). The mechanisms by which CRPC arises are discussed in detail below. CRPC is a lethal form of the disease as there are currently no curative therapeutic options; hence there is an unmet need for the development of alternative therapeutic options. Below, we briefly discuss some of the latest findings and future perspectives in CRPC treatment.

In the UK alone there are 29 clinical trials for PC recruiting participants (Cancer Research UK, 2023). A fair proportion of these are looking at the effects of Poly (ADP-ribose) polymerase (PARP) inhibitors in patients who harbour *BRCA* mutations, as

discussed above. In both the UK and the USA, PARP inhibitors are recommended for patients who have a *BRCA* mutation and when the cancer has metastasised (NICE, 2019). PARP inhibitors have been investigated as monotherapies in TOPARP-A/B (Mateo et al., 2015; Mateo, Porta, et al., 2020) and TRITRON trials (Fizazi et al., 2023) where almost 90% of patients with a *BRCA* mutation responded to PARP inhibition. Numerous clinical trials have used PARP inhibitors in combination with other drugs such as AR targeting agents (Clarke et al., 2018) and Immunotherapies (E. Y. Yu et al., 2019) where combinations appear to have modest improvement in trial endpoints. It should be noted that PC tumours are still seen to be "cold" i.e., immune suppressive and that is why generally trials involving immunotherapies in PC have had limited success (Bansal et al., 2021; I. Wang et al., 2022). The use of radioligand therapies which target prostate-specific membrane antigen (PSMA), an antigen highly specific to metastatic castration-resistant prostate cancer cells was assessed in the Phase III VISION trial (Sartor et al., 2021). To be enrolled patients must have received at least one androgen-receptor–pathway inhibitor and one or two taxane regimens. Whilst the results showed significantly improved overall survival compared to current treatment and improve quality of life, NICE did not recommend the therapy as it did not see cost-effectiveness estimates within the range considered an acceptable use of NHS resources.

Other therapeutic strategies of interest involve AR-V7 targeting agents (discussed in section 1.5.1), PROTACS against AR, epigenetic enzyme inhibitors and target radiotherapies (Choudhury et al., 2022; Hofman et al., 2021; B.-R. Wang et al., 2022). Proteolysis targeting chimeras (PROTACs) were first reported in 2001. They contain three elements: the protein of interest (POI) binding ligand, a linker and an E3 ubiquitin ligase binging ligand. PROTACS work by hijacking the ubiquitin-proteasome system to degrade a specific protein of interest (Z. Liu et al., 2022). Briefly, the POI ligand binds to its selective protein and isolates it to the E3 ligand. Consequently, the E3 ligands recruits an E3 ubiquitin ligase bringing it in spatial proximity of the POI. This allows for the polyubiquitination of the POI permitting its destruction by the proteasome (L. Zhao et al., 2022). Because the PROTACS recruits the E3 ubiquitin ligase itself they can target proteins not normally ubiquinated. Additionally, PROTACS can target previously 'undruggable proteins' which lack enzymatic activity site or bindable site (Kargbo, 2019).

AR targeting PROTACS are plentiful, and some have had positive clinical results in phase I/II trials. The ARV-110 PROTAC entered clinical trials in 2019 and has proven efficacy in degrading both wild-type AR and treatment induced AR mutants. The phase 2 trial showed the response rate in patients with CRPC was between 10- ≥50% (measured by 50% PSA reduction) with best response was seen in patients harbouring treatment induced mutations (Gao et al., 2022a). In addition to ARV-110 other AR targeting PROTACS include ARV-766 (phase II enrolment ongoing) and CC-94676 (phase I/II), whist many others are still in the pre-clinical stage.

1.4 Mechanisms of Resistance and Castrate resistant prostate cancer

1.4.1 Clinical challenges of Castrate resistant prostate cancer prostate cancer

As mentioned above, approximately 10-20% of patients will progress to a disease state termed CRPC which normally occurs 1-5 years post-therapy (Chandrasekar et al., 2015; Crowley et al., 2021; Saad et al., 2021). By definition, CRPC is biochemical progression (detected by PSA levels rising at least 25% over a week) or radiological progression (MRI detection of new lesions) despite the presence of castrate serum testosterone levels (<50 ng/dL) (Conteduca et al., 2021). Current treatment regimens for CRPC are palliative, not curative, and normally involve chemotherapy with docetaxel in addition to the continuation of treatment with anti-androgens and ADT (NICE, 2019; Nuhn et al., 2019; Sartor & de Bono, 2018). In patients with mCRPC, bone targeting therapies, such as bisphosphonates, are recommended to reduce skeletal-related events (James et al., 2016; Kamba et al., 2017; NICE, 2019).

Unfortunately, as shown in **Figure 1.4**, these treatments invariably fail, and the disease ultimately progresses to an incurable form which leads to patient death. The next part of this thesis will detail the molecular mechanisms of resistance to early treatment which ultimately causes CRPC.

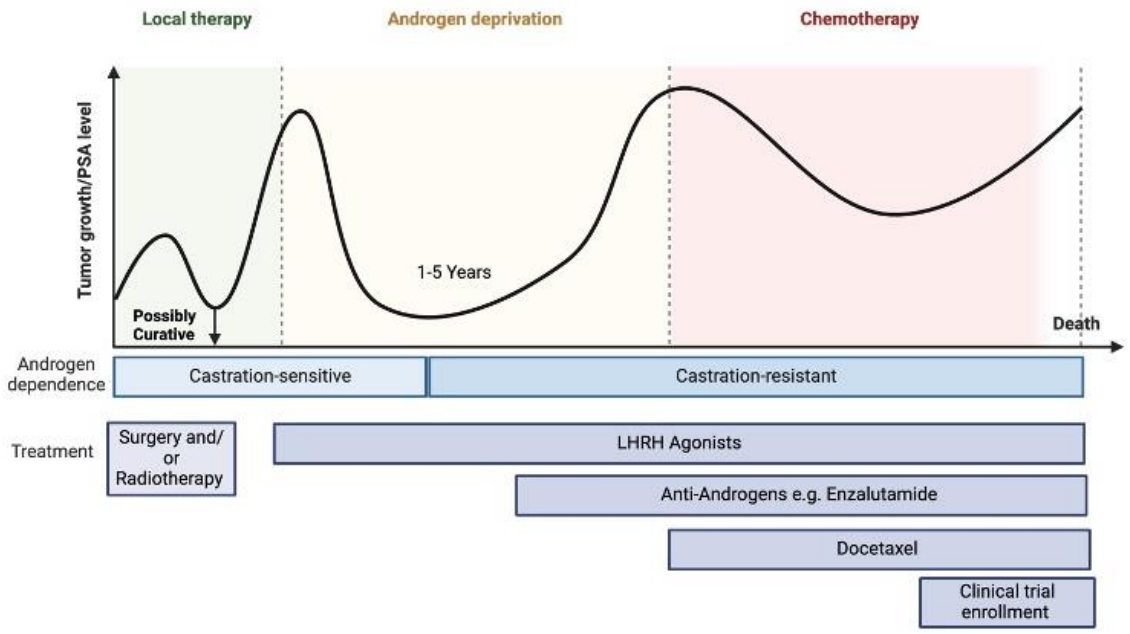

Figure 1.4 Typical prostate cancer progression and treatment intervention. *Localised prostate can be treated with radical proctectomy and/or radiotherapy and is likely to be curative. Men with reoccurrence will be offered ADT and with this anti-androgen also. Unfortunately, despite the initial effectiveness of these drugs, the cancer transforms from CSPC to CRPC. Whilst Docetaxel and possible enrolment in a suitable clinical trial are possible interventions, CRPC will inevitably become fatal (BioRender)*

1.4.2 Androgen receptor gene amplification

AR gene amplifications occur in up to 50% of men with CRPC (Edwards et al., 2003; D. Robinson et al., 2015). Interestingly, the study by Edwards *et al.,* demonstrated that the level of AR expression was significantly higher in CRPC tumours compared to matched hormone-sensitive tumours from the same patient. Similar results were shown in another study where *AR* gene amplification typically results in 6-fold more AR proteins in CRPC patient samples compared to hormone-naïve or benign prostate hyperplasia (Linja et al., 2001). *AR* gene amplification leads to one of the key features of CRPC, which is hypersensitivity within the androgen signalling pathway; allowing prostate cancer cells to utilize the extremely low levels of serum testosterone to drive activation of AR target genes (Merson et al., 2014). Taken together this alludes to the fact this process is one of the key mechanisms to enable progression to CRPC and develops largely because of ADT.

1.4.3 Androgen receptor mutation

AR gene mutations are two-fold more frequent in CRPC as opposed to androgen-dependent PC. To date, around 660 mutations have been described in the AR gene, most of which are gain-of-function point mutations most frequently found in the LBD (Nadiminty & Gao, 2012; D. Robinson et al., 2015). Mutations to the LBD have two effects which allow for continued AR signalling in castrate conditions: (i) they decrease the specificity of the AR-ligand interaction to enable alternative steroid molecules, such as glucocorticoids or progesterone, to activate the AR (Hay & McEwan, 2012; Karantanos et al., 2013); (ii) some mutations, such as W742C and F876L within the AR LBD, enable anti-androgens bicalutamide and enzalutamide, respectively, to act as an agonist of the AR (Lallous et al., 2016; Nadiminty & Gao, 2012; Waltering et al., 2012)Therefore, patients expressing these mutations would invariably become resistant to these treatments.

1.4.4 Intra-tumoral steroidogenesis

Activation of intra-tumoral androgen biosynthesis is another mechanism by which, despite castration levels of testosterone in the serum and prostatic tissue, AR target genes are still activated (Knuuttila et al., 2018). Crucially, intra-tumoral levels of DHT are only reduced by 75% during ADT which, together with *AR* gene amplification or gain of function *AR* mutations, can combines to drive AR target gene activation/expression (Armandari et al., 2014; Hamid et al., 2020).

In addition to this, in CRPC the levels of enzymes including AKR1C3, HSD17B2 and HSD17B3, which are required for metabolising adrenal steroids (such as DHEA-S and cholesterol), are highly upregulated. This allows *de novo* synthesis of androgens from adrenal androgen precursors and continued activation of AR target genes, driving PC growth and proliferation (Hagberg Thulin et al., 2016; Pfeiffer et al., 2011).

1.5 Androgen receptor variants (AR-Vs)

Tepper *et al.,* were the first to describe AR-Vs in PC by identifying an altered AR protein which lacked the LBD in the CWR22Rv1 cell line. The CWR22Rv1 cell line was derived from an androgen-independent xenograft tumour termed CWR22R-2152, which was derived from culturing the CWR22 hormone-dependent xenograft in androgen-depleted conditions. The study showed that the AR-V was only detectable in CWR22 xenograft post-androgen deprivation and had the capacity of constitutive nuclear localisation and androgen independent DNA binding (Tepper et al., 2002). In this study however Tepper *et al* believed the AR-V was a result of proteolytic cleavage and it was not until 2008 where Dehm *et al* showed that in fact, the AR-V was generated through alternative splicing of the AR (Dehm et al., 2008). Since this, over 22 AR-Vs have been discovered in CRPC specimens and whilst most are generated through alternative splicing, *AR* gene rearrangements can also generate AR-Vs as in the case of AR-V^{567es} (Y. Li et al., 2020; D. Robinson et al., 2015; Valentín López et al., 2024).

Alternative splicing of the AR gene leads to the production of most AR-Vs **(Figure 1.5A)**. AR-Vs lack the exons encoding the LBD, but due to retention of exons encoding the NTD and DBD, they can drive AR-target gene expression constitutively without the requirement for cognate ligand binding. AR-V7, the most clinically significant AR-V, is generated through an alternative 3' splice site (Paschalis et al., 2018). The result is a 3' cryptic exon, term cryptic exon 3 (CE3), truncating the AR so it no longer harbours the LBD and therefore no longer requires ligand binding to become activated. AR-V^{567es} is generated through skipping of exons 5, 6 and 7 which causes a frameshift mutation generating a new stop codon after the first 29 nucleotides of exon 8 leading to a truncated AR-V which is constitutively active (S. Sun et al., 2010). Therefore, despite AR-V^{567es} harbouring a small section of the LBD, it is constitutively active and does not rely on ligand binding. AR-V9 is generated through the inclusion of cryptic exons 5 and 3 at the 3' terminus of the AR which, like AR-V7 and AR-V^{567es}, generates a truncated AR lacking the LBD(Kohli et al., 2017). The NLS is encoded by in exon 4 (hinge region) of the AR gene and most AR-Vs do not harbour this region yet still have ability to localise constitutively in the nucleus. There are different explanations to this including NLS-like signals in the unique C-terminal extensions encoded in the different AR-Vs (Hu et al., 2009) and AR-Vs lacking the

nuclear export signal (NES) normally encoded by exon 6 of the *AR* (Saporita et al., 2003). AR-V^{567es} retains the hinge regions and therefore has a full NLS signal whilst other AR-Vs (AR-V1 and AR-V9) show poor nuclear localisation which may account for their reduced transcriptional activity. Given that the LBD is the site for direct anti-androgen binding, AR-Vs are refractory to first- and second-generation anti-androgens, such as bicalutamide and enzalutamide.

The transcriptional activity of AR-Vs varies considerably, constitutively active AR-Vs (AR-V7 and AR-V^{567es}) show strong transcriptional activity whereas cytoplasmic AR-Vs (such as AR-V3) are transcriptionally inactive unless they form heterodimers with AR-FL or AR-V7 (Zhan et al., 2017). AR-Vs can form homodimers to work independently of the AR-fl or form heterodimers with AR-FL allowing the nuclear translocation of AR-FL without ligand binding and/or presence anti-androgens (Antonarakis et al., 2014a; Roggero et al., 2021). These dimers bind DNA driving transcription of both the canonical set of AR-regulated genes plus additional AR-V specific-genes to drive disease progression (Cato et al., 2019; J. Lu et al., 2015; Messner et al., 2020). The N-terminal AF1 region of the AR is solely responsible for transcriptional activity which is unlike other nuclear receptors, such as ER, which require AF2/AF1 synergy for full transcriptional activity (Ji et al., 2023; Tan et al., 2015). AR-V1 has no intrinsic constitutive transcriptional activity however androgens enhance its dimerization to AR-FL, and interestingly AR-V1 reduces AR-V7 transactivation capabilities (Zhan et al., 2017). **Table 2** summaries the transcriptional activity and clinical relevance of different AR-Vs.

Various preclinical studies have shown the significance of AR-Vs in PC. Kounatidou *et al.,* developed a derivative of the CWR22Rv1 cell line, named CWR22Rv1-AR-EK, which has lost expression of FL-AR, but retains all endogenous AR-Vs. They showed that by targeting exon 1 of the AR-Vs by siRNA knockdown they could reduce the recruitment of AR-Vs at cis-regulatory elements of the AR target genes and consequently reduce their expression and slow growth of the cells (Kounatidou et al., 2019). Similarly, Dehm et all used the CWR22Rv1 cell line and demonstrated that by using siRNA targeting cryptic exon 2b, they could reduce AR-V activity and crucially by doing so, re-sensitize the cells to anti-androgens (Dehm et al., 2008).

In addition to the preclinical data, Sharp *et al.,* showed that levels of AR-V7 protein are seen in <1% in primary hormone-sensitive PC but following ADT, AR-V7 expression is

prevalent in 75% of matched castrate-resistant cases **(Figure 1.5B)** (Sharp et al., 2019). Critically, mounting evidence shows that patients with detectable levels of AR-V7 have reduced overall and progression-free survival **(Figure 1.5C)** (Antonarakis et al., 2014b; Scher et al., 2018; Tagawa et al., 2019).

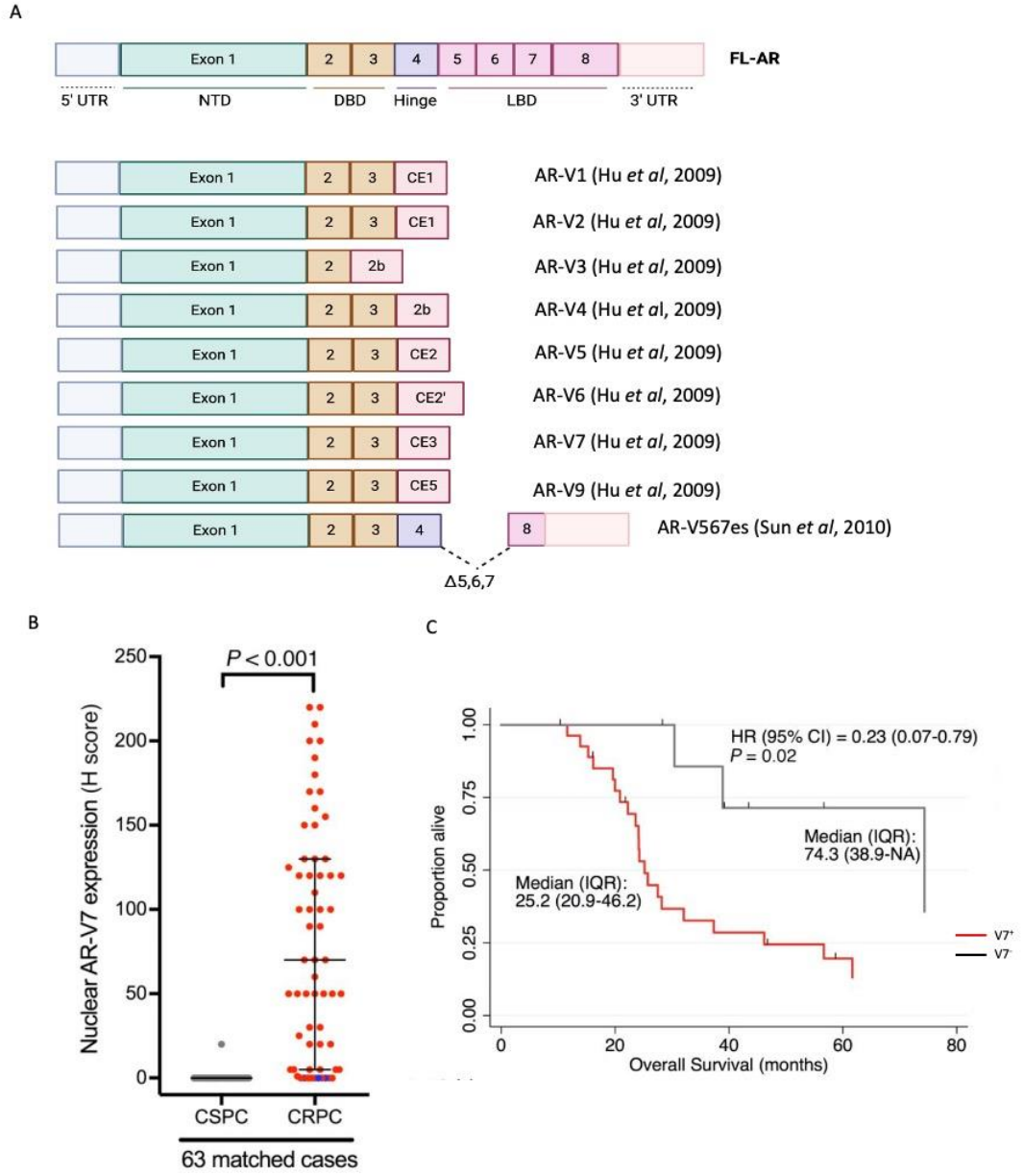

Figure 1.5 Androgen Receptor variants and their clinical significance. *A. Multiple AR-Vs have been identified and described in literature, here highlighting the most common AR-Vs and the year they were discovered, and their structure compared to the full length AR. Most AR-Vs include a cryptic exon leading to a truncated form of the AR which can constitutively activate AREs mentioned earlier (BioRender). B and C adapted from Sharp et al., 2019 utilising 63 tumour matched patients from the Royal Marson Clinical trials unit. B. Demonstrates that in when patients' cancer was castrate sensitive, expression of AR-V7 was very low however when the same patient tumours were assessed following biochemical reoccurrence post ADT (CRPC) expression of AR-V7 was significantly upregulated. C. Kaplan-Meier curve shows that there is a statistical difference in overall survival between AR-V7+(25.2 months) and AR-V7- (74.3months) patients from start of ADT treatment.*

AR Variant	Transcriptional Activity	Response to Androgen	Generation and structure	Clinical Relevance
AR-FL (Full-length)	Strong androgen-dependent transcriptional activation	Activated by androgens (e.g., testosterone)	Full N-terminal, C-terminal, and ligand-binding domains intact	Standard target ADT
AR-V7 (Most studied AR-V)	Constitutive transcriptional activity, even without androgen. Activates androgen-responsive genes and subset of additional ones. Strong transcriptional activity.	Activated without androgen; resistant to androgen-deprivation therapy. Located in nucleus.	Alternative splicing. Lacks the LBD and NLS.	Major driver of resistance in CRPC, predictive biomarker for treatment resistance
AR-V1	Lacks inherent transcriptional activity but can activate AR-FL. Termed conditionally activity as probably cell specific.	Androgens enhance AR-V1/AR-FL dimerization	Alternative splicing lacks LBD as replaced with CE1.	Detectable in CRPC specimens but not associated with worse prognosis.
AR-V3	Constitutive transcriptional activity, but low, unless bound to AR-FL/AR-V7	Cytoplasmic. Activated without androgen, resistant to ADT.	Alternative splicing. Full N-terminal and partial DBD domain. No LBD, no NLS.	Highly expressed and predictive of therapy resistance.
AR-V4	Constitutive transcriptional activity.	Activated without androgen.	Alternative splicing. Full N-terminal and DBD domain. No LBD.	Low prevalence in tumour samples and no clear clinical associations.
AR-V5	Unknown transcriptional activity	Activated without androgen.	Alternative splicing lacks LBD as replaced with CE2.	Low prevalence in tumour samples.
AR-V9	Lacks inherent transcriptional activity but can activate AR-FL. Termed conditionally	Cytoplasmic. Activates AR-FL in androgen independent manner.	Alternative splicing lacks LBD as replaced with CE5.	Expressed in patient samples, can be associated with worse

	activity as probably cell specific.			prognosis and therapy resistance.
AR-V567es	Constitutively active. Activates some androgen response genes and additional AR-V567es specific due to hinge region. Strong transcriptional activity.	Activated without androgen; resistant to androgen-deprivation therapy. Located in nucleus.	AR gene rearrangement leading to loss of exons 5/6/7. Has a truncated Exon 8.	Detectable in CRPC samples and associated with reduced overall survival

Table 2: Summary of the different functions of AR-Vs and their clinical significance. Summary of work by (Haile & Sadar, 2011; Kanayama et al., 2021; C. Lu & Luo, 2013; Luo et al., 2018; Wach et al., 2020; Wadosky & Koochekpour, 2017).

1.5.1 Therapeutic Targeting of AR-V7

Targeting AR-V7 is an active area of drug discovery. There are different approaches to the targeting AR-V7 which include: 1) small molecules that bind to the AR-V7 protein 2) small molecules that cause the degradation of AR-V7 3) agents that act indirectly to target AR-V7 4) anti-sense oligonucleotides and small molecules which disrupts alternative splicing leading to AR-V7 generation (Melnyk et al., 2022). Below we will discuss some of the more promising agents that have some clinical trial data.

Niclosamide is a multi-functional drug with broad anti-tumour activity. In CRPC, pre-clinical data showed a robust reduction in AR-V7 protein expression following Niclosamide treatment (C. Liu et al., 2016). A phase Ib trial of Niclosamide in combination with abiraterone in CRPC patients showed a 62.5% response rate and warranted further investigation (Parikh et al., 2021). A better understating of the specific mechanism of action in CRPC patients may lead to better identification of patients who would benefit from Niclosamide treatment.

Utilising anti-sense oligo nucleotides which binds to specific regions of the AR have had limited success clinical. EN-4176 is a third-generation antisense oligonucleotide that binds to the hinge region to AR mRNA. It had been shown to down regulated both AR-FL and AR-Vs in pre-clinical data but the Phase I trial involving it was halted due to business reasons and poor clinical results (Bianchini et al., 2013).

Both PROTACS mentioned in section 1.3.8 (the only two of which are in clinical trials) unfortunately target the LBD of the AR and therefore are inactive against AR-V7. NTD targeting compounds include EPI-506, which binds to the AF1 region of AR inhibiting its transactivating activity, however this showed lack of efficacy and poor bioavailability in clinical trails (Moigne et al., 2019). EPI-7386, another N-terminal targeting PROTAC, was developed more recently with improve pharmaceutical properties. EPI-7386 in now in Phase I/II clinical trial both as a monotherapy and in combination with Enzalutamide (Laccetti et al., 2023).

Indirect targeting of AR-Vs include the use of bromodomain and extra-terminal (BET) family inhibitors as it is well documented that BRD4 for example can activated both AR-FL and AR-V7 through direct interactions actings as co-regulators of both proteins (Mandl et al., 2023). BET inhibitors, including GS-5829, have reached phase II clinical trials comparing monotherapy and in combination with Enzalutamide but showed limited clinical efficacy (Aggarwal et al., 2022). The histone acetyltransferase paralogues CREB-binding protein (CBP) and p300 are potent coactivators of ARs that epigenetically increase the chromatin accessibility of AR target genes (Daniels et al., 2024). Their functional partly mediated by two conserved regions: a catalytic histone acetyltransferase domain and a bromodomain. These domains interact with a plethora of transcription factors (including AR-FL and AR-V7), as well as the general transcriptional machinery, and therefore regulate multiple cellular processes (Welti et al., 2021). CCS1477 perhaps the best studied inhibitor of CBP/P300 which targets the bromodomain is currently being assessed in a clinical trial as a monotherapy and in combination with standard ADT (NCT03568656) (De Bono et al., 2019). Polo-like kinase 1 (PLK1) is elevated in prostate cancer and plays a role in coordinating the downstream PI3K-AKT-mTOR pathway and the activation of AR signalling through elevating cholesterol biosynthesis during the progression to castration-resistant disease. There is an ongoing trial assessing the effectiveness of onvansertib, a PLK1 inhibitor, in combination with abiraterone and prednisone in CRPC patients however s yet there are no results posted (Einstein et al., 2022).

Therapeutic Agent	Mechanism of action	Reference
Niclosamide	• Hinders AR-V7 recruitment to AREs	(Parikh et al., 2021)
TAS3681	• Down regulation of AR and AR-V7 (mechanism not completely known)	(De Bono et al., 2021)
EPI Compounds	• Targets N-terminal domain of AR • Bind within ARF-1 regions to prevent protein-protein interactions	(Antonarakis et al., 2016; Laccetti et al., 2023)
PROTAC	• Degrade full length AR • Selective targeting of DRB region to degrade both AR-FL and AR-V7	(Gao et al., 2022b; Hung et al., 2023)
VNPP433-3β	• Binds to AR resulting in its ubiquitination and subsequent proteasomal degradation	(Taplin et al., 2019; E. Thomas et al., 2023)
Regulated Induced Proximity Targeting Chimera (RIPTAC)	• binds AR-FL and AR-Vs as well as an essential protein to cell viability which effectively kills cells	(Bae et al., 2025; Raina et al., 2023)
Oligonucleotides	• siRNA directly targeting AR-V7 • Anti-sense oligonucleotides can inhibit splicing (reducing AR-V7 generation)	(Luna Velez et al., 2022; L. Xue et al., 2024)
AUTOphagy-TArgeting Chimera (AUTOTAC)	• Targeted degraded or AR and AR-V7	(Bae et al., 2025)

Table 3: Therapeutics which directly target AR-V7 currently in development

1.5.2 Alternative Splicing

Alternative splicing is an essential process for enhancing transcriptional diversity from genes in multicellular organisms; with over 90% of human genes undergoing alternative splicing (Graveley, 2001). Alternative splicing **(figure 1.6),** the process of removal of introns and joining together of exons in various configurations as mature mRNA, is the reason why the human genome has around 20,000 genes but the human proteome consists of approximately 90,000 proteins (McManus & Graveley, 2011).

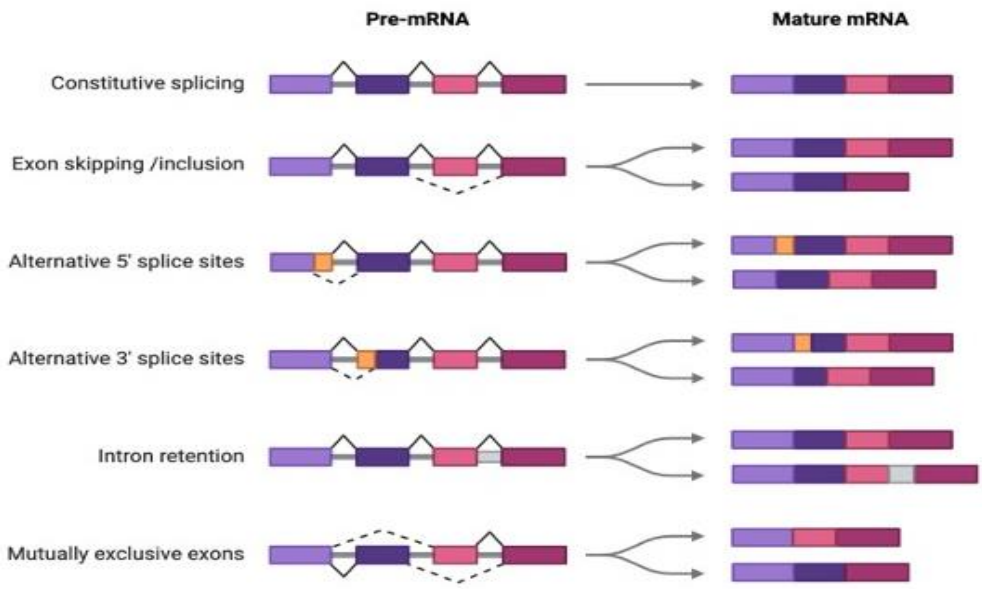

Figure 1.6 Alternative Splicing Patterns. *Numerous splicing patterns have been identified in literature. Exons are separated by longer introns (not shown to scale) and can be configured in multiple mature mRNA transcripts. Constitutive splicing refers to when exons are joined sequentially from the 5' to 3' genomic order. Alternative splicing enables exons to be include mutually exclusive allowing alternative 5' and 3' sites withing exons to be used, exons skipped, or introns retained. (Biorender)*

The spliceosome **(Figure 1.7A)** is comprised of five small nuclear ribonucleoproteins (snRNP) (U1, U2 and the U5/U5/U6 tri-snRNP) as well as their associated cofactors termed splicing factors (SFs) such as U2AF65 and SRSF1 (Paschalis et al., 2018). The first step of alternative splicing is the assembly of these components which is then followed by subsequent splicing of pre-mRNA (Y. Wang et al., 2015).

Initially, U1 recognises a 5' splice site on the intron to be spliced and a three-protein complex comprised of U2AF1, U2AF2 and SF1 recognises the 3' splice site to form Complex E **(Figure 1.7A.2)** (Bonnal et al., 2020). The three-protein complex is highly organised with SF1 interacting with a subunit of U2AF1 but as shown in Figure 3, the SF1 binds to the pre-mRNA whereas the U2 subunits are the part that binds to the 3' splice site (Wahl et al., 2009). Formation of Complex E triggers the ATP-dependent binding of U2 around the branch site which is facilitated by SF3B1, a protein component of U2, which induces a conformation change bringing the 5' splice site to the proximity of the 3' splice site to form Complex A **(Figure 1.7A.3)** (Bonnal et al., 2020; Wahl et al., 2009). Next, the preassembled U4-U5-U6 tri-snRNP joins the pre-B complex to induce further conformational change and protein exchange **(Figure 1.7A.4).** U1 and U4 are destabilised and exit from the complex which results in the formation of the catalytically active complex B **(Figure 1.7A.5).** Two sequential catalytic reactions occur to form Complex C, which contains the free end of the first exon and the remaining intron–exon lariat intermediate (Dvinge, 2018). The second reaction forms the post-spliceosome complex that contains the mature mRNA product, as well as the entire looped intron lariat **(Figure 1.7A.6-7).** Subsequently, U2, U5 and U6 are released and recycled for subsequent splicing reaction **(Figure 1.7A.8)** (Wahl et al., 2009).

Clearly, from the complexity of the splicing process, there is a need for it to be highly regulated. This is achieved through the interactions between *cis*- and *trans*-acting regulatory elements (Y. Wang et al., 2015). The regulatory elements aid in defining exon regions, *Cis*-acting regulatory elements are divided into four functional groups; exonic splicing enhancers (ESEs), exonic splicing silencers (ESSs), intronic splicing enhancers (ISEs) also known as intronic activators of splicing (IASs) and intronic splicing silencers (ISSs) (M. Chen & Manley, 2009). Whilst *cis*-acting regulatory elements refer to the actual regulatory sequences found within the pre-mRNA, *trans*-acting elements are proteins which regulate alternative splicing by interacting with the *cis*-regulatory sequences (Dvinge, 2018; Z. Wang & Burge, 2008). *Trans-acting* elements can be put into two main groups: Serine/arginine-rich (SR) proteins or hnRNPS. SR proteins are generally considered splicing enhancers that promote exon inclusion by interacting with ESEs (Dvinge, 2018). In contrast to this, heterogeneous nuclear ribonucleoproteins (hnRNPs) are considered spicing repressors and do this by binding to ISS motifs (Huelga et al., 2012). Referring to Figure 5,

the 5’ splice site recognised by U1 is an example of a *cis*-regulatory element whilst the SPF protein that is involved in the formation of complex E, is a *trans*-acting factor.

Dysregulation of the spliceosome is documented in PC. For example, it has been shown that treatment of PC cells with enzalutamide can cause excessive recruitment of SFs to the site in the AR mRNA which contains the 3’ splice site of AR-V7 (Liu et al., 2014). Another example is polypyrimidine tract-binding protein 1 (PTB1), a hnRNP, which in over-expression studies has been shown to increase AR-V7 expression levels (Nadiminty et al., 2015). Thus, identifying additional splicing factors that may be crucial for AR-V formation may provide a novel therapeutic opportunity in treating otherwise fatal CRPC.

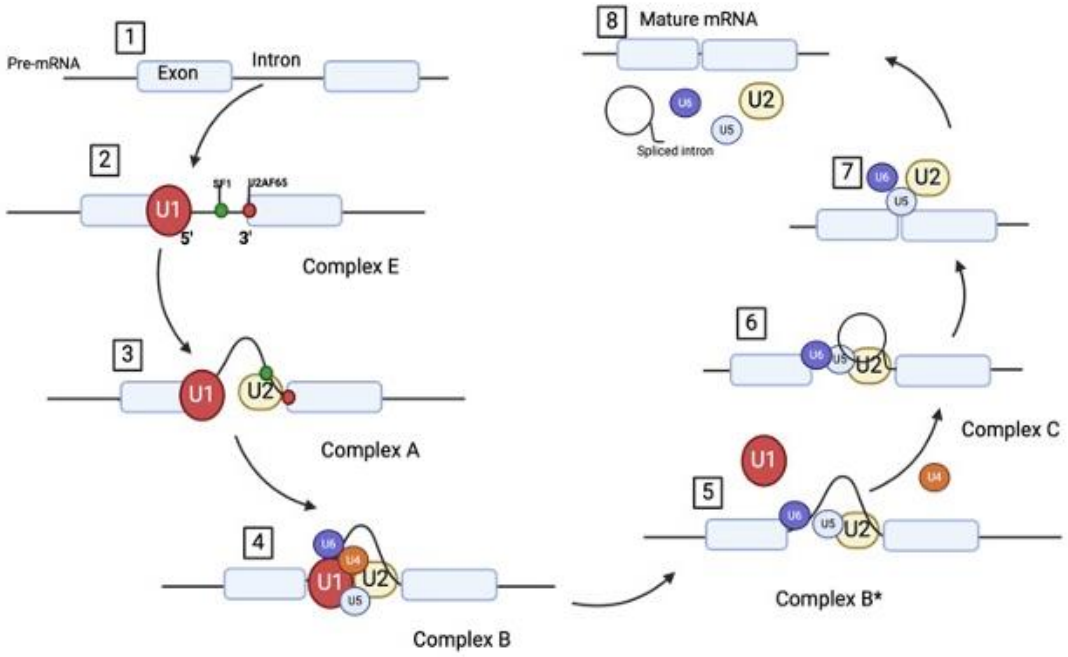

Figure 1.7 Pre-mRNA Splicing by the Spliceosome. *Stepwise process of cross intron assembly and disassembly of the spliceosome to generate a mature mRNA transcript. Spliceosome snRNPs (coloured circles) of importance for the removal of an intron (black line) from pre-mRNA containing two exons (light blue boxes). Splicing factors (SFs) shown by small green and red circles at step one are essential for specific splice site recognition to begin splicing process. Different intermediate complexes formed during the splicing process are highlighted (complex E, A,B,B+ and C) (Figure adapted from Dvinge, 2018, and Wahl et al, 2009).*

1.5.3 Histone Regulation of Alternative splicing

To form a comprehensive explanation of how histone modifications regulate splicing it is essential to first take a step back and over and review DNA order and chromatin compactions. DNA molecules wrap around histone octamers H2A, H2B, H3 and H3 to make up nucleosomes, which is the first order of chromatin compaction (Kang et al., 2017) **(Figure 1.8a).** Histone proteins contain a slight protrusion, known as a histone tail, at their N-terminus which are essential to permit higher-order chromatin structures. They are basic sequences and contain specific amino acids which can be subjected to post-translational modifications such as methylation and acetylation (Armstrong, 2014). These modifications remodel the chromatin thus making it more or less compact. A less compact chromatin state generally allows for other proteins (such as transcription factors or RNAPoII) to bind and thus lead to gene activation whilst a 'closed' chromatin state normally leads to suppression of a gene. Methylation of histone tails is just one form of histone modification with acetylation, phosphorylation and ubiquitination being the other most studied modifications. GlcNAcylation, citrullination, crotonylation, SUMOylating and isomerisation are other, less well studied, modifications of histone. These modifications are carried out by specific enzymes which either add (writers) or remove (erasers) the modifications **(Figure 1.8B).** The writers consist of; Histone acetyltransferase (HATs), Histone methyltransferase (HMTs/KMTs) and protein arginine methyltransferase (PRMTs) or Kinases. The group of "eraser" enzymes have opposing affects in that they remove the histone modification. The erasers consist of; Histone deacetylase (HDACs), Lysine demethylases (KDMs) and phosphatases. Histone modifications are primarily associated with changing chromatin architecture and thus affecting gene expression. However, as this next section will demonstrate, histone modifications can also regulate alternative splicing.

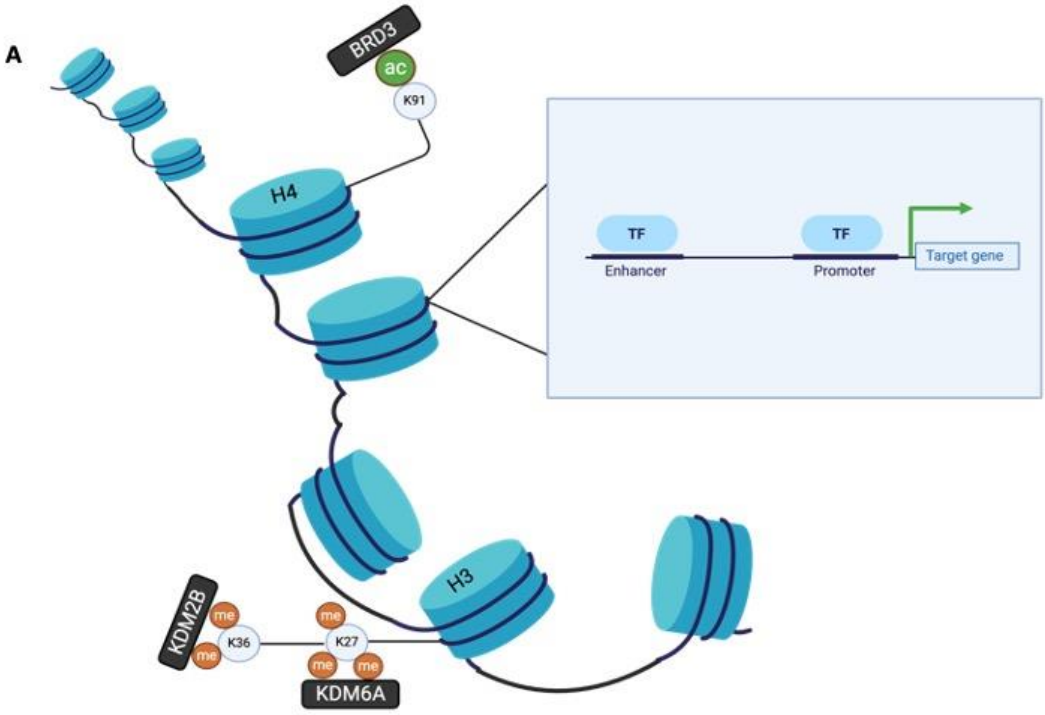

Modification	Writers	Erasers
Acetylation	Histone acetyltransferases (HATs)	Histone deacetylases (HDACs)
Methylation	Histone methyltransferases (HMTs/KMTs) and protein arginine methyltransferases (PRMTs)	Lysine demethylases (KDMs)
Phosphorylation	Kinases	Phosphatases

Figure 1.8 DNA and Chromatin architecture and major writers and erasers. *A) DNA (black line) wraps around histones (blue cylinders) to form nucleosomes. Amnio acid tails (protrusions from histones) which can be modified by a range of epigenetic writers and erasers. These writers and erasers, including the modification the act upon, are summarised in the table below.*

As well as the *cis*- and *trans*-regulatory elements mentioned before, there is mounting evidence that there is epigenetic regulation of alternative splicing through histone modification as well as DNA methylation (Lev Maor et al., 2015; Luco et al., 2010). This became evident in studies which revealed that histone marks, for example, are not randomly distributed along the genome and that different levels of certain histone marks could affect some of the spliceosome machinery (Agirre et al., 2021; Luco & Misteli, 2011; Segelle et al., 2022) . In addition to this, there must be another layer regulating alternative splicing as some tissues exhibit different splicing patterns despite harbouring identical sequences and expression of *cis*- and *trans*-regulatory elements and factors, respectively (Xu et al., 2018).

As originally described by Luco et al., histone modifications appear to be able to affect splicing decisions in two ways; the kinetic model **(Figure 1.9)** and the chromatin-adapter model **(Figure 1.10)**. Firstly, since alternative splicing occurs co-transcriptionally, the first model proposes that the rate of RNA polymerase II (RNAPoII) can influence splicing decision and that histone marks can affect RNAPoll elongation rate. Generally, a slower elongation rate leads to increased inclusions of exons with weak splice sites, by allowing more time for the spliceosome to bind to exons; whereas a quicker elongation rate favours inclusions of exons with strong splice sites (and generally the exclusion of exons with weak splice sites). Strong splice sites are defined as those which are constitutively spliced and have sequences which allow for splicing machinery to easily bind compared to 'weak' splice sites which are generally alternatively spliced exons (Dvinge, 2018). In the context of the *AR* gene, a 'strong' splice site would be seen in the 3' of exon 8 whereas a 'weak' splice site would be in the intron before CE3. Evidence of this model in action has been demonstrated at Exon 18 of the *NCAM* gene which has two isoforms depending on splicing decision. Schor et al., revealed that an increase in active transcription methylation marks (H3K36me3) surrounding a spliced exon caused a quicker RNAPol II elongation rate and thus resulted in exon inclusion (Schor et al., 2009). On the other hand, transcriptionally-repressive methylation marks, such as H3K9me2, have been shown to slow down RNAPolI which can result in the exclusion of certain exons and lead to the inclusion of alternative exons with 'weak' splice sites (Dujardin et al., 2014; Marasco et al., 2022).

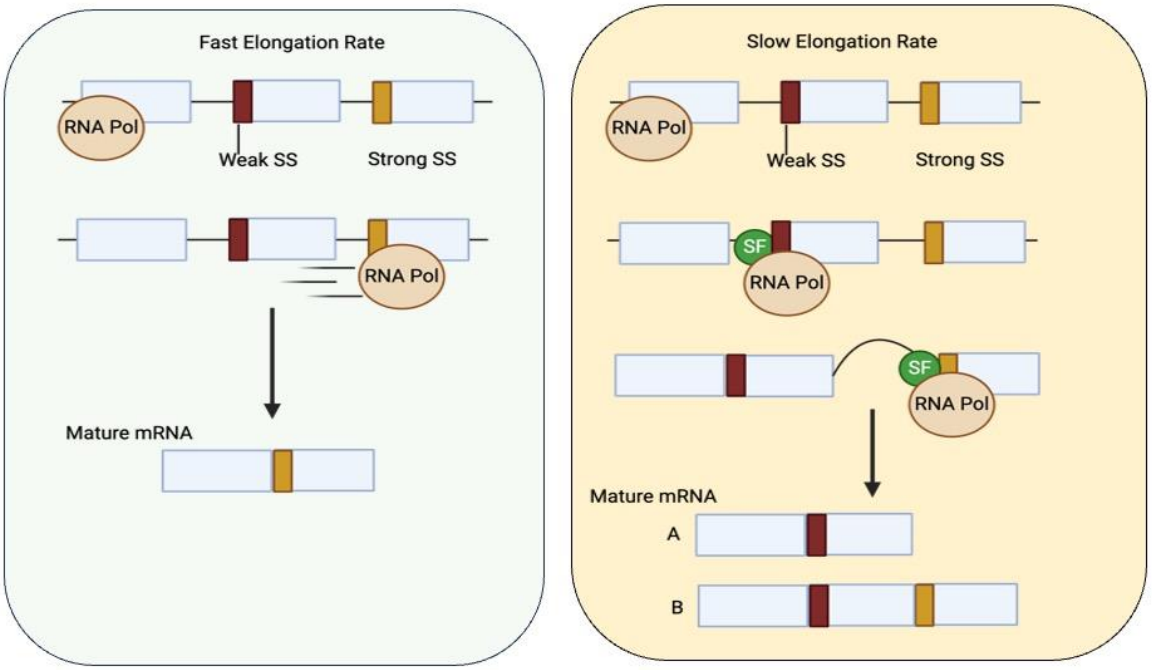

Figure 1.9 Kinetic model of histone modifications affecting splicing. *Some histone marks allow for a fast rate of RNA polymerase elongation rate (Left box). As a result, RNA polymerase moves quickly through a gene and is slowed only by exons with a 'strong' splice site (depicted in the third exon in the diagram). As RNA polymerase binds to said exon it recruits splicing factors and as a result leads to splicing. The resultant mature mRNA then contains the exon with a strong splice site whilst the exon with a weak splice site is excluded. When histone modifications slow RNA Polymerase (right box), it allows RNA polymerase to bind to Exons with weak splice sites (depicted in the second exon here). As before, this recruit splicing machinery (green circle) to the exons and therefore the exon is included in the mature mRNA). RNA polymerase could then move to the next exon and repeat the process. That is why slow elongation rate could lead to two possible isoforms of a protein; A which contains only exons 1 and 2 (as seen with the generation of AR-V7) or B whereby the protein has all three exons included. (Figure adapted from Dujardin et al; 2013, using BioRender)*

In addition to this 'Kinetic Model', Luco et al., described another which they termed "chromatin adaptor model". In this model, they proposed that histone modifications directly recruit splicing factors via a chromatin-adapter system **(figure 1.10)** which consists of a chromatin-binding protein (such as KDM6A) that reads the histone marks and allows splicing factors to bind to the specific splice site on the pre-mRNA. This model is perhaps the most well studied with multiple examples being reported. Recently, Segelle et al., demonstrated how a specific chromatin change in H3K27 methylation abundance at specific exons of a subset of genes was sufficient to induce endothelial-to-mesenchymal transition in multiple cell line models. Mechanistically, this histone post translational modification-dependent influence on splicing was facilitated by chromatin binding proteins binding to these histone marks and recruiting spliceosome components to discriminate exons (Segelle et al., 2022). Significantly, this model has also been shown to lead to AR-V7 expression. Fan et al., demonstrated that KDM3A binds to the H3K9 methylation mark at CE3 and recruits HNRNPF to this location of the pre-mRNA. In turn, HNRNPF subsequently binds U2AF65 to the cryptic exon, facilitating its inclusion in the mature transcript thus leading to the generation of AR-V7 **(Figure 1.9**) (Fan et al., 2018).

It should be noted however that most studies above have focussed on a binary splicing model whereby the resultant protein is either A or B. In terms of prostate cancer progression, we know that AR-V7 are expressed along with other variants, as well as the full-length AR. Therefore, there is not a binary splicing switch *per se*. It is therefore imperative to further understand changes in specific splicing patterns which may lead to novel target strategies through, for example, the use of HDAC, HAT or KDM inhibitors to switch or prevent oncological splicing events.

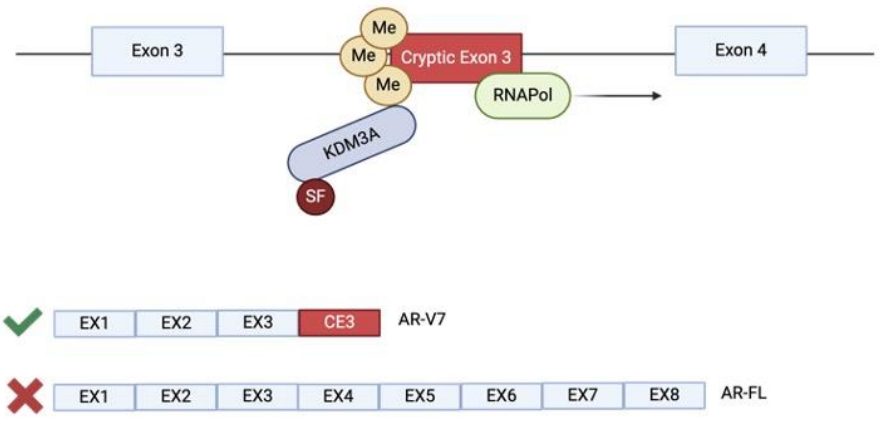

Figure 1.10 Chromatin adapter model. *A specific example of a chromatin-adapter model leading to AR-V7 generation is discussed in the text. H3K9me2 methylation marks (Yellow circle) which are upregulated in castrate conditions at the CE3 are recognised by KDM3A. As part of this recognition, KMD3A recruits specific splicing factor HNRNPF (Red circle attached to KDM3A) to CE3. Consequently, there is increased splicing around CE3 leading to its inclusion and thus favours the generation of AR-V7 mature transcript compared to full-length AR (indicated by green tick and red cross respectively) (BioRender)*

1.6 Histone Demethylases in Prostate Cancer

As discussed above histone demethylases are one epigenetic 'erasers' which catalyse the removal of methyl groups from histones allowing them to either activate or silence genes depending on the site of the residue (Lemster et al., 2022). Histone demethylase fall into one of two categories; amino oxidase homolog lysine demethylases 1 (KDM1A and B) and Jumonji C (JmjC) domain-containing histone demethylases (KDM 2-6) (D'Oto et al., 2016). KDM1 family differs from the other histone demethylases in that it contains a flavin adenine nucleotide (FAD)- dependant enzyme amine oxidase that can remove mono and dimethyl histone marks, but not tri-methylation (Sainathan et al., 2015). During the chemical reactions, KDM1 utilises FAD as its cofactors to specifically demethylate H3K4 and H3K9. On the other hand, the rest of the histone demethylases contain a JmjC domain. These KMDs utilise α-ketoglutarate (α-KG), Fe (II), and molecular oxygen as cofactors in

the demethylation of mono-,di-, and tri-methyl lysine residues (an overview of all demethylases and their target residues can be found in table 2).

Despite KDMs 2-6 sharing the JmjC domain at their N terminal they still exhibit individual specificity to certain amino acid residues (i.e., KDM6A only demethylates at H3K27). This is achieved through specific differences in; active site architecture, helper domains and dimerization ability **(Figure 1.11A)** (Pilka et al., 2015). A single amino acid difference in the active site of KDM4A and KDM4D for example gives KDM4D the ability to demethylase tri- and di- methylated substrates whilst KMD4A has very weak/no activity of di-methylated substrates (Labbé et al., 2014). KDMs contain a wide variety of DNA and histone binding 'helper' domains. The Tudor domain for example is contained in KDM4A but not KDM4D, this creates different lysine binding preference between the KDM4 isoforms (Sterling et al., 2021). As mentioned above selectivity can be aided by KDM dimerization. KDM3A for example, which does not contain helper domains, can form homodimers between its Zinc binding and JmjC domain which is important for its site specificity function (Goda et al., 2013; Yamane et al., 2006a).

Whilst most JmjC domains execute their activity through demethylating lysine residues, there are a few which have been shown to demethylate arginine residues such as JMJD6 and PAD4(J. Zhang et al., 2019).

Subfamily		Domain Architecture	Substrate	Selectivity mechanism and residues involved
KDM2	2A		H3K36me2/me1	Active site architecture Residues F215, V220, G296
KDM3	3B		H3K9me2/me1	Dimersation Residues K1539, Q1650, A1701 Helper Zn-binding domain
KDM4	4A	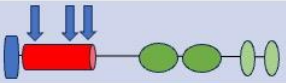	H3K9me3/me2 H3K36me3/me2 H1.4K26me3/m32	Active site architecture Residues F185, K241, S288 Helper Tudor domains
	4D	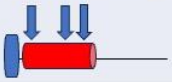	H3K9me3/me2 H1.4K26me3/me2	Active site architecture Residue F189, K245, A292 Dimerisation
KDM6	6A	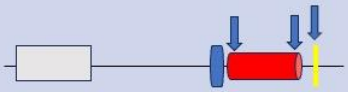	H3K27me3/2	Active site architecture Residues Q113, A1238 Helper Zn-binding domain
KDM7B	7B	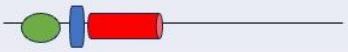	H3K9me2 H3K27me2 H4K20me1	Helper PHD domain Residue F250, V255, G331

Figure 1.11 Chromatin architecture and comparison of JmjC containing KDM family. *Blue arrows indicate residues and domains involved in mediating selectivity. Underlined residues indicate preference for a particular methylation state (Ser towards me3, discussed in text). JmjN, Jumonji N domain; JmjC, Jumonji C domain; Zf-C2HC4, zinc finger domain; GATAL, GATA-like domain; PHD, plant homeodomain; LRR, leucine-rich region; TPR, tetratricopeptide domain. (Figure and legend adapted from Pilka et al., 2015)*

The first histone demethylase KDM1A was described in 2004 (Shi et al., 2004). There is mounting evidence that histone demethylases are deregulated in a range of solid and haematological cancers including; breast, prostate, neuroblastomas and leukaemia (Duan et al., 2019; H. Lu et al., 2020a; G. Xie et al., 2017; S. Xue et al., 2020; J. Yang et al., 2015). KDM1A inhibitors have even reached clinical trials; with some reporting favourable outcomes (Salamero et al., 2021). Unfortunately to date, there are no clinical trials utilising compounds which target JMjC containing KDMs, this is likely due to the high similarity amongst the Jumanji domain which makes the development of potent and specific compounds very difficult. This demonstrates the unmet need to better understand the role of KDMs in cancer to allow for the development of compounds which may target downstream effects rather than the KDMs themselves. A brief overview of the known histone demethylases and their role in prostate cancer can be found in Table 2.

1.6.1 Histone demethylases in AR-V7 synthesis and generation

Constitutively active AR-Vs are a major mechanism of resistance to anti-androgens in PC. Whilst there a numerous known AR-Vs, AR-V7 is the best characterised. AR-V7 is generated through the aberrant mRNA splicing of exons 1-3, loss of exons 4-8, and inclusion of CE3 (Antonarakis et al., 2014b; Sharp et al., 2019). The resultant protein can evade all treatment options due to its exclusion of the LBD whilst demonstrating ligand-independent transcriptional activity (Y. Zhu & Luo, 2020). Due to AR-V7 still containing a functional DNA binding domain and N terminal domain (NTD), it can activate canonical AR targets plus a set of unique genes which allow the progression of cancer (Chan et al., 2012). Whilst targeting AR-V7 seems an attractive prospect for new clinical interventions, this is notoriously difficult as it contains a high degree of structural plasticity and intrinsic disorder (Mohler et al., 2021) . Due to this, looking at the role of histone demethylase in AR-V generation and functions could provide an alternative approach to therapeutically targeting AR-Vs.

Histone demethylases have been implicated in regulating alternative splicing (AS) of the full-length AR. Duan *et al* dissected the role of KDM4B, a H3K9me3 demethylase, in AR-FL splicing. They showed that KDM4B, like other KDMs was over-expressed in CRPC cell lines and metastatic patient tumours (Chianese et al., 2022; Lemster et al., 2022; Tomlins et al., 2007). Interestingly they showed that KDM4B increased splicing of AR-FL through both its catalytic function as an H3K9me3 demethylase and independently of this. As a H3K9me3 demethylase, KDM4B was found to remove heterochromatin-associated methylation marks proximal to CE3. Consequently, this increased the chromatin accessibility, enabling greater coupling of the spliceosome machinery around CE3 and subsequently increasing the inclusion of CE3. Independently of its catalytic function, KDM4B was shown to be highly phosphorylated under androgen-deprived conditions. This led to an increased interaction between KDM4B and SF3B3, a key splicing factor, which led to the KDM4B/SF3B complex binding to RNA sequences near the 5'-CE3, recruiting more components of the spliceosome and increasing its inclusion in mature RNA (Duan et al., 2019).The finding that KDM4B was more active in castrate conditions, akin to those found in patients undergoing ADT, is interesting and warrants further investigation as to exactly how ADT treatment causes a reprogramming of the epigenome.

Similarly, Fan et al., demonstrated that KDM3A, another H3K9me3 demethylase, acted independently of its catalytic activity to promote splicing of AR-FL to form AR-V7. Fan et al., showed that KDM3A interacts with HNRNPF, a splicing regulator. HNRNPF binds to G-tract sequences, for which there are 5 close to the 3' CE3. The group was able to demonstrate that HNRNPF bound to the G-tract sequence closest to the 3' CE3 which increased the inclusion of this exon and consequently increased the AR-V7 mature transcript (Fan et al., 2018). Knockdown of KDM3A in CW22Rv1 and LNCaP95 cells significantly reduces AR-V7 protein and mRNA levels.

A similar mechanism was described by Tong, in relation to JMJD6, a histone demethylase which targets H3R2 and H4R3. Tong showed JMJD6 expression positively correlated with AR-V7 in patient tumours and how JMJD6 is a strong regulator of the spliceosome through its interactions with U2AF65. Like histone demethylase enzymes discussed above, Tong demonstrated that JMJD6 could induce alternative splicing of the AR gene to generate AR-V7 by recruiting U2AF65 to the pre-mRNA (Tong, 2021). Again, under castrate conditions, U2AF65 has been shown to bind to the 3' end of CE3 increasing the inclusion of this CE (L. L. Liu et al., 2014; Z. Zhang et al., 2016). Work from Paschalis et al., provided more evidence that JMJD6 regulates AR-V7 expression through modulating recruitments of U2AF65 to the pre-mRNA splice site described above (Paschalis et al., 2021).

1.6.2 Histone Demethylases in epithelial to mesenchymal transition (EMT) and metastasis

EMT occurs in multiple cancer types and involves the transition of epithelial cells to cells with a mesenchymal phenotype. During this process, cells lose cell-cell adhesion junctions and apical-basal polarity. Consequently, solid tumours become more malignant having increased invasiveness and metastatic properties (Ribatti et al., 2020). Governing this process are changes in gene expression, primarily by reduction in expression of epithelial genes and an increase in expression of a mesenchymal gene signature. Given the fact histone demethylase can govern gene expression, it is rational to speculate that aberrant changes to demethylase enzymes can play a crucial role in the EMT process.

PC patients normally succumb to the disease through primary tumour metastasising to organs vital for survival, such as the lungs or liver (Nauseef & Henry,

2011). In addition to this, prostate cancer regularly spreads to bone; especially the pelvic bone which causes significant pain and reduces the quality of life for patients (Briganti et al., 2014). There is an urgent need to target the initiation and consequence of EMT. What follows next is a review of the current literature demonstrating an involvement of histone demethylase in EMT.

KDM1A is expressed in up to 94% of metastatic CRCP tumours which is significantly higher than in primary tumours (Sehrawat et al., 2018). As discussed above KDM1A is not a JmjC containing KDM. KMD1A is documented to demethylase specifically at H3K4me1 and H3K4me2 and in prostate cancer has been shown to be an AR co-activator (Crea et al., 2012; D'Oto et al., 2016). KDM1A inhibition is effective in reducing the invasive capabilities of prostate cancer cell lines (Chen et al., 2016). Chen et al., demonstrated that inhibition of KDM1A leads to a significant reduction of invasive cell numbers compared to mock controls. Mechanistically, these changes were caused by both decreased expression of TGF-β1 and its substrate Smad2/3 following inhibition of KDM1A. TGF-β1 has been shown to increase PC metastases in other studies (Fournier et al., 2015; Shiota et al., 2021). Interestingly in this study, KDM1A was also shown to negatively regulate the expression of E-Cadherin which fits with other literature (M. Wang et al., 2015). Loss of E-cadherin is considered a hallmark of EMT and tumour cell invasion.

Members of the KDM5 family have been implicated in causing metastases in PC. KDM5B expression was interrogated in datasets by Xiang et al. and was shown to be highly expressed in metastatic tissue compared to healthy prostate (Xiang et al., 2007). In other cancer types, high KDM5B expression has been shown to modulate H3K4me3 levels at the PTEN promoter and inactivating its transcription. Consequently, this affected pathways such as PI3K/ATK which reduced the invasive phenotype of cells (B. Tang et al., 2015; Z. Wang et al., 2015).

KDM5D has been shown to repress invasion-associated genes in PC; *MMP1, MMP2, MMP3* and *MMP7* by removing the active histone mark H3K4me3. Unlike previously discussed demethylases, Li et al., demonstrated that compared to normal tissue the levels of KDM5D were reduced in metastatic samples(Li et al., 2016). This suggests that during PC progression there is an epigenome reprogramming which allows for a more promiscuous cell type able to migrate more readily. Clinically, one could propose the idea

of routinely assessing histone demethylase as prognostic markers for tumours with more metastatic phenotype i.e., $KDM5D^{-}/KDM6A^{+}$.

KDM4C has been reported to regulate metastases of PC cells via its interactions with c-MYC. Lin et al., demonstrated how attenuating KDM4C function, via either CRISPR knockout or therapeutic inhibition with SD70, the MYC pathway was the most significantly decreased. Consequently, MYC target genes, including those involved with EMT, were significantly reduced. The group showed through chromatin immune precipitation (ChIP) assays that KDM4C directly binds to the *MYC* promoter and that low levels of KDM4C reduced *MYC* expression. This suggests that at least in this setting, the demethylase activity of KDM4C regulates MYC target genes (Lin et al., 2022). This interaction between KDM4C and MYC has also been demonstrated in other cancer types (Lee et al., 2021).

1.6.3 Histone demethylases in prostate cancer metabolomics

During the transition to CRPC, prostate cancer cells undergo wide-scale metabolic changes to survive the nutritional stain and hypoxic conditions during both disease progression and therapy and these changes have been recently reviewed in depth by Beier *et al (Beier et al., 2022)*. Altered metabolism is also a hallmark of cancer and, according to the latest Prostate Cancer Foundation scientific retreat report, tumour metabolomics remains a primary area of research (Miyahira & Soule, 2022). Notably, there have been a number of clinical trials investigating the use of metabolomics in the treatment/diagnosis of CRPC (Qu et al., 2021; Sardesai et al., 2021; Stein et al., 2010). A review of the literature on the role that histone demethylase plays in altering tumour metabolomics to evade current treatment options is provided below.

The role of KDM4B in metabolic changes in CRPC was recently investigated by Wu et al. They demonstrated that KDM4B had a demethylase-dependent role in causing metabolic changes in the development of CRPC. Firstly, they showed that following KDM4B knockdown, there was significantly reduced expression of genes involved in glycolysis and pyruvate metabolism, supporting the idea that KDM4B is involved in the regulation of glycolysis in cancer cells (Li et al., 2020; Qiu et al., 2021). Wu et al., next showed that some of these metabolic changes were orchestrated through KMD4A interactions with c-MYC and co-regulating c-Myc target genes (Wu et al., 2021). KDM4B has been shown previously to interact with c-MYC (D. E. Tang et al., 2020; J. Yang et al., 2015), and the H3K4me3 demethylase activity of KDM4B was essential for the effect on MYC-driven gene expression. Indeed, when KDM4B was knocked out there was an accumulation of H3K9me3 marks at metabolism-related genes (*LDHA*, *ENO1*, and *PFK*) resulting in reduced expression. In conclusion, KDM4B inhibition reduces the expression of metabolism-related genes regulated by c-MYC and this is due to a more compact, H3K9me-enriched chromatin environment following KDM4B inhibition.

Other members of the KDM4 family have also been implicated in metabolic changes resulting in aggressive prostate cancer phenotype. KDM4C inhibition was recently shown to significantly reduce the expression of metabolic genes; especially those involved in; glycolysis, TCA and oxidative phosphorylation (Lin et al., 2022). Interestingly the authors demonstrated, through ChIP, that like other members of the KDM4 family, KDM4C

directly binds to MYC promoter. By inhibiting KDM4C, they showed that 54% of MYC activity decreased and it was because of this that those genes involved in the processes mentioned above we reduced.

From the evidence of this strong KDM4/MYC interaction, it is rational to propose the idea of targeting KDM4 to disrupt MYC target gene activity. This may be beneficial considering the "undruggable" nature of MYC itself (Llombart & Mansour, 2022). Alongside this, the fact that KDM4s are significantly upregulated in CRPC and have a targetable enzymatical domain suggests further development of specific inhibitors would have wide benefits.

Sarac et al., identified from an shRNA screen that the KDM3 family were important regulators of CRPC (Sarac et al., 2020). The shRNA screen targeted several epigenetic modifiers, including many of those discussed previously in this review, from a CRPC cell line LNCaP-abi which is a derivative of the LNCaP cell line that is resistant to abiraterone. Sarac et al., showed that inhibition of KDM3B leads to the most significant reduction in proliferation. The group demonstrated, through rescue experiments, that catalytically active KDM3B was required to restore the reduced proliferation following shKDM3B.

Inhibition of KDM3B led to a significant reduction in metabolic gene expression including *ARG2* and *RDH11*. Strikingly, gene set enrichment analysis (GSEA) of RNA sequencing data demonstrated a significant reduction in xenobiotic metabolism and oxidative phosphorylation following KDM3B KD. In keeping with KDM3B in PC, the other members of the KDM3 family have been shown to regulate metabolism in other cancer types including bladder (Wan et al., 2017) and leukaemia (Lynch et al., 2019) .

In summary, the current evidence shows that KDMs show differential expression in CRPC. Also, the data demonstrates that KDMs are involved in CRPC through both catalytically- dependent and -independent functions. This suggests that future drug targeting may need to be based on more than just inhibiting the catalytic domains of KDMs and that perhaps PROTACS, for example, maybe a more robust therapeutic option. Given the lack of options for men with advanced disease, targeting KDM activity may provide a novel option in preventing some of the resistance mechanisms to ADT.

Table 4. Histone demethylase and their roles in Prostate Cancer Progression

KDM	Alias	Target lysine	Role in CRPC
KDM1A	LSD1, AOF2, KIAA0601	H3K4me2/me1, H3K9me2/me1	• Increases invasiveness (Sehrawat et al., 2018; M. Wang et al., 2015)
KDM1B	LSD2, AOF1, C6orf193	H3K4me2/me1	• Recruits AR to gene promoters, and confers enzalutamide resistance (D. Tang et al., 2022)
KDM2B	CXXC2, FBL10, FBLX10,	H3K4me3, H3K36me2	• Cell adhesion, migration and invasion (Su et al., 2019; Zacharopoulou et al., 2018)
KDM3B	JMJD1B, JHDM2B	H3K9me2/me1	Metabolic changes (Sarac et al., 2020)
KDM3C	JMJD1C, JHDM2C	H3K9me2/me1	• AR-negative PC sensitive to KDM3C inhibition (Yoshihama et al., 2021)
KDM4A	JMJD2A, JHDM3A	H3K9me3/me2, H3K36me3/me2, H3K23me3	• Acts on MYC to drive PC proliferation (Cui et al., 2020) • Activates Hippo-Yap pathway in PC (Mu et al., 2019)
KDM4B	JMJD2B, JHDM3B	H3K9me3/me2, H3K36me3/me2, H3K23me3	• C-MYC activator to drive metabolic changes (Wu et al., 2021) • Induces autophagy to increase CRPC cell proliferation • Promotes splicing of AR to generate AR-V7 in castrate conditions (Duan et al., 2022)
KDM4C	JMJD2C, JHDM3C	H3K9me3/me2, H3K36me3/me2	• Activates ATK and MYC increasing growth and glycolysis (Lin et al., 2019, 2022) • AR co-activator (Wissmann et al., 2007)
KDM4D	JMJD2D	H3K9me3/me2	• AR coactivator (Shin & Janknecht, 2007)
KDM5A	JARID1A, RBBP2	H3K4me3/me2	• Actives PI3K/AKT pathways increasing proliferation and migration(Du et al., 2020)n
KDM5B	JARID1B	H3K4me3/me2	• Hyperactivates PI3K/ATK pathway (G. Li et al., 2020) • AR coregulator (Xiang et al., 2007)
KDM5C	JARID1C	H3K4me3/me2	• Promotes EMT (Lemster et al., 2022) • Suppresses TGFβ signalling (Kim et al., 2008)

			• Overexpression represses PTEN (Z. Hong et al., 2019)
KDM6A	UTX	H3K27me3/2	• Prostate cancer metabolism (Chianese, et al., 2022; D. E. Tang et al., 2021)
KDM6B	JMJD3	H3K27me3/me2	• Overexpressed in metastatic disease (Xiang, et al., 2007) • Promotes CyclinD1 transcription (Cao et al., 2021) • Involved in EMT(S. H. Lee et al., 2021)
KDM7A	JHDM1D, KDM7, KIAA1718	H3K9me2/me1, H3K27me2/me1, H4K20me1	• Upregulated in CRPC, AR regulator (K. Lee et al., 2018)
KDM7B	PHF8	H3K9me2/me1, H3K27me2/me1, H4K20me1	• Overexpressed, increases invasiveness (Bjorkman et al., 2012) • Activates FOXA2 to drive NEPC (Q. Liu et al., 2021)
KDM8	JMJD5	H3K36me2	• AR activator and increases glycolysis (H. J. Wang et al., 2019)

1.7 KDM6A

1.7.1 Structure of KDM6A

KDM6A, or UTX, is located on the X chromosome location Xp11.3 and compromises 29 exons resulting in a protein of around 155kDa. KDM6A contains 6 tetratricopeptide repeats in its N-terminal domain and a Jumonji C domain at its C terminus **(Figure 12A, B)** (Tran et al., 2020) . KDM6A catalyses the removal of methylation groups from lysine 27 of histone 3 (H3K27). The methylation of lysine residues can have opposing roles on transcriptional competency; both activation or repression of a gene in a context-specific manner. This is because methylation, unlike acetylation for example, does not alter histone charge or directly impact histone-DNA interactions (Yan, 2023). Instead, histone methylation acts a molecular beacon to attract transcriptional regulators which can then directly or indirectly alter transcriptional state of a genetic locus. It should be noted that methylation of histone 3 at lysine 27 is regarded as a repressive modification and thus, KDM6A demethylation activity generally leads to gene activation (Gažová et al., 2019). Essentially, histone modifications differ between cell types and can be altered by, for example, environmental factors, when this is read by transcriptional machinery it alters

the expression of genes adding complexity to the genome. This is the basis of the 'histone code' hypothesis (Paro, 2021).

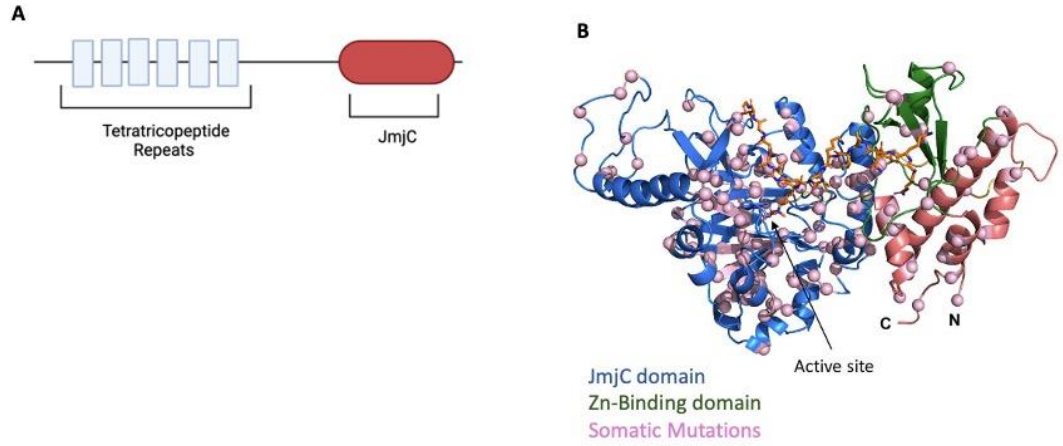

Figure 1.12 Structure of KDM6A and its role in chromatin architecture. A) *Important domains of the KDM6A protein are shown in a schematic. From left to right, the tetratricopeptide domain is essential for protein-protein interactions which are suggested to be essential for KDM6A to have scaffolding, demethylase-independent, functions. The JmjC domain acts as a catalyst to allow the removal of methyl groups from H3K27 in a 2-oxoglutarate and iron-dependent reaction.* ***B)*** *The protein structure of KDM6A generated by the MODDELLER programme shows its distinct domains. Pink dots represent the most common somatic mutations of KDM6A found in pan-cancer studies (Figure from Chi et al; 2022).*

1.7.2 Regulation of KDM6A Expression and Activity

As with all JmjC domain containing KDMs, KDM6A requires ferrous iron Fe(II), α-ketoglutarate (α-KG/2-OG) and oxygen as cofactors and because of this, the activity of KDM6A is regulated through metabolic reactions and hypoxia (Hua et al., 2021a; Sengoku & Yokoyama, 2011). α-KG is an intermediate of the TCA cycle and gain of function mutations to enzymes involved in the TCA such as IDH1/2, produce oncometabolites like D-2-hydroxyglutarate (D-2HG). D-2HG is a competitive inhibitor of α-KG dependent dioxygenases, including KDM6A, and consequently these gain of function mutations observed in IDH1/2 lead to altered histone methylation patterns and contributing to cancer progression (Chang et al., 2019a; Hua et al., 2021a). In addition, the hypoxic conditions which are observed in tumour microenvironments and the core of solid tumours alter KDM6A activity (Kim et al., 2022). During hypoxia, changes in metabolism, including the transition from oxidative phosphorylation to glycolysis which consequently results in reduced levels of α-KG and accumulation in levels of 2-HG thus reducing the activity of α-KG dependant KDM6A (Hua et al., 2021a). Because of this reduced activity, expression levels of KDMs are often elevated to compensate (Kim et al., 2022). The reduced availability of oxygen, which is required for the removal of methyl groups, also reduces KDM6A activity. Work by Chakraborty et al demonstrated KMD6A to be a direct oxygen sensors whereby hypoxic conditions reduced KDM6A activity, leading to increased histone H3K27 methylation and thus effecting gene expression (Chakraborty et al., 2019). Integral to all of this is the Hypoxia-inducible factor (HIF) proteins. HIF-1α can directly regulate the expression of KDM6A by binding to hypoxia-responsive elements (HREs) in the KDM6A promoter region. Under hypoxic conditions, the stabilisation of HIF-1α leads to the upregulation of KDM6A expression in certain cellular contexts (Chakraborty et al., 2019; Gallipoli & Huntly, 2019). HIF-1α is also responsible for the enhanced production of 2-HG by regulating the metabolic shift to glycolysis which upregulates IDH1/2 enzymes thus causing higher levels of 2-HG (Hua et al., 2021a; Kim et al., 2022).

1.7.3 Function of KDM6A

The JmjC domain of KDM6A interacts with methylated lysine 27 of the H3 tail. Once bound, KDM6A acts as a catalyst for oxidative decarboxylation of 2-oxoglutarate **(Figure 1.13a).** This process results in carbon dioxide and succinate resulting in the hydroxylation of the methyl group on the lysine residue. This creates an unstable intermediate which decays, leaving the lysine residue with one less methyl group (Dong et al., 2014; Markolovic et al., 2016). For this process to occur, Fe2+ must be present as it is crucial in the initial oxidative decarboxylation step, mutations in the Fe binding motif of KDM6A can lead to complete loss of enzymatic activity (Lee et al., 2007).

A significant point to discuss, which will become evident from data in this thesis, is that KMD6A can function independently of its enzymatic activity **(Figure 1.13 b and c).** This has been demonstrated in differentiation studies of embryonic stem cells whereby cells with catalytically inactive KDM6A still showed normal differentiation capacities (Wang et al., 2012). This was also further validated in KDM6A knockout cells which were able to regain a normal phenotype when expression was rescued with a catalytically inactive KDM6A (Morales Torres et al., 2013). Studies have demonstrated that KDM6A may adopt a role structurally, acting as a "scaffold protein", through protein-protein interactions with the tetratricopeptide repeats it contains in its N-terminal (Gozdecka et al., 2018)). Koch et al., highlights how KDM6A interacts with components of the SWI/SNF chromatin remodelling complex, specifically CBP/P300 (an H3K27 acetyltransferase), to activate the promoter activity and drive transcription of genes regulated by the complex **(Figure 1.13C)** (Koch et al., 2021)**.** In addition to this, KMD6A forms part of the MLL3/4 or 'COMPASS' complex which can activate the transcription of a specific set of genes. As shown in **Figure 1.13B**, the assembly of the COMPASS complex coordinates the activation of specific response elements, in this case, retinoic acid response elements (RAREs). It should be noted, however, that KDM6A has also been known to interact with other DNA-binding transcript factors including nuclear hormone receptors (AR and ER), and the peroxisome proliferator-activated receptors driving activation of their response elements (Chen et al., 2023; Schulz et al., 2019). In essence, independent of its demethylase activity, KDM6A can convert inactive enhancers to active ones by recruiting MLL4 and p300

proteins to the regions. In the context of this thesis, it is important to consider KMD6A playing a scaffolding role in recruiting splicing factors to cryptic exon 3.

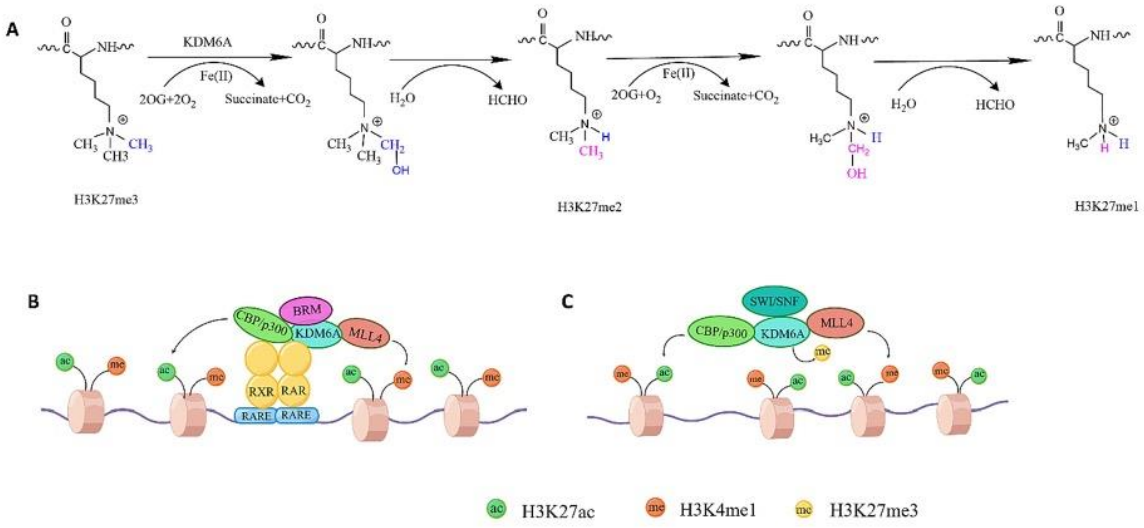

Figure 1.13 KDM6A Catalytic and Catalytic independent function. A) *The catalytic mechanism whereby KDM6A can remove methyl groups at H3K27. Blue indicates the first methyl group removal whilst the second methyl groups to be removed are in pink. This reaction is Fe^{2+} dependent to allow KMD6A to catalyse the oxidative decarboxylation of 20G.* ***B)*** *KDM6A mediated enhancer activation by recruiting MLL and CBP to manipulate the chromatin architecture, causing the activation of specific response elements.* ***C)*** *Promoter activation regulated by KMD6A. KDM6A recruits SWI/SNF complex to promoters as well as interacting directly with RNAPol II to allow for the transcription of SWI/SNF complex target genes (Figure taken from Chen., et al, 2023).*

1.7.4 Role of KDM6A in cancers, friend, or foe?

KDM6A is widely mutated in a range of cancer types, both haematological as well as solid tumours. The MSKCC-IMPACT study, which utilised over 10,000 tumour samples from a range of malignancies, reported that *KDM6A* was mutated in 3.5% of cases with most of those being truncating mutations followed by missense mutation and in-frame indels (Zehir et al., 2017). This mutational rate of ~3% holds true if you interrogate the other publicly available pan-cancer studies of both primary (Weinstein et al., 2013) metastatic tumours (Robinson et al., 2017). Mutational analysis of these pan-cancer studies also reveals that amplification of *KDM6A* is another common mutation, suggesting that KDM6A may also have a potential gain-of-function (Cerami et al., 2012; Schulz et al., 2019). Around 40% of urothelial carcinomas have been reported to harbour *KDM6A* mutations whilst other cancers such as thyroid, medulloblastoma and acute myeloid leukaemia

(AML) have very low/no mutations to the gene (Cerami et al., 2012). As will be shown in more detail later in this thesis, in the case of prostate cancers, around 3% of primary samples have a *KDM6A* mutation whilst this figure increases to ~15% in metastatic, treated, samples. Although there seems to be a good rationale for KDM6A to be a target of interest, as yet it has not been used as a direct target in clinical trials. That said, *KDM6A* genetic alterations (loss, amplification and indels) are used as an inclusion criterion for several trials from a range of cancer types (Holt et al., 2021).

The complexity of KDM6A in cancer considerable with several reports providing conflicting data (summarised in Table 3). In some contexts, KDM6A acts as a tumour suppressor whilst in other cases it has pro-oncogenic effects. KDM6A KO mice have a higher propensity to developing bladder, lung and myeloid leukaemia; suggesti(Gozdecka et al., 2018; Kaneko & Li, 2018)(Gozdecka et al., 2018; Kaneko & Li, 2018). These studies provided evidence that loss of KDM6A led to: i) reduced antagonism of EZH2 (an H3K27 methyltransferase) transcriptional repression; ii) reduced expression of tumour suppressor genes; and (iii) lower expression of cell cycle inhibitors. It should be noted that in the context of prostate cancer, there is no evidence of KMD6A playing a tumour suppressor role. In addition to this, most studies discussed above, have assessed KDM6A in the context of directly affecting gene activation. As mentioned in earlier chapters, there are many more roles to KDM6A than this therefore the work of this thesis may provide a novel insight to KMD6A in PC.

In contrast, many studies have demonstrated KMD6A to have pro-oncogenic roles. KDM6A overexpression has been shown to enhance the proliferation and migration of ER+ breast cancer cell lines as well as indicate a worse overall survival in breast cancer patients (Paolicchi et al., 2013; G. Xie et al., 2017). This occurs by KDM6A and ER colocalising on specific ER-target genes and facilitating ER activity. Furthermore, colorectal cancer studies have demonstrated a negative correlation between KDM6A expression and overall survival, supporting the rationale that targeting KMD6A may be beneficial in these patients (J. Zhang et al., 2020). In addition to breast and colorectal cancers, inhibition of KDM6A in Gliomas and neuroblastoma has been shown to have an anti-tumour effect, supporting the pro-oncogenic role in these settings (Hashizume et al., 2014; Romani et al., 2019).

In terms of PC it is shown that KDM6A has solely a pro-oncogenic. KDM6A appears significantly important in CRPC metabolomics. Recently, Chianese et al., described how

coupled inhibition of KMD6A and KDM1A, using the dual inhibitor MC3324, leads to the reprogramming of PC metabolism by downregulating glycolysis and lipolysis enzymes (Chianese et al., 2022). The group concluded that ATP production was attenuated by key glycolysis-associated genes, such as *GLUT1*, becoming inactivated following KDM6A/1A inhibition and consequently CRPC cell line growth was significantly reduced. Additional data from ChIP experiments would have been useful to demonstrate methylation changes in H3K4me2 and H3K27me3 at affected genes following KDM1A/6A inhibition.

In addition to the role of disrupting ATP production, Chianese et al., demonstrated that KDM6A inhibition reduced fatty acid metabolism and adipogenesis. Consequently, they established that dual KDM6A/KDM1A inhibition induced metabolic plasticity in lipid acquisition. Altogether, their results suggest that inhibition of the two HDMs with MC3324 warrants further investigation *in vivo* due to the wide-scale effect KDM6A/KDM1A has on PC cell metabolomics.

Similarly, KDM6A was shown to regulate fatty acid synthesis in PC cell lines (Tang et al., 2021). Tang et al., demonstrate that KMD6A regulates expression of *SREBP1c*, a gene essential for glucose utilisation as well as fatty acid synthesis (Ferre & Foufelle, 2007) Interestingly, the same study demonstrated that the demethylation of H3K27me3 by KDM6A at the promoter of *SPEB1c* was required for it to become transcriptionally active. The group highlighted how inhibition of KDM6A with GSK-J4 (a prodrug of GSK-J1) significantly reduces tumour size *in vivo* of CW22Rv1 xenografts compared to controls. They concluded that GSK-J4 treatment inhibited SREBP1 protein expression and suppressed prostate tumorigenesis.

Interestingly, high KDM6A demethylase activity has been found in posterior fossa A ependymomas; a tumour which requires hypoxic conditions, high levels of glycolysis and polyamine metabolism, conditions like those seen in CRPC tumours (Michealraj et al., 2020).

As well as affecting metabolomics, studies have suggested that KDM6A is essential for AR activity. KMD6A is shown to be over-expressed in models of CRPC and could be inhibited with the GSK-J4 compound which binds to the catalytic pocket of KDM6A preventing its demethylase activity. The authors hypothesised that GSK-J4 treatment caused stabilisation of methylation marks at androgen response elements and thus hindered AR-driven transcription (Morozov et al., 2017). This is a plausible hypothesis

considering the data from Grasso et al., which showed KDM6A, and other components of the COMPASS complex, were significantly overexpressed in CRPC and interacted directly with AR to impact its signalling (Grasso et al., 2012).

Table 5. Role of KDM6A in cancers where it is commonly mutated according to Pan cancer studies.

Cancer Type	Role	Effect of KDM6A
Bladder	Suppressor	• Loss of KDM6A alters differentiation giving rise to tumour-initiating cells(Lang et al., 2020) • Loss of KDM6A leads to activation of proliferation genes (Ler et al., 2017)
Pancreatic	Suppressor	• Loss of KDM6A caused inactivation of tumour suppressor genes (Watanabe et al., 2019) • Loss of KDM6A upregulated epithelial-mesenchymal pathways (Yi et al., 2022)
Lung	Suppressor	• KDM6A interacts with KMT2B to activate the Wnt/b-catenin/c-MYC pathway driving progression (Leng et al., 2020) • KDM6A loss downregulated tumour suppressor and cell cycle inhibitors (X. Lu et al., 2018)
Prostate	Pro-oncogenic	• Maintains AR activity in castrate conditions (Morozov et al., 2017) • KDM6A inhibition down regulated AR activity and affects metabolic reprogramming in CRPC

		progression (Chianese et al., 2022)
Breast	Pro-oncogenic and Suppressor	• KDM6A inhibits EMT and proliferation (Choi et al., 2015; W. Yu et al., 2019) • KDM6A promotes stemness of cancer cells (Lan et al., 2022; H. Lu et al., 2020b)

2. Project Aims

The aims of this project were to:

1. Better understand the role of epigenetic enzymes, specifically histone demethylase, in the development of CRPC with a focus of AR-V splicing
2. Validate KDM6A as a therapeutic target in CRPC and deepen our knowledge in mechanisms by which KDM6A drives CRPC.

By completing these aims, the work of this PhD will provide a comprehensive insight into the role of histone demethylase in CRPC. In addition, this work will evaluate if inhibition of KDM6A offers further therapeutic potential and determine if it would be a promising candidate in further drug development pipelines. As mentioned in the introduction, up to 20% of patients will progress to CRPC for which there are no curative treatments and thus there is currently an unmet clinical need.

3. General Materials and Methods

3.1 Cell lines and Cell culture Reagents

All cell lines were maintained in 5% CO_2 at 37°C. 10% foetal bovine serum (FBS) (Thermo A5256701) and penicillin-streptomycin (Sigma P0781) were added to culture media. Cells were tested quarterly for mycoplasma contamination. Cells were passaged using trypsin-EDTA solution (Sigma T4174) according to standard protocols for adherent cell lines. Specific media conditions for all cell lines used are listed in **Table 1** Unless specified, all experiments were performed in media conditions listed above. For steroid depletion experiments, FBS was substituted for dextran-coated charcoal stripped FBS (VWR S181F-500). Enzalutamide (Selleckchem S1250) was dissolved in DMSO (Sigma D5879) and used at a final concentration of 10 µM.

Table 6 Cell lines and their corresponding media compositions.

Cell line	Media
CW22Rv1	RPMI-1640 (Sigma R87585)
LNCAP Parental	RPMI-1640 (Sigma R87585)
LNCAP 95	RPMI-160 Phenol Free (R8755)
VCaP	DMEM (Sigma D6171) supplemented with 2mM L-Glutamine (Sigma G7513)
PNT1A	RPMI-1640 (Sigma R87585)
R1-AD1	RPMI-1640 (Sigma R87585)
R1-D567	RPMI-1640 (Sigma R87585)

3.2 Protein Harvest and Western Blotting

Experiments performed in 6-well plates were lysed and harvested in 120 µl SDS sample buffer mixed 9:1 with β-mercaptoethanol (Sigma M3148). Lysates were boiled at 100°C for 10 minutes, before SDS-PAGE was performed by use of a stacking gel cast above a 10% acrylamide resolving gel. Samples were run alongside SpectraTM Multicolor Broad Range Protein Ladder (Thermo 26623). Proteins were transferred for 1 hour at 100 V or overnight at 30V in transfer buffer onto AmershamTM Protran® nitrocellulose membrane (Sigma GE10600016). All steps were performed using a Mini-PROTEAN® electrophoresis and blotting system (Bio-Rad 1658029). Solutions used for PAGE can be found in **Table 2**

Table 7 Western blot buffer composition

Solution	Composition
SDS sample buffer	125 mM Tris-HCl, pH6.8 5% SDS 10% glycerol 10% β-mercaptoethanol 0.01% bromophenol blue
10% resolving gel	Acrylamide (30%) - 3.33 ml diH_2O - 1.67 ml 5ml 2X Buffer A (750 mM Tris-HCl, pH 8.8, 0.2% SDS) N,N,N',N'-tetramethylethane1,2-diamine (TEMED) - 20 µl Ammonium persulphate (APS) (10%) - 100 µl
Stacking gel	Acrylamide (30%) - 840 µl diH_2O - 1.67 ml 2.5 ml 2X Buffer B (250 mM Tris-HCl, pH 6.8, 0.2% SDS) TEMED - 5 µl APS (10%) - 50 µl
Running buffer	25 mM Tris, 190 mM glycine, 0.1% SDS
Transfer buffer	25 mM Tris-HCl, pH8.3, 150 mM glycine, 10% methanol
TBS	500 mM NaCl, 200 mM Tris-HCl, pH 7.5
TBST	500mM NaCl, 200 mM Tris-HCl, pH 7.5, 0.001% Tween-20
Ponceau Stain	0.1% Ponceau in 5% Acetic acid

Transfers were stained using Ponceau S solution (Sigma P7170) where indicated in figures. Briefly, membranes were incubated with Ponceau for 5 minutes at room temperature with agitation. Membranes were imaged and Ponceau was distained by washing membranes with with 0.1 M NaOH (Sigma S5881) for 1 minute at room temperature. Membranes were blocked with 5% (w/v) non-fat milk (Marvel)/TBS (500 mM NaCl (Sigma S9888)), 20 mM Tris-HCl (pH 7.5)) for 1 hour at room temperature, before overnight incubation at 4°C in primary antibody diluted in 1% (w/v) non-fat milk/TBST (TBS + 0.1% Tween 20 (Sigma P1279). Primary antibodies used for western blot are listed in **Table 3.** Membranes were then washed for 3 x 5 minutes in TBST and incubated for 1 hour at room temperature in 1:4,000 goat-anti mouse (Bethyl A90- 516P) or swine anti-rabbit (Bethyl A120-501P) HRP-conjugated secondary antibody diluted in 1% (w/v) non-fat milk/TBST. Membranes were washed again for 3 x 5 minutes in TBST, before signal was developed

using ClarityTM Western ECL Substrate (Bio-Rad 1705061) and imaged using a ChemiDocTM system (Bio-Rad).

Table 8 Antibodies Used for western blot

Antibody	Species	Supplier/catalogue no	Dilution
AR NTD	Mouse	Santa Cruz/sc-7392	1:1,000
AR-V7	Rabbit	RevMAb/31-1109-00	1:1,000
KDM6A	Rabbit	Cell Signalling/ 33510S	1:1,000
H3K27me3	Rabbit	Abcam/ab192985	1:1,000
a-tubulin	Mouse	Sigma/T9026	1:4,000
Flag	Mouse	Sigma/F3165	1:1,000

3.3 RNA Extraction and RT-qPCR

RNA was extracted using the GenElute mammalian total RNA miniprep kit (Sigma RTN350), manufacturer instruction for RNA exttractions from 'Attached Cell cultures' were followed. Concentration and purity of extracted RNA was measured using the NanoDrop ND-100 (Thermo) spectrophotometer.

To remove genomic DNA from RNA preparations, RNA was treated with DNase prior to reverse transcription using DNase I (Thermo EN0521). 1µg RNA was combined with 1µl 10X reaction buffer, 1µl DNase I-RNase-free and DEPC-treated water (Thermo R06061) to a total volume of 10µl. This was incubated at 37^{o}C for 30 minutes. 1µl of 50mM EDTA was then added to the RNA and incubated at 65^{o}C for 10 minutes to inactivate the DNase, the EDTA prevents hydrolysis of the RNA during the heating process. The RNA is them ready to be used as a templated for reverse transcription.

cDNA was generated by reverse transcription of RNA in a 20 µl reaction consisting of 4 µl 5x MMLV-RT buffer (Promega M531A), 2 µl 4mM dNTP mixture (Bioline BIO-39044), 1 µl 100 µg/ml oligo(dT)$_{15}$ (Promega C1101), 1 µl 100 µg/ml random primers (Promega C1181), 0.3 µl MMLV-reverse transcriptase (Promega M170A), and 500 ng - 1 µg RNA + nuclease-free water (Thermo 10977) to a final volume of 20 µl. Reverse transcription reactions were performed for 1 hour at 37°C, before incubation at 100°C for 10 minutes. Resulting cDNA products were then diluted 1:5 - 1:10 in nuclease-free water.

qPCR analysis of cDNA was performed using 384-well plates on a QuantStudioTM 7 Flex Real- Time PCR System (Thermo 4485701). 10 µl reactions were analysed consisting of 5 µl 2x SYBRTM Green PCR Master Mix (Thermo 4309155) or 2x PowerTrackTM SYBR Green Master Mix (Thermo A46113), 0.4 µl of each of forward and reverse 25 ng/µl primer, 2.2 µl nuclease-free water and 2 µl cDNA. Comparative CT method was used to determine the relative gene expression in unknown samples. These were then directly compared using the equation below where [delta] Ct, sample and [delta] Ct, reference is the Ct value of the sample of interest and the control or untreated sample, respectively. RPL13A was used as a house keeping gene for normalisation. Primers used for qPCR analysis are listed in **Table 9.**

$$[delta][delta]Ct = [delta]Ct,sample - [delta]Ct,reference$$

Table 9 PCR Primer Sequences

Target Gene	Forward Primer Sequence	Reverse Primer Sequence
RPL13A	CCTGGAGGAGAAGAGGAAAGAGA	TTGAGGACCTCTGTGTATTTGTCAA
AR-FL	AACAGAAGTACCTGTGCGCC	TTCAGATTACCAAGTTTCTTCAG
AR-V7	AACAGAAGTACCTGTGCGCC	TCAGGGTCTGGTCATTTTGA
AR-V1	AACAGAAGTACCTGTGCGCC	TGAGACTCCAAACACCCTCA
AR-V9	AACAGAAGTACCTGTGCGCC	GCAAATGTCTCCAAAAAGCAGC
KDM6A	AGCGCAAAGGAGCCGTGGAAAA	GTCGTTCACCATTAGGACCTGC
PSA	CCTCACAGCTGCCCACTGCA	GATGAAACAGGCTGTGCCG
TMPRSS2	CTGCTGGATTTCCGGGTG	TTCTGAGGTCTTCCCTTTCTCCT

3.4 Bacterial transformation, Plasmid DNA isolation and gel electrophoresis

3.4.1 Bacterial Transformation

100-500ng of plasmid DNA was added to 50µl of NEB heat stable DH5-A (NEB C2987H) or Thermofisher Stbl3 (Thermofisher C737303) compenent cells. Cells wereleft to recover on ice for 30 minutes prior to 40 second heat-shock (42 °C), and then returned to ice for a further recovery of 30 minutes. Post-recovery, 350 µl of SOC outgrowth media (NEB) was added and cells were transferred to a 37 °C incubator, with shaking for 1 hour. Bacterial cells were then pelleted (3,000rcf, 5 minutes), 300 µl of supernatant removed, and pellet resuspended in the remaining 100 µl. 50 µl ofthe resuspension was then spread onto LB agar plates containing appropriate antibiotic (1% (w/v) NaCl, 1% (w/v) tryptone, 0.5 % (w/v) yeast extract, 1.5 % (w/v) agar and 100 µg/ml ampicillin). Plates were incubated for 16 hours overnight at 37 °C to allow for colony growth.

3.4.2 Recovery of cells from glycerol stock

If plasmid arrived as a glycerol stock or bacterial slab, a sterile P200 pipette tip was dipped into the cells. The tip was then gently swabbed across LB agar plates containing appropriate antibiotic (1% (w/v) NaCl, 1% (w/v) tryptone, 0.5 % (w/v) yeast extract, 1.5 % (w/v) agar and 100 µg/ml ampicillin). Plates were incubated for 16 hours overnight at 37 °C to allow for colony growth.

3.4.3 Culture of bacterial colonies

Colonies from LB Agar plates were selected at random and used to inoculate 5 ml of LB media (1% (w/v) NaCl, 1% (w/v) tryptone, 0.5% (w/v) yeast extract) and relevant antibiotic for positive selection. 5 ml culture were propagated overnight in a 37 °C incubator with rotation (220 rpm).

For plasmids with previously confirmed sequences, larger cultures of 200ml were set up and subjected to maxiprep DNA extraction. 5 ml starter cultures containing relevant antibiotic, were set up as described above, and incubated for 8 hours (37 °C and rotation 220 rpm). Following propagation of 5 ml colonies, 1 ml of the 5 ml starter was used to inoculate 200 ml of fresh LB media, again, containing the relevant antibiotic. 200 ml cultures were incubated (37 °C with rotation 220 rpm) overnight in an incubator.

3.4.3 Isolating plasmid DNA

GenElute™ Plasmid Miniprep Kit (sigma) was used to extract plasmid DNA from small 5 ml cultures in accordance with the manufacturers protocol. For larger 200 ml cultures the PureLink® HiPure Plasmid Filter Maxiprep Kit (Life Sciences, Invitrogen) was used, according to manufacturer's protocol. Briefly both protocols pelleted bacterial cells, before lysis in an alkaline buffer and neutralisation. Resultant cell debris was filtered from the solution before DNA was precipitated, washed and purified of contaminants (protein and genomic DNA) before resuspension in molecular grade water. Plasmid DNA was quantified using a Nanodrop 2000 (Thermo Scientific) spectrophotometer.

3.5 Agarose gel electrophoresis

Gel electrophoresis was used to ensure DNA, PCR products and digested DNA were the expected sizes to indicate a successful experiment. Samples were prepared as follows 500 ng of plasmid DNA or 10 µl PCR product were mixed with water to a final volume of 16 µl. To this 4 µl of 5x DNA loading buffer (NEB) was added. Dependent on expected DNA size, an array of agarose gel concentrations was used (predominantly 0.75-1.5%) in TAE buffer (40 mM Tris, 20mM Acetate, 1 mM EDTA). 1 X GelRed Nucleic Acid Gel Stain (Biotium) was added to gels. Agarose gels were ran in a Mini-sub Cell GT Cell (Bio-Rad) system at 90V until an adequate band separation was achieved. Suitable molecular weight markers were ran alongside samples to evaluate DNA size 1kb and 100 bp ladders (NEB). Gel images were captured using a ChemiDoc™ system (Bio-Rad).

3.6 Plasmid Transfection

Unless otherwise specified, all plasmids used throughout were reverse transfected at the amounts indicated with *Trans*IT®-LT1 transfection reagent (MIR 2300) according to manufacturer instructions using a 3:1 (µl:µg) LT1:plasmid ratio. Opti-MEMTM I (Thermo 31985062) was used as serum-free media for creation of transfection complexes.

3.7 Chromatin-Immune Precipitation (ChiP) Experiments

Chromatin immunoprecipitation (ChIP) assays were carried out according to the Schmidt et al protocol (Schmidt et al., 2009). Briefly cells were fixed in 1% Formaldehyde for 7

minutes before the reaction was quenched with the addition of 1.25mM of Glycine. Cells were washed twice in ice cold PBS containing protease inhibitors (Roche 04693132001) prior to cell scraping and centrifugation at 2000xg for 5 minutes at 4^{o}C. Supernatant was removed and cell pellets were snap frozen and stored at -80^{o}C until processing.

Pellets were thawed and resuspended in 5ml LB1 (50 mM HEPES-KOH, pH7.5, 140 mM NaCl, 1 mM EDTA, 10% glycerol, 0.5% NP- 40 and 0.25% Triton X-100) and incubated on ice with agitation before centrifugation at 950xg for 5 minutes at 4^{o}C. This step was repeated using LB2 (10 mM Tris-HCl pH8, 200 mM NaCl, 1 mM EDTA and 0.5 mM EGTA). Supernatant was removed and pellets were resuspended in 600µl LB3 (100 mM Tris-HCl, pH8, 100 mM NaCl, 1mM EDTA, 0.5 mM EGTA, 0.1% Na- deoxycholate and 0.5% N-lauroylsarcosine) and transferred to a 1.5ml Eppendorf tube. The samples were sonicated using the Soniprep 150 Plus (MSE, Discontinued) consisting of cycles of 10 seconds 'on' and 50 seconds 'off' at an amplitude of 6.5. Following sonication's, samples were centrifuged at 11,000 x g for 10 minutes at 4^{o}C.

Prior to use in experiments, successful sonication was confirmed through analysis of DNA fragments as per Pchelintsev et al (Pchelintsev et al., 2016). 10–30 µL of the sonicated chromatin samples were combined with 10 µL of 10 mg/mL Proteinase K (Sigma, P2308), 50 µL of 2x reverse cross-linking master mix (100 mM Tris pH 8.0, 600 mM NaCl, 1.0% SDS, 100 mM EDTA pH 8.0; kept at +37°C to avoid SDS precipitation) and brought to a final volume of 100 µL with water. Samples were combined with 10 µL of 1 mg/mL RNaseA (Qiagen, 1018048) an incubated for 1 h at +60°C, and the resulting DNA was purified with a PCR purification kit (Qiagen, 28104). Purified DNA was analysed on ethidium bromide-stained agarose gels.

The DNA concentration was measured using a Nanodrop. 50µg chromatin was prepared in a total volume 700 µl using LB3 + 1% triton X-100 solution. From this, 10% was taken as an input sample (stored at -20°C until DNA cross link reversal). 40 µl of Protein A-conjugated Dynabeads (Life Sciences) were washed twice in 0.5% BSA/PBS before 700µl of 0.5%BSA/PBS was added to the beads along with 2µg specific antibody. This was then left for 8 hours, rotating at 4°C, to enable antibody conjugation to beads. Magnetic separation was used to remove the solution from the beads, to which the remaining 630

µl of chromatin preparation was added to the beads and then left for 16 hours at 4°C with rotation.

Following incubation, the supernatant was discarded, and beads washed 4 times in RIPA buffer (50 mM HEPES pH 7.5, 500 mM LiCl, 1 mM EDTA, 1% NP-40, 0.7% Na- deoxycholate) followed by a final wash in TBS (20 mM Tris pH 7.6, 150 mM NaCl). Dynabeads were then resuspended in 200 µl of ChIP elution solution (50 mM Tris-HCl pH8, 10 mM EDTA, 1% SDS) for 8 hours at 65 °C, with an additional re-suspension after the first 20 minutes to allow maximum complex elution. Input samples collected on the previous day were also subject to this process. Post incubation, supernatants were transferred to a fresh tube and mixed with solution and 200 µl TE buffer (10 mM Tris pH 8, 1 mM EDTA) to dilute before storing at 20°C overnight.

Samples were thawed and 4 µl of Proteinase K was added to each before incubating at 55°C for 1 hour. DNA was then purified using the GenEluteTM genomic mammalian miniprep kit (Sigma Aldrich G1N350) as per manufacturers specifications. Purified DNA samples were stored at -20°C until required.

DNA was analysed using qPCR (see section 2.3)**.** Data was analysed by either percentage input using cycle threshold (CT) values or by fold enrichment over IgG control. For % input, the following equation was used:

$$\% \text{ input} = 100 \times 2^{((\text{input CT } 3.2)-\text{IP CT})}$$

Where input CT – 3.2 was used to overcome the discrepancy of using 10% of chromatin amount in the input samples. Data is then normalised to the experimental control.

For fold enrichment the following equation was used:

$$\text{Fold enrichment} = 2^{(-(\text{Ct IP} - \text{Ct IgG})}$$

The fold enrichment method assumes that the level of background signal is reproducible between different primer sets, samples, and experimental replicates.

Chapter 4: Identifying and validating KDM6A as an epigenetic regulator critical in castrate-resistant prostate cancer.

4.1 Introduction

As discussed in the introduction, the progression of PC to CRPC is orchestrated by several mechanisms of resistance to anti-androgens, including the generation of AR-Vs. Considering up to 75% of patients show expression of alternatively spliced AR-Vs following anti-androgen treatment there is an urgent need to improve our understanding of AR-Vs to provide new therapeutic options. Whilst alternative splicing itself is relatively well understood, there is a need to further our knowledge of the regulation of AS and how different factors can influence splicing decisions. Multiple epigenetic enzymes, including histone demethylases, demonstrate significantly altered expression over the progression of PC (Duan et al., 2019; Ragavi et al., 2023; Z. Zhang et al., 2023). This coupled with the work demonstrating that epigenetic enzymes can act as splicing regulators (Metzler et al., 2023a; Segelle et al., 2022) provided a rationale for investigating the role epigenetic enzymes play in the generation and regulation of AR-Vs and whether it is feasible to therapeutically target them.

Previous small-scale epigenetic screens have identified a range of histone demethylases which were shown to be important for PC progression, but only a limited amount focussed on AR-V generation (Bjorkman et al., 2012; Sarac et al., 2020). An overview of histone demethylases and their involvement in PC progression is shown in the introduction.

From a HDM siRNA library knockdown (KD) performed by a student in the laboratory, it appeared that depletion of KDM6A led to a significant reduction in AR-V7 at both a transcript and protein level. siRNA transfections were carried out as described in Chapter 2.6. The siRNAs used targeted all known HDMs encompassing both subgroups (discussed in the introduction) and therefore provided a broad overview of the impact of HDM depletion on AR-V7 levels. KD of KDM6A appeared to have a similar or better reduction in AR-V expression than histone-modifying enzymes that have already been shown to be regulators of AR splicing; JMJD6 (Paschalis et al., 2021) and KDM3A (Fan et al., 2018). This provides a clear opportunity to employ methods which identify epigenetic regulators specifically upregulated in AR-V^{+} setting. To make this work as translational as possible,

we utilised publicly available patient data, tissue microarray on primary patients' samples and patient-derived organoids. Additionally, we developed novel cell line models which better model Enzalutamide resistance, and latterly, KDM6A overexpression (the most common alteration of KDM6A in advanced disease) to better understand the mechanism of KDM6A in CRPC. Utilising all these methods helped us to improve the robustness and clinical relevance of the data regarding KDM6A.

4.2 Aims

This chapter aims to first utilise publicly available data sets and tissue microarray assay to validate that KMD6A has a role in CRPC. The second aim is to assess the effect of common KMD6A mutations in PC cell lines. Finally, we aim to develop novel *in vitro* cell line models which will be used throughout the PhD. These models better reflect both advanced disease as well as common KDM6A alterations observed in PC patients.

The aims will be achieved by:

1. Interrogating publicly available data sets to compare chromatin modifier expression differences in tumours which are AR-V7^{+} or AR-V7^{-}
2. Assess the effect of KDM6A overexpression in PC cell lines.
3. Develop translationally relevant *in vitro* models to allow us to investigate the role of KMD6A in CRPC

4.3 Chapter-Specific Materials and Methods

4.3.1 Analysis of publicly available RNA-Seq clinical cohorts

TCGA-PRAD dataset, *TCGAbiolinks* (v2.15.3) was used to extract raw gene expression counts. Information on patient V7 status was obtained from cBioPortal (Cerami et al., 2012) entries, with the presence or absence of AR-V7 defined as in the TCGA-PRAD 2015 analysis (Abeshouse et al., 2015). Differential gene expression analysis between AR-V7 positive and negative patients was performed using *edgeR* (v3.32.0) (Robinson et al., 2010). log2 counts- per million (CPM) were generated using the *edgeR* trimmed-mean of M values normalisation.

4.3.2 Overexpression of KMD6A plasmids in cell lines

KDM6A wild-type (Wt) and Mutant (Mt) plasmid were ordered from Addgene (#17438 and #40619 respectively). The KDM6A mutant is identical to the wild-type except for two amino acids (H1146 and E1146) which reside within the Jmj domain of the protein and are essential for enzymatic activity. Plasmid DNA was extracted from bacterial slabs following the protocol in Chapter 2 (from 2.4.2-2.4.6). Plasmid DNA was transfected into cells following the protocol in Chapter 2.5.

4.3.3 Overexpression of KDM6A plasmid in patient-derived xenograft organoids (PDXOs)

The PC346C cells were a kind gift from Dr Van Weerden of the Erasmus MC, Rotterdam. These cells were established from the PC-346 Xenograft. For proliferation, cells require the addition of androgens and their growth can be inhibited with anti-androgens. Their doubling time as a 2D monolayer is approximately 4-5 days.

PDXOs were transfected with KDM6A WT or Mut plasmid as previously described (Broutier et al., 2016). Briefly, organoids were cultured until 80-90% confluence at which point a single cell suspension was prepared by disrupting the Matrigel containing the organoids. Organoids were added to a 15 ml Falcon tube along with additional ice-cold basal media and centrifuged at 200g x 5 minutes at room temperature. The supernatant was removed, and the organoids were resuspended in 2 ml TrypLE and pipetted vigorously before incubation at 37^{o}C for approximately 5 minutes. The digestion was stopped by adding 10 ml of cold basal medium when 90% of the material consisted of single cells. The

single cell suspension was centrifuged at 300g x 5 minutes at 4°C, the supernatant was removed and the pellet resuspended in 450 µl full growth media and stored on ice until transfection. Transfection mixtures consisting of 1 µg of plasmid DNA, 3 µl FuGENE (Promega E2691) and 50 µl of Opti-MEM were combined and left at room temperature for 20 minutes. The transfection mixture was combined with the single-cell suspension and transferred to one well of a 24-well plate. The plate was centrifuged at 600g x 1 hour at 32°C and then incubated for a further 4 hours at 37°C. The transfection mix was transferred to a microcentrifuge tube and centrifuged at 400g x 5 minutes. The supernatant was removed, and the pellet was resuspended in 30 µl of Matrigel and seeded onto one well of a 24-well plate. Full growth media was overlayed on top. 72 hours post-transfection, protein and RNA were harvested, and respective western blot and RT-qPCR were performed as described in Chapters 3.2 and 3.3 respectively.

4.3.4 Lentiviral production, cell line transduction and clonal isolation

6 x 10^6 HEK293FT were seeded in 100 mm dishes in 10 ml media and incubated overnight. The next day, media was replaced, and cells were transfected, using *Trans*IT®-LT1, with 7.5 µg lentiviral packaging plasmid psPAX2 (Addgene #12260), 5 µg VSV-G plasmid pMD2.G (Addgene #12259) and 2 µg lentiviral transfer plasmid (a custom generated KDM6A plasmid from VectorBuilder) (Supplementary 1). 48 hours post-transfection, HEK293FT media was harvested and stored at 4°C, and culture media was replaced. Media was harvested again the next day, and 48/72-hour lentiviral media harvests were combined, spun at 500 x *g* for 5 minutes and the supernatant was filtered through 0.45µm syringe filters. Lentivirus aliquots were subsequently frozen in cryovials at -80°C.

For lentiviral transduction of CWR22Rv1, 1 x 10^6 cells were seeded in 10 cm dishes with 1 ml lentivirus to a final plate volume of 10 ml. 1 ml media was used in place of 1 ml lentivirus as a non-transduced control for puromycin selection. Cells were incubated for 48 hours before lentiviral transduction media was removed and replaced with fresh media containing 2 µg/ml puromycin (Sigma P7255). Cells were maintained in 2 µg/ml puromycin until 100% cell death occurred in non-transduced controls.

To derive a clonal population of KMD6A overexpressing cells, puromycin-resistant cells were picked as single clones and propagated until there were enough cells to conduct

a western blot as described previously. Two clones which appeared to have KDM6A overexpression were then maintained for additional experiments.

4.3.5 Developments of a Novel Enzalutamide Resistant Cell Line Model

To develop a novel model of CRPC which showed resistance to Enzalutamide, a second-generation anti-androgen, VCaP cells were cultured in full media + 10 µM Enzalutamide. Media was replenished every 72 hours. Initially, there was a large amount of cell death however after approximately three months, surviving VCaP cells began to proliferate. After 12 months in culture, VCaP-EnzaR cells grew at a similar rate to parental cells and were sent for RNA sequencing.

4.3.6 VCaP-EnzaR RNA-Seq Analysis

RNA-Seq libraries were prepared using poly(A) selection and ~25-40 million 2x 150 bp reads were sequenced per sample on illumina NovaSeq 6000. The FASTQ files were kindly processed by Nick Brittain who conducted quality checks utilising *FastQC* and *MultipQC.* Illumina universal adapter sequences were trimmed from reads using *Cutadapt (v3.5 Martin, 2011),* and successful adapter removal was confirmed by running trimmed FASTQ files through *FastQC* again.

A genome index was generated using STAR (Dobin et al., 2013)genomeGenerate mode with the GENCODE GRCh38 primary assembly and associated GTF annotation (release v43). SAM files were generated against this index with STAR (v2.7.0e), using default settings. SAMtools was subsequently used for sorting files by genomic coordinate. SAMtools was also used for the conversion of files to BAM format. A gene counts matrix was created with featureCounts (Subread v1.4.0) (Liao et al., 2013) using GENCODE primary assembly GTF annotation (release v43).

For differential gene expression analysis, gene-level counts generated by featureCounts were exported. DESeq2 (Love et al., 2014) was used with default settings for the calculation of differential gene expression between samples, and the ashr algorithm for log2 fold change shrinkage was implemented within DESeq2. Genes were sorted by log2 fold change for gene set enrichment analysis using GSEA software (v4.0.3) (Subramanian et al., 2005) Gene expression counts, normalised by DESeq2, were extracted for plotting.

4.3.7 Spheroid Formation Assay

VCaP parental and VCaP-EnzaR cells were trypsinised and a cell count was performed. $5x10^3$ cells were required per 50 µl Matrigel (Corning 354277). The desired number of cells was aliquoted into a 1.7ml Eppendorf tube and centrifuged at 1000g x 5 minutes. Supernatant media was removed, and the cells were resuspended in Matrigel. 30 µl drops of cell/Matrigel mixture were dispensed into the centre of wells on a 96-well plate. The plates were inverted and placed in an incubator at 37^{o}C for 15 minutes. After 15 minutes, plates were removed and 500 µl of growth media was added per well.

4.4 Results

4.4.1 Analysis of clinical datasets reveal KDM6A is significantly upregulated in CRPC

The expression of KMD6A and any alteration to this, including somatic mutation, was profiled using publicly available clinical data sets from cBioPortal. The key aim of this work was to assess if KDM6A expression was altered in PC and if it correlates with AR-V7 transcript levels.

Firstly, the expression of KDM6A was assessed in patients whose tumours expressed AR-V7 (AR-V7$^+$) (N=80) and those which did not (AR-V7$^-$) (N=240) utilising the TCGA dataset (Cancer Genome Atlas Research, 2015). Importantly, AR-V7$^+$ tumours were found to have significantly higher mRNA expression of KMD6A than AR-V7$^-$ tumours (**Figure 4.1A**), suggesting that KDM6A may be involved in regulating the expression of AR-V7 in PC. Considering that the TCGA data set is limited to only containing treatment-naive patients, which could account for the low number of patients who are AR-V7$^+$ in this cohort, it was important to next examine KDM6A expression in clinical data from advanced pre-treated PC patients.

The International Stand-up to Cancer/Prostate Cancer Foundation (SU2C/PCF) consortium contains RNA-Seq gene expression data for over 200 samples of CRPC patients (Abida et al., 2019). To assess KMD6A expression between AR-V7$^{-/+}$ patient samples, the samples were firstly separated based on AR-V7 spliced reads per million (SRPM). Samples with a SRPM of 0 were considered AR-V7$^-$ whilst samples with an SRPM >0 were considered AR-V7$^+$. Fragments per kilobase millions (FPKM) RNA-Seq expression value of KMD6A was then taken for corresponding patients. In total, there were 134 samples for which both AR-V7 and KDM6A expression were available; with 115 patients categorised

as AR-V7^{+} and 19patients defined as AR-V^{-}. Crucially, consistent with the findings from the TCGA data set, KDM6A was found to be significantly higher expressed in AR-V7^{+} patients compared to AR-V7^{-}(**Figure 4.1B**; $p<0.05$).

Outside of KDM6A expression in PC, it was important to understand if the mutational landscape of the *KDM6A* gene was different between primary, treatment naïve PC and pre-treated CRPC samples. To do this, genomic alteration frequency for samples from the TCGA data set (primary untreated) was compared to patients from the SU2C/PCF consortium (pre-treated CRPC). Genomic alterations, including mutational and amplification data, for both datasets were extracted from cBioPortal. Strikingly, in CRPC patients, *KDM6A* was found to be altered in around 15% of patients compared to approximately 5% in primary samples (**Figure 4.1C**).

The next important finding based on the SU2C/PCF data, was that ~10% of the *KDM6A* alterations in CRPC patients are amplifications. This was much greater than any other alteration to *KMD6A,* for example, deep deletion and mutations which made up 1.2% and 2%, respectively, of all mutations in CRPC patients. It was also notable that amplifications to *KMD6A* were much more common in CRPC samples than primary samples (9.23% v 1.2% respectively). It was also noteworthy that there was a positive correlation between both AR-FL and KDM6A (Pearson = 0.27, P= <0.005) and between AR-V7 and KDM6A (Pearson=0.15, P=0.03) when the data from the SU2C/PCF cohort was analysed **(Figure 4.1D and E).**

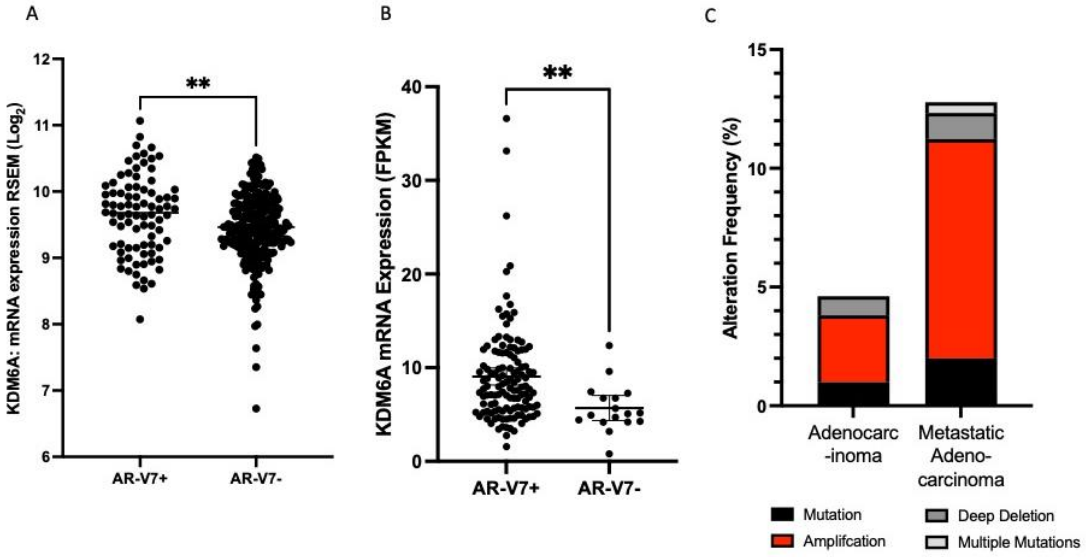
A
KDM6A: mRNA expression RSEM (Log2)
**
AR-V7+
AR-V7-
B
KDM6A mRNA Expression (FPKM)
**
AR-V7+
AR-V7-
C
Alteration Frequency (%)
Adenocarc -inoma
Metastatic Adeno- carcinoma
Mutation
Amplifcation
Deep Deletion
Multiple Mutations

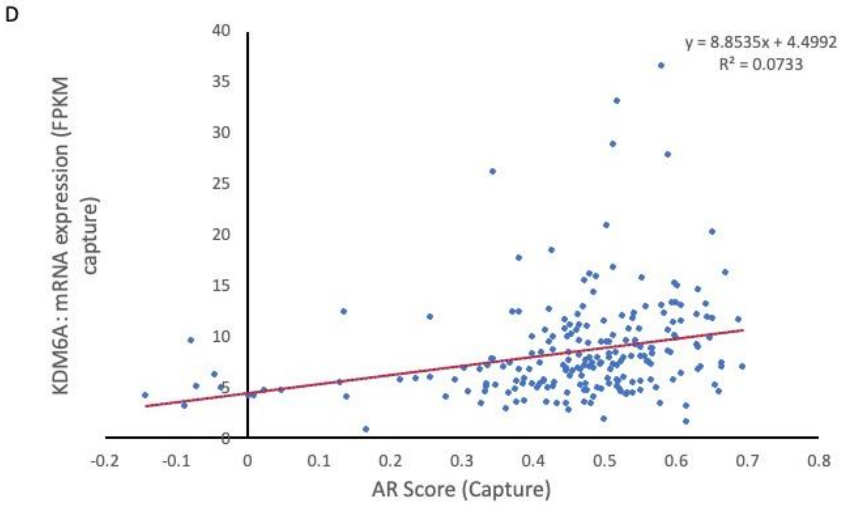
D
y = 8.8535x + 4.4992
R² = 0.0733
KDM6A: mRNA expression (FPKM capture)
AR Score (Capture)

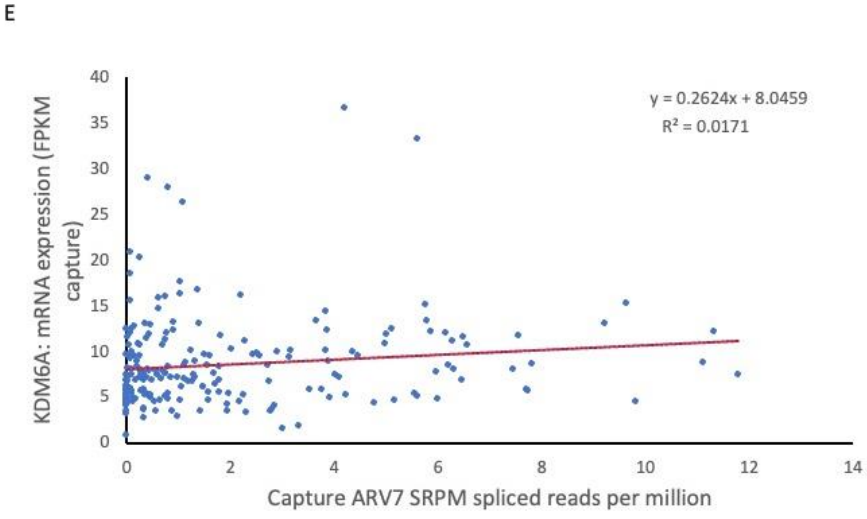
E
y = 0.2624x + 8.0459
R² = 0.0171
KDM6A: mRNA expression (FPKM capture)
Capture ARV7 SRPM spliced reads per million

Figure 4.1 KDM6A is overexpressed in AR-V7+ patients and commonly mutated in advanced disease. A) *Comparison of KMD6A expression between AR-V7+ and AR-V7- patients from the TCGA-Prostate adenocarcinoma dataset, KDM6A is significantly higher expressed in AR-V7 patients.* ***B)*** *Comparison of KMD6A expression between AR-V7+ and AR-V7- patients SU2C/PCF Consortium. KDM6A is significantly higher expressed in AR-V7+ patients.* ***C)*** *Mutational analyses and alteration frequency in both primary, treatment-naive (TGCA) and metastatic, heavily treated (SU2C/PCF) patient tumours.* ***D-E)*** *Correlation analyses of expression between AR-FL, AR-V7 and KDM6A. Data available for 208 samples from SU2C/PCF Cohort. Unpaired t-test was used to calculate statistical significance in A and B (*=p<0.05, **=p<0.01, ***=p<0.001 and ****=p<0.0001).*

To see if there were mutational hotspots within KDM6A, somatic mutation data was extracted for both studies from cBioportal. The limited number of mutations from the TCGA data set were spread across the KDM6A gene **(Figure 4.2A).** There was only one mutation *(E1182)* within the JmjC domain. This mutation is a splicing event resulting in a truncated form of KMD6A likely to cause a loss of function. It is worth noting three mutations within Exon 28 at the C-terminal of the KDM6A gene. All three mutations also result in a truncation of the KDM6A protein likely leading to a loss of function. One of the mutations, *KDM6A X1335_splice* is present in bladder urothelial carcinoma, breast invasive ductal carcinoma, neuroendocrine tumour and pancreatic adenocarcinoma (AACR Project., 2017). A full list of mutations and their expected effect on function is shown in **Table 8.**

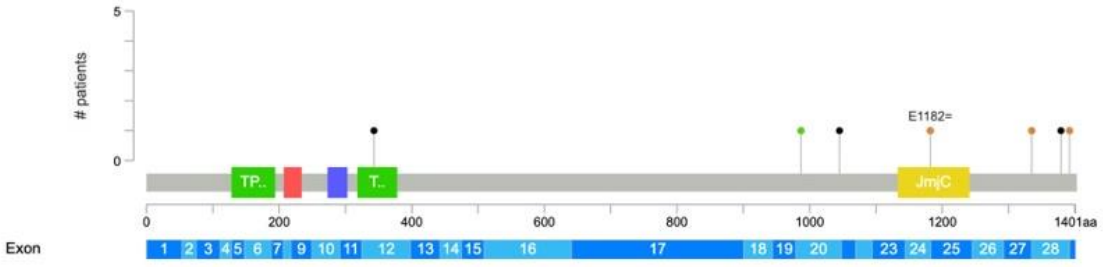

Figure 4.2 Somatic mutations across KDM6A in Prostate Adenocarcinoma. *Data from the TCGA cohort showing location of KDM6A mutation in primary prostate adenocarcinoma and mutation type. Mutation type indicated by colour of dot. Black (Truncating), Orange (Splice), Green (Missense).*

Patient	KDM6A Mutation	Mutation Type	Functional Change
1	E1182(Driver)	Splice	Truncating mutation causing loss of function

2	AMP		
3	AMP		
4	X1392_splice (Driver)	Splice	Truncating mutation causing loss of function
5	M1380Wfs*4 (Driver)	Frame shift deletion	Truncating mutation causing loss of function
6	E1045*(Driver)	Nonsense	Truncating mutation causing loss of function
7	AMP		
8	HOMDEL(Driver)		
9	C343Wfs*21	Frame Shift insertion	Truncating mutation causing loss of function
10	K987R	Missense	Truncating mutation causing loss of function
11	HOMDEL(Driver)		
12	AMP		
13	X1335_splice (Driver)	Splice	Truncating mutation causing loss of function

From the SU2C/PCF consortium cohort, there was a spread of mutations across the KDM6A gene **(Figure 4.3A).** In these patients, other than amplifications, Frameshift deletions or missense mutations were the dominant mutation types. For all the frameshift deletion OncoKB predicted the functional change to be a truncation leading to inactivation of KDM6A (Chakravarty et al., 2017; Suehnholz et al., 2024). For samples with missense mutations, no information on the functional change was known. In Exon 16 of KMD6A there were four frameshift deletion mutations from four individual samples which led to truncation of the protein and consequently loss of function. Exon 16 lies within what is termed the intrinsically disordered region (IDR) which connects the TPR and JmjC domains (Özden-Yılmaz et al., 2023). A functional IDR in KDM6A is necessary for tumour suppressor activity through the formation of liquid condensates (Fotouhi et al., 2023; Shi et al., 2021) (Shi et al., 2021, Fotouhi et al., 2023). Mutations to KDM6A IDR have been found commonly in other cancers including bladder and lung (Biagini et al., 2022; Özden-Yılmaz et al., 2023). All samples and corresponding mutations are found in **Table 2.** One patient (Patient 21 from Table 2) had two separate missense mutations *(N1158H and C1164S)* in Exon 24 of the KMD6A gene as well as an amplification to KMD6A. Suggestive of an overexpression of a mutant form.

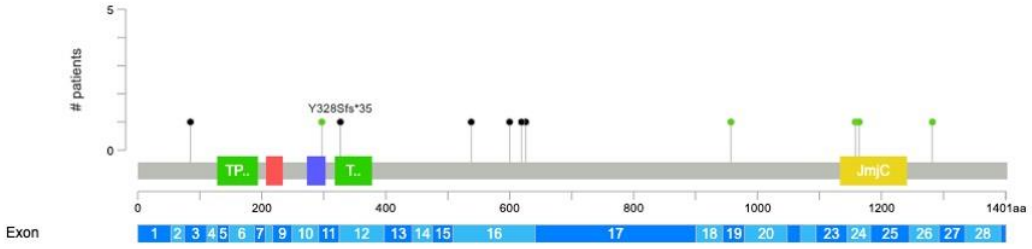

Figure 4.3 Somatic mutation across KDM6A in Metastatic Prostate Cancer. *Data from the SU2C/PCF cohort showing the location of KDM6A mutation in primary prostate adenocarcinoma and mutation type. Mutation type is indicated by the colour of the dot. Black (Truncating), Orange (Splice), Green (Missense).*

Table 11 KDM6A Mutation in SU2C/PCF Cohort. *Breakdown of KDM6A mutations in individual patients. The location of the mutation, mutation type and the expected function change to KDM6A where known, are shown. Function change predicted by ONCOkb (Suehnholz et al., 2024, Chakravarty et al., 2017)*

Patient	KDM6A Mutation	Mutation Type	Functional Change
1	AMP		

2	S601Vfs*24*(Driver)*	Frame Shift deletion	Truncation
3	AMP		
4	AMP		
5	AMP		
6	AMP		
7	AMP		
8	AMP		
9	HOMDEL*(Driver)*		
10	AMP		
11	HOMDEL*(Driver)*		
12	HOMDEL*(Driver)*		
13	AMP		
14	AMP		
15	AMP		
16	S627Rfs*60*(Driver)	Frame Shift deletion	Truncation
17	AMP		
18	AMP		
19	AMP		
20	AMP		
21	N1158H, C1164S, AMP	Missense	
22	Y328Sfs*35*(Driver)	Frame Shift deletion	Truncation
23	AMP		
24	H619Qfs*19*(Driver)	Frame Shift deletion	Truncation
25	K1282N	Missense	
26	AMP		
27	AMP		
28	I297F	Missense	
29	AMP		
30	AMP		
31	AMP		
32	AMP		
33	HOMDEL*(Driver)*		
34	AMP		
35	AMP		
36	AMP		
37	AMP		
38	AMP		
39	AMP		
40	AMP		
41	A87Lfs*13*(Driver)	Frameshift deletion	Truncation
42	AMP		
43	AMP		
44	AMP		
45	AMP		
46	Q544Lfs*14*(Driver), AMP	Frameshift Insertion	Truncation
47	HOMDEL*(Driver)*		

48	AMP		
49	AMP		
50	AMP		
51	AMP		
52	AMP		
53	H957Q	Missense	
54	AMP		
55	AMP		

Subsequently, additional metastatic prostate cancer data sets on cBioPortal were examined to discover if this higher alteration frequency of *KDM6A* in CRPC is commonly observed. The two additional studies utilised, which contained mutational analysis data on CRPC tumours, were the SU2C/PCF consortium 2015 (n=150) (Robinson et al., 2015) and the Grasso *et al.,* dataset (n=50) (Grasso et al., 2012). Although these studies report a lower frequency of *KDM6A* alterations of 4% and 10%, respectively, compared to the SU2C/PCF data set, they still reflect a considerable patient cohort who have mutations/amplifications of KDM6A which could be important for future personalised treatment strategies.

4.4.3 Expression of KDM6A in prostate cancer cell lines and organoid models

To establish a background understanding of KDM6A biology in the range of PC cell lines used in the study; *KDM6A* mutational analysis as well as mRNA and protein expression of each cell line was conducted. Mutational analysis was conducted by interrogating the Depmap and COSMIC portal for each cell line. For the PC346C cells, copy number analysis was provided by Wytske Van Weerden. All cell lines tested, or where the data was available, showed no amplification of or mutation in the *KDM6A* gene across the PC cell lines tested **(Figure 4.4A).**

For investigating the mRNA expression of KDM6A between PC cell lines, RNA was extracted from all cell lines over three separate passages. Relative expression of genes was calculated by normalising the data to PNT1A, a non-cancerous prostate cancer cell line. KDM6A showed some variation across cell lines and was significantly upregulated in the following cell lines compared to the PNT1A: LNCAP, VCaP, CW22Rv1 and LNCAP95 **(Figure 4.4B).** Differences in both AR-FL as well as AR-V7 expression were also assessed in the same cell line panel. Importantly, PC3 and LNCAP showed no expression of AR-V7 as is well documented in the literature (Hille et al., 2019). VCaP, CW22Rv1 and LNCAP95 all showed

significant upregulation of AR-V7 compared to the PNT1A, with LNCAP95 showing the highest expression **(Figure 4.4C).** In terms of AR-FL, its expression was found to be significantly higher in LNCaP, VCaP, CW22Rv1 and LNCAP95 which, except for LNCaP cells, is consistent with AR-V7 expression **(Figure 4.4D).** Protein expression analysis revealed levels of KDM6A appeared to be highest in the LNCaP cells, compared to PNT1A. Although it should be noted that expression of loading control (α-tubulin) was lower in VCaP and CW22Rv1 cells, suggestive of lower cell content being loaded. If the protein expression was normalised to loading control it is likely both cell lines would have considerably higher KDM6A expression than PNT1A. High AR-FL expression was detectable in LNCaP/95s, VCaP and some expression was detectable in CW22Rv1. AR-V expression was detectable in VCaP, CW22Rv1 and LNCaP95 cells validating previous literature. The AR-V detected in the LNCaP cells is likely to be ARV3 as AR-V7 expression is not detectable (**Figure 4.4E and F).**

A

Cell Line	KDM6A Status
CW22Rv1	Wild-type
VCaP	Wild-type
LNCaP	Wild-type
LNCaP95	
PNT1A	
PC346C	Wild-type (CNA only)
PC3	Wild-type

B

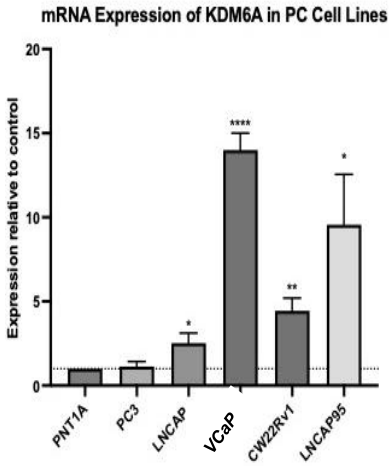

C

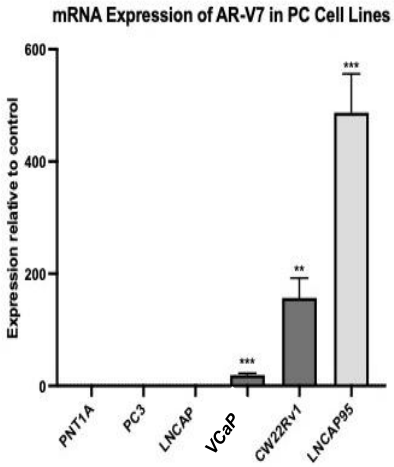

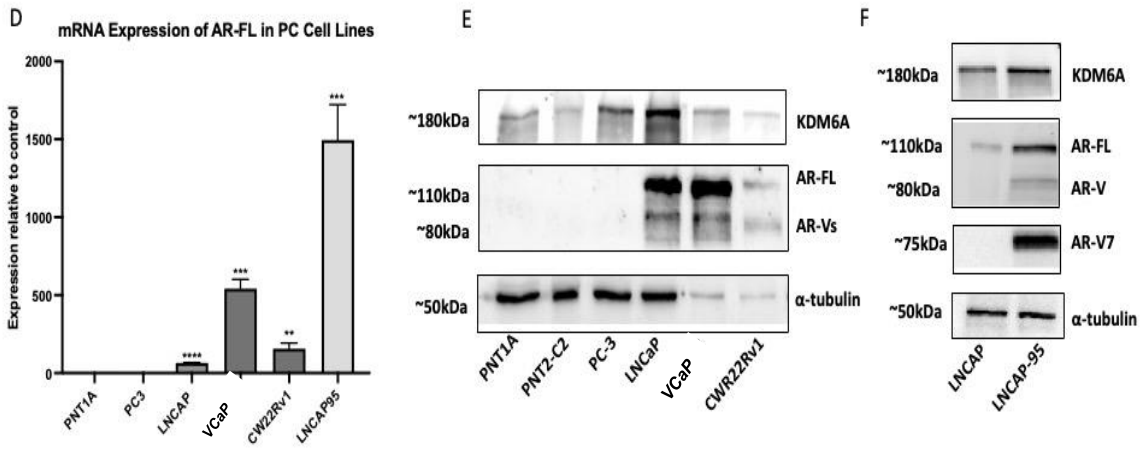

Figure 4.4 Profiling the expression of KMD6A, AR-FL and AR-V7 in a range of prostate cancer cell lines. A) *Mutational analysis from COSMIC and DepMap confirming that cell lines used in this work were KDM6A wild type.* ***B-D*** *mRNA expression of KDM6A, AR-V7 and AR-FL in prostate cancer cell line used in the study.* ***E-F*** *Protein profiling of KDM6A, AR-V7 and AR-FL in the same prostate cancer cell lines as B-D. An unpaired t-test was used for B-E where cell lines were compared to the PNT1A (BHP) cell line. qPCR data comprises n=3 independent biological replicates, plotted as mean +/- SEM (*=p<0.05, **=p<0.01, ***=p<0.001 and ****=p<0.0001). E-F show a representation of N=3.*

4.4.4 Effect of KDM6A overexpression in prostate cancer cell lines

Based principally on findings from the SU2C/PCF publicly available dataset which demonstrated amplification of *KMD6A* occurred in around 15% of cases, it was important to model and investigate the effect of KDM6A overexpression in prostate cancer cell lines. This study would potentially replicate *KDM6A* gene amplification *in vitro* and provide a better understanding of the role of elevated KDM6A expression in disease progression.

To that end, transient overexpression of either KDM6A wild-type (Wt) or a catalytically inactive KDM6A Mutant (Mt) was conducted across a range of PC cell lines to assess if elevated expression and catalytic activity impacts AR isoform levels and cell growth. Considering the potential for impact on AR-FL and AR-V7 transcript abundance by both Wt and Mt KDM6A (as discussed in the introduction), expression data was normalised to an empty vector control (control).

To first validate the expression of the plasmids and their FLAG tag, 1 and 3µg of each plasmid were transfected into HEK293T cells for 48 hours before protein lysates were harvested. Both KDM6A Wt and KDM6A Mt plasmid were expressed as shown by increased expression of FLAG in a dose-dependent manner whilst non transfected cells (Con) showed no FLAG expression **(Figure 4.5A).** To validate if KDM6A Wt and Mt plasmid

affected levels of H3K27me3 different CW22RV1 cells were subjected to transfection of both plasmids for 72 hours before cells were either lysed for protein analysis or fixed to perform immuno-fluorescence (IF) staining. This way the level of H3K27me3 could be quantified by two independent methods. With western blot analysis, it was difficult to determine differences in levels of H3K27me3 (**Figure 4.5 B).** Overexpression of KDM6A Wt did not appear to reduce levels of H3K27me3 as would have been expected whilst both KDM6A Wt and KDM6A Mt appeared to increase levels of H3K27me3 at 3µg. Despite the results of KDM6A Wt and Mt overexpression being slightly inconclusive, the plasmids were still used given the fact they have been more thoroughly profiled previously (S. Hong et al., 2007; C. Wang et al., 2012). These studies used a range of assays including demethylase assay, western blot and multi-parameter IF imaging to validate KDM6A Wt caused demethylation of H3K27me3 whilst the KDM6A Mt plasmid did not affect levels of the methylation mark.

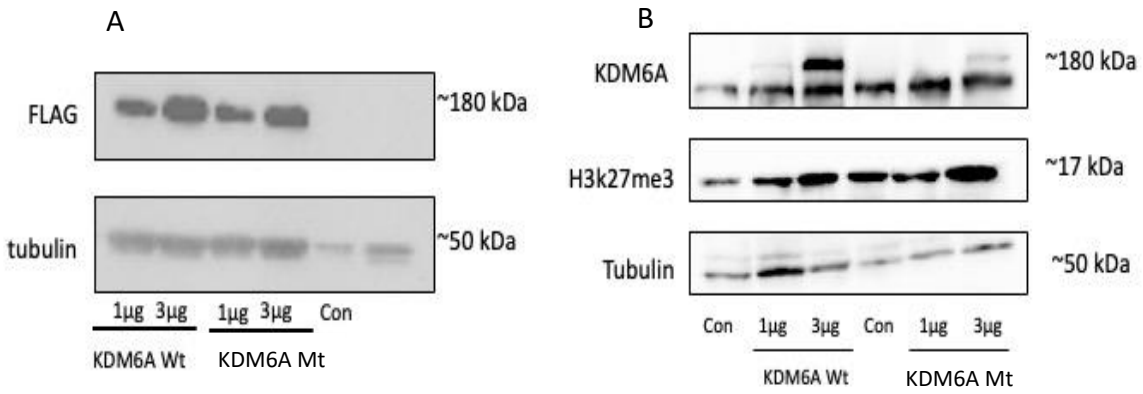

Figure 4.5 Validation of the KDM6A Wt and Mt Plasmids. *KDM6A Wt or Mt were transfected into cells for 72 hours before protein lysates were taken.* ***A)*** *Transfection of plasmids into HEK293T cells prior to profiling of FLAG to determine expression of the plasmid in cells. Control cells were transfected with an empty GFP vector of a similar size to the KMD6A plasmids.* ***B)*** *Transfection of KMD6A plasmid into CW22RV1 cells to assess the effect on H3K27me3 levels to validate loss of demethylase activity in KMD6A Mt plasmid.*

As shown in **Figures 4.6 A and B**, both Wt and Mt plasmids increased expression of KMD6A in multiple PC cell lines by between 90-6000-fold compared to empty-vector-transfected control cells. The increase in expression was less so in cells (around a 3-fold increase) which was expected as these cells are notoriously more difficult to manipulate.

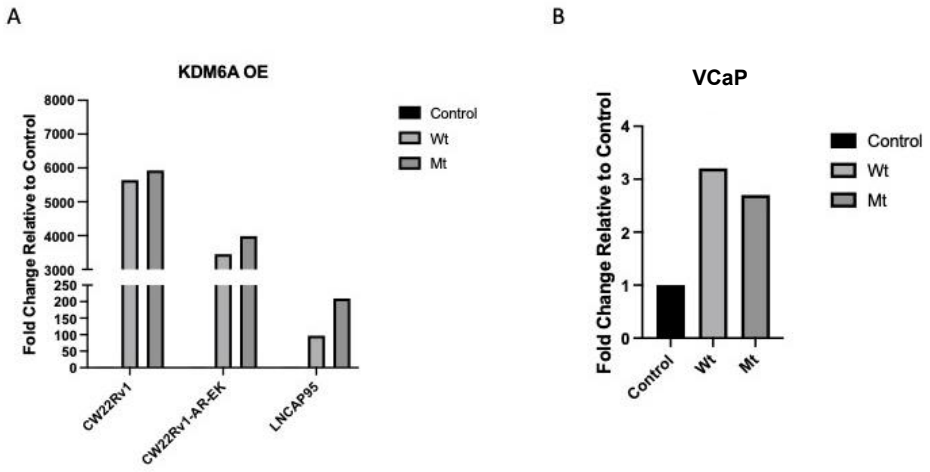

Figure 4.6 Profiling the mRNA expression of KMD6A after transient transfection*. Cells were transiently transfected with 1µg of KDM6A Wt or Mt plasmid for 72 hours before RNA was harvested. A-B) Expression of KMD6A mRNA following transfection compared to empty vector control. N=1 qPCR data from samples used in further experiments.*

Given the correlation between KDM6A and AR isoform expression in advanced PC, the effect of KMD6A Wt and Mt overexpression on AR-FL and AR-V7 levels was next examined. Furthermore, *PSA* (*KLK3*) expression was also examined as this is activated by both AR-FL and AR-V7 (Sobhani et al., 2021). In the CW22Rv1 cell line, overexpression of Wt, but not Mt, KDM6A caused a significant increase in AR-FL, AR-V7 and PSA mRNA **(Figure 4.7A)**. As shown in **Figure 4.7C**, KDM6A overexpression was confirmed for both plasmids, although marked differences in protein abundance for Wt and Mt were observed despite equal amounts of each plasmid being transfected into the cell. There also appeared to be no significant changes in AR-V7, despite the increase in AR isoform mRNA in the presence of Wt KDM6A, or H3K27me3 levels.

In the CW22Rv1-AR-EK cells, over-expression of Wt, but not Mt KDM6A, caused an increase in AR-V7 transcript levels, although not statistically significant **(Figure 4.7B).** The CW22Rv1-AR-EK cells do not express AR-FL at the protein level (Kounatidou et al., 2019) however will still give a transcript signal due to primers utilised which bind to Exon 3 forward and Exon 4 reverse. It is therefore no surprise that KDM6A overexpression did not alter AR-FL transcript levels significantly. Overexpression of KDM6A Wt and Mt caused a minimal change in PSA expression in the CW22Rv1-AR-EK cells; the latter leading to a significant increase in PSA expression, but how physiologically relevant this remains questionable.

Surprisingly overexpression of both KDM6A Wt and Mt caused a decrease in expression of AR-FL, AR-V7 and *PSA* in the VCaP cell lines although this was statistically insignificant **(Figure 4.7D).** At the protein level, however, this was not the case. As shown in **Figure 4.7F,** levels of AR-V7 seem consistent between the control and both Wt and Mt KDM6A experimental arms, while AR-FL levels seem to slightly increase in both Wt and Mt cells compared to the control. It was promising to see that despite low changes in the KDM6A transcript level, KDM6A OE by both Wt and Mt appeared to increase KDM6A protein levels.

In the LNCAP95 cell line, there was little change in AR-FL expression following overexpression of either KDM6A Wt or Mt. There was a small increase in AR-V7 expression with transfection of the Wt plasmid, but this was statistically insignificant. Overexpression with Wt, but not Mt KDM6A, caused a statistically significant increase in *PSA* expression but, like findings from CWR22Rv1-AR-EK cells, how physiologically relevant this is

questionable. **(Figure 4.7D)**. At the protein level there appeared to be little change in KDM6A, AR-FL and AR-V7 between control, Wt and Mt across the range of proteins assessed suggesting that the subtle differences observed at the transcript level may be a consequence of minimal KDM6A overexpression in this cell line. (**Figure 4.7F).**

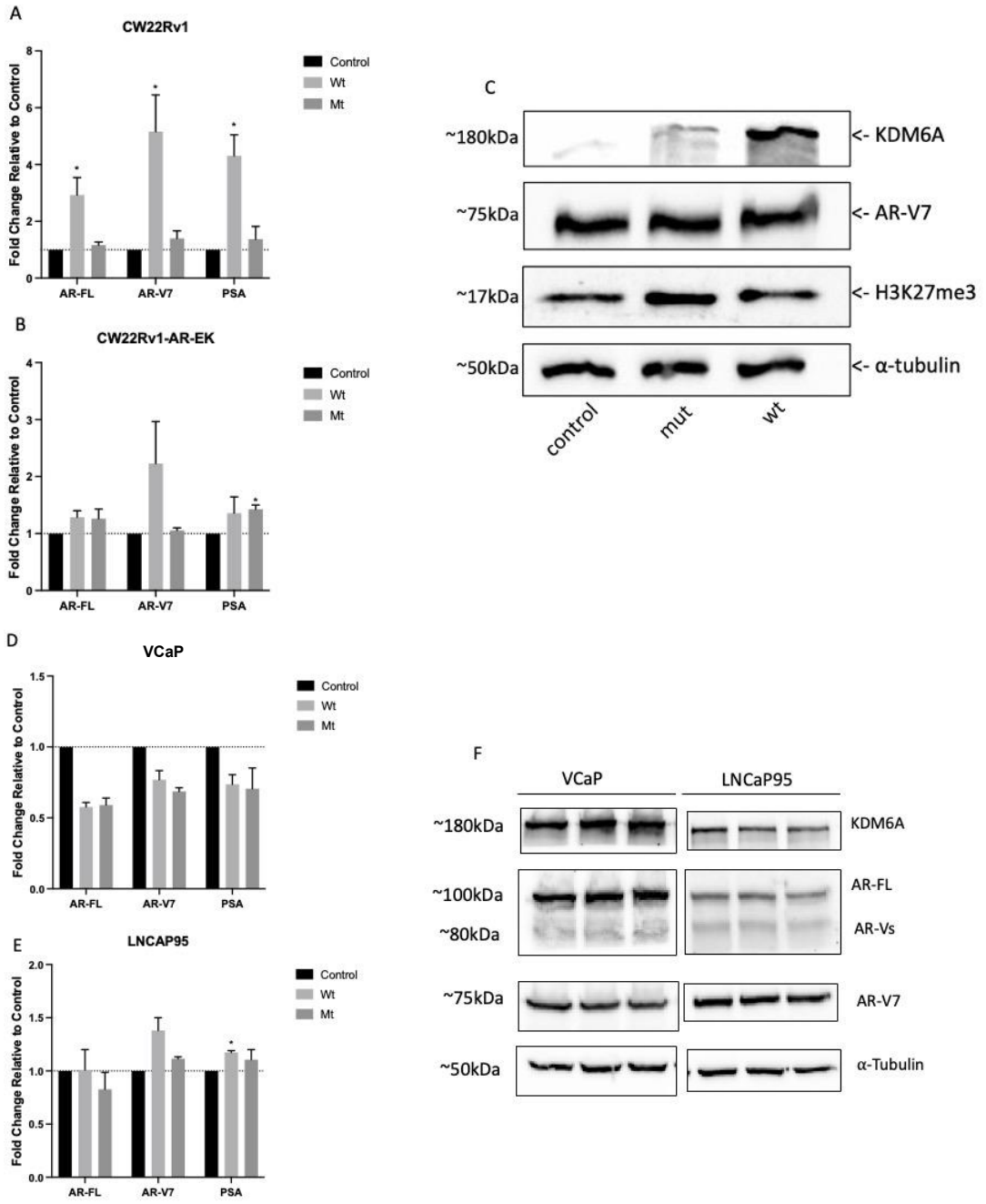

Figure 4.7 Effect of KDM6A Overexpression on AR-V7, AR-FL and PSA expression in a range of Prostate Cancer Cell lines. *Analysis of multiple cancer cell lines 72 hours after transfection with KDM6A Wt or Mt plasmids. AR-V7 specifically detected by RevMAb AR-V7 specific antibody (RevMAb 31-1109-00). AR-FL antibody (Santa Cruz/sc-739) targets the N-terminal of AR and therefore detects both AR-FL and AR-V7.* ***A-B****) Effect of KMD6A overexpression in CW22rv1 and CW22RV1-AR-EK cells on expression of KMD6A, AR-FL and AR-V7.* ***C)*** *Effect of KDM6A overexpression in CW22Rv1cells 72*

hours post-transfection. ***D-F)*** *Effect of KMD6A overexpression in VCaP and LNCaP cells on expression of KMD6A, AR-FL and AR-V7 at mRNA and protein level. qPCR data comprises n=3 independent biological replicates, plotted as mean +/- SEM. Unpaired t-test used to calculate statistical significance (*=p<0.05, **=p<0.01, ***=p<0.001 and ****=p<0.0001). Only statistically significant results are marked by an asterisk, all others are non-significant.*

We next assessed the effect of KDM6A overexpression in a patient-derived organoid model, the PC346C. This cell line was generated through the implantation of a prostatic carcinoma specimen into male NMRI nu/nu mice. After multiple passages in mice, the tumours were resected, dissociated and grown in cell culture flasks **(Figure 4.8)** (Marques et al., 2006). As highlighted in Figure 6, multiple derivatives of the PC246C have been developed with unique molecular features to model mutations seen in patients.

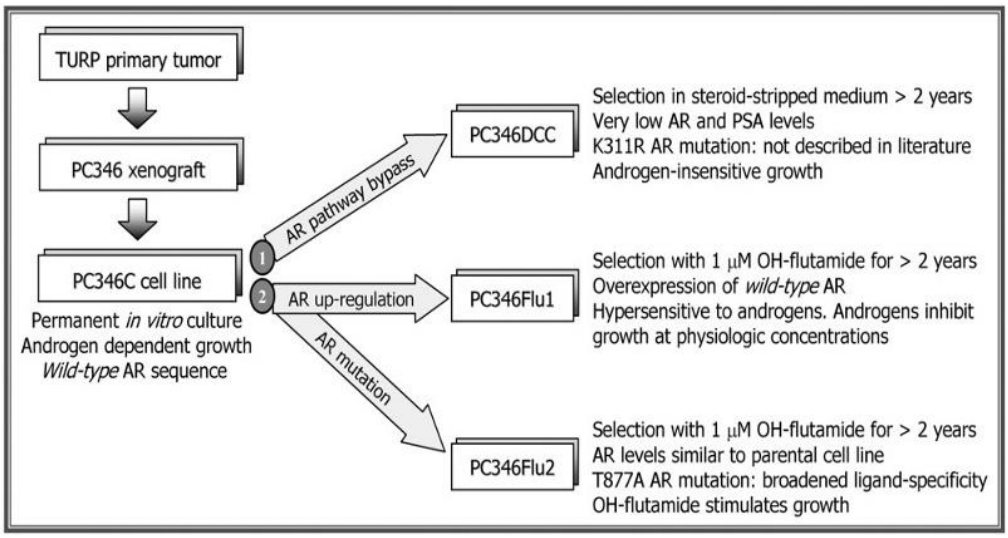

Figure 4.8 The Development of PC346C Cell line. *Experimental workflow of how the PC346C cell line was generated from a TURP primary tumour. The PC346DCC, PC346Flu1 and PC346Flu2 lines were further developments to model resistance mechanism present in patients.*

Firstly, it was critical to validate that the KDM6A plasmids had been successfully transfected into the organoid line (Described in 4.3.2). Transfection of both Wt and Mt plasmids gave rise to a large increase in expression of KMD6A transcript levels; approximately a 5,000-6,000 fold increase compared to control mock-transfected cells **(Figure 4.9A).** Both Wt and Mt plasmids lead to a decreased expression of AR-FL **(Figure 4.9B)**. Wt KDM6A plasmid led to a small but statically insignificant increase in AR-V7 expression whilst the Mt plasmid reduced expression of AR-V7. Both Wt and Mt plasmid transfection resulted in a reduced expression of PSA. It should be noted that no results for

these experiments were statistically significant. Regarding protein level changes, overexpression of both Wt and Mt KDM6A was confirmed using western blotting incorporating a Flag antibody to detect the Flag-tagged KDM6A isoforms expressed from the respective plasmids **(Figure 4.9C).** However, there appears to be little increase in KMD6A expression in the Wt experimental arm using the KDM6A Ab which is at odds with observations using the Flag Ab. Furthermore, no change in AR-V7 protein levels was observed after transfection with both KDM6A plasmids compared to the control.

Overall the data from this section suggest the demethylase activity of KMD6A is important for regulating expression AR-V7, and possibly essential for changes in alternative splicing patterns. This is the result of KDM6A Wt plasmids appearing to drive higher expression of AR-V7 than KMD6A Mt plasmids despite having similar expression levels in the cell lines tested. The limitation of this data is that transient transfections were used which notoriously have multiple variables such as transfection efficiencies between experiments and cell types and non-physiologically relevant levels of the protein of interest (Chong et al., 2021; Di Blasi et al., 2021). In addition to this, the loss of demethylase activity in the KMD6A Mt plasmid was reliant on data from other studies meaning caution should be aired when interpreting results from this data.

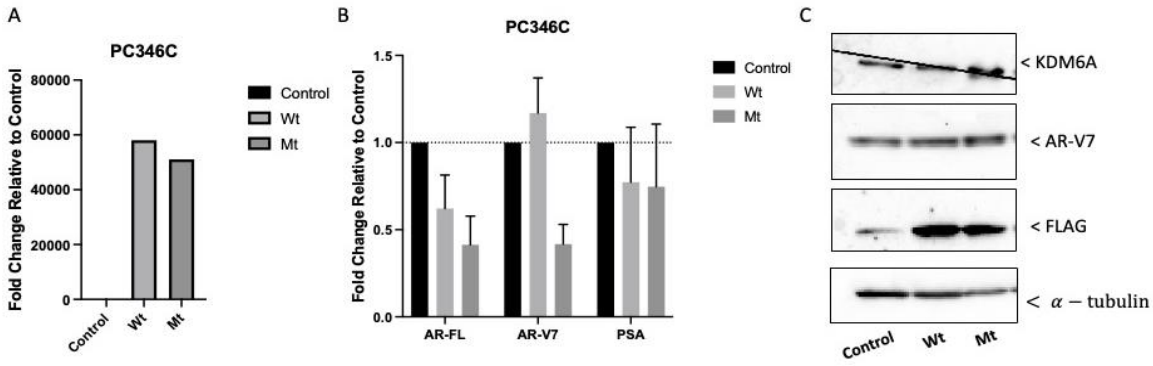

Figure 4.9 Overexpression of KDM6A in the PC346C Organoid Model. *All samples taken 72 hours post transfection. A-B) mRNA expression of KDM6A as well as gene of interest after over expression with KMD6A plasmid. C) Protein expression of lysates used in A and B. Plasmid contains FLAG tag in frame on KDM6A therefore used as surrogate of KMD6A expression. qPCR data comprises n=3 independent biological replicates, plotted as mean +/- SEM.*

4.4.5 Generation of a stable KDM6A over-expressing cell line

Due to problems associated with transient transfection of plasmids into recipient cell lines and organoids, including considerable variation in transfection efficiencies between experimental repeats which are likely contributing factors to variability in our previous findings, it was important to develop a CW22Rv1 cell line with stable expression of KMD6A Wt. The Wt KDM6A plasmid was chosen for two reasons: (i) patients with amplified *KDM6A* are typically wild-type, and (ii) time constraints prevented the successful generation of a Mt KDM6A overexpressing cell line derivative.

CWR22Rv1 cells were transfected with KDM6A Wt plasmid as described in 4.3.4 and clonal populations were isolated. Two clones were subsequently selected (Clone 28 and Clone 31) which appeared to show the highest expression of KDM6A compared to parental CWR22Rv1 control cells **(Figures 4.10A and B).** Both clones were further passaged and subjected to western blotting to determine if KMD6A overexpression was retained over multiple passages.

As shown in **Figure 4.10C**, initially at passage one (approximately one week after lysates from A and B were taken) C28 and C31 did not appear to have a higher expression than parental cells. At passage 10, C 28 appeared to have increased expression in KMD6A compared to the parental whilst clone C31 had reduced expression. This same trend was found at passage 15 suggesting a consistent upregulation of KMD6A in Clone 28.

KDM6A transcript levels were found to be approximately 3-fold up-regulated in Clone 28 by RT-qPCR **(Figure 4.10D)** which was significantly higher than the control. Clone 31 demonstrated reduced expression which supported the western blot data showing KMD6A levels lowered in this clone over time.

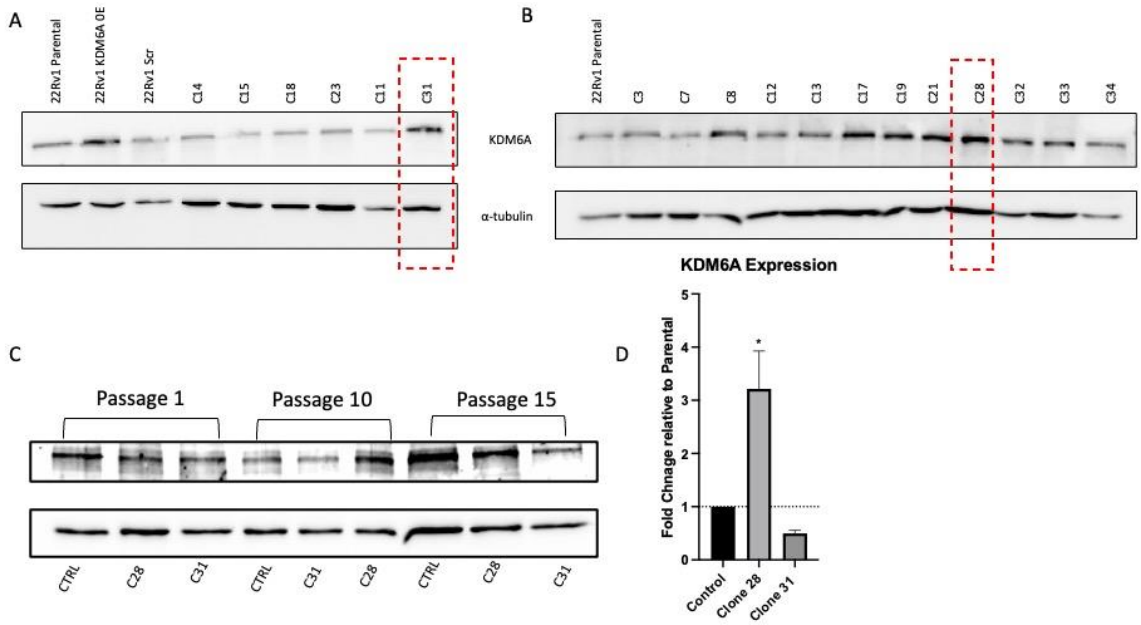

Figure 4.10 Profiling KMD6A Expression in stable cell line clones. A and B) *Protein expression by Western Blot. KDM6A expression of multiple homogenous clones transduced with KDM6A, compared to parental CW22Rv1s. Two highlighted clones are the ones we took forward for further studies. C) Protein expression by Western Blot. KMD6A expression of CW22Rv1 (Control), Clone 28 and Clone 31 over multiple passages. D) Comparison between CW22Rv1 (control), Clone 28 and Clone 31 of KDM6A mRNA expression. qPCR Data comprises n=3 independent biological replicates, plotted as mean +/- SEM. Statistical significance was calculated using an unpaired t-test where clones were compared to control (*=p<0.05, **=p<0.01, ***=p<0.001 and ****=p<0.0001).*

In addition to assessing KDM6A levels, expression of AR-FL, AR-V7 and PSA in both Clone 28 and Clone 31 were analysed **(Figure 4.11A-C).** Interestingly, Clone 28 which has detectably higher KDM6A transcript levels, had significantly higher expression of AR-V7, AR-FL and PSA compared to parental CWR22Rv1 control cells. In contrast, Clone 31 had a significantly lower expression of AR-V7 but no change in the expression of AR-FL and PSA compared to the control. The same lysates from passage 10 (shown in Figure 8) were utilised to profile AR isoforms at the protein level. There was higher expression of KMD6A, AR-FL and AR-Vs in Clone 28 compared to the control. Whilst Clone 31 appeared to have levels of AR isoforms equal to that of the parental line **(Figure 4.11D).**

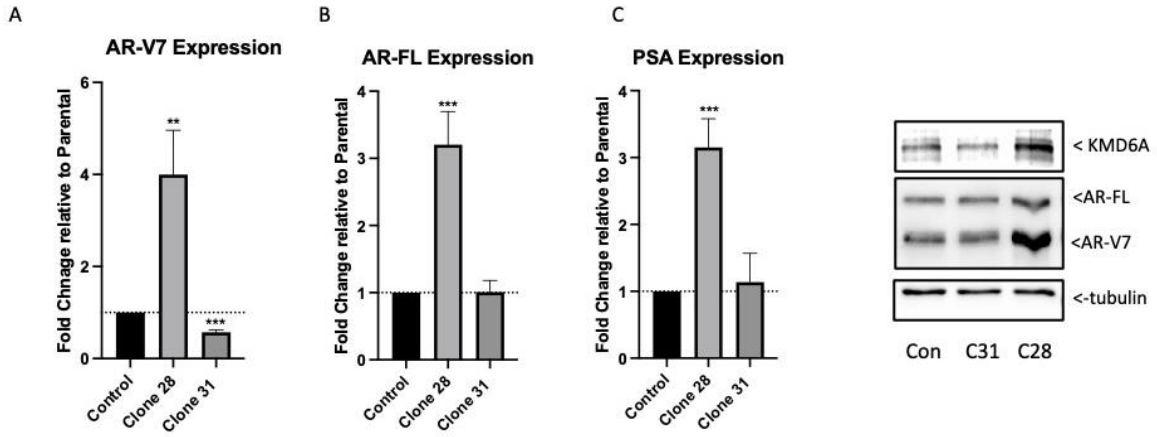

Figure 4.11 Profiling the expression of AR-FL, AR-V7 and PSA in stable cell lines. A) *Expression of AR-V7 is significantly higher in clone 28 compared to the parental line. Clone 31 has significantly lower expression.* ***B)*** *AR-FL is significantly higher expressed in Clone 28 compared to parental. There is no change in AR-FL expression in Clone 31 compared to parental.* ***C)*** *PSA expression is significantly higher in Clone 28 compared to the parental. PSA is unchanged in Clone 31.* ***D)*** *Protein expression by western blot. Clone 28 shows elevated levels of KDM6A, AR-FL and AR-V7 compared to the parental. qPCR data comprises n=3 independent biological replicates, plotted as mean +/- SEM Unpaired t-test used to calculate statistical significance (*=p<0.05, **=p<0.01, ***=p<0.001 and ****=p<0.0001). Only statistically significant results are marked by an asterisk, all other are non-significant.*

Proliferation assays revealed over 7 days there was no significant difference between the parental cell line and either OE clones **(Figure 4.12A).** The sensitivity of the overexpression clones to a KMD6A inhibitor (GSK-J4) was compared to the parental cells **(Figure 4.12B).** The difference in IC_{50} concentration between all three cell lines was minimal. Parental cells had an IC_{50} value was 0.95µM whilst C28 and C31 had IC_{50} of 1.23µM and 1.11µM respectively.

Given this lack of changes in drug sensitivity and proliferation, combined with time constraints no further work was conducted on the KDM6A OE cell lines.

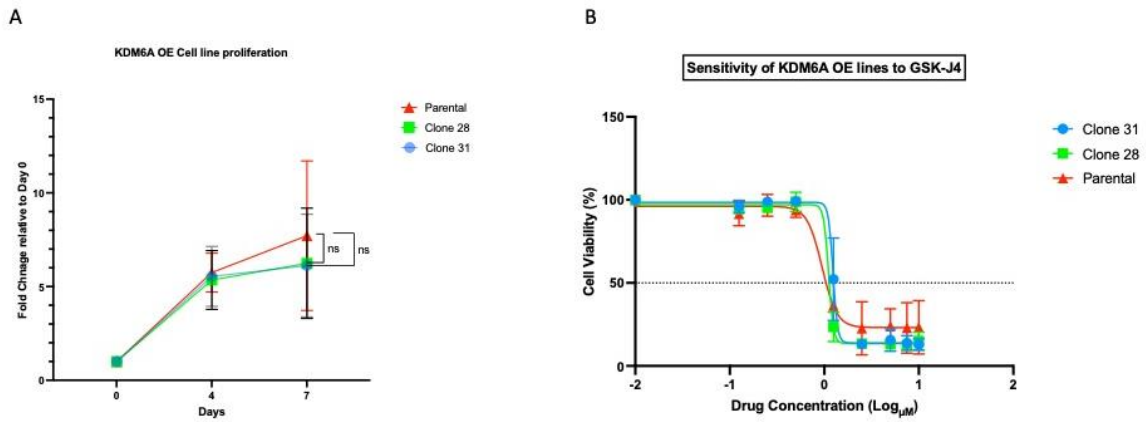

Figure 4.12 Proliferation and Drug sensitivity comparison between Parental cells and KMD6A OE clones. *A) SRB assay comparing proliferation of C28 and C31 to Parental cells over a 7 day period. Data for each cell line normalised to individual day zero. B) Survival curves of cells exposed to KDM6A inhibitor. Cells were exposed to inhibitor for 4 days before SRB assay was conducted. Data was normalised to DMSO untreated control.*

4.4.6 Generation of Enzalutamide Resistant Cell Line Model

We sought to establish an Enzalutamide-resistant VCaP model to understand the mechanism which drives Enzalutamide resistance and KDM6A involvement in this. Given that a large percentage of patients harbour KMD6A amplifications after treatment with anti-androgens, such as Enzalutamide, it was essential to develop an *in vitro* model to understand the role of KMD6A in disease progression. Considering HDMs can regulate mechanisms of resistance in PC such as; AR-V synthesis and AR amplification this model allows us to investigate KMD6A involvement in these processes and potentially unveil novel therapeutic options.

The VCaP cell line was chosen as a recipient model for making an enzalutamide-resistant derivative for multiple reasons which included: (i) VCaP cells are not resistant to Enzalutamide, unlike other cell lines such as the CW22Rv1; and (ii) VCaP cells respond to Enzalutamide by upregulating AR-V7s and therefore provide an interesting model to investigate AR-V synthesis and a potential role for KDM6A in this process.

VCaP Enzalutamide Resistant (VCaP-EnzaR) were generated as described in 4.3.5. To initiate the characterisation of the new derivative cell line, growth rates of the VCaP-EnzaR derivative was compared to the parental control. These experiments were conducted for approximately 18 months of culturing with Enzalutamide. There was no difference in growth rates between the two cell lines over six days **(Figure 4.13A).** A key

point to highlight is that both VCaP Parental and VCaP-EnzaR were cultured in FBS (10%) media. The only addition in media compositions was the addition of 10µM Enzalutamide. This was a useful control as it suggests that any changes seen between the two cell lines were because of the Enzalutamide only. Next, it was important to profile the expression of genes of interest, including *AR* isoforms, *PSA* and *KDM6A* between the VCaP-EnzaR and parental cells. The VCaP-EnzaR cell line had significantly higher expression of *KDM6A*, *AR-FL*, *AR-V7* and *PSA* **(Figure 4.13B)** as determined by RT-qPCR which was also validated at the protein level by western blotting **(Figure 4.13C).** The next step was to compare the expression of these genes between the VCaP-EnzaR cell lines and other cell lines resistant to Enzalutamide. For this, the CW22Rv1 and LNCaP95s were utilised as both harbour resistance to Enzalutamide (Leung et al., 2021, Li et al., 2013). For the analysis, expression of the genes was normalised to PNT1A as in Figure 4.4. The analysis reveals that the VCaP-EnzaR has significantly higher expression of both AR isoforms, PSA and KDM6A compared to the non-cancerous PNT1A cell line **(Figure 4.13 D-F).** The VCaP-EnzaR cell line has the highest expression of KMD6A compared to other Enzalutamide-resistant cell lines **(Figure 4.14 D).** In terms of AR isoform expression, the VCaP-EnzaR cell line had a higher expression of AR full length than the Cw22Rv1 but not as high of an expression as the LNCAP95s **(Figure 4.14 E).** Finally, whilst the VCaP-EnzaR cell line has a substantially high expression of AR-V7, its expression is less than that found in the CW2RV1 and LNCAP95s **(Figure 4.14 F).** Taken together, these results show that the novel VCaP-EnzaR cell line has comparable expression of AR isoforms and KMD6A to well-established Enzalutamide-resistant cell lines. Whilst there are some differences, this is to be expected given that cell lines have differences in AR copy numbers, methods of development and mechanisms of resistance.

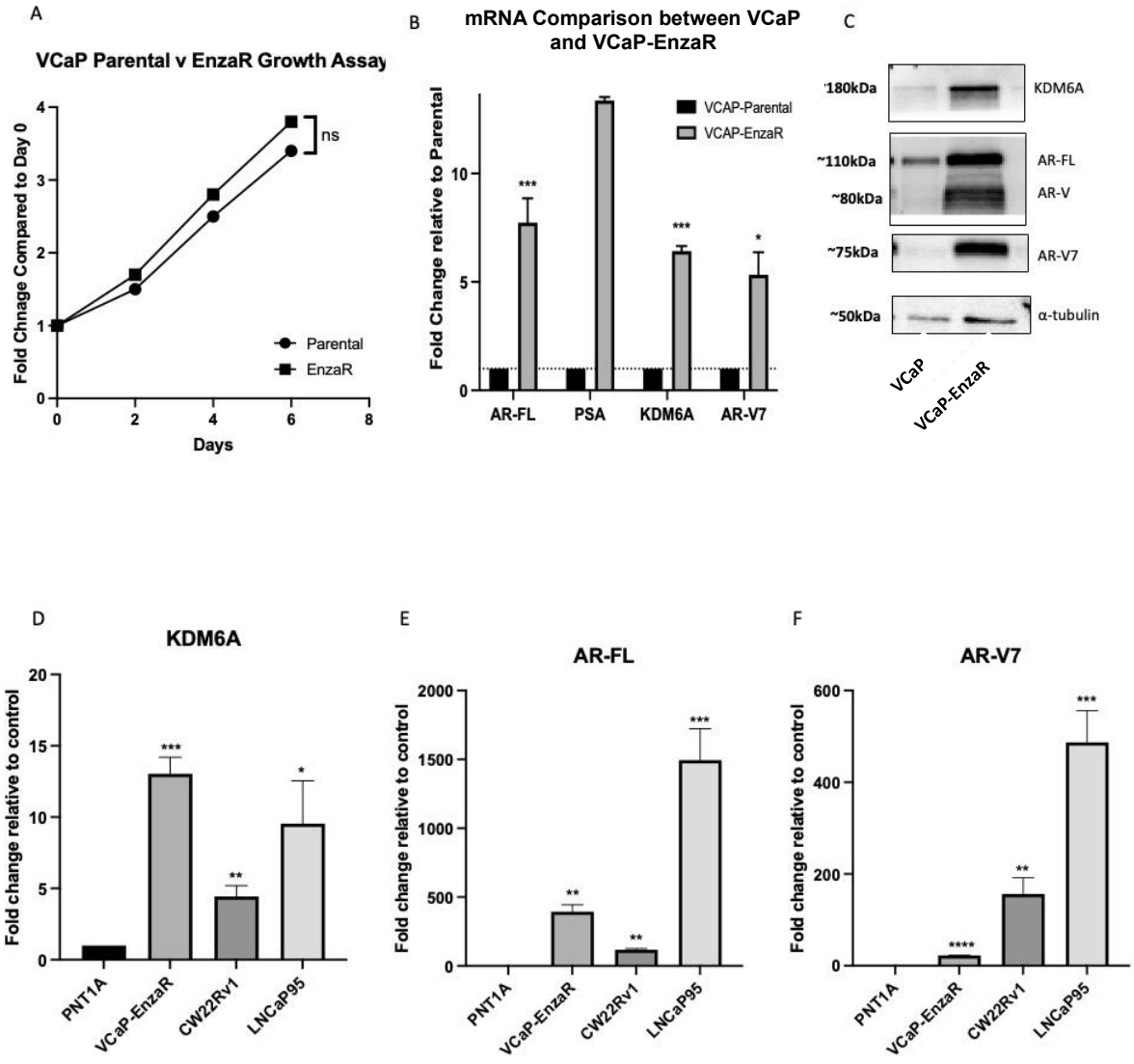

Figure 4.13 Characterising the VCaP-EnzaR cell line. *A) SRB assay to evaluate growth of both VCaP parental and VCaP-EnzaR cells. No difference in growth rates between cell lines when normalised to day 0. N=3. B) Expression comparison of AR-FL, AR-V7, PSA and KDM6A mRNA between VCaP parental and VCaP-EnzaR. All genes were significantly upregulated in the VCAP-EnzaR cell lines. C) Protein expression by Western Blot. VCaP-EnzaR had elevated levels of AR-V7, AR-FL and KDM6A when compared to the parentals. D-E) Comparison of Expression of AR Isoforms and KDM6A in Enzalutamide resistant cell lines. qPCR data comprises n=3 independent biological replicates, plotted as mean +/- SEM. Unpaired t-test used to calculate statistical significance (*=p<0.05, **=p<0.01, ***=p<0.001 and ****=p<0.0001). Only statistically significant results are marked by an asterisk, all other are non-significant.*

To comprehensively understand mechanisms driving enzalutamide resistance in this model, triplicate RNA samples of both parental and VCaP-EnzaR were subject to RNA sequencing. For this, both cell lines had been propagated in full media +/- Enzalutamide for approximately 12 months and were of similar passages. RNA lysates were generated from both cell lines from sequential passages. In total 6 samples were sent for paired-end RNA-Sequencing (3 Parental cell lines and 3 VCaP-EnzaR). Parental cells (no Enzalutamide) were used as the control for these experiments as the addition of Enzalutamide was the only difference in the culturing of the two cell lines. Additionally, because both cell lines were of a very similar passage this eliminated the chance of any differences being induced through passage differences.

Data was received through GENEWIZ in the form of raw FASTQ files. Each sample has two FASTQ files with ~30-40 million reads at ~150bp in length. The first process with the FASTQ files was to conduct a quality control assessment to ensure the quality of the data could be used in downstream analysis. Firstly, the RNA-Seq library was assessed using *FastQC (Andrews, 2010)* and a quality report for all samples was created with *MultiQC (Ewels et al., 2016)*. FastQC measures a range of metrics such as GC content and, the presence of overrepresented sequences which is indicative of contamination (Andrews, 2010). The result of the metrics for each sample are shown in **Figure 4.14.**

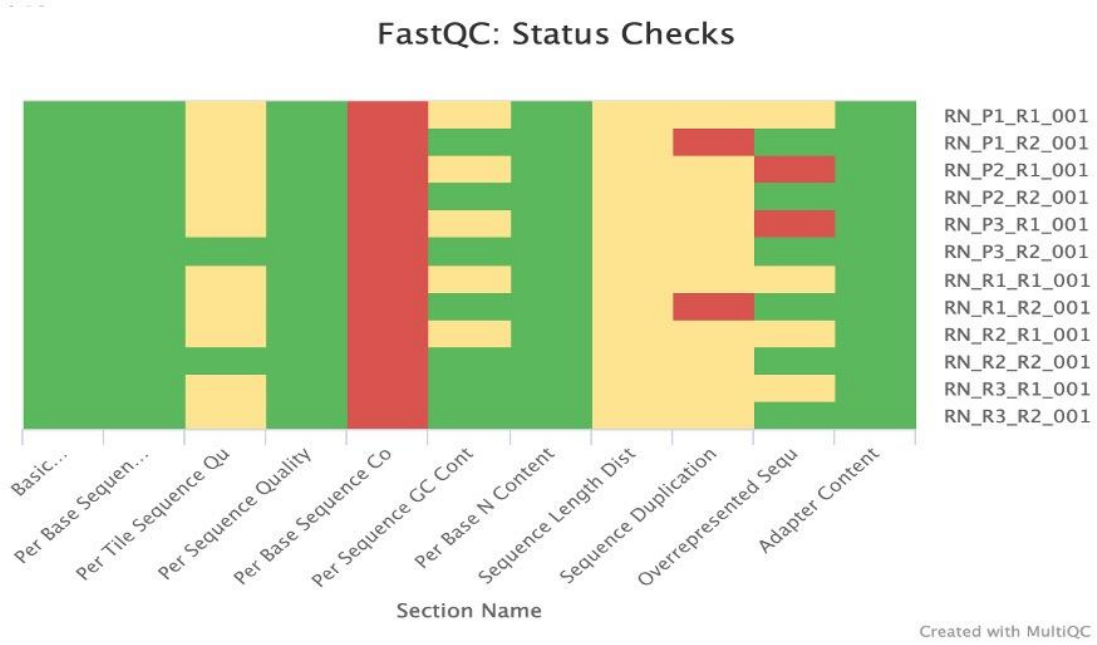

Figure 4.14 Result of FastQC for samples used in RNA-Seq Experiments. *The X-axis shows different parameters measured in FastQC analysis. The Y-axis shows reads for each sample; Parental cells (P1-3), VCaP-EnzaR (R1-3), each sample has two reads (R1 and R2) 12 reads in total. Green = passed QC, Amber = passed with warning, Red = Failed QC.*

Overall, the data reveals good-quality sequencing. Whilst it is apparent that all samples failed the 'Per Base Sequence Content'(Figure 4.14 7th Column) generally this issue does not have any implications for downstream analysis (Hansen et al., 2010). To give this issue more context, Per Base Sequence Content is essentially the proportion of each base position for which each of the four normal DNA bases has been called. In a normal library, the expectation is that the proportion for each base should be almost equal. The results received from these experiments failed this parameter due to a difference of <20% between A and T or G and C. However as shown in **Figure 4.15A** these divergences occurred in approximately the first 10bp in all samples, whilst for the rest of the read the lines run in parallel suggesting equal proportions (Andrews, 2010). The cause of this is the random hexamers used in the library preparation binding non-randomly as they should. It is unrelated to adapter sequences and simply 'trimming' the affected base pairs does not solve the issue (Hansen et al., 2010; Minshall & Git, 2020) Because the issue is limited to the 5' end of the read we do not exclude samples.

The next QC result to discuss is the 'Sequence Duplication' for which 10/12 samples have a warning whilst 2/12 samples have 'failed'. Again, this does not mean the samples

cannot be used for downstream analysis. As discussed by Parekh et al, 'Sequence Duplication' QC score tends to fail in RNA-Seq due to the presence of highly expressed genes and deduplication is not recommended (Parekh et al., 2016).

The final point to discuss from Figure 4.14 is 'overrepresented sequences'. For all samples, the first read (R1) had a warning, with two samples (Parental n=2 and parental n=3) failing this parameter due to them containing a sequencing which made up >1% of the total. Over-representative sequences can either be caused by a highly biology-significant sequence or perhaps library contamination. Investigating these 'Overrepresented sequences' revealed that the sequence was 'NNNNNNNNN…'. **(Figure 4.15B).** N sequence occurs when the sequencer is unable to make a base call. The N sequence occurred for all affected samples (R1s) early in the read **(Figure 4.15C)** and therefore can be disregarded.

Overall, whilst *FastQC* provided some warnings, upon further investigation none of them warranted a sample to be removed from further analysis.

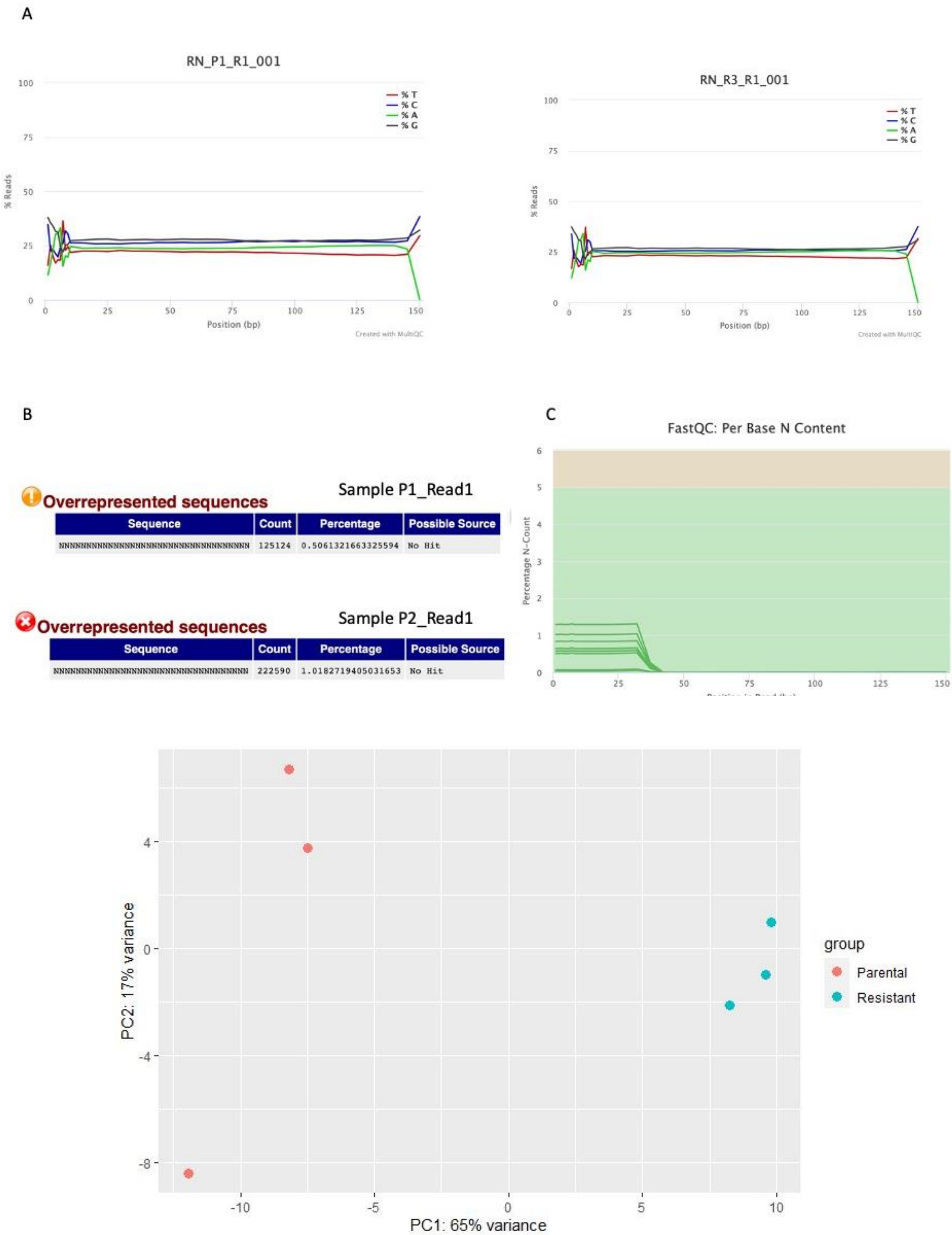

Figure 4.15 Analysis of parameters that failed FastQC. A) *Per Base Sequence Content of two samples (P1 and R3) to investigate proportionality of bases over reads. Samples failed this parameter due to discrepancies in the first 10bp of reads.* ***B)*** *The overrepresented sequences warning given for samples. Multiple Ns occur due to sequencers inability to assign correct base with confidence.* ***C)*** *Demonstration that N sequences from B were clustered in the start of the read.* ***D)*** *Principal component analysis (PCA) of DESeq2 normalised gene counts*

Once the quality control checks were completed, differential gene expression analysis (DGEA) was conducted between parental VCaP and VCaP-EnzaR derivative samples. To do this, RNA-SeQ reads were aligned using *STAR (Dobin et al., 2013)* to an hg38 human reference genome. The reads were assigned to exons which allowed a gene-level expression count using *featureCounts (Liao et al., 2013)* and the resulting count matrix was used for DGEA between experimental arms using the DESeq2 package. DESeq2 normalises data against unchanging genes for a specific library depth and composition. Samples which have been normalised can then be viewed using principle component analysis (PCA) which essentially reveals intra-arm similarities and inter-arm differences (Groth et al., 2013). The result reveals that experimental arms (VCaP-EnzaR and VCAP Parental for this work) clustered closely together meaning there is little variation within experimental arms **(Figure 4.15 D).** As PC1 (X-axis) represent a greater percentage of variability between samples than PC2 (Y-axis) (Groth et al., 2013) it was evident that between experimental arms there were significant differences. The PCA data reveals that i) intra-samples have little variance and i)inter-samples (i.e. between experimental arms) have good separation indicating a larger change in gene number.

There was a total of 1146 significantly differentially expressed genes (SDEGs) between the two cell lines; 493 genes were upregulated in the VCaP-EnzaR line (Log_2 FC greater than 0.5) and 653 genes were downregulated in the VCaP-EnzaR cell line (Log_2 FC less than -0.5). **Figure 4.16A** gives an overview of the 20 most up and downregulated genes between the two cell lines. Subsequently, DEGs from this study were next compared to two other transcriptomic data sets in which Enzalutamide-resistant VCaPs had been generated and subject to RNA-sequencing (Kregel et al., 2016; Lelong et al., 2022) The Kregel data set was generated by a very similar experimental setup to our study. VCaP cells were plated and continuously cultured in 10μM Enzalutamide for at least six months. The study had 4 experimental repeats for each arm sent for sequencing. The second data set from LeLong *et al.* was generated from VCaP xenograft tumours subject to prolonged exposure to Enzalutamide (Lelong et al., 2022).

Between the three datasets there were 70 genes commonly significantly upregulated **(Table 3)** Reassuringly, genes such as AR, KLK3 and YAP1 which are essential in Enzalutamide resistance and disease progression were amongst the genes commonly upregulated (Conteduca et al., 2017; Marx et al., 2020). In contrast, there were only 25

genes commonly significantly downregulated between all three data sets **(Table 4) (Figure 4.16 B).** Given that all three datasets had the same cut-off for DEG expression applied (Log_2 FC >0.58, FDR <0.05) it is surprising to see how many more DEG the LeLong data set contains. A possible explanation may come from the experimental set. In the LeLong experiment, VCaP cells were implanted into mice before the establishment of Enzalutamide resistance and therefore there may be differences in growth rate, nutrient/growth factor availability and cell cycle which could explain this (Duval et al., 2017; Hum et al., 2020). Overall it was comforting to see a good number of overlaps between the datasets.

To gain a better understanding of altered pathways which may give rise to enzalutamide resistance in the VCaP-EnzR cells, the total set of differentially expressed genes (DEGs) were run through Gene Set Enrichment Analysis (GSEA) against the 'Hallmarks" signatures which define a range of specific and well-defined biological states or processes **(Figure 4.16C).** From our data set only 3 gene sets were significantly downregulated (NES <-1.5, FDR q-value <0.25). On the other hand, 15 gene sets were significantly upregulated with several gene sets involved in immunobiological processes (NES >1.5, FDR <0.25).

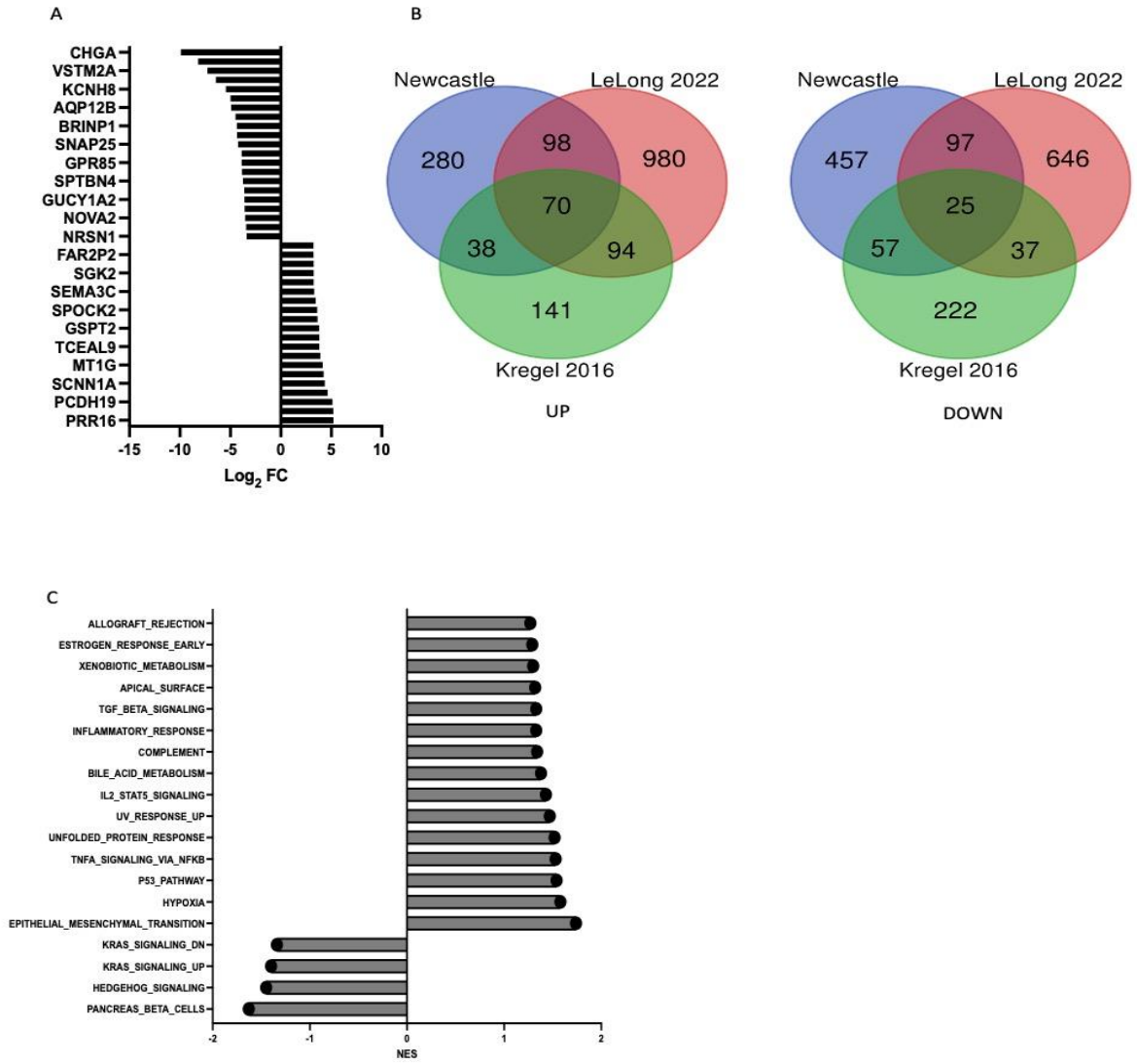

Figure 4.16 Transcriptomic analysis of VCaP-EnzaR characterised by an aggressive phenotype. A) *20 most significantly up and downregulated genes in the VCaP-EnzaR cell line compared to the parental based on Log2FC.* ***B)*** *Overlap of significantly DEG in our dataset compared to two other datasets which had generated/ characterised VCaP-EnzaR cells (See in text for reference). 70 genes are commonly upregulated in all three data sets, whilst 25 genes are commonly downregulated.* ***C)*** *GSEA of our data set on the 'Hallmarks'. Pathways significantly altered in the VCaP-EnzaR cell are shown. Epithelial to mesenchymal transition is the most enriched pathway.*

Table 10 List of genes commonly Significantly differentially upregulated between VCaP-EnzaR data sets

MPZL2	GMPR	FZD7	SLC7A8	TAX1BP3	YAP1	SMAD6
MBNL2	UGT2B15	TLL2	SHMT1	TMC5	IGFBP3	SAT1
NWD1	RGS4	PI15	CA12	FBLN2	EPAS1	AGR2
AGR3	BAMBI	RASSF10	CCNO	KCNK13	LGR4	HOPX
SOX13	CLSTN2	SGK2	TSPAN15	TGFA	AR	
AIDA	IRF6	SMPDL3A	CRABP2	SRPX	TRNP1	
TGM2	PRKCD	GPX2	MGLL	ZDHHC14	VAV3	
A1CF	ANTXR2	CDKN2B	PDLIM1	KRT19	KLK3	
SHROOM1	CROT	CSRNP1	REG4	MATN2	FXYD3	
TAGLN2	ITPR2	SLC31A2	AQP3	ARHGAP6	SELENBP1	
PLA2G2A	DHRS3	CWH43	KLHL5	ADM	TRIB2	

Table 11 List of genes commonly Significantly differentially Downregulated between VCaP-EnzaR data sets

TRPM8	CAMK1D	ST7
CNTFR	KCNN2	HSD17B6
ETS2	KCNH8	PROCR
ATP8B4	WNT2	
CNRIP1	SIRPA	
ASTN2	PCDHB10	
NPY	LIPG	
CUX2	CNTNAP2	
BEND4	FAT1	
MCCC2	CLDN8	
SESN3	F3	

Of interest was that epithelial to mesenchymal transition (EMT) was the top hit from the GSEA analysis (NES 1.74, FDR 0.04) **(Figure 4.17A).** To validate the enrichment of this pathway, the creation of spheroids in Matrigel was utilised to assess the 3D forming ability of the VCaP-EnzaR versus parental cells. As shown in **Figure 4.17B,** both at day 0 and day 10, the parental VCaP cells had significantly larger spheroids compared to the VCaP-EnzaR; which rarely formed spheroids. At day 10, the parental spheroids had statistically significantly larger diameters than the VCaP-EnzaR with an average of 365 micron compared to 94.67 micron, respectively **(Figure 4.17C).** Loss of spheroid forming capacity has previously been characterised as an EMT phenotype and could be an explanation for VCaP-EnzaR failing to form spheroids (Chu et al., 2009; Stadler et al., 2018).

A scratch assay was also conducted as this is a simple method to measure the migration capacity of cells (X. Lu et al., 2018; Shao et al., 2017). Cells with a mesenchymal phenotype should migrate to the scratch site and thus there should be a difference between the two cell lines. Given the increased doubling time with VCaP cells, images were taken 5 and 8 days after the scratch was conducted. Unfortunately, as shown in **Figure 4.17D** the results of this experiment were inconclusive. This was due to the scratching of VCaP-EnzaR cells causing 'snagging' and 'tearing' of the monolayer (Indicated by red arrows). This does not occur in the parental cells where a smooth scratch is formed. Additionally, the VCaP-EnzaR cells showed a loss of adhesion to the culture ware and as a result, washing of the cells caused significant cell loss. Whilst this made measurements of wound healing impossible, loss of adherence is a key phenotype of cells undergoing EMT due to loss of cell polarity, cell-cell adhesion and attachment to basement membranes which allowed them to become more invasive (Bornes et al., 2021; Cervantes-Arias et al., 2013; Morata-Tarifa et al., 2016). This suggests that the VCaP-EnzaR cells have a phenotype that is associated with EMT however additional experimental work could confirm this.

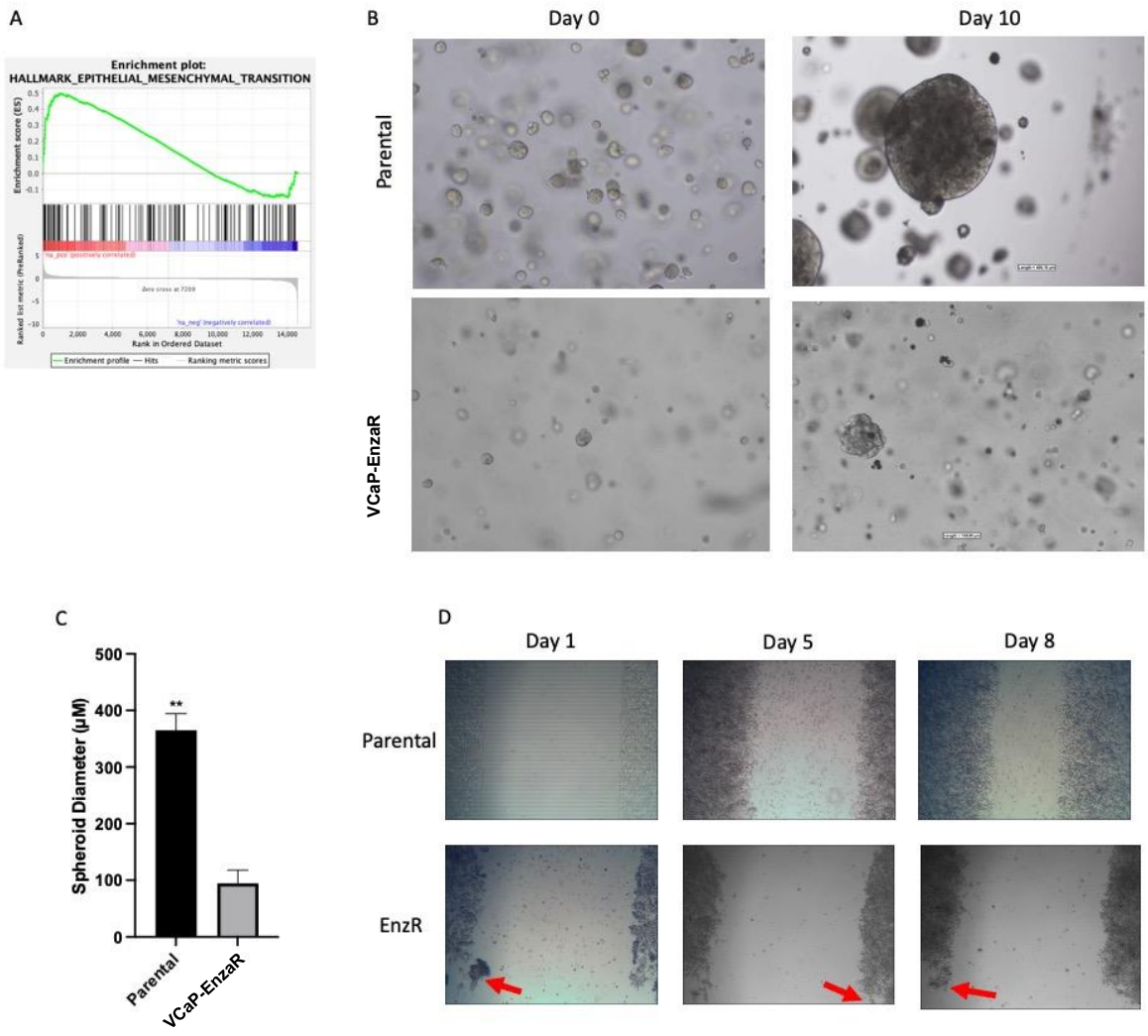

Figure 4.17 Validation of EMT upregulation in the VCaP-EnzaR Cell line. *A) Epithelial mesenchymal transition plot confirming strong upregulation of the pathways. NES 1.7, FDR <0.25. B) 3D spheroid formation assay in Matrigel. Parental VCaPS are able readily form large spheroid in culture whilst the VCaP-EnzaR do not form sturcutures. C) Average diameter of VCaP parental spheroid at day 10 are significantly larger than those from VCaP-EnzaR. N=9, 3 spheroids imaged from three different wells for both cell lines at day 10. D) Scratch assay in cell lines and recovery over wound over multiple days. Data comprises n=3 independent biological replicates, plotted as mean +/- SEM. Unpaired t-test used to calculate statistical significance. (*=p<0.05, **=p<0.01, ***=p<0.001 and ****=p<0.0001).*

To further investigate the functional roles of DEGs in the VCaP-EnzaR data set, GO and KEGG term enrichment analyses were conducted on the Database for Annotation, Visualisation, and Integrated Discovery (DAVID) **(Figure 4.18 A and B).** Three categories were included in the GO analyses: Biological processes (BP), molecular function (MF) and cellular component (CC). For upregulated DEGs, BP terms included lipid metabolism, Angiogenesis and Cell adhesion, which coincides with the EMT gene-set upregulation. The CC terms from these genes include cytoplasm, cytoskeletons, and endoplasmic reticulum. MF terms include developmental proteins, acetyltransferase and both Ion and voltage-gated channels. Using the same process, but for the significantly downregulated genes, we see BP terms largely associated with transport, sodium, potassium, and ion as well as neurogenesis. MF terms include differentiation and both ion and potassium channels. For CC terms were dominated by membranes. We had very few KEGG pathways which were significantly altered (NES > 1.5 or < -1.5, FDR <0.25) **(Figure 4.18C).**

Due to the elevated levels of AR-V7 in the VCaP-EnzaR cell line, a bespoke AR-V7 signature data set containing 59 genes associated with nuclear AR-V7 protein expression was next compared to the VCaP-EnzR data set (Sharp et al., 2019). This gene set was significantly enriched in the VCaP-EnzaR cell line compared to the control (NES +1.75, FDR 0.005) **(Figure 4.19A).** It is also noteworthy that the VCaP-EnzaR cell line had a significant enrichment for the Hallmark 'Androgen Response' (NES 1.18, FDR 0.15) **(Figure 4.19B).** Given the increases in AR-V7 expression as well as the enrichment for AR-V7 gene signature, it was perhaps surprising that both the KEGG Spliceosome Gene set and a bespoke 268 gene "Splicing Signature" gene set were not positively enriched in the VCaP-EnzaR cells (NES +1.16, FDR 1 and NES -0.84, FDR 0.83 respectively) **(Figure 4.19C).**

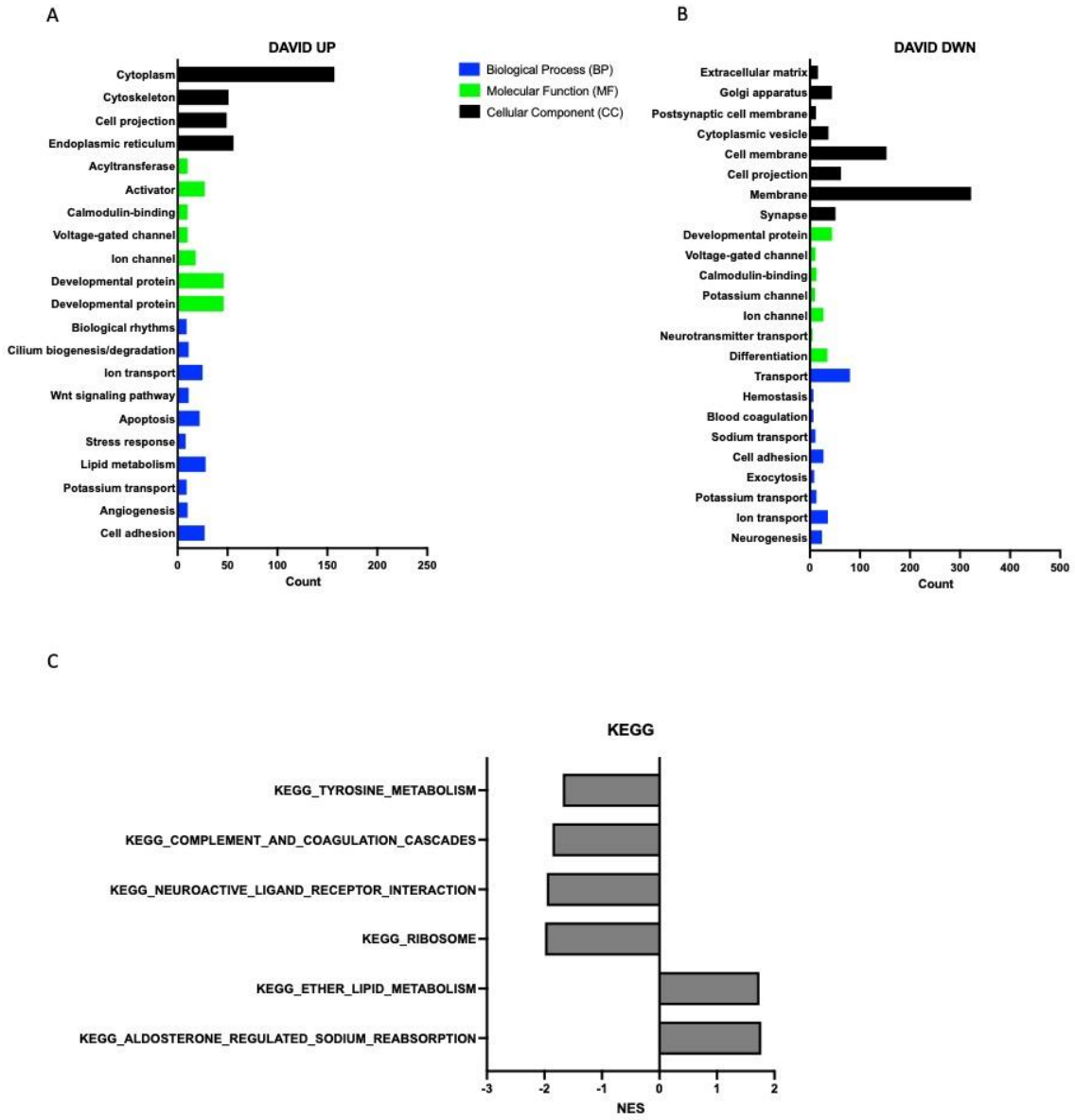

Figure 4.18 DAVID analyses of GO terms and KEGG pathway alterations in VCaP-EnzaR cells. A) *GO terms significantly upregulated in the VCaP-EnzaR cells.* ***B)*** *GO terms significantly downregulated in VCaP-EnzaR cells.* ***C****) KEGG pathways significantly altered in the VCaP-EnzaR cell line.*

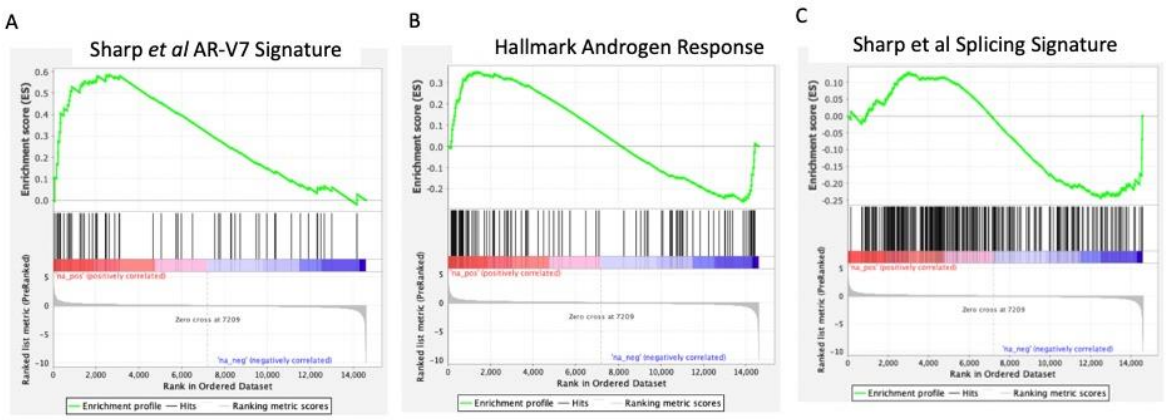

Figure 4.19 Bespoke enrichment plots of interest for the VCaP-EnzaR Cell line. A-C *Bespoke gene sets from Sharp et al 2019 relevant to the VCaP-EnzaR line.* ***A)*** *Enrichment for AR-V7 signature, that is genes which are supposed to be regulated by AR-V7.* ***B)*** *Enrichment for genes known to be regulated by androgen.* ***C)*** *The gene list associated with known splicing factors was not enriched in the VCaP-EnzaR cells.*

4.5 Discussion

The scope of this work was to deepen our understanding of HDMs, specifically KDM6A, and how they aid the progression of prostate cancer. The rationale for this is that current treatments which target the AR signalling cascade are unsuccessful over a prolonged time due to resistance. Targeting alternative proteins which play a role in CRPC progression may make current treatments more effective for longer. As mentioned in the introduction, HDMs regulate many signalling cascades and functions within cells such as splicing, transcription factor binding and metabolism which may be hi-jacked in cancers. A previous pilot study conducted in the laboratory identified KDM6A, amongst other HDMs, as being potentially involved in AR-V generation since data demonstrated that KDM6A knockdown significantly reduced AR-V7 expression in PC cell lines. Studies have shown KMD6A to regulate AR activity and physically interact with the AR although further validation of this was missing (Grasso et al., 2012; Morozov et al., 2017). It was also implicated that KDM6A was essential in regulating metabolic changes which could play a role in therapy resistance and the progression to CRPC (Chianese et al., 2022). Given that other KMDS has previously been shown to regulate AR-V7 generation we believed that KMD6A may regulate a range of pathways essential for cancer progression thus being an attractive therapeutic target (Duan et al., 2019; Fan et al., 2018; D. E. Tang et al., 2020).

By analysing publicly available data, it became evident that KDM6A was overexpressed in advanced disease and showed elevated expression in AR-V7+ compared

to AR-V7^{-} tumours. This was of particular interest given the role of other histone demethylases in regulating alternative splicing such as KDM4B and KDM3A (Duan et al., 2019; Fan et al., 2018). It was noteworthy that in the SU2C/PCF consortium data set, which contains 444 patients, *KDM6A* was altered in almost 15% of samples. This was higher than other data sets which focussed on metastatic tumours, namely Grasso *et al. (Grasso et al., 2012)* and Robinson *et al.* (Robinson et al., 2015), however, these datasets were very limited in size (n=50 and n=155 respectively). To put this into context, genes well known to play a role in PC such as SPOP and BRCA2 (Dai et al., 2017; Messina et al., 2020; Nakazawa et al., 2022) had a mutational rate of 11% and 12% respectively in the same patient cohort (Abida et al., 2019). This suggests KDM6A is important to CRPC disease and therefore warrants further investigation.

As mentioned in the results, 10% of patients from the SU2C/PCF data set harbour a copy-number amplification to *KMD6A*. Recently, collaborators of the Newcastle Prostate Group demonstrated that *KDM6A* amplification was present in approximately 60% of CRPC xenograft models, while no HSPC xenograft models harboured detectable *KDM6A* alterations (Moll et al., 2022). This suggests that KMD6A is important in treatment resistance. Whether this is through KDM6A regulating resistance mechanisms such as alternative splicing and AR gene amplification or KMD6A being altered during the epigenome reprogramming in disease progression (Goel et al., 2022; Pomerantz et al., 2020; T. Severson et al., 2022) remains unclear. Perhaps both ideas are not mutually exclusive, and it could be the case that KDM6A is heavily altered during epigenome reprogramming which in turn causes it to influence resistance mechanisms.

Whilst some of the initial ectopic KDM6A overexpression work was of interest, in that it showed upregulation of AR-V7 upon KDM6A overexpression, there were perhaps some results which were initially surprising. The reduced expression of AR isoforms in the VCaP cell after KDM6A overexpression can perhaps be explained by other studies. Previously it has been demonstrated that the VCaP cell line has a novel feedback loop by which the AR can downregulate expression of its own gene when stimulated by cognate ligands (Cai et al., 2011). As will become evident later in this work, there is an interaction between KMD6A and AR and therefore by over-expressing KDM6A, we may potentially hyperactivate selective AR-mediated transcription which, in VCaPs cells, downregulates

AR gene expression. This may be a contributing factor in the observed reduction in *PSA* expression.

Extending these KDM6A overexpression studies into the patient-derived organoid PC346C demonstrated minimal changes in *AR* isoform and *PSA* expression. There are factors to consider when interpreting these results. Firstly, because it was not possible to verify transfection efficiencies, for example by immunofluorescent microscopy, which may explain the low levels of KMD6A after transfection with either Wt or Mt plasmids. Due to time constraints, and lack of a working protocol whilst in Rotterdam there was no time to optimise the transfection protocol. Also, we were unable to profile the H3K27me3 marks in the organoid lines following transfections and thus it is unclear as to how much of the plasmid integrated into the cells. Additionally, whilst there was a substantial expression of the FLAG tag, assessed by western blot, this did not transpire to elevated levels of KDM6A. It would be interesting to carry out similar work in the newly generated and characterised CRPC organoid models from the Van Weerden lab. The new organoid lines come from heavily pre-treated patients to span diverse patient profiles of CRPC. For example, the organoid lines harbour a range of genomic alterations in members of clinically actionable pathways previously reported to be affected in PCa including the AR, PI3K, WNT, MAPK/ERK, DNA repair pathways and the cell cycle (Van Hemelryk et al., 2021). In addition, the organoid lines show a range of AR-V7 expression which would be relevant to this work.

Modelling the most common KDM6A mutation found in CRPC patients, gene amplification, is a critical tool to dissect the role this mutation has on the development of the disease. As highlighted in the introduction KDM6A is known to alter the metabolomics of PC and has been implicated to interact with the AR (Chang et al., 2019; Chianese et al., 2022). It therefore warranted the establishment of in vitro models to deepen our understanding of KDM6A and whether it had additional functions to those already in literature. As mentioned previously, the cells were generated through lentiviral transfection followed by clonal isolation. The CW22Rv1 backbone was used due to it having expression of multiple AR isoforms thus we could assess the effect of KMD6A OE on these. Also, the CW22Rv1 cell line does not harbour mutations in KMD6A and therefore any changes seen in AR isoform expression were because of KMD6A overexpression. In the future, the CW22Rv1 cells would also be an ideal model for introducing additional

KDM6A mutations discussed in section 4.4.1 such as frameshift indels. These mutations could be induced through CRISPR-Cas9 techniques as previously described (D. Chen et al., 2018; Lalonde et al., 2017).

Clone 28 and Clone 31 appeared to have increased KDM6A expression compared to the parental cells that were propagated and used for experiments. It was startingly the difference in AR-V7, AR-FL and PSA levels between the two derived clones. It was comforting to see that the increased expression of KDM6A Wt in Clone 28 was also reflected in the levels of AR-FL, AR-V7 and PSA both at the transcript and protein level. Because these cells were generated late in the project, there was insufficient time to characterise them further using RNA-Seq experiments which would be a hugely beneficial step to understand the global transcriptomic impact of elevated KDM6A. An observation from the work was that in the later passages of the KDM6A OE clones appeared to have lower expression of KMD6A compared to early clones. The plasmid used to generate the KMD6A OE clones contained an E1A promoter which is usually refractory to methylation-based silencing which may occur through KMD6A OE (X. Wang et al., 2017). A possible explanation is that KDM6A OE in the background of CW22RV1 cells is cytostatic, which may explain why KDM6A OE clones have slightly lower rates of proliferation. This may lead to clones without KMD6A OE overtaking the culture despite the presence of puromycin. In hindsight, the generation of a KDM6A Mt cell line in parallel would have been beneficial and this is ongoing work in the lab. This will be especially insightful given that overexpression of KDM6A Mt did have some effect on PSA and AR-FL expression in LNCaP96 and CW22Rv1-AR-EK cells. Combined with the literature demonstrating that KDM6A has catalytic independent functions through the TRP domain(Shpargel et al., 2017; C. Wang et al., 2012; G. Xie et al., 2017) development of KDM6A Mt overexpression lines will be insightful to see these roles in the context of CRPC.

The novel VCaP-EnzaR cell line which was generated through continuous propagation of VCaP cells with 10µM Enzalutamide for over 12 months is an excellent in vitro tool to understanding Enzalutamide resistance, as seen in CRPC patients, and the role of KDM6A in this process. The VCap-EnzaR cell lines proved to have significantly higher expression of AR-FL, AR-V7 and PSA compared to VCaP-Parenal which models what is seen in CRPC patients treated with Enzalutamide (Del Re et al., 2019; Sharp et al., 2019) Given the high expression of AR isoforms, it was interesting to see also an increase in KMD6A

expression. Expression of KDM6A in the VCaP-EnzaR was around 6-fold higher than in the parental cells, and a noticeable increase was also seen at the protein level. This is promising as it replicated KDM6A amplifications seen in CRPC patients but also suggests a correlation between KMD6A expression and AR isoforms. It was also interesting to note that KDM6A was highly expressed in other Enzalutamide-resistant cell lines compared to Enzalutamide sensitive (LNCaPs) and non-cancer prostate cell lines (PNT1A). Suggestive of a role for KDM6A in treatment resistance.

Additional work will be conducted to validate the significance of KMD6A expression and AR isoform expression. Additionally, it was exciting to see a comparable expression of AR isoforms and KDM6A compared to the other Enzalutamide-resistant cell lines; CW22Rv1 and LNCaP95. Whilst the LNCaP95 cell lines appear to have the highest mRNA expression of AR isoforms, our work demonstrates that at the protein level, the expression of AR isoforms is very comparable if not slightly higher in the VCaP-EnzaR cells. A possible explanation may be that the LNCaP95s have a significantly quicker doubling time compared to the VCaP-EnzaR (55 vs ~220 hours) thus having higher expression of genes such as AR (Crissman & Steinkamp, 1973; Kempe et al., 2015). AR is also a driver of G1 progression in the cell cycle therefore more rapidly dividing cells may have higher expression (Balk & Knudsen, 2008; Koryakina et al., 2015).

Chapter 5: Assessing the effect of KDM6A knockdown and enzymatic inhibition on AR signalling and enzalutamide resistance in PC

5.1 Introduction

As there was some indication from chapter 4 that overexpression of KDM6A correlated to an upregulation of AR-V7 levels, the effect of inhibiting KMD6A expression through small interfering RNA (siRNA)-mediated knockdown (KD) or with a KMD6A inhibitor was assessed. It was hoped that these approaches would deepen our understanding of the role KMD6A in regulating AR isoform generation and activity in PC cell lines.

siRNAs are a powerful tool in molecular biology. siRNAs comprise a 20-30 nucleotide double-stranded RNA sequence complementary to the mRNA transcript of a gene of interest. Once siRNAs are transfected into cells, they become incorporated into the RNA-induced silencing complex (RISC); whereby they are unwound to enable guide strand engagement with the target mRNA of interest, thus recruiting the RISC complex to the mRNA. As a result, the target transcript is degraded leading to inhibition of protein synthesis and a reduction in protein abundance; a term referred to as 'knockdown' (KD) (Alshaer et al., 2021; Dana et al., 2017). KD with appropriately designed siRNA normally results in around a 50%-75% reduction in the target of interest for approximately five days (Han et al., 2018).

Due to the robust reduction in target expression, as well as specificity of the siRNA, they have extremely high therapeutic potential. Concerns surround siRNAs regarding their potential off target effects; however, these can be mitigated with advances in the technologies. Using siRNA pools (multiple siRNA targeting same gene), adding chemical modifications to the guide strand and improved design algorithms have all vastly reduced off target effects (Bramsen et al., 2010; Kittler et al., 2007; Parsons et al., 2009). Whilst efforts to utilise siRNAs in the clinic have been hampered by inefficient delivery systems, it should be noted that a handful of siRNAs have been approved by NICE and/or the FDA suggesting a new era of siRNA therapeutics may be arising (Ali Zaidi et al., 2023; Walker, 2023).

Whilst siRNAs are a useful tool, in the case of KMD6A, for example, which has a catalytic function, a more targeted approach to inhibiting this can be achieved using small-

molecular inhibitors. GSK-J4, the pro-drug of GSK-J1, was first described in 2012 as a specific inhibitor of KDM6A/6B (Kruidenier et al., 2012). The compound is a competitive inhibitor of both 2-oxoglutarate (a-ketoglutarate) and Fe^{2+} which are essential co-factors for the JmjC demethylase catalytic activity. According to the original article, GSK-J4 was specific to the KMD6A family by both structural and inhibitor interaction mechanisms. Kruidenier et al., concluded that these key structural and recognition determinants were only possessed by members of the KMD6 family. More recently, however, the specificity of GSK-J4 has come under question as it was demonstrated that, at higher concentrations, GSK-J4 also inhibited catalytic activities of other KMD subfamilies such as KDM5B/C and KDM4A (Heinemann et al., 2014). It should be noted that according to Heinemann et al, GSK-J4 has half-maximum inhibitory concentration (IC50) towards KDM6A and KDM6B of 6.6µM and 8.8µM respectively. With this in mind, no doses above a final concentration of 5µM were use in the following work to ensure effects were not due to inhibition of other KDM activity. Currently, there are no other potent inhibitors of KDM6A, and GSK-J4 is still a useful compound for studying the catalytic function of KDM6A. It is worth noting that to date very few drugs that modulate the epigenome have been approved by the FDA largely due to poor pharmacokinetic and safety/tolerability profiles, largely induced by off-target effects (Feehley et al., 2023).

To date, there are no RNA-Seq data sets which have combined both siRNA KD and GSK-J4 treatment from the same experimental setup. Given that mechanisms of Enzalutamide resistance are poorly understood, we sort to interrogate global transcriptome effects of KDM6A KD and inhibition to provide insight into the role, if any, of KMD6A in the development of Enzalutamide resistance. In addition to this, as our experimental set-up included both KD and a catalytic inhibitor, it was anticipated we would be able to understand both catalytic-dependent and -independent genes and processes regulated by KDM6A. This is significant to explore given that other histone demethylase have been shown to regulate processes such as AR activity, alternative splicing and PC metabolomics through both catalytic-dependent and -independent means (Fan et al., 2018; Metzler et al., 2023b; Sehrawat et al., 2018; Z. Yang et al., 2020). Along with Enzalutamide resistance, it was anticipated that experiments from this chapter would also address the possible role of KMD6A in regulating AR splicing.

5.2 Aims

This chapter aims to utilise both siRNAs and KDM6A inhibitors to better understand the role of KMD6A in regulating AR signalling and prostate cancer progression in different disease models. By combining these experiments with transcriptomic analysis, we can build a comprehensive understanding of the role of KDM6A in global transcriptional regulation and ascertain the existence of non-catalytic roles of the demethylase.

The aims of this chapter are as follows:

1. Investigate the effect of KDM6A KD and inhibition on AR signalling and PC growth
2. Combine public and in-house datasets to assess pathways regulated by KDM6A which are prevalent in CRPC
3. Assess the effect of KDM6A inhibition on Enzalutamide sensitivity

5.3 Materials and Methods

5.3.1 Drug treatments of cell lines

GSK-J4 (Selleckchem S7070) was received in powder form and resuspended in 100 % DMSO to a final concentration of 100 mM. Stocks were stored at -80^{o}C until required.

Enzalutamide (Selleckchem S1250) was received in powder form and resuspended in 100% DMSO to a final concentration of 30 mM. Stocks were stored at -80^{o}C until required.

For obtaining IC_{50} values of prostate cancer cell lines to GSK-J4, cells were seeded at $2x10^3$ (or $10x10^3$ for VCaP cells) cells per well of a 96-well plate and incubated until 80% confluent. Once confluent, media was removed and replaced with fresh media containing the desired concentration of GSK-J4. Cells were incubated with the compound for four days after which the cells were fixed and processed using an SRB assay.

For Enzalutamide re-sensitivity assays, cells were seeded as described above. However, when the media was replaced, it contained the desired concentration of both Enzalutamide and GSK-J4. Cells were subsequently incubated for 4 days after which the cells were fixed and processed using an SRB assay. Cell viability was normalised to untreated DMSO control. Synergy scores were calculated using SyngerFinder (Ianevski et al., 2022). For re-sensitivity assays involving KDM6A KD, cells were seeded into 96-well plates as described above. The next day, the media was replaced with media containing siRNA to a final concentration of 25 nM. 24 hours later, the desired concentration of Enzalutamide was added to corresponding wells. Plates were incubated there harvested at stated time points.

To assess the effect of GSK-J4 on the expression of AR-V7 and AR target genes, cells were seeded in 6-well plates at $2\text{-}5x10^5$ cells per well depending on the cell line. Once the cells reached 80% confluency, media was replaced with fresh containing the desired concentration of GSK-J4. Cells were harvested 48 hours after treatment and RT-qPCR or western blot was performed as described previously.

5.3.2 siRNA transfection

All cell lines other than VCAPs were forward transfected in 6-well plates with siRNA at a 25 nM concentration using 0.2% lipofectamine RNAiMAX according to the manufacturer's protocol. Opti-MEM was used as a serum-free media for generating transfection complexes. 72 hours post-transfection, protein or RNA was harvested and RT-qPCR or western blot was performed as described previously.

VCaP cells were seeded in 6-well plates and grown until 80% confluent. At 80% confluence, the siRNA was transfected as described above. Cells were harvested 72 hours post-transfection, protein or RNA was harvested and RT-qPCR or western blot was performed as described previously.

For siRNA work, ON-TARGETplus Human KMD6A siRNA (Dharmacon #7403) or scrambled siRNA (Sigma-Aldrich) were purchased and resuspended in RNase/DNase-free water to a final concentration of 100µM and stored at -20 until required.

5.3.3 Seahorse assay

For the Seahorse assay, CW22Rv1 cells were seeded into the specialised 96-well microplate (provided with the kit) at $2x10^3$ cells/well. The next day, media was replaced, and cells were treated with either siRNA or 750 nM GSK-J4. Cells were left for 48 hours before the media was replaced with Seahorse Assay media. The seahorse assay was carried out as per the manufacturer's protocol. Briefly, on the day of the assay, injection ports were loaded with metabolic effectors. At the starting point, baseline levels of oxygen consumption rate (OCR) and extracellular acidification rate (ECAR) were measured using the Seahorse XF Analyser. Following sequential injection of effort compounds, OCR and ECAR were measured to assess changes in metabolic activity. I would like to thank Hannah Kendall for her assistance in the Seahorse Assay.

5.3.4 *In vivo* experiments

For *in vivo* work, GSK-J4 HCL (Selleckchem S7070) was dissolved in sterile water and sonicated until dissolved. The drug was made up fresh before each dosing.

Mouse work was kindly conducted by Huw Thomas of the Newcastle Drug Discovery Unit. All experiments were conducted under local ethical approval under the project license number: PP5794374.

Male CD1 nude mice were inoculated with $5x10^6$ CW22Rv1 cells subcutaneously on the right flank. Tumours were allowed to develop for approximately 7 days to an average volume of 66 (± 14.4) mm^3. At this point, mice were randomised into two groups:

1. 10 mice received water I.P. x5 per week for 6 weeks
2. 10 mice received 50 mg/kg GSK-J4 I.P. X5 per week for six weeks

Mice were weighed and the tumours were measured using electronic callipers three times per week. Mice were sacrificed when tumours reached x4 starting volume (RTV4) or if there were signs of toxicity.

5.4 Results

5.4.1 KDM6A Knockdown reduces PC Cell lines Proliferation

First, the effect of KDM6A KD on the growth of multiple AR-V7-expressing prostate cancer cell lines over five days was assessed. KD of KDM6A resulted in a significant growth reduction of the CW22Rv1, CW22Rv1-AR-EK and LNCAP95 cell lines at day five compared to non-targeting control ($P < 0.05$). There was no change in proliferation in VCaP cells over the same five-day period **(Figure 5.1A-D).** This may be due to the slow doubling time of VCaPs which is generally around 5 days and thus the experimental set-up did not allow enough time for a proliferation to be reduced (Cowley et al., 2014). Next, the effect of KDM6A KD on cell growth was compared in CW22Rv1 and PNT1A cells. As PNT1A are a non-cancerous prostate cell line, this would determine if cell growth was more dependent on KMD6A in cancerous cells compared to normal prostate epithelium cell lines. It is important to evaluate if targeting KDM6A has a cytotoxic effect on cancerous cells only or if it would also be detrimental to healthy cells. KDM6A KD caused a significantly greater growth reduction in the cancer cell line compared to the normal prostate epithelium cell (42% compared to 22% reduction) **(Figure 5.1E).** Reduction in cell number following KDM6A KD in the CW22Rv1 cell line was validated with brightfield microscopy. Images were taken 72 hours after KDM6A KD, with KDM6A targeting siRNAs causing a significant reduction in well confluency compared to non-targeting control.

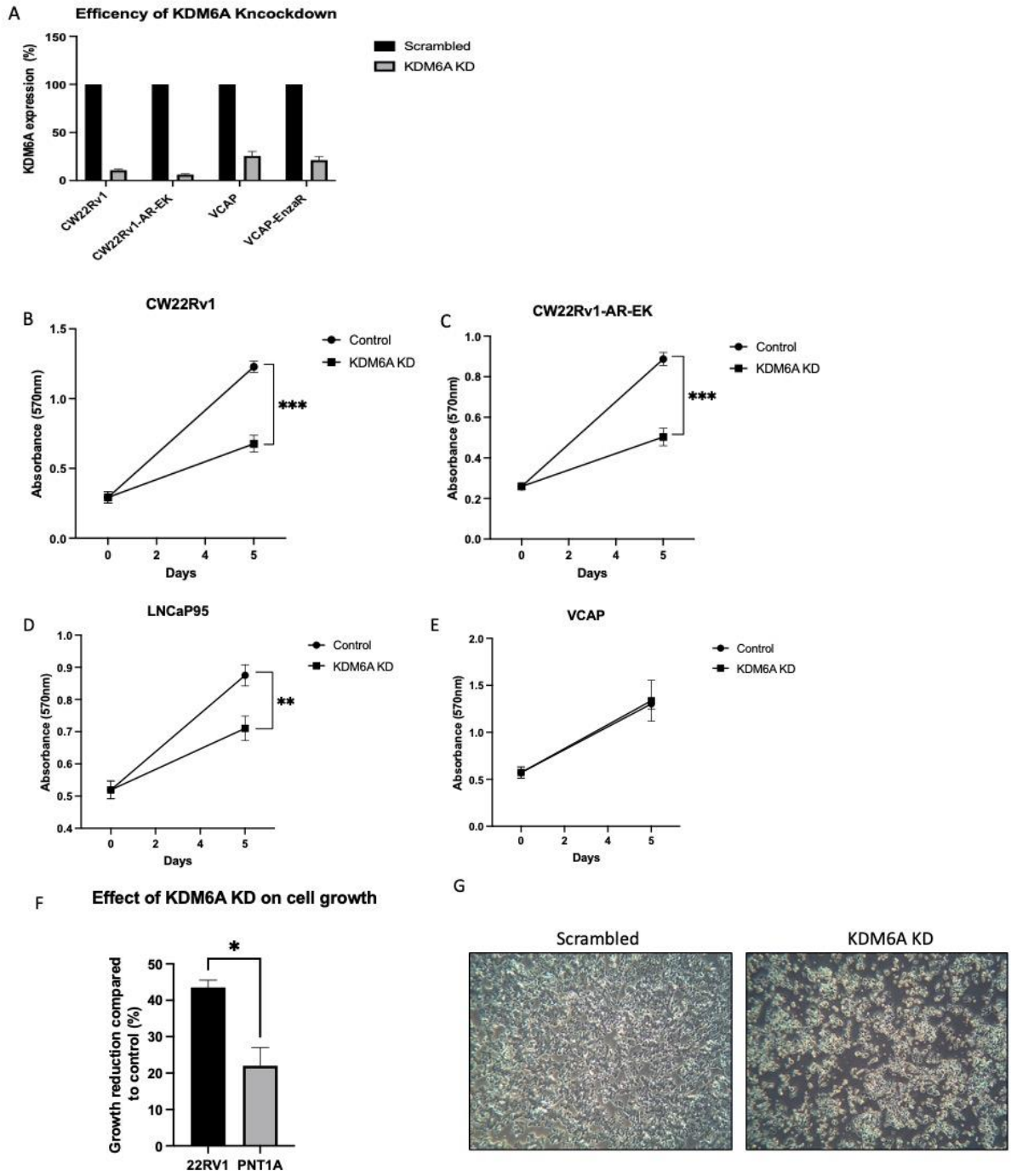

Figure 2 Effect of KDM6A Knockdown (KD) on Prostate Cancer Cell line proliferation. A) *Expression of KDM6A mRNA following knockdown compared to scrambled control.* ***B-D*** *Changes in cell proliferation 120 hours post KDM6A KD compared to non-targeting control in prostate cancer cell lines.* ***E****. Comparison of growth reduction induced by KDM6A KD in CW22Rv1 and noncancerous PNT1A cell lines. Growth reduction calculated as difference between KDM6A KD and control cell number for individual cell lines.* ***F.*** *Brightfield images of KDM6A KD and non-targeting control in CW22Rv1 cells 72 hours after siRNA transfection at x10 magnification. SRB datapoints were calculated as an average of technical triplicates within each biological replicate, all data presents n=3 biological replicate plotted a mean +/- SEMs. Unpaired t-test was used to calculate statistical significance between day 6 datapoints in B-F (*=p<0.05, **=p<0.01, ***=p<0.001 and ****=p<0.0001).*

Next, the effect of KMD6A KD on the expression of selected AR pathway components (AR-V7, AR-FL and PSA) was assessed. KDM6A KD caused a significant reduction in the expression of both AR isoforms and PSA at both the transcript and protein levels in the CW22Rv1 and CW22Rv1-AR-EK cell lines **(Figure 5.2 A-D).** The levels of H3K27me3 were also profiled, with the assumption that reducing levels of KDM6A would increase H3K27me3 levels. However, there did not appear to be a significant change in H3K27me3 levels after KDM6A KD although the use of a total histone H3 antibody may have been a useful loading control to ensure endogenous levels of H3 were equal across samples.

Interestingly, KD of KDM6A in the VCaP parental caused an upregulation of AR-FL and AR-V7 although not statically significant. It was surprising to see that despite the increased levels of AR isoforms, PSA expression significantly decreased by around 50% **(Figure 5.2E).** This would suggest that AR signalling is not upregulated despite levels of AR isoforms being higher. It should also be considered that the increased AR levels following KDM6A KD may go some way in explaining why there was no marked reduction in the VCaP cell proliferation following KDM6A KD as shown in figure 1.

Finally, the effect of KDM6A expression was profiled in the VCaP-EnzaR cell line. In contrast to the parental cell line, KD in the VCaP-EnzaR cells caused a significant reduction of AR-FL, AR-V7 and PSA. AR-FL and AR-V7 mRNA expression was reduced by around 25% whilst PSA expression was reduced by around 50% suggesting AR signalling is being inhibited **(Figure 5.2F).** At the protein level, these changes to the AR isoforms were difficult to detect which may be due to the higher copy number of AR in the VCaP cells **(Figure 5.2G).**

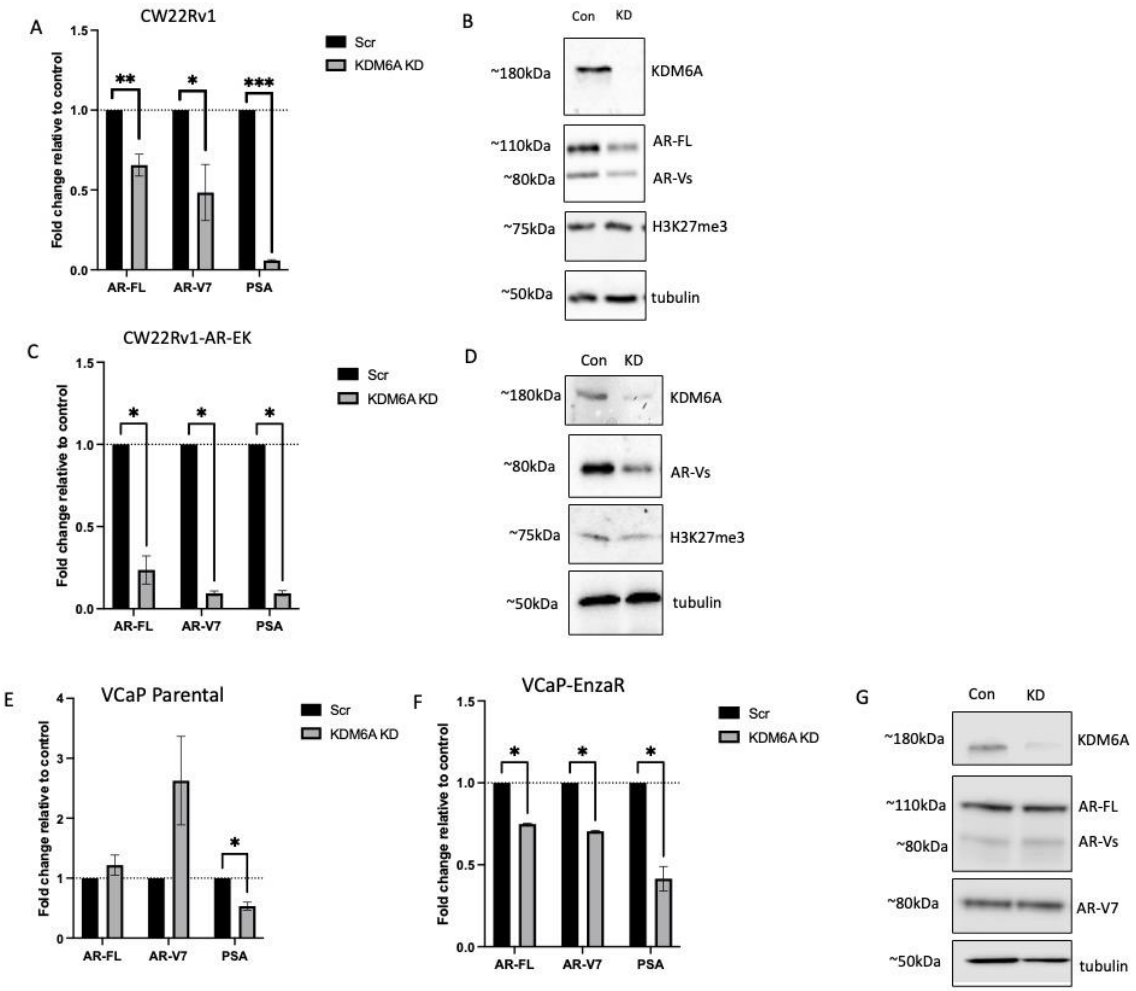

Figure 5.2 Effect of KDM6A KD on AR isoform and PSA expression at transcript and protein level. *Cells were treated for 72 hours with siRNA targeting KDM6A or non-targeting control before RNA and protein lysates were harvested.* ***A)*** *KDM6A mRNA expression in KD compared to non-targeting control.* ***B-C****. CW22RV1 cells.* ***D-E.*** *CW22Rv1-AR-EK.* ***F****. VCaP* ***G-H****. VCaP-EnzaR. qPCR data comprises n=3 independent biological replicates plotted as mean +/- SEM. Unpaired t-test was used to calculate statistical significance in A-F (*=p<0.05, **=p<0.01, ***=p<0.001 and ****=p<0.0001).*

5.4.2 Effect of KDM6A inhibition with GSK-J4

As mentioned in the introduction, GSK-J4 is a competitive inhibitor of both 2-oxoglutarate (a-ketoglutarate) and Fe^{2+} and is proposed to inhibit the catalytic activity of KMD6A. Firstly, the IC_{50} was determined for a range of prostate cancer cell lines by exposing the cells to varying doses of the drug for five days. IC_{50} values for GSK-J4 varied between 0.72 - 5.28 µM **(Figure 5.3 A-B).** The CW22Rv1 cell line was the most sensitive to the compound whilst the VCaP-EnzaR was the least sensitive. Comparing the IC_{50} of VCaP Parental and VCaP-EnzaR cells, there was a shift from 1.37 µM to 5.28 µM which perhaps can be explained by the increased levels of KMD6A in the VCaP-EnzaR cells demonstrated in *Chapter 4.4.6*. The VCaP-EnzaR cells also have higher expression of pathways involved in drug metabolism, as a result of continuous exposure to Enzalutamide, potentially allowing them to metabolise GSK-J4 more efficiently thus dampening its effect. This was revealed in the RNA-Seq results in *Chapter 4* whereby VCaP-EnzaR cells had significantly higher expression of the Hallmark "*Xenobiotic Metabolism*" for example. Analysis of intracellular GSK-J4 levels in the VCaP cell line derivatives would therefore be a useful extension to this study.

The CW-RV-AD1 cells, which harbour only AR-FL, had a relatively high IC_{50}. Previous studies have reported the same trend in that CW-RV-AD1 cells tend to be less sensitive to GSK-J4 than AR-V-expressing PC cell lines (Morozov et al., 2017). Morozov et al., demonstrated that this was due to a faster reduction in H3K27me1 levels in AR-V expression cell lines compared to the CW-RV-AD1 cells.

A

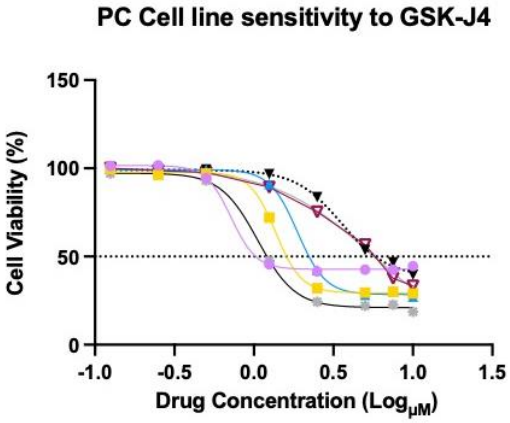

B

Cell line	IC_{50} (µM)
CW22Rv1	0.72
VCAP Parental	1.37
CW-R1-D567	1.88
CW-R1-AD1	3.56
VCAP-EnzaR	5.28
PNT1A	1.08

Figure 3 Determining the IC50 of Prostate Cancer cell lines to GSK-J4*. Cell lines were treated with titrating doses of GSK-J4 for 94 hours before harvesting for SRB assays.* ***A)*** *Dose response curves of GSK-J4 treatment on PC cell lines. Data was normalised to the DMSO control for each cell line to assess changes in cell viability.* ***B)*** *IC50 calculated from Y intercept at 50% viability.*

Next, a range of GSK-J4 concentrations were tested on *AR* isoform, *PSA* and *KDM6A* expression in multiple PC cell lines. Drug concentrations ranged from 10 nM to 5 µM. Based on the elevated sensitivity to GSK-J4 for CW22Rv1 and CW22Rv1-AR-EK cells, they received a maximum dose of 1.25 µM, whilst VCaP, VCaP-EnzaR and LNCAP95 cells received a higher final dose of 5 µM to reflect their lower sensitivity to the compound. All drug ranges covered at least a 100-fold difference between the lowest and highest doses to give a wide range of concentrations. This method is recommended for drugs with limited data on specific cell lines as in the case of GSK-J4 in PC cell lines (Francies et al., 2019; Niepel et al., 2017). RNA and protein lysates were harvested 48 hours after GSK-J4 treatment. All data was normalised to DMSO control samples.

Both the CW22Rv1 and CW22Rv1-AR-EK showed a robust response to GSK-J4 at low drug concentrations of 0.1-1.25 µM; causing a significant reduction in both *AR* isoform, *PSA* and *KMD6A* expression **(Figure 5.4 A-D).**

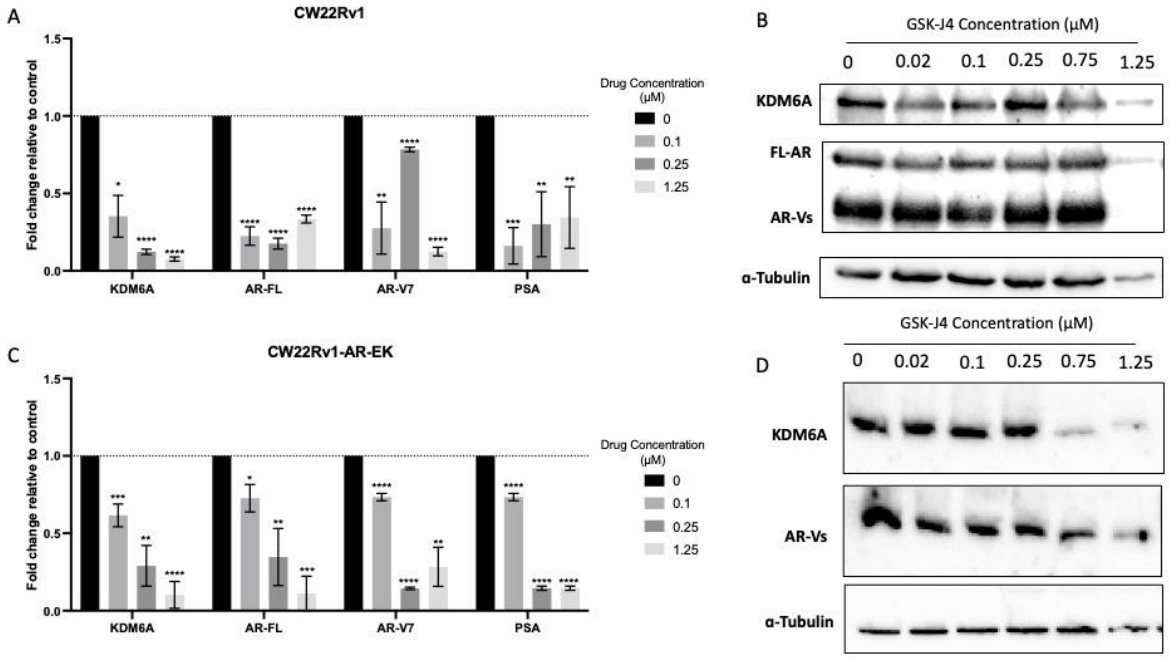

Figure 5.4 Effect of GSK-J4 treatment on CW22Rv1 and CW22Rv1-AR-EK cells. *Cells were treated with varying concentration of GSK-J4 for 48 hours before RNA and protein lysates were harvested. For assessing transcriptional changes in target gene expression, data was normalised to DMSO control for each gene.* ***A-B.*** *CW22Rv1* ***C-D****. CW22Rv1-AR-EK. qPCR data comprises n=3 independent biological replicates plotted as mean +/- SEM. Unpaired t-test was used to calculate statistical significance in A and C (*=p<0.05, **=p<0.01, ***=p<0.001 and ****=p<0.0001).*

The VCaP parental cells provided some interesting observations. Treatment of the VCaP parental cells with 0.25 µM GSK-J4 resulted in ~3x increased expression of KMD6A at the mRNA level. At this dose, there was also an increase in the expression of *AR* isoforms and *PSA*, although none of these increases were statistically significant. At the higher doses of 1.25 µM and 5.0 µM, KMD6A expression was comparable to that of the untreated control whilst causing increased expression of *AR* isoforms and *PSA* **(Figure 5.5 A).** In contrast, GSK-J4 treatment of the VCaP-EnzaR caused a robust reduction in the expression of the genes profiled **(Figure 5.5 B-C).** Interestingly, in this cell line, there appeared to be a strong dose-dependent effect in that at the highest GSK-J4 dose (5 µM) there was the greatest reduction in *AR* isoform, *PSA* and *KDM6A* expression. Remarkably, in the VCaP-EnzaR cell lines, 5 µM of GSK-J4 reduced expression of profiled genes by 80% (+/- 10%) at the transcript level. It should be noted that as with KMD6A KD, changes at the protein level were more difficult to clearly detect, but there was evidence for reduction to AR-V protein levels at the higher doses of the KDM6A inhibitor. Considering this model best represents CRPC patients resistant to treatment, from a therapeutic standpoint, these results are promising.

Finally, GSK-J4 treatment was tested on the LNCaP95 cells. As mentioned previously, the LNCaP95 cell line is AR-V7 positive and Enzalutamide resistant (Leung et al., 2021). Given the focus of this study, which is to identify the role of KMD6A in AR-V7 generation and CRPC progression, they offer an additional relevant PC model to test. Consistent with the VCaP-EnzR cells, GSK-J4 treatment of LNCaP95 also showed a robust dose-dependent effect in reducing the expression of *KDM6A*, *AR* isoforms and *PSA*; with the highest concentration of GSK-J4 (5 µM) reducing expression of all genes profiled by approximately 50% (**Figure 5.5 D).** At the protein level, 5 µM of GSK-J4 treatment appeared to cause a reduction in KDM6A and AR-V7 however the loading control, α-tubulin, suggests this may be a result of lower cell numbers driven by cytotoxicity of the compound.

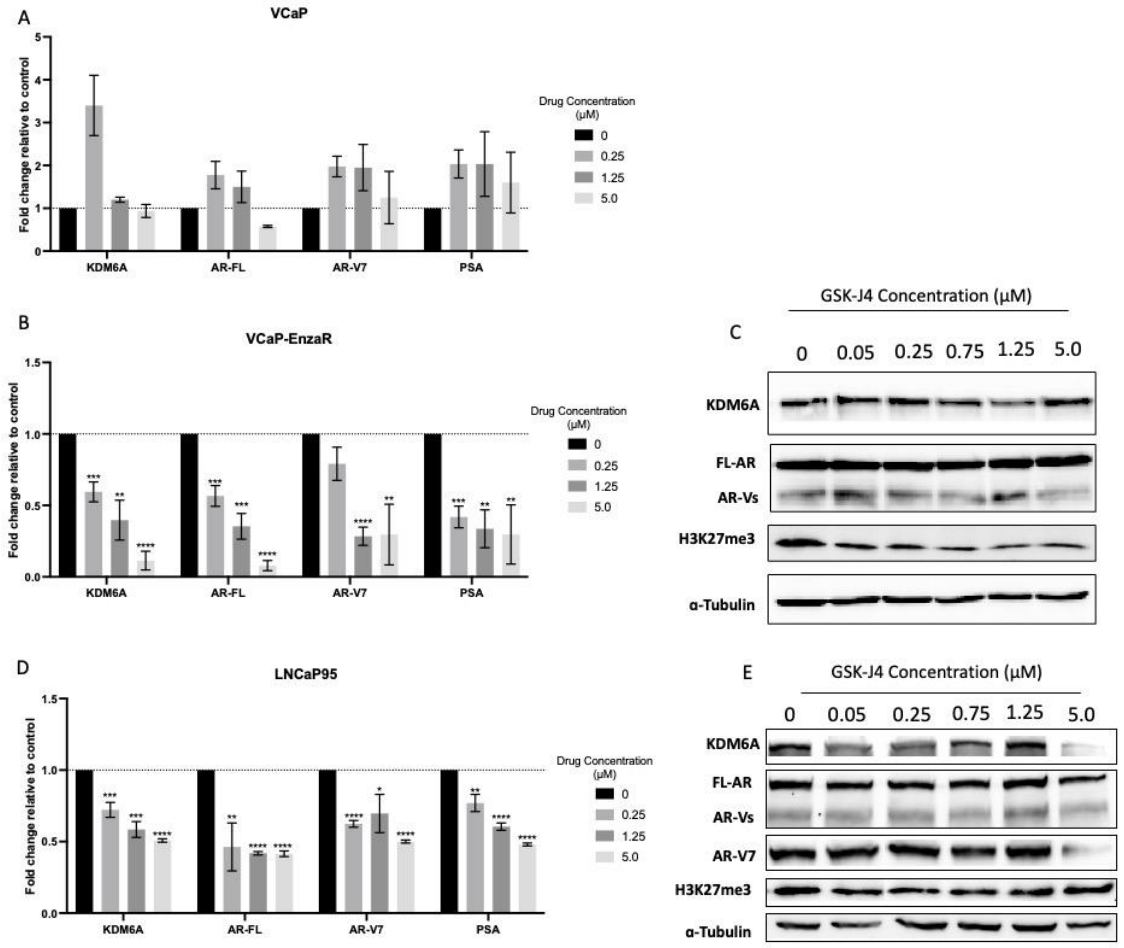

Figure 5.5 Effect of GSK-J4 treatment on VCaP Parental, VCaP-EnzaR and LNCAP95s*. Cells were treated with varying concentration of GSK-J4 for 48 hours before RNA and Protein lysates were harvested**. For assessing transcriptional changes in target gene expression, data was normalised to DMSO control for each gene.* ***A****. VCaP* ***B-C*** *VCaP-EnzaR* ***D-E*** *LNCaP95. qPCR data comprises n=3 independent biological replicates plotted as mean +/- SEM. Unpaired t-test was used to calculate statistical significance in A, B and D (*=p<0.05, **=p<0.01, ***=p<0.001 and ****=p<0.0001).*

GSK-J4 treatment did not appear to alter H3K27me3 levels in any cell lines tested. Given that KDM6A is a demethylase there was an expectation that its inhibition would cause accumulation of H3K27me3. Other studies which utilised the compound have reported the same results (Morozov et al., 2017; Ntziachristos et al., 2014). A possible reasoning behind this is that GSK-J4 treatment does not affect global levels of H3K7me3 but instead alters it at specific genomic regions. This will be tested later in the thesis through Chromatin-Immunoprecipitation assays (ChIP) to investigate methylation changes at CE3 following GSK-J4 treatment.

The results from the GSK-J4 work were both interesting and promising. The three Enzalutamide resistant cell lines (CW22Rv1, VCaP-EnzaR and LNCaP95s) showed a robust sensitivity to the inhibitor whereby treatment reduced expression of *AR* isoforms and *PSA* between 50-90%. In hindsight, treatments of the cells for a longer time such as 72 or 96 hours may have caused a more pronounced reduction at the protein level.
An observation from this work is the possibility of a relationship between KMD6A and the AR. In the VCaP parental cells, GSK-J4 treatment resulted in an increased *AR* isoform expression corresponding with increased *KDM6A* following treatment, whilst in other cell lines there was an inverse relationship. Given that the AR interacts with and is transcriptionally activated by other KDMs, including KMD3A (Yamane et al., 2006b), KDM4A and KDM4D (Shin & Janknecht, 2007), this warrants further investigation. Work by Morozov et al., suggested AR may recruit KDM6A complex to AREs for H3K27me3 demethylation however this was not investigated further. Additionally, it was unexpected that GSK-J4 treatment reduced the expression of KMD6A itself given it binds the catalytic pocket of KDM6A. Despite many studies utilising GSK-K4, very few profiled KDM6A expression in response to GSK-J4. One study showed that GSK-J4 treatment reduced KDM6A expression on a transcript level, although at a much higher concentration used in our study (N. Yan et al., 2017). It was therefore hypothesised that there was possibly reciprocal feedback between AR and KMD6A meaning the expression of one altered the other. It was important to answer this to determine whether the reduction in KMD6A seen after GSK-J4 was a result of reduced AR-mediated *KDM6A* gene transcription as opposed to the compound itself.

5.4.3 Investigating the interactions between AR and KDM6A

A body of evidence was starting to demonstrate a relationship between AR and KMD6A. This was built on the fact that i) KDM6A and AR have a positive correlation in tumour samples; ii) the GSK-J4 data suggested a relationship in the expression of KMD6A and AR isoforms; iii) studies demonstrating other KDMs regulate AR activity and implication of KDM6A regulating AR activity.

Firstly, a simple approach of comparing Delta Ct values of AR and KDM6A mRNA expression in a range of PC cell lines was conducted. Delta Ct values are the difference between the Ct value of target genes and the housekeeping gene thus, assessing the Delta Ct values gives the relative expression of AR and KDM6A across different cell lines. A lower Ct value indicated a higher expression of the gene of interest. There appeared to be a relationship between the expression of AR and KDM6A in the cell lines tested, with VCaP-EnzaR cell line, for example, having the lowest dela Ct value (highest expression) of both AR and KMD6A. On the other hand, the LNCaP cell line has the highest value for both AR and KDM6A **(Figure 5.6A)**. Whilst this is not quantifiable, it demonstrated a trend in cell lines that those with high AR expression also have high KDM6A expression and vice versa.

Next, the effect of AR knockdown on KMD6A expression was assessed. The aim of this was to determine if AR KD reduced the expression of KMD6A. CW22Rv1 and CW22Rv1-AR-EK were subjected to siRNA transfection of AR exon 1-targeting siRNAs which would deplete all AR isoforms. KDM6A levels in response to total AR knockdown were assessed by RNA and protein profiling at 48 and 72 hours. Depletion of AR caused a significant reduction in KDM6A mRNA expression in the CW22Rv1 cells after 72 hours at both the transcript and protein levels **(Figure 5.6B-C).** There were no changes to KDM6A expression after 48 hours in these cells. For the CW22Rv1-AR-EK, AR knockdown did not reduce KDM6A expression; on the contrary, it led to an increase in mRNA expression although this was statistically insignificant and not detectable at the protein level **(Figure 5.6B-C).**

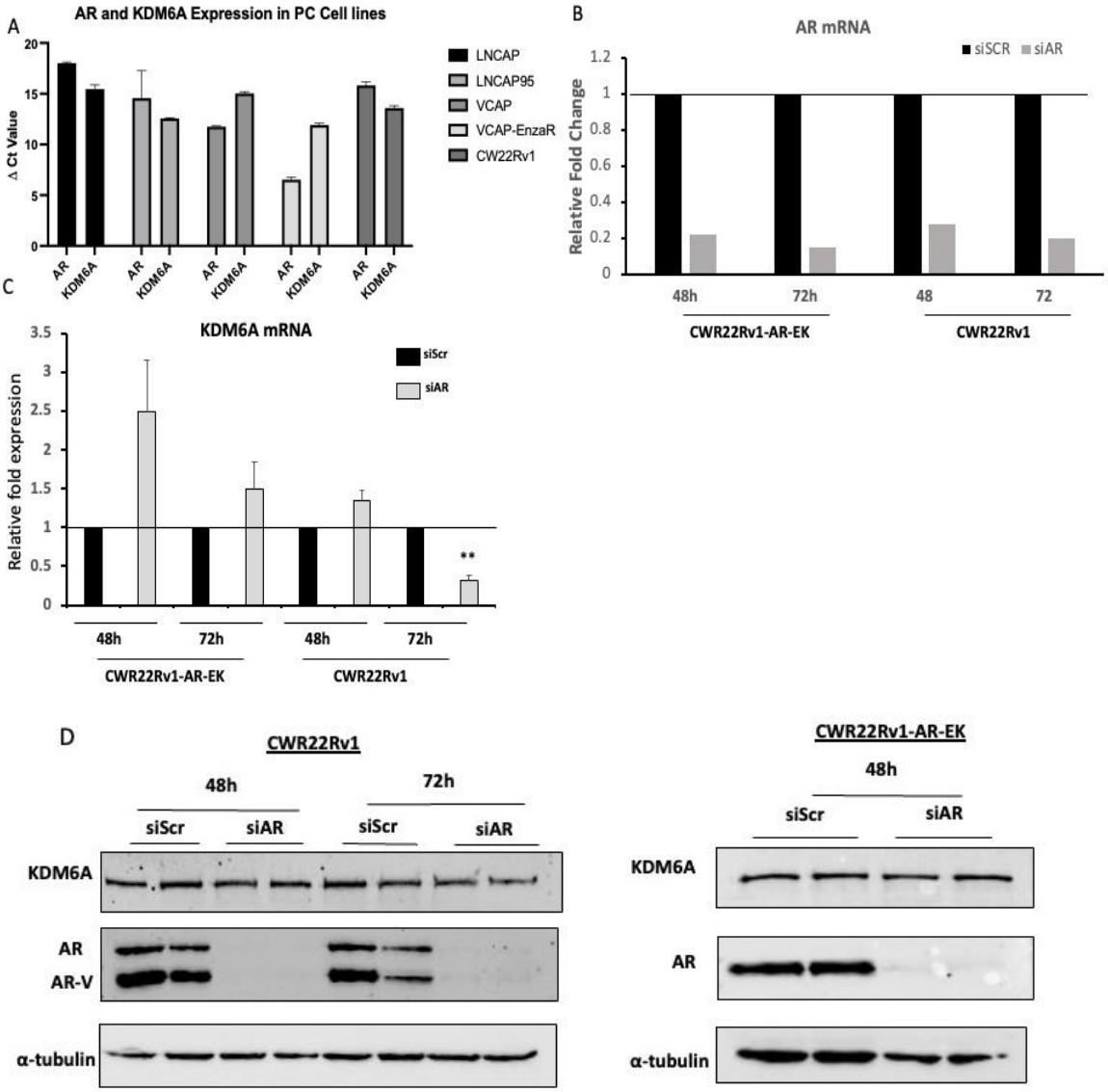

Figure 5.6 Profiling the interaction between AR and KDM6A. A) *Delta-Ct values of KDM6A and AR for PC cell lines. Data was generated by subtracting KDM6A Ct values from HKG (RPL13A) Ct values for each cell lines. B) AR mRNA expression in cell lines following KD. qPCR data shown comprises n=1.* ***C-D)*** *Effect of AR KD on KDM6A mRNA and protein expression in CW22Rv1-AR-EK and CW22Rv1 cells. Cells were treated for 48 and 72 hours with siRNA targeting AR. Data is normalised to non-targeting control for respective timepoint. qPCR data in C comprises n=3 independent biological replicates plotted as mean +/- SEM.. Unpaired t-test was used to calculate statistical significance in C (*=p<0.05, **=p<0.01, ***=p<0.001 and ****=p<0.0001).*

Next, chromatin-immunoprecipitation (ChIP) assays were utilised to validate if AR is bound to regions within the KMD6A promoter. Firstly, ChIP-seq data was analysed using CistromeDB (Zheng et al., 2018), a user-friendly depository of ChIP-Seq data sets whereby the binding of transcript factors can be assessed. AR binding peaks within the KMD6A promoter were identified by interrogating datasets using two different prostate cancer cell lines, C4-2 and LNCaP grown in full media without androgen supplementation (Barfeld et al., 2017; Y. Zhao et al., 2016). Data from both cell lines showed consistent AR binding in distinct regions of the *KDM6A* gene. From this, primers were designed to amplify these distinct regions of the *KMD6A* promoter to validate AR binding. As a control, primers amplifying a region within exon 2 of *KDM6A* were also generated, which would reveal if AR bound indiscriminately to *KDM6A* or, importantly, more selectively at *cis*-regulatory elements which may support a role in AR regulating *KDM6A* expression. ChiP assays were conducted as described in *Chapter 3.3*, in which cells were grown until 90% confluent in full media before being harvested for ChIP experiments. In the CW22Rv1 cells, a 5-fold enrichment of AR binding compared to IgG control was detected in both regions of the *KMD6A* promoter, but not in Exon 2 of KMD6A **(Figure 5.7 B).** In the CW22Rv1-AR-EK cells, there were similar results, in that AR bound to KDM6A promoter regions significantly more than IgG control **(Figure 5.7 C).** Overall, in the CW22Rv1-AR-EK, there is less AR enrichment shown by lower Fold % input values (~0.08% v ~5%, respectively). In both experiments, primers which amplify cis-regulatory elements of the *KLK3* and *KLK2* genes were used as positive controls. In both cell lines, AR bound robustly to both *KLK2* and *KLK3* (Avg. Fold % input of 85 and 115, respectively) validating the specificity of the AR antibody. The ChIP data suggests the AR may bind to promoter regions of KDM6A but required further experimental work.

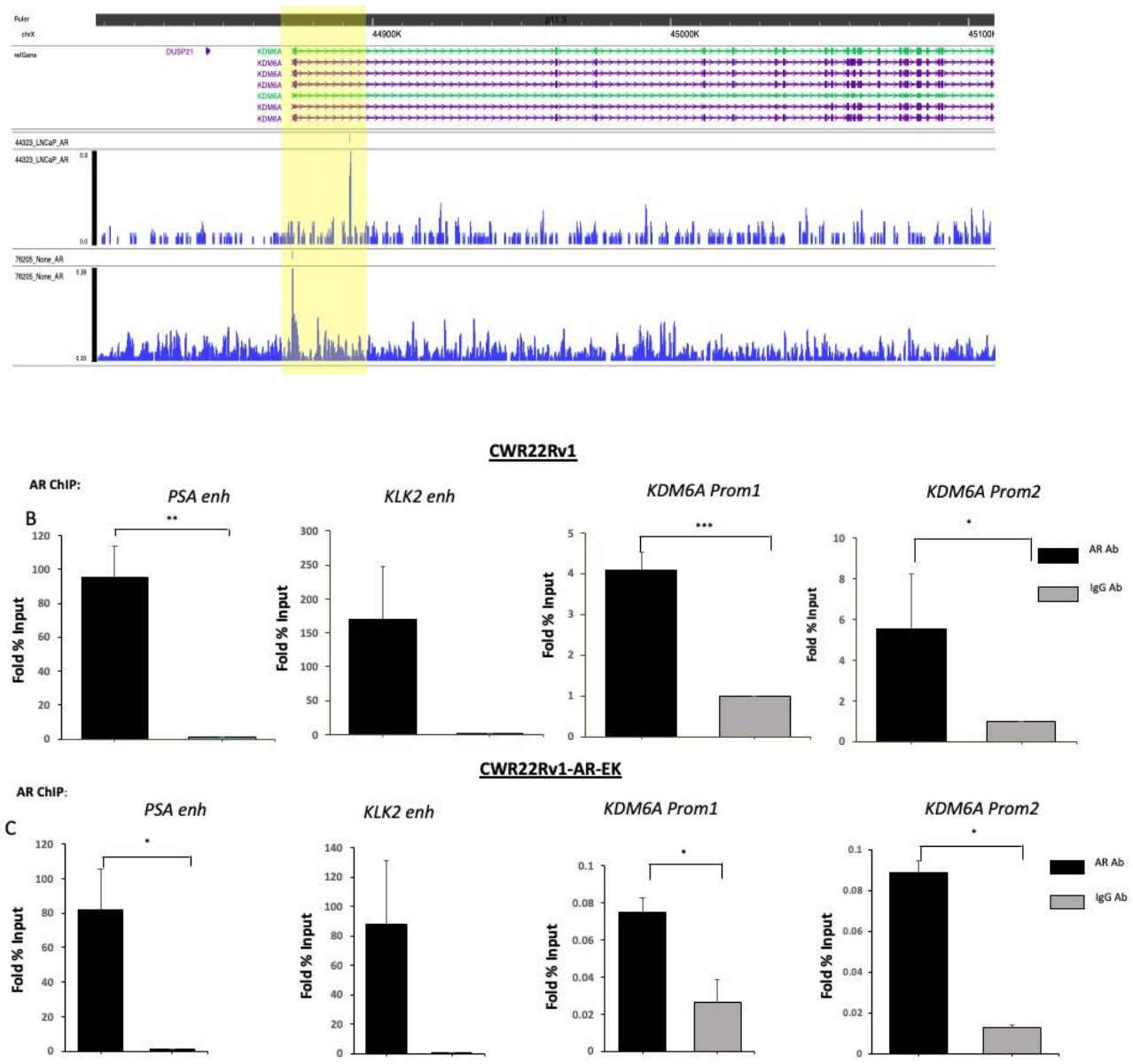

***Figure 5.7 Assessing the Enrichment of AR in distinct KMD6A regions**. **(A)** AR binding peaks identified in CbioPortal in two separate experiments. Enrichment of AR at AR target genes (PSA, KLK2) and KDM6A promoter regions described in text in **(B)** CW22Rv1 and **(C)** CW22Rv1-AR-EK cells. qPCR data comprises n=3 independent biological replicates plotted as mean +/- SEM. Significance shown is the result of unpaired T-test between AR and IgG antibody (*=p<0.05, **=p<0.01, ***=p<0.001 and ****=p<0.0001).*

In a final experiment to investigate AR and KDM6A interaction, VCaP cell lines were utilised as it is well documented that in response to DHT, VCaP cells down-regulate AR isoform expression (Cai et al., 2011). It was therefore hypothesised that in response to DHT treatment, both levels of AR and KMD6A may be reduced. VCaP cells were grown in 10

nM DHT for 24 hours before protein and RNA lysates were taken. In response to DHT treatment, there was a significant reduction in AR expression at the mRNA level whilst KMD6A expression increased almost 2-fold compared to the -DHT arm, although statistically not significant **(Figure 5.8A).** At the protein level, although the loading control is problematic, the reduction in AR expression was evident, while expression of KMD6A appeared to remain the same between experimental arms **(Figure 5.8B).**

To understand if this phenomenon was consistent with other literature, datasets from other groups with similar experimental setups were interrogated using GEO2R (https://www.ncbi.nlm.nih.gov/geo/geo2r/). GEO2R supplies a Fragments Per Kilobase Million (FPKM) value for the gene of interest from each sample. FPKM is a simple expression level normalisation method where read counts are normalised based on gene length and the total number of mapped reads. The effect on *AR* and *KDM6A* expression was assessed in the work by Guo et al*.,* whereby VCaP cells were treated with DHT for 24 hours before global transcriptomic analysis by RNA-Seq (H. Guo et al., 2021). In line with our data, Guo et al., also demonstrated a significant reduction in AR expression and a modest upregulation of KMD6A in response to DHT treatment in VCaP cells **(Figure 5.8C).**

Collectively this data provides some insight into the AR and KDM6A relationship. Firstly, cell line data shows a trend in which the expression of *AR* and *KMD6A* are generally close to one another. Secondly, depletion of AR in the CW22Rv1 cells leads to a reduction in KDM6A expression at the mRNA level but no change is apparent at the protein level. ChIP data reveals that AR binds to distinct areas of the KDM6A promoter and this seems specific binding considering AR does not bind to exon2 of KMD6A. Finally, in the VCaP cell lines there appeared to be the inverse occurring in that when AR expression was high, KDM6A expression was lower. It should be noted however that studies by others have demonstrated a physical interaction between AR and UTX through immunoprecipitation of VCaP protein lysates (Grasso et al., 2012).

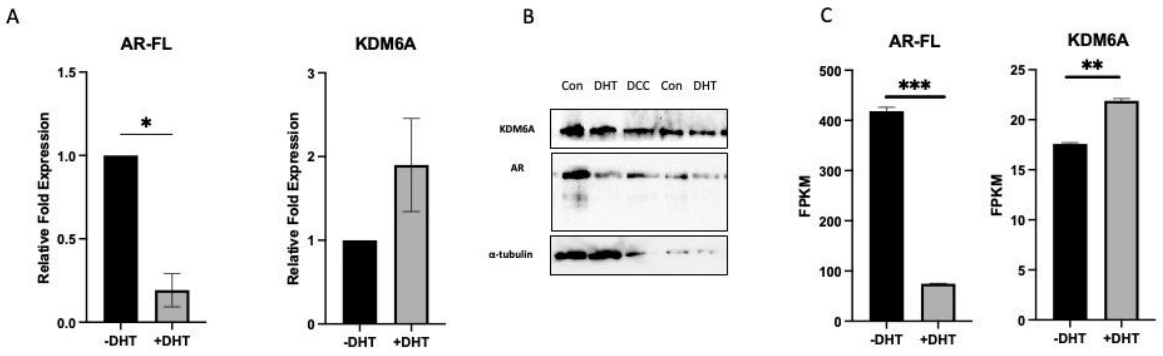

***Figure 5.8 Assessing the effect of DHT treatment on KMD6A expression in VCaP cells**. A) Gene expression of AR-FL and KMD6A in VCaP cells treated with DHT for 24 hours. Data normalised to -DHT control. B) Two technical repeats of experiments from A. C) Gene expression of AR-FL and KDM6A from work by Guo et al., 2012. qPCR data comprises n=3 independent biological replicates, plotted as mean +/- SEM Significance shown is the result of unpaired T-test (*=p<0.05, **=p<0.01, ***=p<0.001 and ****=p<0.0001).*

5.4.4 Differential gene expression using DESeq2.

To gain an understanding of the global changes occurring in response to GSK-J4 treatment or KMD6A knockdown, CW22Rv1 cells subject to enzyme depletion or inactivation were analysed by RNA sequencing. There were three conditions to the experimental design: control (DMSO, scrambled siRNA), treatment with GSK-J4 (750 nM) and siRNA KD of KDM6A (using siRNAs from 5.4.1). The concentration of 750 nM GSK-J4 was used as it was near to the IC_{50} (720 nM as shown in Figure 5.5) and had been shown to reduce AR-V7 expression. Before samples were sent for RNA sequencing, a total of 5 experimental replicates were produced and gene expression profiled. mRNA and protein expression of KDM6A, AR isoforms and PSA was assessed from all repeats and three replicates with the most substantial changes to profiled genes were sent for RNA-Seq **(Figure 5.9 A).** As had been previously shown, KDM6A KD or GSK-J4 treatment reduced AR isoform and PSA expression at the transcript level. GSK-J4 treatment did not reduce KDM6A expression at the protein whilst KD did, whilst both caused a reduction in AR isoform expression. Given that the expected effects were observed, samples were subsequently sent for RNA-Seq.

Data was received through GENEWIZ in the form of raw FASTQ files. Each sample has two FASTQ files with ~30-40 million reads at ~150bp in length. The first process with the FASTQ files was to conduct a quality control assessment to ensure the quality of the data could be used in downstream analysis. Firstly, the RNA-Seq library was assessed using *FastQC* (Andrew, 2010) and a quality report for all samples was created with *MultiQC* (Andrews, 2010). FastQC measures a range of metrics, such as GC content and the presence of overrepresented sequences which is indicative of contamination(Andrews, 2010). The results of the metrics for each sample are shown in **Figure 5.9B.** Overall, the sequencing data was of good quality. There were similar issues in some samples as reported in *Chapter 4.4.6* and no QC warning which warranted further investigation. Therefore, differential gene expression analysis (DGEA) was conducted between experimental arms. To do this, RNA-SeQ reads were aligned using *STAR* (Dobin et al., 2013) to an hg38 human reference genome. The reads were assigned to exons which allowed a gene-level expression count using *featureCounts* (Liao et al., 2013) and the resulting count matrix was used for DGEA between experimental arms using the DESeq2 package. DESeq2 normalises data against unchanging genes for a specific library depth and composition. Samples which have been normalised can then be viewed using principal component

analysis (PCA) which essentially reveals intra-arm similarities and inter-arm differences (Groth et al., 2013). PCA plot highlighted that samples clustered well (**Figure 5.9 C).** KDM6A KD has greater separation based on PC1 compared to control and GSK-J4 arms. This is to be expected given the large number of genes affected by KD in comparison to the GSK-J4 treatment. The GSK and control arms did have some variance based on PC2 although samples clustered close together. Due to the specific nature of GSK-J4 and the low concentration used in the study, it is to be expected for there not be a large variance.

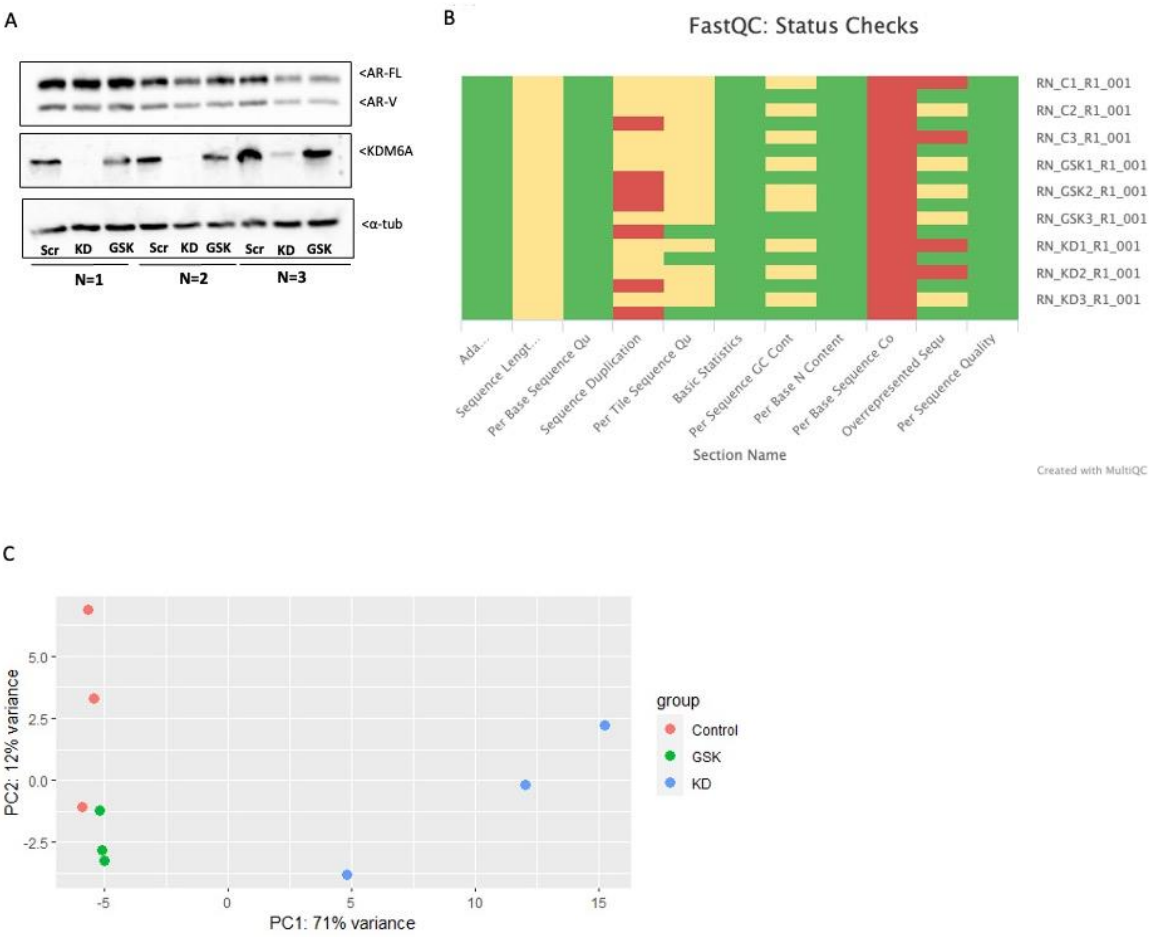

Figure 5.9 Sample validation and QC results for RNA-Seq experiments. *A) Three independent repeats of KMD6A KD or GSK-J4 treatment in CW22Rv1 cells used for RNA-Seq experiments. B) FastQC results of samples used in RNA sequencing. X-axis shows different parameters measured in FastQC analysis. Y-axis shows reads for each sample. Green = passed QC, Amber = passed with warning, Red = Failed QC C) PCA plots of samples shows clustering of experimental arms.*

Next, volcano plots were created to summarise all fold change and FDRs (adjusted p-value) of differentially expressed genes (DEGs) across each experimental condition **(Figure 5.10 A and B).** KDM6A expression was significantly reduced in the KD arm (Log -3, adjust 6.98^{-E14}) but not in the GSK-J4 treatment (Log 1, adjust 0.9) despite qPCR validation before sample submission. This is likely due to differences in data processing. Whilst in qPCR data is normalised to a reference gene, in RNA-Seq reads are mapped to exons which can create differences. DGE between the two experimental arms and control cells were assessed to investigate which genes were significantly affected because of KMD6A KD or GSK-J4 treatment. Genes were deemed significantly upregulated if they met the criteria of LogFC >1.5, padj <0.05. From the GSK-J4 treated and KMD6A KD experimental arms, there were 17 and 368 genes significantly upregulated, respectively **(Figure 5.10 C and D).** From this, there was a total of 12 genes which overlapped between both experimental arms. Differentially downregulated genes were defined by Log FC <-1.5, padj <0.05. In total, there were 37 and 756 genes significantly downregulated in response to GSK-J4 and KMD6A KD, respectively **(Figure 5.10 B).** Of these, 13 genes were significantly altered by both GSK treatment and KDM6A KD. Lists of overlapping genes both significantly up and downregulated are shown in **Figure 5.10.** Given that there was little overlap between gene sets, primarily because of overall DGE being low in the GSK-J4 experimental arm, this made STRING and DAVID analysis difficult due to too few input genes. There are, however, genes differentially expressed which have already been studied in the prostate field. *Hairy and enhancer of split 2 (HES2)* and *Hairy and enhancer of split 6 (HES6*) were both significantly downregulated in response to both KMD6A KD and GSK-J4 treatment. *HES2* and *HES6* are both target genes of the NOTCH signalling cascade, although there is evidence that *HES6* can function independently of NOTCH signalling (Krossa et al., 2022). *HES6* is better known for its functions in the nervous system, although work by Ramo-Montoya et al., demonstrated that HES6 drives castration resistance by enhancing the transcriptional activity of AR, even in the absence of androgens (Ramos-Montoya et al., 2014). Additionally, *HES6* expression is positively regulated by AR signalling, independent of NOTCH signalling in PC, and AR binds upstream of the *HES6* coding sequence to upregulate *HES6* expression (Carvalho et al., 2015; Ramos-Montoya et al., 2014). Other candidates from the gene list including *Claudin 3* and *4 (CLDN3/4)* (Carvalho et al., 2015; Maeda et

al., 2012) and *Metallothionein 1X/2A* have previously been reported as essential in CRPC.

z

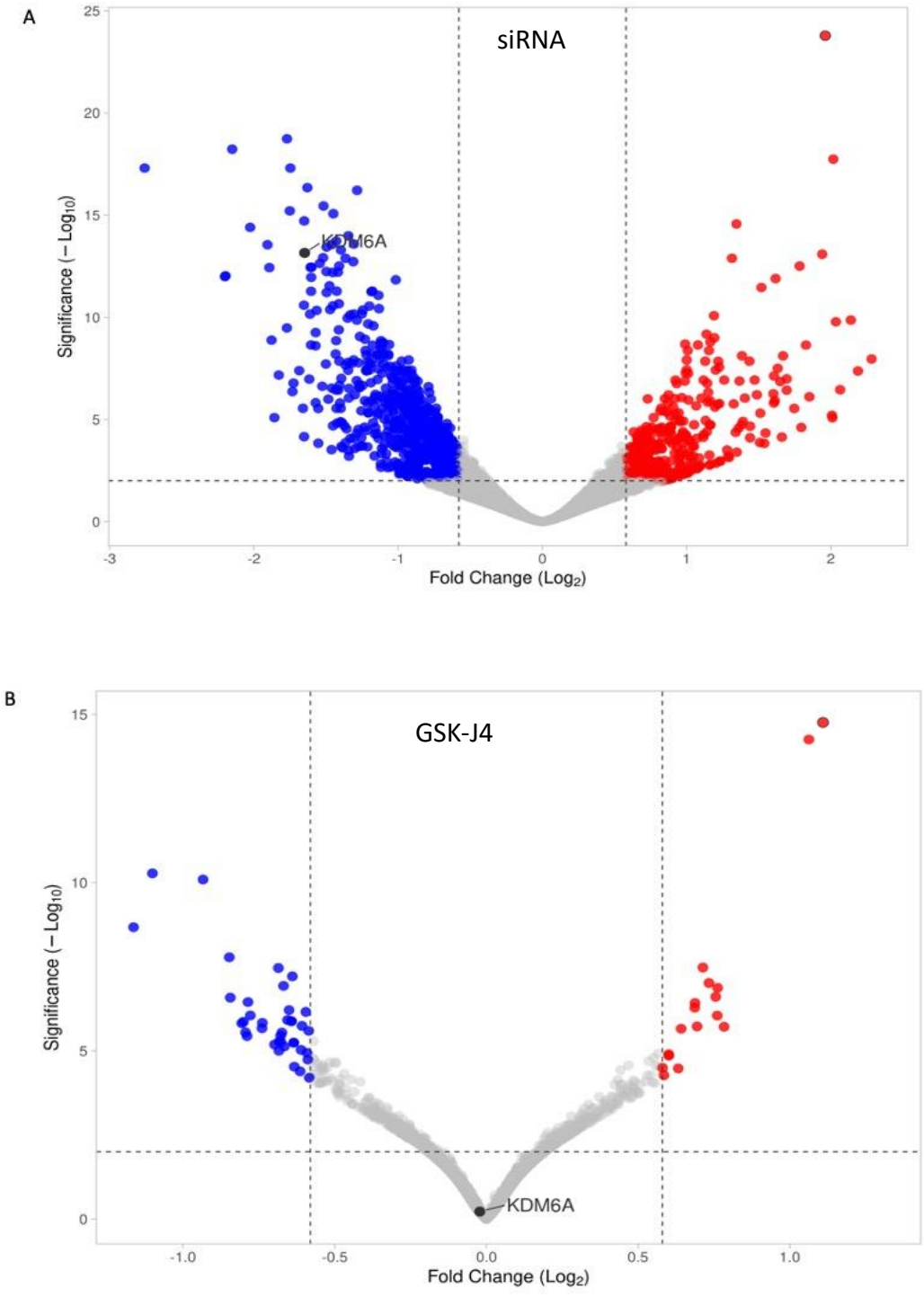

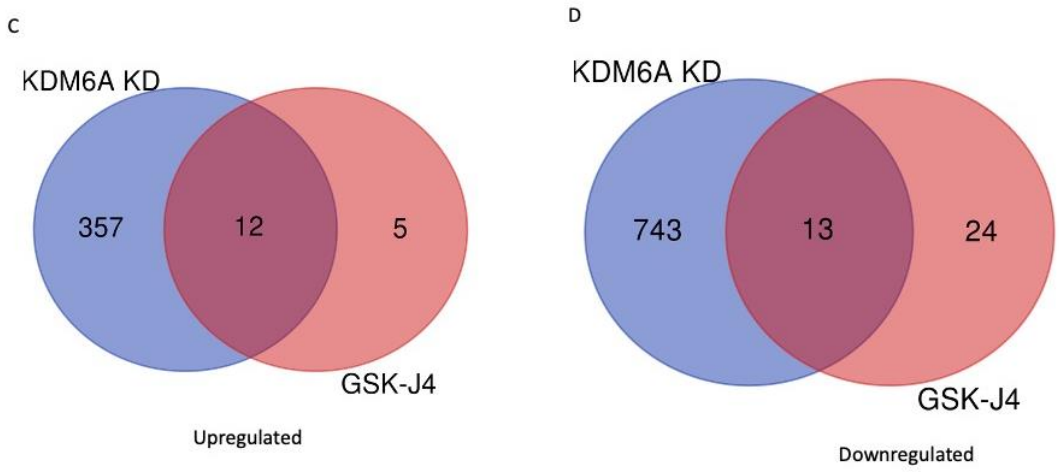

Upregulated	Downregulated
LINC01029	HES2
CDK14	CLDN4
TNC	CLDN3
TPM4	HES6
MESD	MMP17
ZDHHC16	CDKN1C
DCBLD2	HID1
WIF1	QSOX1
IGFBPL1	SFN
ZNF616	MT1X
OGFR	MT2A
ZW10	WNT7B
	COLEC12

Figure 5.10 Gene expression analysis from RNA-Seq Data. A-B) *Volcano plot of DEGs resulting from KDM6A KD and GSK-J4 vs NT. Cutoffs for significantly DEGs (points in red and blue) are FDR < 0.05 and linear fold change +/- 1.5.* ***C)*** *Upregulated DEG following KDM6A KD (369) or GSK-J4 (17) treatment. 12 genes commonly upregulated listed in table.* ***D)*** *Downregulated DEG following KDM6A KD (756) or GSK-J4 treatment (37). 13 overlapping genes listed in table.*

5.4.5 GSEA reveals pathways that are impacted in response to KDM6A manipulation.

Gene Set Enrichment Analysis (GSEA) (Subramanian et al., 2005) was used to reveal pathways affected by KDM6A KD and GSK-J4 treatment. For this, sets of DEGs from both experimental arms were run through GSEA '*Hallmarks'* signature gene lists which define a range of specific and well-defined biological states or processes. Pathways were deemed significantly altered if there was a Normalised Enrichment Score (NES) >1.5 or <-1.5 and FDR q-val <0.25. In response to GSK-J4 treatment, there were no pathways significantly enriched. However, there were four pathways with FDR <0.25 which have been shown in the analysis **(Figure 5.11A).** '*Unfolded Protein Response*' was the most enriched pathway (NES 1.4, FDR 0.21). Upregulation of this pathway suggests cells are under stress such as hypoxia or altered glycosylation (Read & Schröder, 2021). KDM6A KD resulted in the significant upregulation of 7 pathways **(Figure 5.11B).** These included *Hypoxia* (NES 1.56, FDR 0.019) which coincides with the upregulation of unfolded protein response seen in GK-J4 treatment. The pathway most upregulated was *TNF alpha signalling via NFKB* (NES 2.56, FDR 0). This may be driven by the reduction in AR expression given that this causes an increase in inflammation markers which can activate NFKB signalling (Staal & Beyaert, 2018). The only Hallmark enriched in both experiential arms was the *Epithelial Mesenchymal Transition*.

GSK-J4 treatment resulted in significantly more pathways being downregulated, a total of 15 pathways were significantly altered in response to GSK-J4 treatment **(Figure 5.11C).** *NOTCH signalling* was one such pathway (NES -1.75, FDR 0.0007) which would support the changes seen in *MES* gene expression discussed in section 5.4.3. In response to KMD6A KD, 6 pathways were significantly reduced **(Figure 5.11D),** however it should be noted that 16 pathways had an FDR <0.25. KMD6A KD affected metabolic pathways predominantly such as *Fatty acid metabolism*, *oxidative phosphorylation* and *Adipogenesis* which was interesting given the literature showing KMD6A plays a role in CRPC metabolomics (Chang et al., 2019; Chianese et al., 2022; Tang et al., 2021) . Between both experimental arms, there were 13 pathways commonly downregulated with an FDR <0.25. Oxidative Phosphorylation was the most downregulated gene set between the two experimental arms **(Figure 5.11 E and F).**

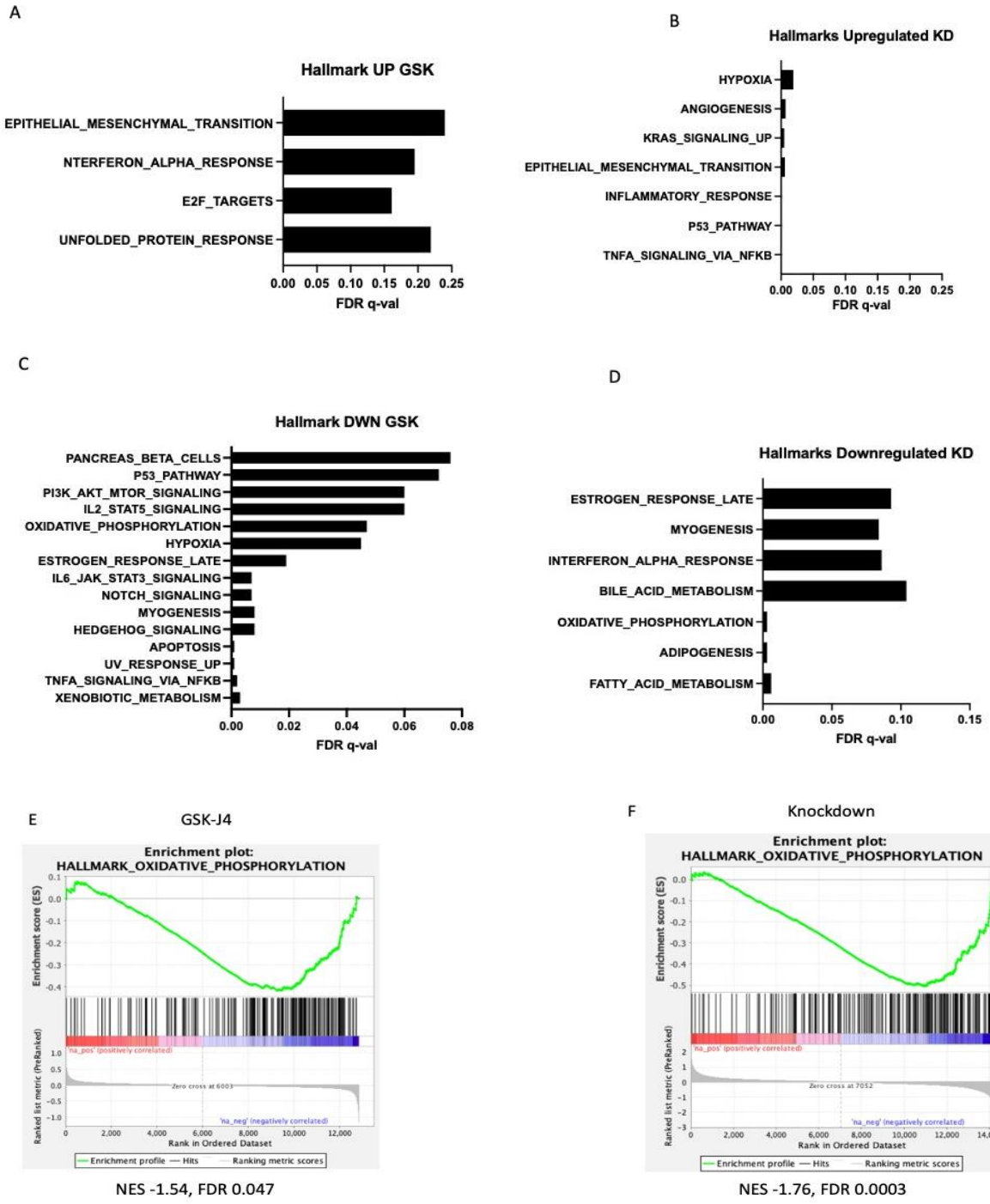

Figure 5.11 Pathway analysis from RNA-Seq experiment. *Gene lists from experimental arms were put into a ranked list based on Log2FC before processing in the GSEA software.* ***A -B)*** *Pathways from the HALLMARK gene set significantly upregulated in KDM6A KD and GSK-J4 treated cells respectively.* ***C - D)*** *Pathways from the HALLMARK gene set significantly downregulated in KDM6A KD and GSK-J4 treated cells respectively.* ***E-F)*** *Effect of GSK-J4 and KDM6A KD on the Hallmark "Oxidative Phosphorylation"*

In terms of the 'Androgen Response' Hallmark, both KDM6A KD and GSK-J4 treatment caused a reduction in the expression of this signature although neither achieved statistical significance (NES -1.2, FDR 0.175 and NES -1.2, FDR 0.2 respectively) **(Figure 5.12 A and B).** The Log_2 FC of a range of AR and AR-V7 target genes were profiled individually in response to KMD6A KD or GSK-J4 treatment **(Figure 5.12 C).** Lines on the Y-axis at 0.58 and -0.58 indicate significance thresholds. GSK-J4 did not significantly alter any of the profiled genes. KDM6A KD led to a significant reduction in *KLK3* and *TMPRSS2*. Whilst not statistically significant, KDM6A KD also reduced the expression of *KLK2* and *NUP210* which are AR and AR-V7 target genes. On the contrary, KDM6A KD led to an increased expression of *ETS2* which is proposed to be an AR-V7 target gene (Miller et al., 2023; Sugiura et al., 2021).

In conclusion, reducing KDM6A expression appears to largely affect metabolic pathways which is consistent with literature in both prostate and other cancers (Chang et al., 2019b). Whilst KDM6A KD and GSK-J4 treatment appear to have some effect in reducing AR signalling it does not appear to directly affect many AR/AR-V7 target genes, therefore it is interesting to further investigate mechanisms by which this occurs. It appears that GSK-J4 is a specific inhibitor as this was evident by the total number of genes affected by compound treatment. Even though GSK-J4 resulted in a low number of significant DEGs, there was good overlap with gene significantly altered from KDM6A KD (70% up overlap, 35% down overlap). Both KDM6A KD and GSK-J4 treatment resulted in more genes being downregulated which is to be expected given that KDM6A normally activates genes through removal of H3K27me marks.

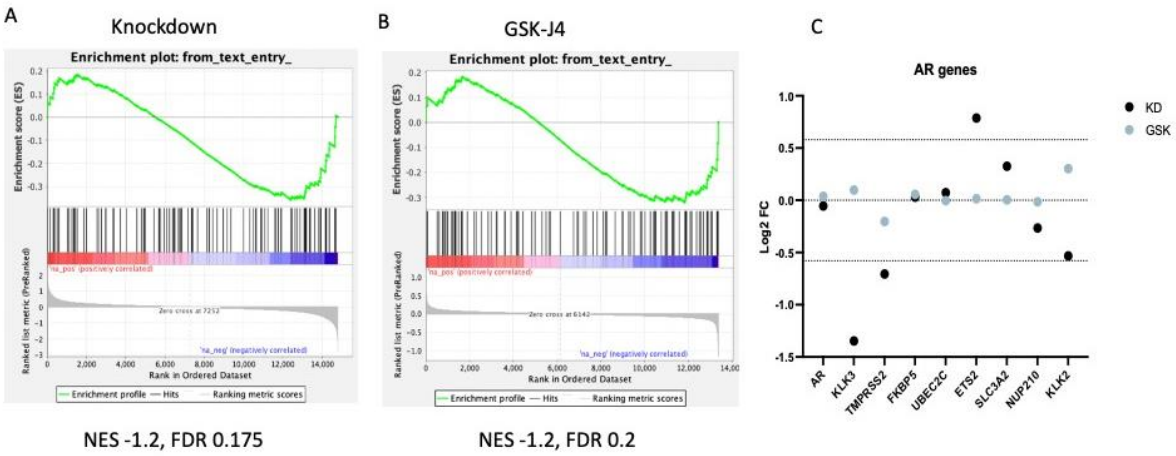

Figure 5.12 AR Pathway analysis from RNA-Seq Experiments. A-B *Changes in Hallmark "Androgen Response" following KMD6A KD or GSK-J4 respectively****. C)*** *Change in expression (LogFC) of AR and AR-V7 target genes following KMD6A (black) or GSK-J4 (Blue) treatment. Fold change relative to untreated control, dotted lines indicate significance threshold.*

5.4.6 KMD6A KD affect prostate cancer cell metabolomics.

Given the finding in section 5.4.5 that KDM6A KD and GSK-J4 treatment altered metabolic pathways, further validation of this was pursued. To validate these findings the Seahorse assay was employed. The Seahorse assay performs automatic, real-time measurements of oxygen consumption rate (OCR), proton efflux rate (PER) or extracellular acidification rate (ECAR), as well as ATP production rates of live cells in a multi-well plate; interrogating key cellular functions like mitochondrial respiration and glycolysis (Caines et al., 2022). The assay contains four compounds; Oligomycin, Carbonyl cyanide-4 (trifluoromethoxy) phenylhydrazone (FCCP), Rotenone, and Antimycin which modulate respiration. Each compound targets a different complex of the Electron Transport Chain (ETC) **(Figure 5.13A)** and through the sequence by which the compounds are added to the cells, different parameters of mitochondrial function can be measured **(Figure 5.13B).** The injection of oligomycin, which, by inhibiting ATP synthase, rapidly hyperpolarizes the mitochondrial membrane, thereby preventing protons from passing through the complexes. FCCP, an uncoupling agent of oxidative phosphorylation, reverses the hyperpolarized state caused by oligomycin by carrying the protons across the mitochondrial inner membrane. Finally, the injection of R/A inhibits mitochondrial complexes I and III thus completely stopping the mitochondrial respiration (Gu et al., 2021a).

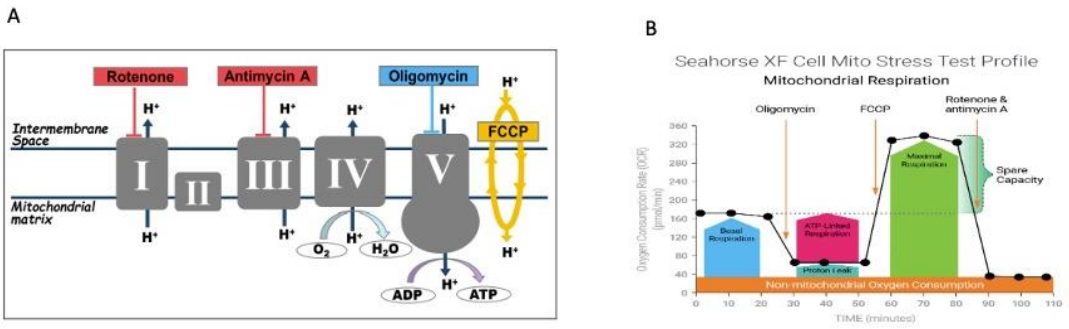

Figure 5.13 Seahorse assay set-up. A) *Targets within the Electron Transport Chain of the Seahorse assay kit compounds.* ***B)*** *Schematic of the Seahorse assay including parameters measured and timing of compound addition. Images taken from Agilent Technologies.*

CW22Rv1 cells, the same cell line used in RNA-Seq experiments, were seeded into specialised 96-well plates provided with the kit. KDM6A KD and GSK-J4 (750nM) treatment were conducted as described in *section 5.4.4*. After appropriate incubation times with either siRNA (72 hours) or GSK-J4 (48 hours), cells were ready for the Seahorse assay. At this point, growth media is removed and replaced with assay media 1 hour before the assay commences. Compounds supplied with the kit (Oligomycin, FCCP, ROT/AA) were resuspended and loaded into injection cartilage, this ensures compounds are added to the cells at precise timings as shown in **Figure 5.13B.** The 96-well plate was then run on the Agilent Seahorse Analyser and data was extracted onto an Excel worksheet. The data shown is n=10 of technical repeats of each condition. This is due to the cost implication as well as the possible lack of consistency if biological replicates were used.

An overview of the effect of KDM6A KD (Green line) or GSK-J4 treatment (Blue line) on metabolic parameters measured by the Seahorse assay can be seen in **Figure 5.14A**. The significance values shown are the result of One-way ordinary ANOVA. KDM6A KD had significantly greater effects on all parameters measured than the GSK-J4 treatment. Whilst RNA-Seq results indicated GSK-J4 treatment caused a significant reduction in the *Oxidative Phosphorylation hallmark* (NES -1.54, FDR 0.0047), these effects were not observed in parameters measured in the seahorse assay. No significance was observed between GSK-J4 treated or control cells. KDM6A KD cells had significantly reduced basal respiration, maximal respiration, ATP production and spare respiratory capacity **(Figure 5.14B).** Reductions in basal respiration and ATP production confirmed that in KMD6A KD cells there was a reduction in oxidative phosphorylation. The reduction in maximal respiration in KMD6A KD cells is likely indicative of reduced cell fitness (Gu et al., 2021b; Hill et al., 2012). Conversely, KDM6A KD cells had significantly increased levels of non-mitochondrial oxygen consumption and increased amounts of proton leaks, although this was statistically insignificant **(Figure 5.14C).** Increased levels of non-mitochondrial oxygen consumption were calculated through OCR levels after treatment with Rotenone and antimycin as these completely shut down the ETC through inhibition of complexes I and III (Campioni et al., 2022). Increased levels of non-mitochondrial oxygen consumption could indica(Plitzko & Loesgen, 2018)lysis (Plitzko & Loesgen, 2018), but also other oxygen-consuming processes, including peroxisomal reactions, Cytochrome P450 enzymes, oxidative

reactions plus oxidase and oxygenase enzymes. Increased levels of proton leak can be indicative of damaged mitochondria (Campioni et al., 2022b; Gu et al., 2021b).

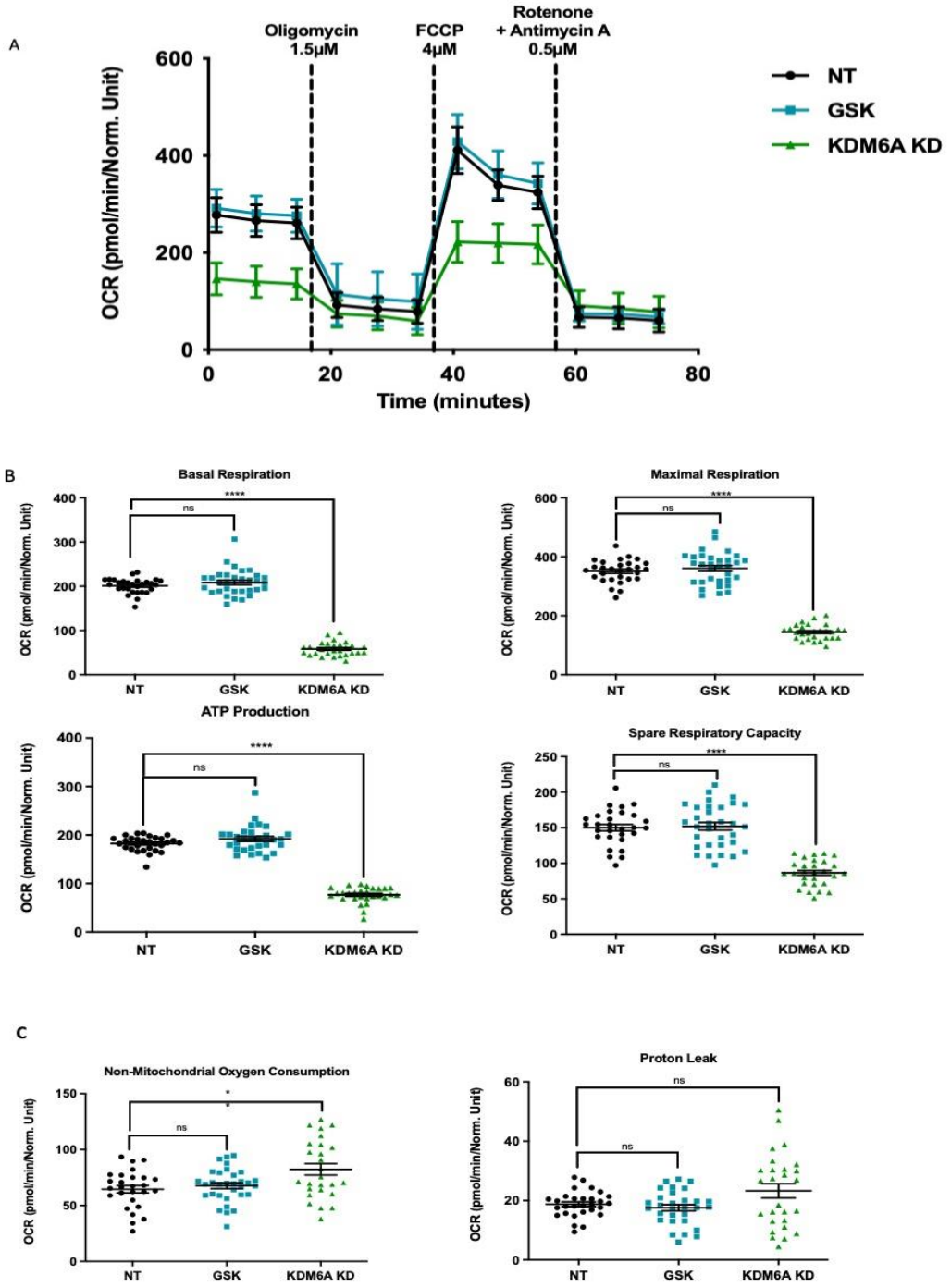

Figure 5.14 Results of the Seahorse assay in KDM6A KD and GSK-J4 treated cells. *A) Overview of OCR changes in response compound treatment in experimental arms. B) Parameters significantly reduced following KDM6A KD C) Parameter s which increased or remained unchanged following KDM6A KD. GSK-J4 did not significantly alter any parameters. Mean and standard error of difference of data points shown. Statistical significance calculated with One Way ANOVA (*=p<0.05, **=p<0.01,*

Collectively these results show that KDM6A KD has a marked impact on CWR22Rv1 metabolism. Due to the lack of changes observed in response to GSK-J4 treatment, it remains unclear if these changes are catalytic-dependent or independent. Experiments at higher dosages of GSK-J4 may provide a more insightful experimental set-up.

5.4.7 GSK-J4 treatment alters pathways which confer Enzalutamide re-sensitivity.

Given the data from *5.4.6*, in which KDM6A KD or inhibition reduced expression of the Hallmark *Androgen Receptor* and AR/AR-V7 regulated genes, I next sought to identify if GSK-J4 affected genes and pathways which conferred Enzalutamide resistance. As previously discussed, almost all patients will develop resistance to Enzalutamide and other anti-androgens (Vander Ark et al., 2018). Prior studies, using CRISPR screens, showed KDM6A to be an essential gene in Enzalutamide resistance specifically and did not affect other anti-androgen treatments (Haldrup et al., 2023).

Firstly, to identify genes that may be essential in treatment resistance and CRPC progression, significantly DEGs were identified from both the Grasso data set (Grasso et al., 2012) and CW22Rv1 cells treated with GSK-J4 (from section 5.4.4). It should be noted that whilst all patients in the Grasso data set received hormone therapy, exactly which compound they received is not specified. Therefore, this dataset provides a general list of genes affected by ADT.

In total, there were 27 genes which were significantly differentially expressed in both data sets **(Figure 5.15A).** Of these 27 genes, 51% (14), of them had opposing effects (highlighted in blue) suggesting that GSK-J4 may alter genes essential for CRPC. An additional comparison was made in comparing significantly DEGs between the TCGA data set (Cancer Genome Atlas Research, 2015) and GSK-J4 treated genes. For this, genes which were significantly altered between AR-V7+ and AR-V7- patients and in GSK-J4 treated cells were compared. In total, there were 12 genes significantly differentially expressed in both datasets. Interestingly, 75% of these genes have opposing effects; i.e. upregulated in AR-V7+ patients and downregulated with GSK-J4 treatment **(Figure 5.15B).** There were three genes *(TNC, ITGB8 and HID1)* common amongst both data which GSK-J4 treatment effects, all of which have previously been shown to be significant in CRPC (H. Li et al., 2024a; Rao

et al., 2002; R. Thomas et al., 2022a). It should be noted, as discussed earlier, that the TCGA data set is limited in that the tumours were treated. Therefore, genes from this dataset may be associated with AR-V7 expression as opposed to Enzalutamide resistance.

To assess if there were genes specifically associated with Enzalutamide resistance upon which GSK-J4 caused opposing effects, DGE in the VCaP-EnzaR cell line, described in 4.2, and GSK-J4 treated cells were compared. Again, with the idea that if GSK-J4 treatment caused an opposing effect on a DEG in the VCaP-EnzaR cells then it was likely that this gene was important for Enzalutamide resistance. In the EnzaR cells, 486 genes were significantly upregulated whilst GSK-J4 treatment caused 24 genes to be significantly downregulated **(Figure 5.15C).** Of these, 4 genes *(CROT, MT1X, MT2A, TNFRSF19)* overlapped. Next, the inverse comparison was made. In total, there were 636 cells significantly downregulated in EnzaR cells whilst GSK-J4 resulted in 19 genes becoming significantly upregulated (Figure 5.15D). Of these, 3 genes overlapped *(DCBLD2, SYT4, TNC)*. In total this leaves 7 genes in which GSK-J4 treatment has opposing effects in expression than what is seen in patient samples. Future work to further validate the sensitivity effects of inhibiting these genes would be imperative. Tenascin C *(TNC)* was persistent in all data-sets tested implicating its significance in CRPC. TNC has been shown to regulate levels of AR-V7 and is regularly amplified in aggressive PC (Mishra et al., 2019a; R. Thomas et al., 2022b). Interestingly, when the same comparison was conducted in a Darolutmaide-resistant LNCaP derivative, no overlaps were observed **(Figure 5.15 E-F).** This implicated that perhaps GSK-J4 and thus KMD6A have more specific effects on genes altered during Enzalutamide resistance. However, as this model is in a background of the LNCaP cells, any assumptions should be aired with caution. A VCaP-Darolutamide-resistant cell line would be required to validate this suggestion.

To attempt to understand pathways in which GSK-J4 may elicit an effect against Enzalutamide-resistant cells, a comparison of Hallmark Pathway analysis was conducted between the dataset of both experimental sets up. As shown in **Figure 5.15F** there were 5 Hallmark Pathways which had significant (NES <1.5, FDR <0.25) opposing changes in expression between EnzaR and GSK-J4. *Androgen Receptor* Hallmark was used as a positive control which is upregulated in EnzaR cells but downregulated following GSK-J4 treatment.

Both *TNFα* and *IL2/Stat5* pathways are strongly upregulated in CRPC patients. Inhibitors for both of these signalling pathways are currently in early-stage clinical trials in CRPC patients, however, it is too early to determine their effectiveness (Maranto et al., 2020) (ClincalTrial.gov.2024 *NCT05960578)*. This does suggest, however, that inhibition of KDM6A does inhibit pathways which are clinically relevant in CRPC. No pathways observed the inverse comparison i.e. upregulated in response to GSK-J4 treatment and downregulated in EnzaR cells.

To conclude the various comparisons made in this section, GSK-J4 treatment has a positive effect in altering the expression of genes and pathways significant in the development of CRPC. GSK-J4 treatment appears to influence gene alteration in Enzalutamide resistance as opposed to other anti-androgens and therefore may be an attractive additional treatment for patients with CRPC.

A

Gene	adj.P Value	Up or downregulated in metastatic CRPC versus localised PCa p atients samples	GSK treatment
TPM4	0.0000406	Downregulated	Upregulated
GANAB	0.00000433	Upregulated	Upregulated
IGFBPL1	0.00313	Upregulated	Upregulated
OGFR	3.65E-07	Upregulated	Upregulated
DCBLD2	2.24E-07	Downregulated	Upregulated
ZDHHC16	0.0105	Upregulated	Upregulated
TNC	4.41E-13	Downregulated	Upregulated
ZNF616	0.000118	Downregulated	Upregulated
ZW10	1.57E-08	Downregulated	Upregulated
ITGB8	1.86E-15	Downregulated	Upregulated
CHST14	0.000401	Upregulated	Upregulated
DLG2	1.88E-10	Downregulated	Upregulated
CASP7	0.00381	Downregulated	Upregulated
CROT	0.0000401	Downregulated	Downregulated
DAZAP2	1.34E-13	Downregulated	Downregulated
CDKN1A	0.00124	Upregulated	Downregulated
TNFRSF19	0.0000045	Downregulated	Downregulated
CLDN4	0.0068	Downregulated	Downregulated
CCND1	0.00755	Upregulated	Downregulated
ARHGAP29	0.00183	Downregulated	Downregulated
COLEC12	0.00000114	Downregulated	Downregulated
CDKN1C	0.0149	Downregulated	Downregulated
RHPN2	0.0183	Upregulated	Downregulated
NGFR	0.0000155	Upregulated	Downregulated
MMP17	0.00000413	Upregulated	Downregulated
HID1	0.00156	Upregulated	Downregulated
HES2	0.00549	Downregulated	Downregulated

B

Gene	PValue	Up or downregulated in AR-V7 positive CRPC patients samples	GSK treatment
TNC	0.0178164 6	Downregulated	Upregulated
ITGB8	0.0441471	Downregulated	Upregulated
SYT4	0.049176	Downregulated	Upregulated
QSOX1	0.0136586 5	Downregulated	Downregulated
ZNF217	0.0167936 9	Upregulated	Downregulated
CLDN3	0.0204406 2	Upregulated	Downregulated
ARHGAP29	0.0326846 6	Upregulated	Downregulated
CDKN1C	0.0164395 1	Downregulated	Downregulated
TOB1	0.0018184	Upregulated	Downregulated
NGFR	0.0024169 1	Downregulated	Downregulated
HID1	0.0243539 5	Upregulated	Downregulated
MT2A	0.0146352 9	Upregulated	Downregulated

C

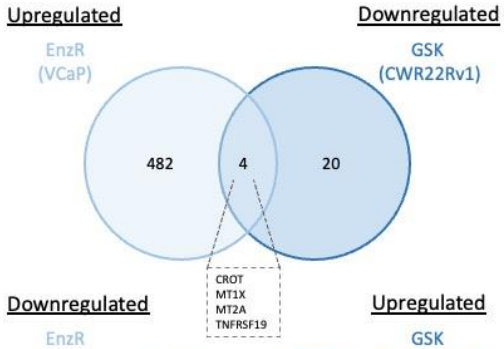

D

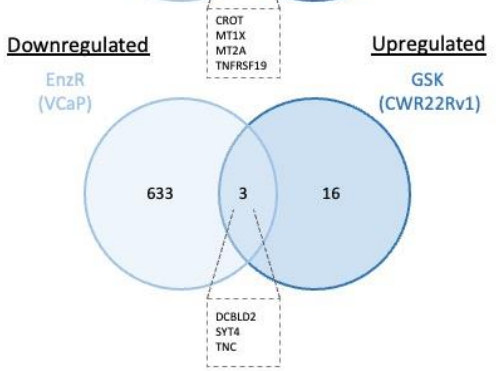

E

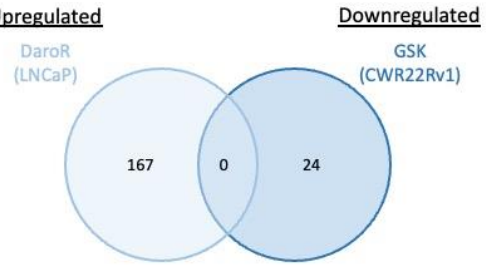

F

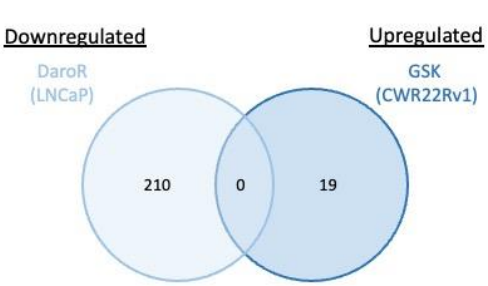

F

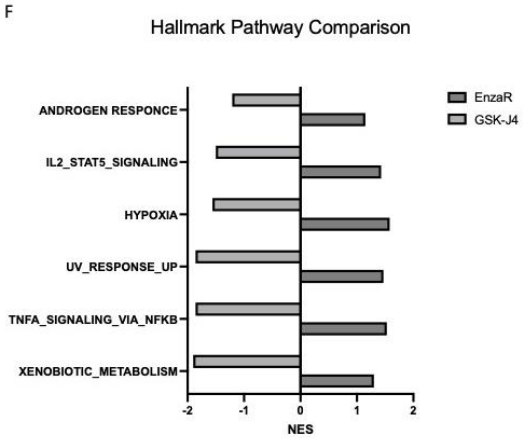

Figure 5.15 Investigating the effect of GSK-J4 treatment on genes and pathways associated with Enzalutamide Resistance. A) *SDEG expression comparison between GSK-J4 treated cells and genes from Grasso et al data set.* ***B)*** *SDEG expression comparison between GSK-J4 treated cells and genes from TGCA data set.* ***C-D)*** *Comparison of SDEG in VCaP-EnzaR cells and GSK-J4 treated cells.* ***E-F)*** *Comparison of SDEG in LNCaP-Daro cells and GSK-J4 treated cells.* ***G)*** *Comparison in changes to Hallmark Pathways in VCaP-EnzaR and GSK-J4 treated cells*

5.4.8 GSK-J4 treatment re-sensitises cells to Enzalutamide

Given the results from the previous section in which GSK-J4 treatment altered genes and pathways essential for Enzalutamide resistance, the next hypothesis was that GSK-J4 treatment could resensitise cells to Enzalutamide. Previous data showed GSK-J4 treatment to reduces mRNA levels of AR-V7 which may interfere with AR target gene expression. Secondly, as discussed above, GSK-J4 treatment affects several genes shown to be essential in Enzalutamide resistance. To test this, the CW22Rv1 cells with known resistance to Enzalutamide (Q. Liu et al., 2017), were exposed to a drug combination of Enzalutamide and GSK-J4.

Enzalutamide concentrations which are clinically relevant were chosen for the study. GSK-J4 concentrations were selected based on the CW22Rv1 IC_{50} of 750 nM. Data is normalised to an untreated DMSO control. During the SRB assay, absorbance was converted as a readout of cell proliferation. Both treatments were added to the cell simultaneously, and experiments were harvested four days after treatment. Synergy was calculated using SynergyFinder (Ianevski et al., 2022). Firstly, resistance to Enzalutamide was confirmed through minimal changes in cell viability even at the highest concentration of 30 µM of the drug (**Figure 5.16A).** Next, inhibition at each well of the combination drug matrix was calculated **(Figure 5.16B)** and data shown is the median viability of three individual experiments (N=3). The intensity of red indicates the reduction in cell growth. Finally, using the HSA model, a synergy score for the drug combinations was calculated. The combination of GSK-J4 and Enzalutamide returned a synergy score of 17.1 which is considered synergistic **(Figure 5.16C)** (Value >10 Synergistic) (Ianevski et al., 2017).

To additionally validate the re-sensitivity effect of KMD6A inhibition, CW22Rv1 cells were exposed to KDM6A KD followed by Enzalutamide treatment. As shown in **Figure 5.16D,** KDM6A KD plus 30 µM or 50 µM Enzalutamide led to a significant (P=<0.05) reduction in

cell growth over six days compared to KD alone. Also at a single time pint, 6 days after KDM6A KD, it was shown that 50 µM Enzalutamide plus KDM6A had the most significant reduction in cell proliferation **(Figure 5.16E).** Taken together, this work demonstrates that GSK-J4 treatment can resensitise cells to Enzalutamide. This work is highly promising and warrants further investigation given the clinical unmet need for men who inevitably become resistant to current anti-androgen treatments.

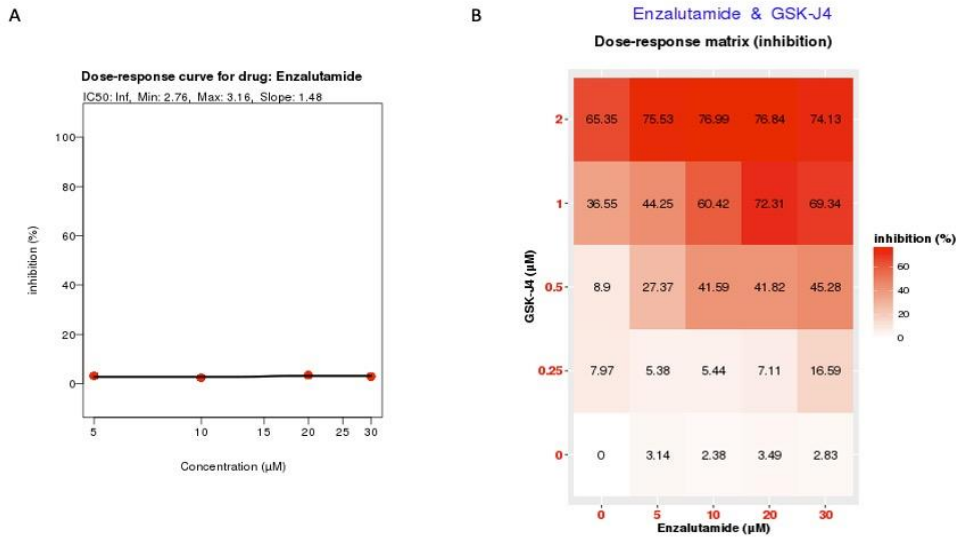

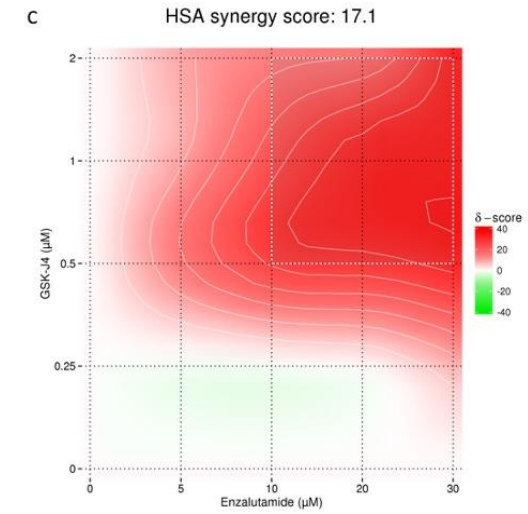

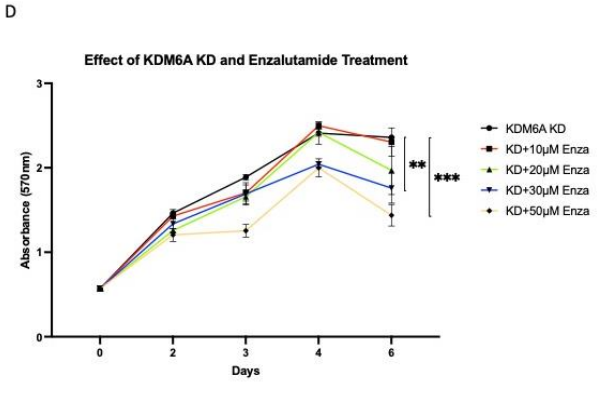

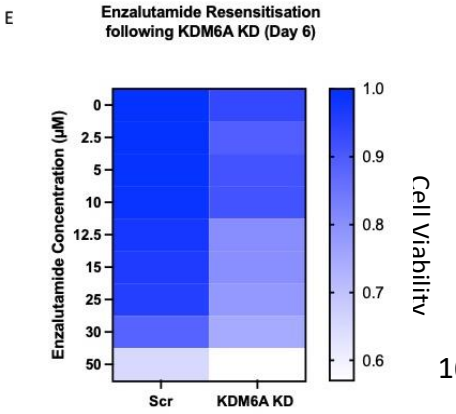

Figure 5.16 Investigating the synergistic effect of GSK-J4 and Enzalutamide in CW22Rv1 Cells A) *Validation of CW22Rv1 resistance to Enzalutamide after 96 hours of treatment.* ***B)*** *Combination matrix of GSK-J4 and Enzalutamide with corresponding reduction in cell growth in each cell. Data for each well is normalised to control (bottom left) to give change in viability.* ***C)*** *HSA calculation for drug matrix from B, deepening of red indicated stronger synergistic effect. A-C images taken directly from SynergyFinder report file.* ***D****) Effect of KDM6A KD and Enzalutamide combination on proliferation of CW22RV1 cells over a six-day period. Data is normalised to KMD6A only (black line)* ***E****) Cell viability in CW22Rv1 cells treated with increasing doses of Enzalutamide and either KDM6A KD or non-targeting control. Data normalised to Scrm, no Enzalutamide control cells (uppermost left). SRB datapoints were calculated as an average of technical triplicates within each biological replicate (n=3). Unpaired t-test was used for determination of statistical significance between day 6 datapoints. (* = p < 0.05, ** = p < 0.01, *** = p < 0.001)*

5.4.9 Assessing the effect of GSK-J4 *in vivo.*

Given the promising results of GSK-J4 on reducing PC cell line proliferation both as a single agent and in combination with Enzalutamide, the next natural experiment was to assess this *in vivo*. Firstly, to establish a concentration of GSK-J4 for dosing, a review of studies that had previously used the compound was conducted (**Figure 5.17A).** Collectively the literature review revealed that 50 mg/kg of GSK-J4 administered five times a week via intraperitoneal injections was the most common dosing schedule, this included two studies using PC cell lines.

Following subcutaneous injection of CW22Rv1 cells, mice were left for 7 days until visible tumours had formed. On the day of the first treatment, tumour volume for each mouse was measured and showed no significant difference between the control and treatment groups **(Figure 5.17B).** It was essential to establish that tumours were a similar volume before dosing as this could affect the results. Tumour volumes were measured three times weekly and by 15 days of treatment there was a surprising result in that the GSK-J4 treatment arm had significantly higher tumour volumes than control mice (P=0.04) (**Figure 5.17C).** An interesting observation on day 15 was that in the GSK-J4 treatment arm, there are two populations, responders, and non-responders. Initially, it was checked to ensure this was not a cage effect. However, upon investigation, it was clear this was not the case as both responders and non-responders were equally split between both treatment cages. The GSK-J4 treatment group had a higher relative tumour volume (RTV) at day 15 although this was statistically insignificant (P=0.135) **(Figure 5.17D).** The same trend was seen for the remainder of the experiment. By day 45 the control group had a higher time to RVT4 (P=0.028) **(Figure 5.17E)** and a higher time to RTV4 survival, although this was not significant (P=0.056) **(Figure 5.17F)** suggesting that administration of GSK-J4 surprisingly had a negative impact by increasing tumour growth. One slightly optimistic observation is that as days elapsed, the difference in tumour volumes became less prominent **(Figure 5.17G).** There was no difference in mouse weight during the study suggesting that the compound had no toxicity effects.

A

Authors	Cancer Type	Route of Administration	Dosage
Cao *et al,* 2021	PC3 and C42B PC cell lines	I.P.	50mg/kg
Yi *et al*, 2018	Kasumi-1 AML cells	I.P.	50mg/kg
Heisey *et al,* 2021	5106 Ewing Sarcoma Cells	i.p.	50mg/Kg
Sanchez *et al*, 2022	PC3, DU145, LNCaP PC cell lines	I.P.	50mg/kg

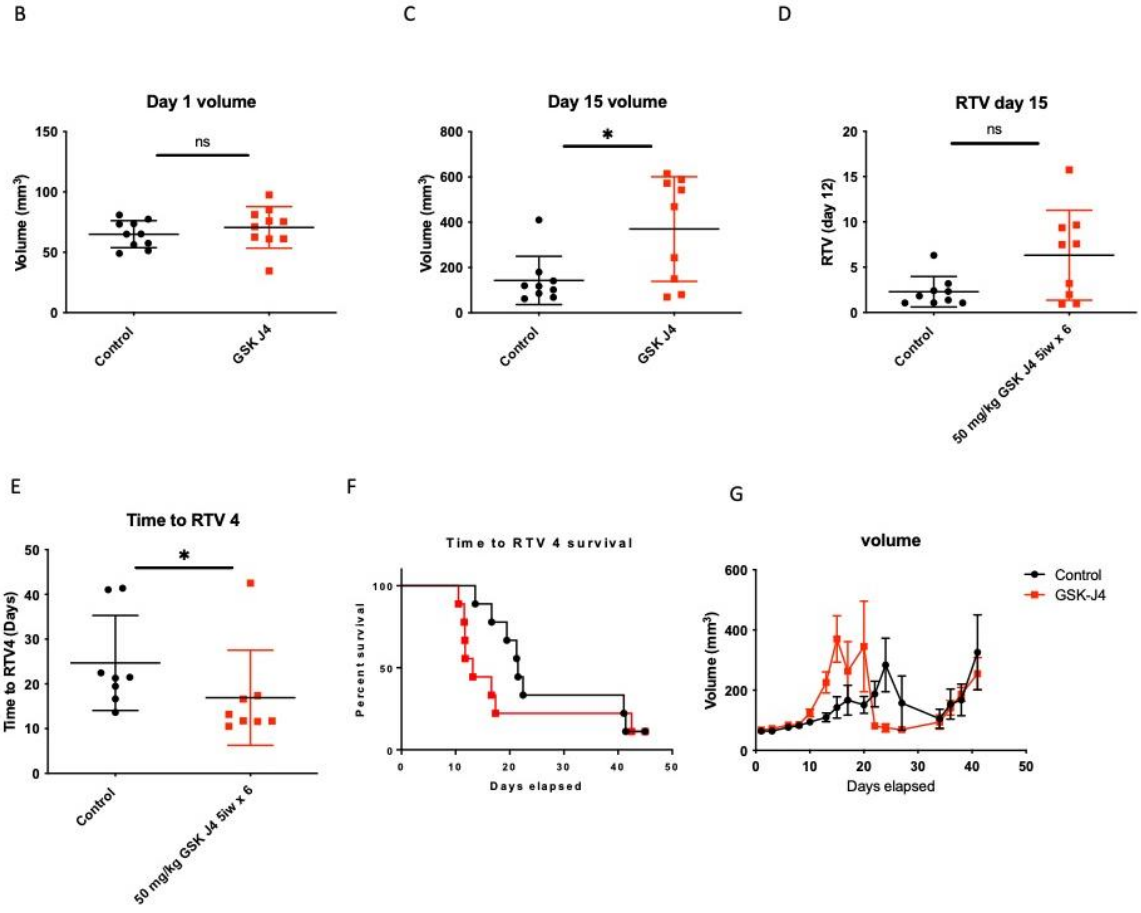

Figure 5.17 The effect of GSK-J4 on CW22Rv1 Subcutaneous Xenograft tumours. A) *Results of literature review to assess dosing schedule for GSK-J4 in vivo experiments.* ***B-C****) Volume of tumours at day 1 and day 15.* ***D)*** *Relative tumour volume of tumours calculated by normalising tumour volumes at day 15 to day 0.* ***E)*** *Time taken for tumours to reach 4 times their starting volume.* ***F)*** *RVT4 (four times the volume of day 0) used as a surrogate endpoint for survival. Each point represents when tumours had reached RVT4.* ***G)*** *Average tumour volumes of mice from experimental groups at each day measured. B-E show median and standard deviation of data points. Mann-Whitney test used to calculate statistical significance, (ns=p>0.05, *=p<0.05, **=p<0.01, ***=p<0.001 and ****=p<0.0001).*

To try and understand the results from the *in vivo* experiments, as mice were sacrificed, tumours were removed and subject to IHC using the following antibodies: AR, PSA, KMD6A, H3K7me3, H3K27ac and Ki67. Tumours were harvested from six mice (3 per experimental arm) with one mouse from each of the following time points; early, median, and late in the study. By selecting mice from different time points in the study, it was anticipated any changes in biomarker expression induced with GSK-J4 treatment would be detected with IHC staining.

The H-score of biomarkers was compared between mice from experimental arms. When comparing the expression of all biomarkers tested none were significantly altered between experimental arms **(Figure 5.19 A-E).** The treated group, however, had lower expression of PSA and AR whilst levels of KDM6A and Ki67 remained almost identical between groups. Interestingly, levels of H3K27me3 were reduced in the treatment arm, an unexpected result. Whether this was due to KDM6A not being inhibited at 50mg/kg or perhaps a form of compensatory mechanism from other epigenetic enzymes remains unanswered.

To conclude the *in vivo* work, GSK-J4 alone was not an effective compound in reducing CWR22Rv1 subcutaneous tumour growth in this single study.

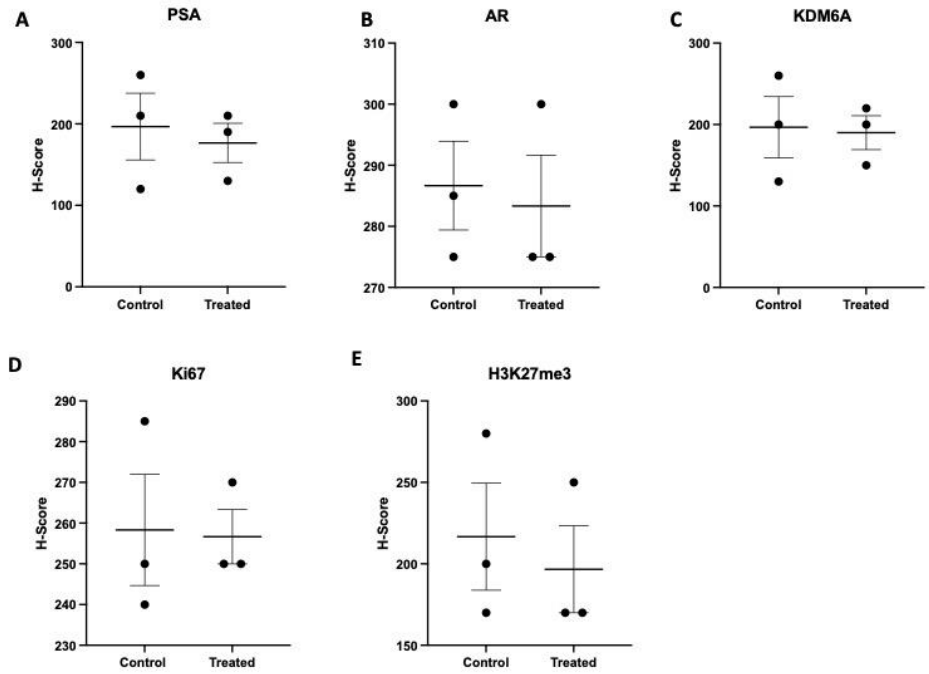

Figure 5.18 Assessing the effect of GSK-J4 on expression of biomarkers in xenograft tumours. A-E) *Comparison of H-score between control and treated tumours for each antibody used in IHC analysis. Data comprises n=3 independent tumours, mean and standard deviation indicated. Statistical comparison of H-scores using unpaired t-test between experimental arms shows no significant changes in expression.*

5.5 Discussion

The overarching aim of this chapter was to assess global changes in PC cell lines in response to either KDM6A KD or inhibition of its enzymatic activity with GSK-J4. Firstly, the effect of KDM6A KD was validated in a range of AR-V7-expressing cell lines. KDM6A KD had a robust effect in reducing proliferation and attempting to generate a KDM6A KO line was lethal which is supported by other studies (Haldrup et al., 2023). Both KDM6A KD and drug treatment with GSK-J4 resulted in a similar reduction in the expression of AR-FL, AR-V7 and PSA. It was also demonstrated that GSK-J4 treatment did not reduce levels of KDM6A itself, however still had a robust effect in reducing expression of candidate genes implicating that perhaps inhibition of KMD6A catalytic activity was enough to reduce target gene expression. It would be interesting to validate this more. Given that GSK-J4 treatment did not affect levels of H3K27me3 it would be important to profile other histone marks such as H3K27me1 which have been described in the literature to alter with GSK-J4 treatment. Due to this reported phenomenon of GSK-J4 not affecting H3K27me3 levels, it makes it difficult to determine whether demethylase activity is vital in the generation of AR-V7. In the next chapter, ChIP assays will be utilised to assess changes in the chromatin architecture around CE3 in response to GSK-J4, this will help determine if indeed GSK-J4 does affect H3K27me3 levels.

As with other KDMs, KMD6A had been implicated to be essential for AR activity (Hua et al., 2021), but mechanistic validation of this was lacking. In the CW22Rv1 cells, it was apparent that KD of AR resulted in reduced expression of *KMD6A*. Furthermore, it was shown that AR bound to distinct regions within the *KDM6A* promoter. This appeared to be a specific interaction given that at different regions of *KMD6A* (Exon 2) there was no enrichment of AR. These regions were selected through investigation of AR binding peaks from publicly available ChIP-Seq datasets. The importance of these binding regions requires further exploration as only less than 10% of AR binding sites display androgen-

dependant activity (Huang et al., 2021). The issue with the CW22Rv1 cell is that they are insensitive to androgens and therefore it was impossible to differentiate an AR binding site from an AR-regulated gene.

The VCaP cell line was utilised due to its sensitivity to endogenous androgens. Upon DHT stimulation, levels of KMD6A increased whilst levels of AR were reduced in both our dataset and an independent study (H. Guo et al., 2021). It should be noted, however, that the time point for both studies was 72 hours after the addition of DHT and therefore a multitude of factors could be changing KDM6A levels, not AR itself.

RNA-Seq from GSK-J4 and KMD6A KD cells were highly informative. Given that KDM6A removes the repressive H3K27me3, it was unsurprising to see KDM6A inhibition led to more genes being significantly repressed than upregulated. From the data, we attempted to define catalytic independently-regulated genes (those reduced in KD but not by GSK-J4 treatment). This was however difficult; firstly due to the small number of genes affected by GSK-J4 treatment and secondly, it was not clear if the concentration of GSK-J4 used in the work affected the catalytic activity of KMD6A. An experiment which would have been extremely insightful alongside the drug sensitivity work would have been a demethylase assay. This would have provided comprehensive validation that the drug concentrations used were indeed inhibiting the demethylase activity of KMD6A. It was insightful to show that KDM6A KD and GSK-J4 significantly altered PC cell line metabolomics. This validated previous work in PC cell lines where KMD6A inhibition had been shown to inhibit mitochondrial ATP production and maximal respiration (Chianese, et al., 2022).

Given that treatment resistance to second-generation anti-androgens, such as Enzalutamide, occurs in occurs in almost all patients (Vander Ark et al., 2018b), there is an unmet clinical need to resensitise men to these treatments and better understand key genomic drivers of Enzalutamide resistance. Previously, it was shown that GSK-J4 treatment could reduce AR transcriptional activity in Enzalutamide resistant cell lines models; hence it was hypothesised that GSK-J4 treatment may affect genes and pathways which are critical for Enzalutamide resistance. In the first part of addressing this, the significantly differentially-expressed genes were compared between GSK-J4 treated cells and AR-V7+ and CRPC tumours. As shown, there were three genes *(TNC, ITGB8 and HID1)* which were common amongst both datasets where GSK-J4 treatment had opposing effects as to that seen in samples. It should be noted that due to the relative small number

of genes studied in the datasets (n=39) the probability of this occurring is quite high (p=0.698 using hypergeometric porbabilitly) Interestingly, despite very few genes becoming significantly upregulated in response to GSK-J4 treatment, both *TNC* and *ITGB8* were significantly upregulated after GSK-J4 whilst in CRPC their expression is normally reduced. The *ITGB* family participate in cell survival, proliferation, and migration (Giancotti & Ruoslahti, 1999). Low expression of *ITGB8* has been shown as a poor prognostic factor in non-small cell lung cancer and renal cell carcinoma (X. Lu et al., 2016; C. Zhang et al., 2021). In prostate cancer, studies have shown conflicting evidence with some confirming downregulation of ITGB8 in PC (H. Li et al., 2024b; Taheri et al., 2022) and other studies suggesting inhibition of ITGB8 reduced PC cell mobility (Mertens-Walker et al., 2015). Differences in the studies are likely due to different datasets and cell lines used. Similar comparisons in the VCaP-EnzaR cells demonstrated that GSK-J4 treatment resulted in the downregulation of four genes (*CROT, MT1X, MT2A and TNFRSF19*) which were significantly upregulated in VCaP-EnzaR cells. Metallothioneins, of which MT1X and MT2A are part, are cytosine-rich metal-binding proteins activated by a range of stimuli such as metal ions, cytokines, and growth factors (Ruttkay-Nedecky et al., 2013). Consistent with the high expression of MT proteins in the VCaP-EnzaR line, previous studies have shown MT family members to be upregulated in PC with a direct link to chemotherapy and radiation resistance (Cherian, 2003; Gumulec et al., 2012; Smith et al., 2006). MTs regulate Zinc homeostasis and oxidative stress, processes which become upregulated during carcinogenesis (Masarik et al., 2012). One can therefore speculate that GSK-J4 treatment impedes this ability and consequently leaves the cancer cells vulnerable. Interestingly, MT has been shown to interact with NF-KB which can regulate apoptosis within cells by affecting expression, activity, and transactivation of NF-kB (Butcher et al., 2004; C.-Y. Wang et al., 1999). Our data set demonstrated that GSK-J4 resulted in a significant reduction in the *TNFα signalling via NFKB* hallmark which may have been mediated through changes in expression of MT genes. MT2A is the most highly expressed metallothionein in prostate cells and is associated with a higher incidence of biochemical reoccurrence (Forma et al., 2012; MA et al., 2015) and has also been implicated in Enzalutamide resistance (Kregel et al., 2016).

As discussed in the text, *Tenascin C* (*TNC*) was the only gene in all data sets tested in which GSK-J4 elicited an opposing effect. In CRPC, *TNC* is down-regulated whereas GSK-J4 treatment resulted in a robust upregulation. TNC is an extracellular matrix glycoprotein and is mainly studied in the context of tumour initiation, cell adhesion, migration, and differentiation (Mishra et al., 2019b). Most studies implicate TNC to be over-expressed in PC leading to increased metastasis as well as reciprocal regulation of AR-V7 expression (Y.-C. Lee et al., 2022; Ni et al., 2017; R. Thomas et al., 2022c).

With more comparative analysis we were able to show that GSK-J4 treatment repressed pathways commonly upregulated during Enzalutamide resistance such as AR response, hypoxia and STAT5 signalling (Erb et al., 2020; Maxwell et al., 2022; Schalken & Fitzpatrick, 2016). This generated the hypothesis that GSK-J4 treatment could potentially resensitise CW22Rv1 cells to Enzalutamide. A robust synergist effect was shown when both GSK-J4 and Enzalutamide were used in combination, a significant reduction in proliferation was also observed in KDM6A KD combined with GSK-J4. It is still unclear whether this effect is due to AR inhibition following GSK-J4 treatment or due to the number of genes important in Enzalutamide resistance which are affected by GSK-J4.

Unfortunately, the *in vivo* drug efficacy study did not provide positive results. The study showed that mice treated with GSK-J4 appeared to have faster-growing tumours. As mentioned previously in the work, there appeared to be two distinct populations in the treatment arm however these were not for the same cage. Whilst 50 mg/kg was effective in reducing tumour size of PC subcutaneous models, none had been conducted in the background of CW22Rv1 cells. Recently, Pecci et al., had shown that GSK-J4 treatment alone had little effect on tumour growth in both CW22Rv1 and PC3 subcutaneous models (Pecci et al., 2024). This study used the same drug dosing and scheduling of our in vivo work which suggests that GSK-J4 treatment alone is not effective in reducing tumour size, however it may change chromatin architecture which makes tumours more vulnerable to the likes of anti-androgens or inhibitors of pathways upregulated in CRPC. It would have been interesting to assess the uptake of GSK-J4 into the tumours by utilising mass spectrometry. This would have validated that the drug was penetrating the tumours to a sufficient concentration to cause an effect. However the financial implications of this were too great in the context of this study.

As discussed in the *in vitro* drug assays, GSK-J4 itself does not alter H3K27me3 levels but does reduce expression of AR isoforms and PSA which is why these biomarkers were selected for the IHC work. The IHC work was interesting in that it showed the treatment group had lower expression of AR and PSA suggesting transactivation of AR was being reduced in response to GSK-J4 as shown in *in vitro* studies, but not enough so to reach statistical significance. Levels of KMD6A levels were similar which was to be expected given that GSK-J4 would not deplete KMD6A levels. Ki67 levels also remained very similar which implies that the proliferation rate of the tumours was not significantly different. A significant finding was that levels of H2K27me3 were lower in the treated group which goes against the expected finding but also what other groups have shown with GSK-J4 increased H3K27me3 levels (B.-J. Hong et al., 2019). It is worth noting however that this study used 100 mg/kg. In retrospect, conducting an *in vivo* drug sensitivity assay first may have provided more robust results despite several studies having used 50 mg/kg with other cell lines. Additionally, the *in vivo* study from this thesis used a relatively small number of mice for the experiment which became problematic when the treatment group formed two distinct populations. Using more mice may have possibly provided some more insight. Other considerations to improve the in vivo study would be using CRISPR technology to generate a KMD6A knockout CW22Rv1 cell line. This would have had a more robust reduction in KMD6A and removed protein-protein interaction that may have still occurred with GSK-J4 treatment.

Chapter 6: KDM6A Regulates Cryptic Exon 3 of the AR Gene Through Alterations in Chromatin Structure

6.1 Introduction

Some evidence from this thesis suggests KDM6A may have a role in. However, the mechanism by which this occurs is still poorly understood. As mentioned previously, other histone demethylases have been shown to have both catalytic-dependent and independent functions in PC, such as regulating AR activity, influencing alternative splicing and allowing changes in cancer cell metabolomics (Hua et al., 2021b; Sarah & Fujimori, 2023; Tran et al., 2020). It was therefore imperative to develop assays which could investigate the mechanisms by which KDM6A was involved in processes presented in this thesis including changes to AR-V7 expression, Enzalutamide sensitivity and possible changes to alternative splicing patterns. Fundamentally, these assays would answer whether KMD6A regulates these processes in a catalytic-dependent or -independent manner. From a drug discovery perspective, it is important to determine this as it would dictate the best targeting strategy. If KDM6A was eliciting its effect in a catalytic-dependent manner, a small molecular inhibitor, such as GSK-J4, may be a suitable therapeutic option. However, if KMD6A elicits its effect through, say, protein-protein interactions, as with the chromatin adapter model previously discussed, then a more attractive option may be something such as a PROTAC to diminish levels of the complete protein.

At the time of writing this thesis, there is little data relating to KMD6A in prostate cancer, other than it being deemed “important” in AR activity following ADT treatment. However, there was little mechanistic investigation into this, and the hypothesis was primarily based on observations that expression of AR and KMD6A correlates in disease (Morozov et al., 2017).

Data from previous chapters had shown that AR-V levels were reduced following KDM6A KO and GSK-J4 treatment. Additionally, through profiling of the VCaP-EnzaR cell line and patient tumour transcripts there was a clear correlation between AR-V7 and KDM6A expression. Together this indicated the potential for KMD6A to regulate AR-V7 synthesis. Previously, groups have shown that other KMDs such as KDM4B can act as a trans-acting splicing factor and scaffold to recruit spliceosome components to CE3 (Duan et al., 2019).

In this instance, KDM4B elicits its function through protein-protein interactions as well as by manipulating histone modifications. Alternatively, Fan et al showed KDM3A, exclusively regulated the expression of AR-V7 through protein-protein interactions with spliceosome components (Fan et al., 2018). Between both studies, evidence for both the chromatin-adapter and RNA polymerase elongation rate model of alternative splicing changes have been described. Importantly in terms of KMD6A, there were no studies demonstrating if it could specifically interreact with CE3 and other regions of the AR.

In addition to this, GSK-J4 had a robust effect in reducing AR-V7 expression within PC cell lines but mechanistic understanding of this was still unclear. Data from this thesis and other studies have been able to demonstrate that GSK-J4 treatment does not affect global levels of H3K27me3 (Morozov et al., 2017). However, these conclusions were drawn from western blot analysis which provides global protein expression and therefore a more bespoke method to measure changes in H3K27me3 levels at specific loci is required. It was hypothesised that GSK-J4 may cause methylation change at specific loci, such as CE3, which are essential for AR-V7 generation thus reducing the expression of AR isoforms by altering alternative splicing. Hence, this results chapter aimed to investigate KDM6A recruitment and methylation changes in response to Enzalutamide across the AR gene, including CE3, in appropriate PC models which could possibly highlight the role of KDM6A in regulating splicing decisions of the AR transcript.

VCaP cells represent an ideal model to study the impact of flux to epigenetic post-translational modifications across the *AR* locus on AR splicing as AR-V7 transcript is upregulated in response to enzalutamide treatment. Unfortunately, publicly available ChIP-Seq portals such as Cistrome DB and ChIP-Atlas returned no results for VCaP cells treated specifically with 10 µM Enzalutamide for 72 hours. Recent work by Severson et al., using primary patient material demonstrated Enzalutamide-induced changes in H3K27ac at specific loci which are associated with castration resistance (T. M. Severson et al., 2023) . H3K27me3 levels have been profiled in other PC models, such as LNCaP cells, following Enzalutamide treatment, showing changes at specific loci (Asberry et al., 2022). However, as LNCaP cells do not upregulate AR-V7 expression following Enzalutamide treatment, they do not allow for the investigation of treatment-induced epigenomic changes and possible effects on alternative splicing regulation. As a result of this, a bioinformatics approach could not be used to assess methylation changes following Enzalutamide

treatment and therefore this Chapter provides experimental exploration to answer this key question. Despite a range of histone-modifying enzymes being implicated in alternative splicing of the AR, all are described in the context of protein-protein interactions with no studies into their effect on RNA polymerase elongation.

Overall, this concluding chapter looks to investigate mechanisms by which KMD6A elicits the effects seen on cell growth, AR-V7 generation and Enzalutamide resistance which have been mentioned in previous chapters of this thesis.

6.2 Aims

This chapter aims to investigate the changes, if any, on KMD6A abundance around CE3 in conditions where the expression of AR-V7 is high. The next aim is to assess if KDM6A changes the histone architecture around CE3 through demethylase activity or by catalytic-independent functions. Finally, it was important to investigate the effect of any changes seen on RNA polymerase elongation rates given this is one of the mechanisms histone changes can affect alternative splicing. Collectively this would provide a comprehensive mechanistic investigation into the role of KMD6A in AS of the AR.

To answer this question, I will:

1. Utilise ChIP assays to compare the abundance of KM6A and H3K27me3 in high and low AR-V7 expression models
2. Utilise ChIP assays to compare the abundance of KMD6A and H3K27me3 in +/- GSK-J4
3. Develop a novel CRISPR-KDM6A fusion which allows for the manipulation of chromatin architecture around CE3

6.3 Materials and Methods

6.3.1 Chromatin Immunoprecipitation assay

To assess the effect of Enzalutamide treatment on H3K27 methylation, KDM6A and RNA polymerase abundance at the CE3 locus, VCaP cells were seeded at $5x10^6$ cells per 150-mm dish in full growth media. Once the cells reached 80% confluency, they were treated with Enzalutamide to a final concentration of 10 µM, or DMSO control, and left for 72 hours before being harvested for ChIP. For the ChIP assay, 2 µg of the following antibodies were used per 50 µg of Chromatin (KMD6A Cell signalling Technologies #33510, H3K27me3 Abcam #ab6002, RNA Polymerase Abcam #a817, Mouse IgG control Santa Cruz sc-7392, Rabbit IgG Diagenode #C15410206)

To assess the effect of GSK-J4 on the chromatin landscape around CE3 in CW22Rv1 cells, $2.5x10^6$ cells were seeded per 150-mm dish in full growth media. Once the cells reached 80% confluency, they were treated with 750 nM of GSK-J4 and left for 72 hours before being harvested for ChIP. For the ChIP assay, 2 µg of the following antibodies were used per 50 µg of Chromatin (KMD6A Cell signalling Technologies #33510, H3K27me3 Abcam #ab6002, Mouse IgG control Santa Cruz sc-7392, Rabbit IgG Diagenode #C15410206)

6.3.2 5,6-dichlorobenzimidazole (DRB) assay

For the DRB assay, $5x10^5$ VCaP cells were seeded per 35-mm dishes in full growth media. The following day, media was removed and replaced with full growth media + 10 µM Enzalutamide and incubated at 37°C for 72 Hours. After 72 hours, the media was removed and replaced with full growth media + 10 µM Enzalutamide and 100 µM DRB. The cells were incubated with DRB for 6 hours after which the media was removed, and the cells were washed twice with PBS. Fresh full-growth media + 10 µM Enzalutamide was added to the cells. Cells were harvested for RNA, as previously described, at indicated timelines and RT-qPCR was conducted as previously described with an additional DNase treatment step prior to reverse transcription. Primer used for RT-qPCR are shown in Table 1.

Primers were designed using PrimerQuest (IDT) to span the Exon/intron junction of the AR gene to ensure that detection was only that of newly transcribed Pre-mRNA. Primer sequences are shown in table 1.

Table 14 Sequences of primers used in the DRB assay.

Target	Forward Sequence	Reverse Sequence
AR Exon 1/Intron 1 pre-mRNA	CCA GTC CCA CTT GTG TCA AA	GGC GAC ATT TCT GGA AGG AA
AR Exon 2/Intron 2 pre-mRNA	AAG CTT CTG GGT GTC ACT ATG	CTC TGG AAG GTA AAG GAG AAA GG
AR Exon 3/Intron 3 pre-mRNA	GTT ATG AAG CAG GGA TGA CTCT	TGG CCA CGT TGC CTA TG
AR CE3 Intron/ CE3 Exon pre-mRNA	GCCTGCTAGATACAAGCCCG	AGCCTTTCTTCAGGGTCTGG

6.3.3 Plasmids and Molecular cloning

TLCV2-dCas9 was generated by digestion of the TLCV2 plasmid (Addgene #87360) with Anza Restriction enzymes *Age* 1 (Thermo IVGN0074) and *Bam* H1 (Thermo IVGN0056), followed by removal of the Cas9 ORF and gel Extraction of the TLCV2 backbone using the Monarch DNA gel extraction Kits (Neb T1020). dCas9 template was amplified using the Q5 High Fidelity DNA polymerase (NEB M0491) using primers listed in Table 2. The PCR product was isolated by gel extraction using the Monarch DNA gel extraction Kits (Neb T1020). dCas9 was also digested with Anza *Age* 1 and *Bam* H1 enzymes and gel extracted as above before ligation into the TLCV2 backbone using T4 Ligase (NEB M0202). Ligation reactions were then transformed into *E. Coli* cells. All bacterial transformations for cloning products were performed in *Stbl3* cells generated in-house. Bacterial colonies were propagated in LB broth with selection antibiotic before plasmid purification by miniprep (Thermo K210011) or maxiprep (Sigma PLEX15). Plasmid sequences were checked by Sanger sequencing (GENEWIZ).

Table 15 Primers used to amplify dCas9. *Restriction Enzyme sites are in Caps followed by complementary sequence.*

Forward	Reverse
ACC GTT ATG gac aag aag tat tct atc gga ctg gcc atc	GGA TCC ctt gcg ctt ttt ctt ggg agc tcc ctc atc

6.4 Results

6.4.1 Enzalutamide treatment causes an increase in KDM6A accumulation around CE3

In response to Enzalutamide, VCaP cells upregulate levels of AR-V7 at both the transcript and protein levels (Kregel et al., 2016). This replicates what is seen in patients whereby Enzalutamide treatment drives the generation and expression of AR-V7 leading to CRPC (Sharp et al., 2019). To establish the role of KDM6A in this process, VCaP cells were treated for 72 hours with Enzalutamide before being harvested for ChIP assays. ChIP assay would allow for the quantification of KDM6A at specific genomic loci, CE3 in this work. ChIP primers were designed to span the breadth of CE3. The location of primer target sites are shown by blue boxes (for upstream on CE3) and red boxed (within CE3 coding region) **Figure 6.1A.**

Firstly, to validate the experimental setup, VCaP cells were treated with 10 µM Enzalutamide for 72 hours before RNA and protein lysates were harvested. From this, the increased levels of AR-V7 were validated at both the transcript (**Figure 6.1B)** and protein level **(Figure 6.1C).** Next, the same assay was conducted with the exception that cells were harvested for ChIP, using an anti-KDM6A antibody, as discussed in Chapter 3.3. Treatment of VCaP cells with Enzalutamide resulted in a significantly higher abundance of KMD6A around CE3 at all areas profiled compared to the DMSO control **(Figure 6.1D).** Interestingly, at intron 2 of the *AR* gene, levels of KDM6A remained unchanged between experimental arms suggesting the changes seen in KDM6A abundance are CE3-specific.

As KDM6A catalyses the demethylation of H3K27me3, the abundance of this histone mark was also profiled in the same experimental setup. The expectation was that, given KDM6A demethylates H3K27me3, the abundance of this mark would decrease following Enzalutamide treatment. It was observed that in response to Enzalutamide there was a general reduction in H3K27me3 abundance, which coincided with higher levels of KDM6A **(Figure 6.1E).** Two regions (-1.8kb and CE3 #3/4) have significantly reduced levels of H3K27me3, although it should be noted all regions were very close to significance. As with the abundance of KDM6A, H3K27me3 levels at intron 2 also remained unchanged. Taken together, these results suggest that during the emergence of AR-V7 expression, high levels of KDM6A accumulate around CE3 and alter levels of the methylation mark H3K27me3. Changes to the methylation landscape are known to affect RNA Polymerase activity which

can alter splicing decisions therefore it is imperative to develop an assay to investigate if indeed this is the case here.

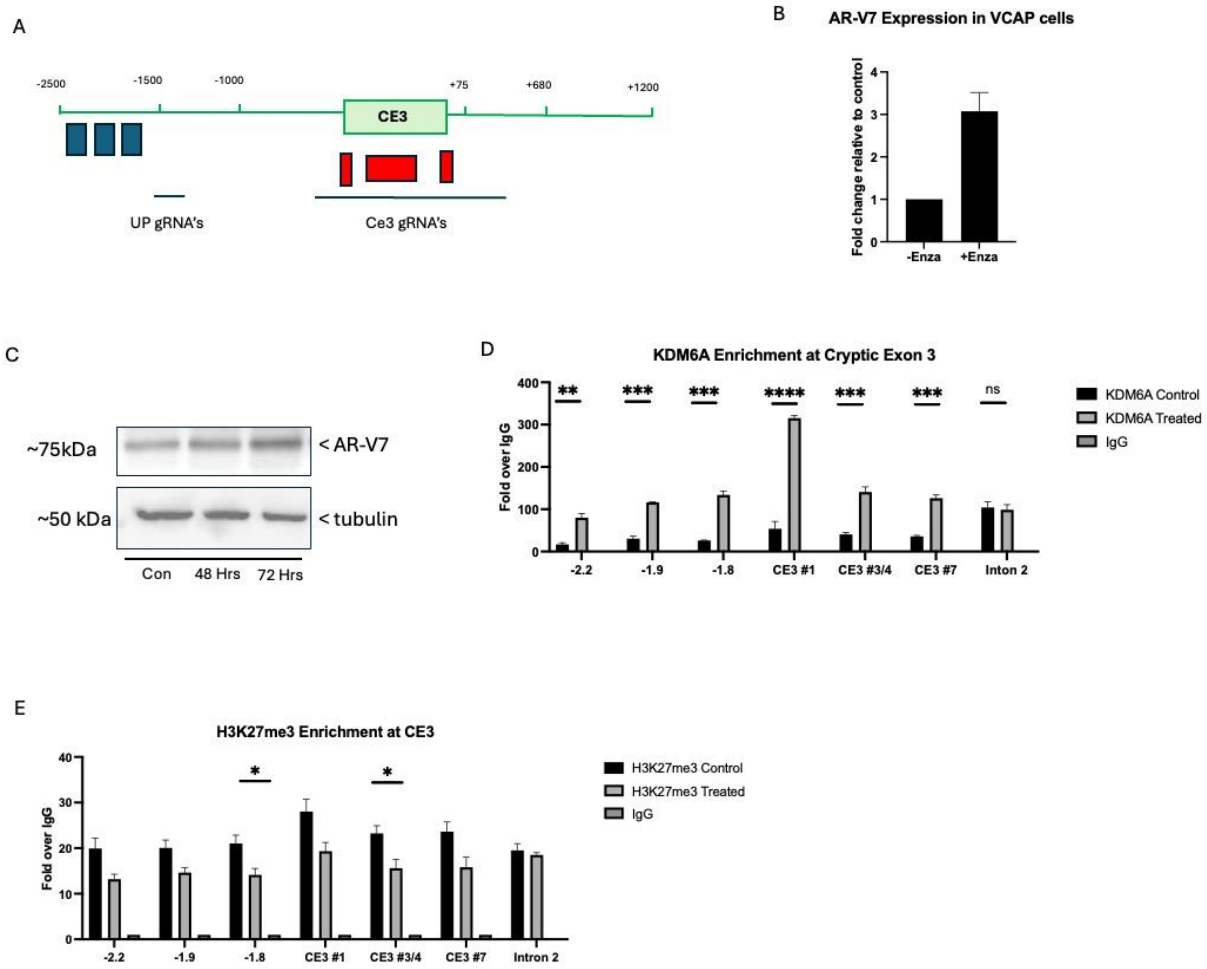

Figure 6.1 Investigating changes to the epigenetic landscape around CE3 in response to Enzalutamide. A) *Region of CE3 amplified designed for the ChIP experiment.* ***B-C)*** *Profiling the changes in AR-V7 expression in VCaP cell at the transcript and protein level in response to enzalutamide treatment.* ***D-E)*** *Changes in abundance of KMD6A and H3K27me3 following enzalutamide treatment. Statistics show the difference in fold over IgG between treated and control. qPCR data comprises n=3 independent biological repeats plotted as mean +/- SEM. Unpaired t-test was used to calculate statistical significance in D-E (*=p<0.05, **=p<0.01, ***=p<0.001 and ****=p<0.0001).*

6.4.2 Developing a novel assay to assess changes in RNA Polymerase elongation rate following Enzalutamide treatment

This section aimed to dissect whether KDM6A accumulation following Enzalutamide treatment, shown in section 6.4.1, altered RNA polymerase elongation rate given that this was one of the mechanisms by which epigenetic enzymes can alter splicing decisions as discussed in the introduction **(Figure 6.2A).** If there was no change in RNA Polymerase elongation rate this would indicate that KMD6A is affecting splicing through the "Chromatin adapter model" discussed in the introduction.

To assess the RNA polymerase elongation rate, a 5,6-dichloro-1-beta-D-ribofuranosylbenzimidazole (DRB) assay was optimised. DRB assays have previously been used in other cell lines to measure rates of RNA polymerase elongation and splicing (Singh & Padgett, 2009; Veloso et al., 2014) however key steps of the protocol had to be optimised for this specific assay. The DRB assay involved the addition of DRB which inhibits initiation of transcription. After a specific incubation time, the media is washed to remove DRB and allows transcription reactivation to commence. RNA is harvested at specific time intervals to allow new pre-mRNA expression to be assessed with qPCR. A schematic of the DRB assay is shown in **Figure 6.2B.** As the readout for the DRB assay was qPCR, specific primers were designed to span exon-intron junctions of the *AR* gene **(Figure 6.2C)** to ensure only pre-mRNA was amplified and detected in the assay (Singh & Padgett, 2009). Times indicate approximately how long it should take for new transcripts to be generated, this is based on literature which suggests RNA Polymerase elongates at approximately 1.5kb/min (Veloso et al., 2014). Primer efficiencies were calculated using a standard curve as described previously (Sreedharan et al., 2018). The HKG to be used in the experiments, RPL13A, was used as a control to compare the efficiencies of the new primer sets too. As shown in **Figure 6.2D,** all primer efficiencies were similar (median 112.5% +/- 4%) suggesting efficient amplification of their respective targets.

Next, the effect of DRB on *RPL13A* expression was tested to ensure it could remain a reliable housekeeping gene. The addition of DRB did not affect the expression of RPL13, demonstrated by consistent CT values between samples, even after 18 hours of the compound **(Figure 6.2E).** This shows that *RPL13A* is not affected by DRB and thus can continue to act as a robust housekeeping gene for qPCR analysis. The final variable to

optimise was the length of time for which cells should be incubated with the DRB compound. Compared to no DRB control, the most robust effect was observed with 8 hours of DRB treatment shown by reduced expression in all transcripts screened **(Figure 6.2F).** For this assay, cells were treated with 10 µM Enzalutamide for 72 hours, the same conditions used in previous ChIP work which elicited a robust increase in KDM6A abundance across CE3.

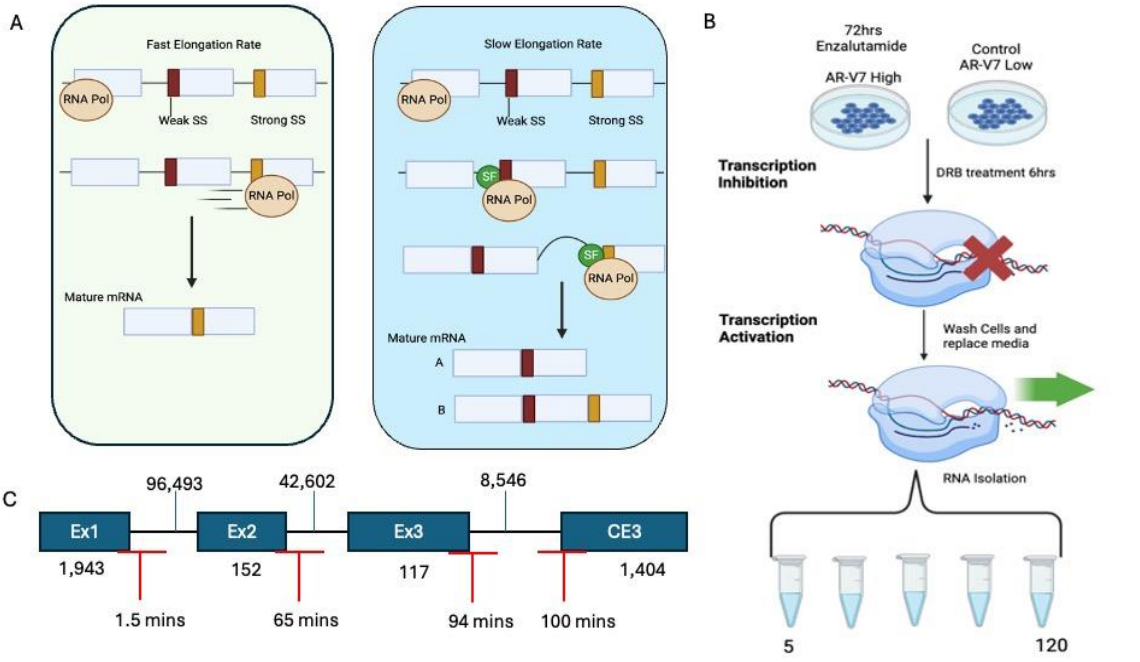

D

Primer	Slope Regression	Primer Efficiency (%)
RPL13A	-3.11	109.53
Exon1/Intron 1	-3.02	114.32
Exon2/Intron 2	-3.13	108.92
Exon3/ Intron 3	-2.99	116.27
Intron 3/CE3	-3.03	113.77
Exon 3/CE3	-3.00	115.66

E

Condition	Ct Value
NO DRB	20.77575
3 HOURS	20.55622
6 HOURS	20.99515
8 HOURS	20.92486
18 HOURS	20.21925

F

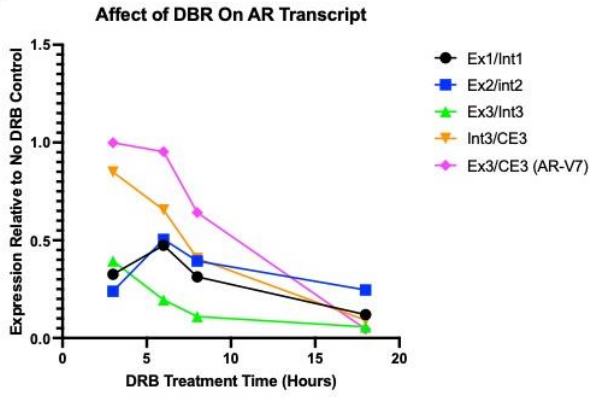

Figure 6.2 Design and optimisation of the DRB assay to investigate RNA Polymerase Elongation Rate. A) *Model of how changes in RNA polymerase can alter splicing decisions.* ***B)*** *Experimental overview of the DRB assay to investigate if enzalutamide effects RNA polymerase elongation rate.* ***C)*** *Schematic of the AR gene including Exons (Blue boxes), introns and approximate time taken for region to be transcribed (Red lines) up to CE3. Number under Exon refers to number of base pairs per that Exon. Number above intron refers to base pairs in that intron. These figures were used to determine approximate time for transcript to be generated.* ***D)*** *Efficiency of primers used in the assay.* ***E)*** *Expression of HKG, RPL13A, following different incubation times with DRB.* ***F)*** *Expression of pre-mRNA following different incubation periods with DRB. Colour corresponds to same primers from D.*

Profiling the expression of new transcripts, across all time points, it appears that the addition of Enzalutamide did not alter the generation of new transcripts significantly, implying that the RNA polymerase elongation rate was unaffected **(Figure 6.3A-F)**. An interesting observation at locations CE3 3 and CE3 7 **(Figure 6.3E and F**, respectively) where Enzalutamide appeared to reduce pre-mRNA transcript levels possibly suggesting RNA polymerase stalling. It should be noted however that as these primers are within exonic regions of CE3 and therefore it cannot be verified that this is detecting newly transcribed pre-mRNA. Taken together, from this assay, results would indicate that the changes in the chromatin architecture following the addition of Enzalutamide do not affect the RNA polymerase elongation rate.

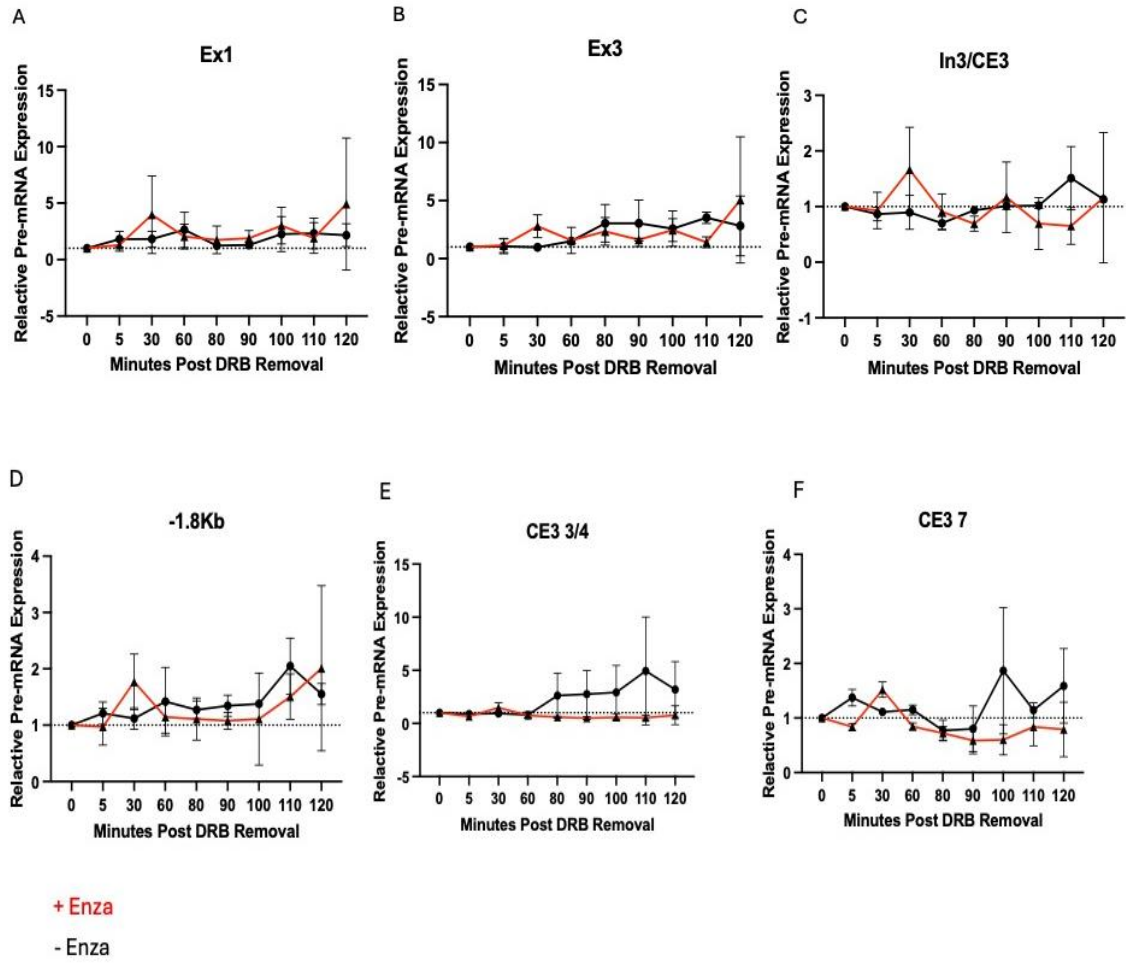

Figure 6.3 Investigating the changes in RNA Polymerase elongation induced by Enzalutamide. A-C) *Comparison of pre-mRNA transcript expression following removal of DRB.* ***D-F)*** *Comparison of mRNA expression across CE3 regions using primers from Figure 1.* ***A-F)*** *All data is normalised to 0 minutes i.e. immediately after DRB is removed. Data comprises n=3 independent biological repeats plotted as mean +/- SEM. Unpaired T-test between +/- Enzalutamide experimental arms for each time point revealed no statistical significance.*

To look further into this, RNA Polymerase ChIPs were conducted in VCaP cells treated with 10 µM Enzalutamide for 72 hours (same conditions as above). The rationale of this experiment was that if RNA polymerase was indeed stalled or slowed, then there may be an increased abundance of it across CE3 (Brodsky et al., 2005). The addition of Enzalutamide led to an increased abundance of RNA polymerase at sites across and upstream of the CE3 with statistically significant higher levels at -1.9Kb upstream, and at CE3 regions 1 and 5 **(Figure 6.4).** Higher levels of RNA polymerase across the CE3 in the

+Enzalutamide arm could implicate RNA polymerase stalling thus increasing exon inclusion (Ip et al., 2011).

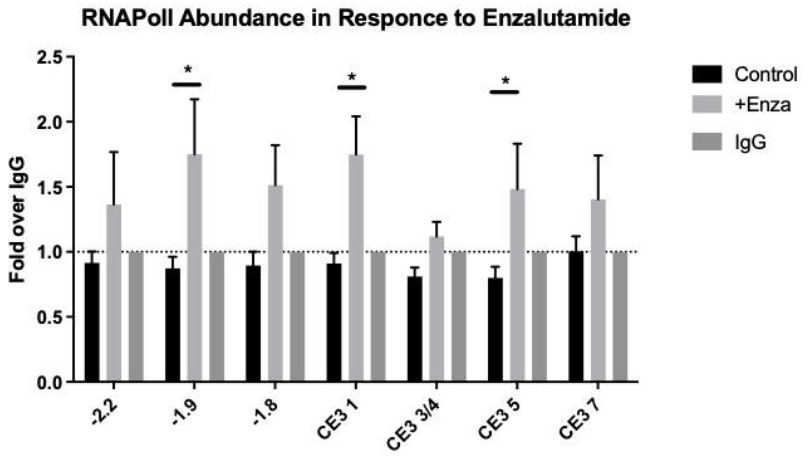

Figure 6.4 Abundance of RNA Polymerase across CE3 in response to Enzalutamide. *Abundance of RNA polymerase across CE3 was profiled 72 hours after enzalutamide treatment using same primers as Figure 1. Statistics show the difference in fold over IgG between treated and control. qPCR data comprises n=3 independent biological repeats plotted as mean +/- SEM. Unpaired t-test was used to calculate statistical significance in D-E (*=p<0.05, **=p<0.01, ***=p<0.001 and ****=p<0.0001).*

The DRB assay showed that there appeared to be no difference in the levels of pre-mRNA produced between experimental arms after the removal of DRB. This would indicate that RNA polymerase elongation was not affected by the chromatin changes induced by Enzalutamide treatment. Whilst there was a higher abundance of RNA polymerase across CE3 in response to Enzalutamide this may be due to the higher expression of AR-V7 after 72 hours of treatment with Enzalutamide. Further assays such as CO-IP or proximity-ligation assays may reveal splicing factors interacting with KDM6A during this process. Alternatively, the development of a novel system to deposit KDM6A around the cryptic exon may also better the understanding of KDM6A in the splicing process.

6.4.3 Assessing the effect of GSK-J4 treatment at CE3

It was hypothesised that GSK-J4 treatment may alter the chromatin state around CE3 which could reduce AR-V7 expression. Previously, western blot profiling of H3K27me3 post-GSK-J4 treatment had revealed no global changes to the methylation mark, however it was speculated there may be more selective changes around specific AR exons.

For this work, CW22Rv1 cells were treated with GSK-J4 to a final concentration of 750 nM for 48 hours. This concentration was selected for two reasons: (i) it was the concentration used in the RNA-Seq experiments thus allowing for comparison between experiments; and (ii) 750 nM had consistently been shown to reduce levels of AR-V7. Whilst treatment with GSK-J4 caused a reduction in KMD6A abundance across and upstream of CE3, this was not statistically significant **(Figure 6.2A).** Importantly, at intron 2, a similar pattern was observed which indicates that the changes to KMD6A after GSK-J4 treatment may be a global effect as opposed to exon-specific. In addition to this, levels of H3K27me3 were also slightly reduced in response to GSK-J4 which was surprising given that KDM6A was also less abundant **(Figure 6.2B).** This experiment was conducted to assess if GSK-J4 altered the expression of H3K27me3 at specific loci given that data from this thesis and other studies had shown no changes in global levels of H3K27me3 following GSK-J4 treatment (Morozov et al., 2017). This experiment revealed that the abundance of KDM6A around CE3 is subtly reduced following GSK-J4 although not significantly. In addition, H3K27me3 levels are also reduced suggesting that the demethylase of KMD6A is not inhibited or other epigenetic modifying enzymes compensate for its inhibition. These patterns of reduction are also seen at intron 2 of the AR suggesting any changes are not CE3 specific. It is worth highlighting that Morozov et al., demonstrated that, in fact, levels of H3K27me1 changed in response to GSK-J4 and therefore future work profiling this methylation mark in response to GSK-J4 will be an important extension to the study (Morozov et al., 2017). Results from this assay would suggest that reduction in AR-V7 generation following GSK-J4 treatment is not a direct result of inhibiting KDM6A demethylase activity.

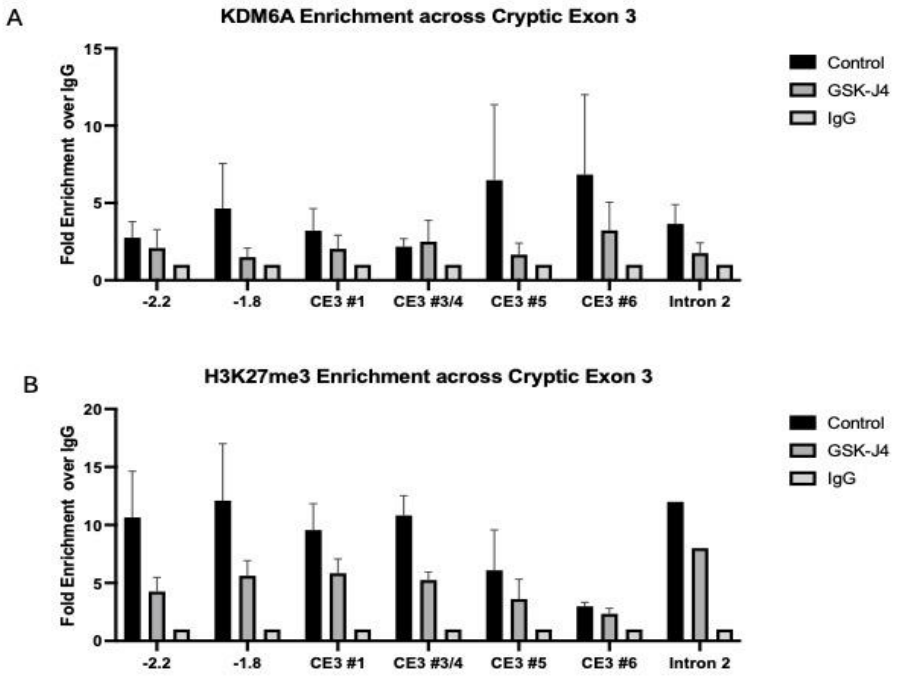

Figure 6.5 Assessing the Effect of GSK-J4 treatment on the abundance of KDM6A and H3K27me3 across CE3. *CW22Rv1 cells were treated with 750 nM GSK-J4 for 48 hours prior to ChIP analysis. ChIP primers used to profile CE3 were the same as those used in Figures 1 and 4. qPCR data comprises n=3 independent biological repeats plotted as mean +/- SEM. Statistical assessment using an unpaired T-Test between treated and untreated cells but reveals no statistical difference between experimental arms.*

6.4.4 Generation and validation of CRISPR-KDM6A fusions to manipulate CE3 chromatin architecture

To gain a better understanding of the involvement of KMD6A in the splicing of CE3, a work plan was set out to generate a novel dCas9-KMD6A fusion protein. It was predicted that this fusion protein could be used as a tool to deposit KDM6A to the specific site within the *AR* gene and assess the effect of this. This would utilise CRISPR's ability to target specific regions using custom sgRNAs. Previously, groups had attempted similar models but had targeted full exons as opposed to specific exon regions (Segelle et al., 2022; Tsui et al., 2018).

As this work required the DNA targeting abilities of Cas9 but not the nuclease activity, the first task was to generate a dCas9 model. The nuclease activity of Cas9 is diminished through the mutation of D10 and H840 of the Cas protein (Karlson et al., 2021). Previously, the lab has utilised the TLCV2 plasmid **(Figure 6.6A)** to generate multiple Cas9-expressing PC cell lines. The U6 promoter of the plasmid is under doxycycline control and therefore the system is inducible as opposed to being constitutively active. This feature was useful as it would allow for KDM6A deposition to be regulated rather than constitutively deposited. Initially, attempts were made to conduct Site-directed Mutagenesis (SDM) on the TCLV2 plasmid to generate a dCas9 form. For this work, the Q5 SDM kit from NEB was utilised. This relies on primer being designed with the desired mutation being in the middle of the targeted sequence. After PCR with the Q5 polymerase, the product should contain the desired mutation. Unfortunately, despite several rounds of modifying the assay, the Q5 SDM kit did not generate any mutations. Alignment studies from five SDM-derived clones reveal no difference in DNA sequence to the Wt TLCV2 plasmid implying unsuccessful SDM **(Figure 6.6B).** The cause of this was likely due to the size of the TCLV2 plasmid, despite kits stating plasmids up to 20 Kb could be mutated no data for this was shown.

Given the difficulties with the SDM approach, a molecular cloning strategy was planned to clone a dCas9 fragment from one vector into the TLCV2 in place of the wild-type Cas9 **(Figure 6.6C).** The removal of Cas9 from the TCLV2 by restriction digest was confirmed by gel electrophoresis **(Figure 6.6D).** Lane 1 was a no-restriction enzyme control whereby the whole TCLV2 was variable around 15 Kb. Lane 3 represents the experimental arm whereby there are two clear products, one of which at ~4Kb was deemed to be the Cas9. PCR

amplification of the dCas9 from a dCas9 donor template (Addgene #44247) was conducted with PCR primers containing complementary restriction sites allowing for the ligation into the TLCV2 vector. Successful PCR amplification was validated through gel electrophoresis **(Figure 6.6E).** Lanes 1 and 2 show no DNA and no polymerase control wells, respectively, whilst lanes 3-5 show wells containing PCR products of approximately 4 Kb which corresponds to the size of dCas9. Following ligation and transformation, 5 clones were selected for sanger sequencing to confirm insertion of dCas9 into the TLCV2 backbone. The LNCX sequence upstream of dCas9 would allow for the detection of the insertion. Alignment analysis indicated that 2 (Clones 3 and 4) out of the 5 clones sequenced were an exact match to the parental dCas9 suggesting successful integration of the dCas9 into the TLCV2 vector **(Figure 6.6F).** To validate if the TLCV2-dCas had successfully been generated, 1µg of DNA from either parental TLCV2 or TLCV2-dCAS9 was transfected into HEK293T cells. Following doxycycline induction for 72 hours, protein was harvested for Western Blot. Unfortunately, whilst doxycycline resulted in Cas9 expression of the WT TLCV2 plasmid, no expression of dCas9 was detected in cells transfected with TLCV2-dCas9 **(Figure 6.6G).**

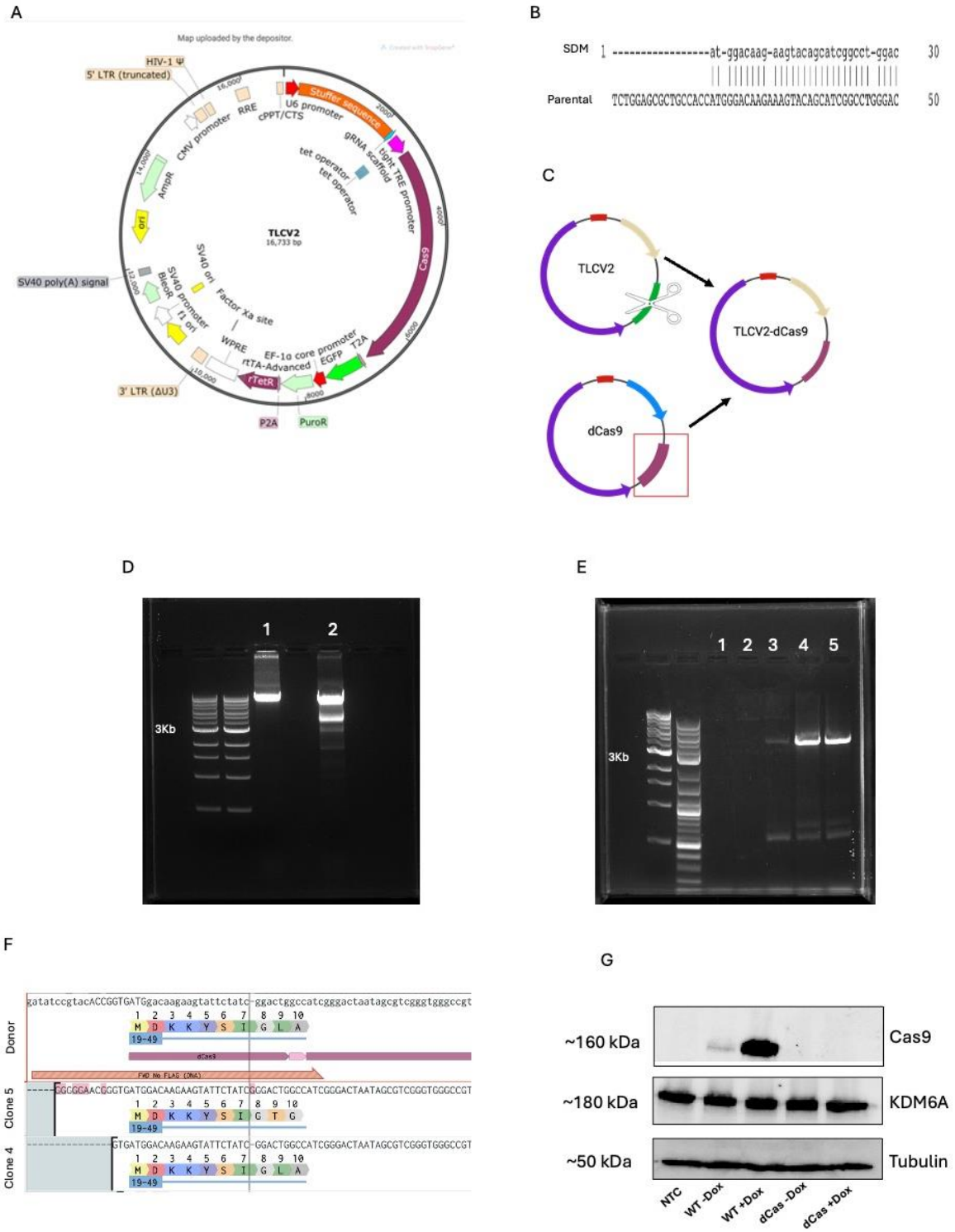

Figure 6.6 Development of a dCas9-KDM6A fusion protein. A) *Plasmid map of the TLCV2 Cas9 lentivirus plasmid which was used as recipient vector for cloning strategy.* ***B)*** *DNA alignment following Sanger sequencing of parental and mutated plasmid allowing for the identification of changes in the DNA sequence.* ***C)*** *Cloning strategy of cloning donor dCas9 into TLCV2 plasmid* ***D-E)*** *Gel electrophoresis confirming successful digestion and PCR amplification of TCLV2 and dCas9 plasmid respectively.* ***F)*** *DNA alignment following sanger sequencing to compare DNA sequence of dCas9 donor and 2 TLCV2-dCas9 clones* ***G)*** *Western blot analysis 72 hours after transfection of parental TCLV2 and TLCV-dCas9 into HEK293T cells.*

Due to time constraints, at this point the generation of a TLCV2-dCAS9 and resulting dCas9-KDM6A was halted. Later investigation demonstrated that the primers used in the amplification of dCas9 have resulted in a frameshift in the plasmid generated. Therefore, dCas9 was not in-frame and thus not expressed. Work within the lab is now ongoing with newly designed primers to allow for the generation of a TLCV2-dCas9 plasmid.

In parallel to the cloning of the TLCV2-dCas9 plasmid, initial experiments were conducted to assess if short sgRNA could be utilised in pre-existing Cas9-expressing PC cell lines developed in-house. Short sgRNA, typically around 16 nucleotides in length, have significantly reduced DNA cleavage but can still bind to genomic regions. The hypothesis was that if short sgRNA could be effective in targeting Cas9 to specific loci, then KDM6A could be more easily cloned into the TCLV2 parental plasmid. Firstly, the lack of DNA cleavage was validated by comparing the reduction in protein expression of the AR following transfection with either 16nt or 21nt sgRNAs. As shown in **Figure 6.7A,** whilst 21nt sgRNAs caused a significant reduction in AR expression, 16nt sgRNAs did not affect AR expression at the protein level. This validated that the 16nt sgRNAs had no DNA cleavage effect and therefore could be a useful tool in targeting Cas9-KMD6A fusions to desired genomic regions. Next, the specificity of 16nt sgRNA investigated if they could recruit Cas9 to specific genomic loci. For this, a doxycycline-inducible Cas9 expressing PC cell line produced in-house (CW22Rv1-AR-Ek-iCas9) was utilised. Abundance of Cas9 at specific genomic locations was calculated using ChIP assays, previously described. As small chromatin fragments were essential for this assay, successful sonication was validated by running ChIP lysates on a SDS gel **(Figure 6.7 B).** As indicated by the red arrow, all samples appeared to be approximately 200bp in size following sonication.

The enrichment of Cas9 to CE3 and regions upstream was interrogated using specifically designed primers which were utilised throughout this chapter (sections 6.4.1-3). Whilst the addition of doxycycline resulted in increased enrichment of Cas9 at genomic locations, this was not specific. Using CE3 or -1.8Kb targeting 16nt sgRNA resulted in increased enrichment of Cas9 in a non-specific manner, this included enrichment at intron 2 of the AR gene used in previous experiments **(Figure 6.7 C and D).** Due to the lack of specificity in this system, no further experiments were conducted. In addition, more recent literature

has shown that 16nt sgRNAs can have similar cleavage effects as 21nt sgRNA meaning that this system would be unsuitable for such applications (Fu et al., 2014; Y. Li et al., 2023). This section highlights the technical complexity of developing epigenome-modifying systems. Whilst it was disappointing that a dCAS9-KDM6A fusion could not be generated, which would allow for manipulation of chromatin at specific loci, additional experiment- such as the DRB provided more mechanistic insight into the effect of increased KDM6A abundance at CE3.

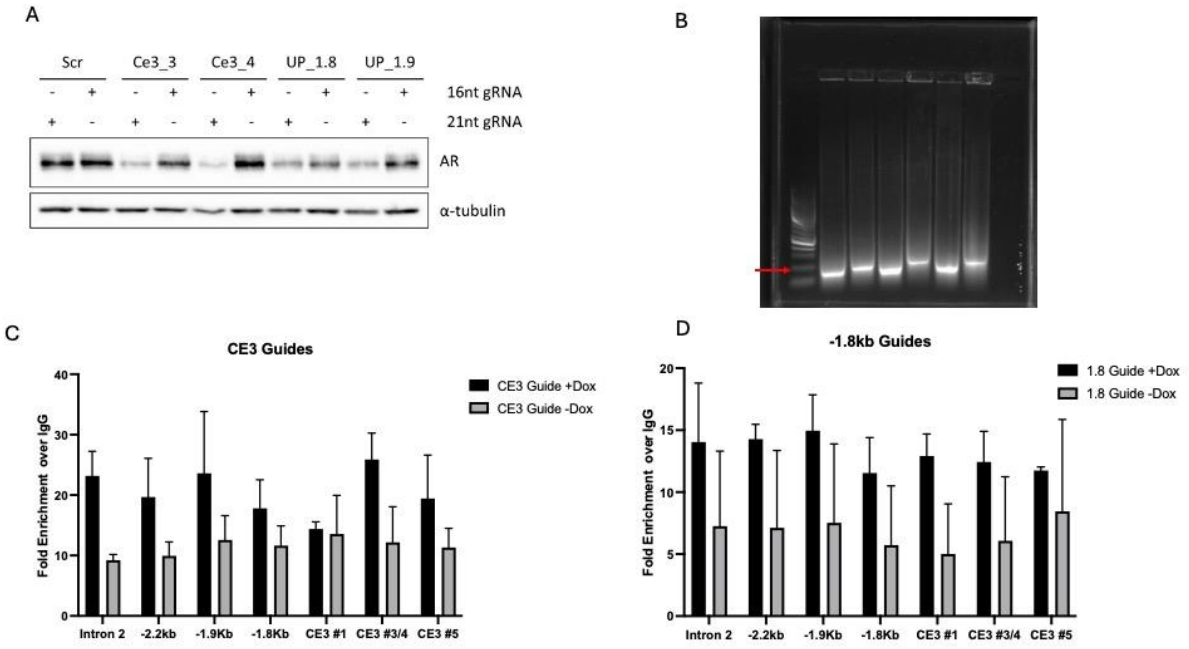

Figure 6.7 Assessing the specificity of short sgRNA as an alternative approach to cloning. A) *Comparing the knockdown efficiency of short sgRNA and regular sgRNAs. AR was targeted in PC CW22Rv1-AR-EK cells to assess if short guides had reduced knockdown efficiency. B) ChIP samples were ran on a 10% gel to ensure successful fragmentation. Red arrow indicated 200bp marker of the DNA loading ladder.* ***C-D)*** *Assessing the enrichment of Cas9 at specific regions across the CE3 using respective sgRNAs. Enrichment at specific regions was compared between +/- doxycycline given the TLCV plasmid is under doxycycline control. ChIP primers used to profile CE3 were the same as those used in Figures 1, 4 and 5. qPCR data comprises n=3 independent biological repeats plotted as mean +/- SEM. Unpaired t-tests were conducted between experimental arms at each region but showed not statistical differences.*

6.5 Discussion

This chapter aimed to explore mechanisms by which KMD6A elicited changes to AR-V7 expression, enzalutamide sensitivity and possible changes to alternative splicing patterns which led to the development of CRPC. Through ChIP assays, one could demonstrate that in response to enzalutamide, there was an increase in the abundance of KMD6A around CE3. Levels of the KDM6A methylation target, H3K27me3, were reduced although not significantly across the whole CE3 gene. Given that KMD6A was so highly enriched (over 300-fold increase at some regions profiled), it was surprising that levels of H3K27me3 did not diminish more.

This suggests that perhaps KMD6A itself, rather than its demethylase activity, was more important in AR-V7 generation. In other studies which have investigated the effect of other KDMs on AR-V7 generation, KDM3A is independent of its demethylase activity (Fan et al., 2018), whilst KMD4B was shown to regulate AS by both a demethylase and an independent demethylase function (Duan et al., 2019). ChIP assays following GSK-J4 treatment also supported the idea that KDM6A elicits changes in a catalytic-independent manner. GSK-J4 treatment resulted in reduced, but not significant, levels of KMD6A as well as the H3K27me3 mark. This would suggest that changes to the methylation mark, and thus the demethylase activity of KMD6A, are not essential for changes seen in AR-V7 expression. It is therefore likely that the changes in AR-V7 expression following GSK-J4 treatment are a result of pathways and genes affected by the inhibitor, discussed in Chapter 5. Alternatively, GSK-J4 treatment may effect some mechanism not tested here such as transcript stability or translation rate.

The DRB assay was conducted to investigate if the epigenomic changes seen in response to enzalutamide (accumulation of KDM6A) affected RNA polymerase elongation rate given this is one of the proposed mechanisms for how histone modification and epigenetic enzymes affect alternative splicing. DRB assays had been used successfully in other studies to investigate RNA Polymerase kinetics and RNA splicing rates (Segelle et al., 2022; Singh & Padgett, 2009) and therefore were an attractive assay due to the simplicities and relatively low cost. A reduction in RNA polymerase rate would have been demonstrated through a longer time for pre-mRNA transcripts to be formed. Previously, a slower rate of RNA polymerase has been shown to increase alternative splicing at specific exons as it

allows more time for the spliceosome to be recruited to weak splice sites (Jin et al., 2023). The results from this work show that at all time points, there was no significant difference in the amount of pre-mRNA or the time for pre-mRNA to be synthesised between experimental arms. This could suggest that RNA polymerase elongation is not different between the experimental arms and thus is not the mechanism of splicing changes. It should be noted that the levels of pre-mRNA transcripts post-DRB removal seen in this work are consistent with those in other papers (around 1.5-fold increase in pre-mRNA expression after DRB removal) (Jin et al., 2023; Singh & Padgett, 2009). One consideration from this work is the possibility of a 'lag' effect from the DRB reagent once washed off the cells. A possible solution to determine if DRB still influences transcription even after being washed off the cells would have been the use of nascent RNA labelling assay. Here, 4-thiouridine or bromouridine treatment could have been assessed in post-DBR treated and non-treated cells to assess if the DRB reagent caused a lasting effect even after being washed from the cells. Alternatively, rather than profiling the expression of region after the addition of DRB (as in Figure 6.6F), a better approach may be to profile the expression of the regions after DRB removal to ensure the effect of DRB is not long lasting.

As mentioned in the results section, primer pairs CE3 #3/4 and CE3 #7 appear to show a reduction in RNA Polymerase elongation. However, these primers amplify an exonic region within CE3, not Exon/intron junctions and therefore it cannot be determined if the change is a true reflection of reduced RNA polymerase elongation or simply detection of residual mature mRNA from before the DRB inhibitor was added. It is worth noting that cell lysates were treated with DNase and therefore there should not be DNA contamination. An additional experimental arm that could have been included is DRB plus actinomycin D for example. Actinomycin D would have blocked recovery of the pre-mRNA following DRB release thus validating that pre-mRNA detected in this assay was from the transcriptional activity of RNA polymerase. The RNA polymerase ChIP was conducted as a secondary validation for the DRB assay with the hypothesis being that if RNA polymerase was stalled, then there would likely be higher abundance of it across CE3. Despite there appearing to be no changes in RNA polymerase elongation, the RNA polymerase ChIP revealed a significantly higher abundance of RNA polymerase in response to enzalutamide. This is likely a reflection of increased amounts of the transcript. Previously, the distribution of RNA Polymerase has been shown to positively correlate with the amount of the pre-mRNA

signal detected by qPCR (Singh & Padgett, 2009). A better refinement of this experiment would have been to use an antibody which detected phosphorylated (active) RNA polymerase, rather than the antibody used in this work which detected total RNA polymerase. The use of the total RNA polymerase may be the reason for the discrepancy between the DRB and ChIP work. The RNA polymerase ChIP data indicated that in the presence of enzalutamide, there was a significantly higher abundance of RNA polymerase. However, the DRB assay showed in general, the addition of enzalutamide caused a reduced transcriptional output. Both assays included three common primer pairs which allowed for this comparison (primer pair -1.8kb, CE3 ¾, CE3 7). It should be noted however that DRB had not been added to the ChIP plates and this itself is likely to affect RNA polymerase abundance.

A critical consideration for this work, given that it was set up to identify if chromatin modification could affect RNA polymerase elongation, was whether DRB treatment itself changed chromatin architecture. Previous studies, however, have demonstrated that the addition of DRB does not significantly affect histone modification or chromatin structure and thus was an appropriate tool to analyse the effects of histone modifications on RNA Polymerase elongation rate (Bandau et al., 2024; Singh & Padgett, 2009).

CRISPR technology can be utilised to modulate and manipulate the epigenome through DNA methylation and histone modifications (Fadul et al., 2023; N. Xie et al., 2018). Firstly, in hindsight an off shelve dCas9-KDM6A plasmid should have been purchased, attempts were made to utilise a dCas9-KDMD6A plasmid from Segelle et al., (Segelle et al., 2022) but unfortunately, time pressure did not allow for this to work out. Initially, the development of our own dCas9-KMD6A plasmid proposed in this chapter would have given us the benefit of using a doxycycline-inducible system, although this was not essential as the comparison could have been made between non-targeting and CE3 targeting sgRNAs. Given the strong body of evidence in the VCaP +/- Enzalutamide ChIP assays, where KMD6A abundance increased around CE3, it was also discussed what added value the generation of an epigenome modifying vector would be. Therefore, at this point, more efforts were put into investigating mechanistic insight into how KMD6A accumulation affected splicing, which led to the development of the DRB assay.

Taking the work of this chapter and assessing it to the aims it would appear that KMD6A affects alternative splicing of the AR around CE3 in a catalytic independent function, probably through a chromatin adapter model as with KMD3A (Fan et al., 2018). The evidence for this is that KMD6A is highly abundant across the CE3 in response to Enzalutamide (over 100-fold) but there are no consistently significant changes to H3K27me3 marks. In addition to this, the addition of GSK-J4 causes a global change to KMD6A and the H3K27me3 methylation marks are reduced which also indicates changes to AR-V7 generation are catalytically independent. Finally, the work here demonstrates that changes in the chromatin architecture in response to enzalutamide do not appear to alter RNA polymerase elongation rate which would suggest the chromatin adapter model of KMD6A inducing AR-V7 generation. To test this hypothesis, further interrogation of RNA-Seq data sets in response to KMD6A KD could identify SFs which are regulated through KMD6A. If these splicing factors were to have motif sequences in or around CE3 it could be tested whether KDM6A induces changes to these SF in response to enzalutamide which led to AR-V7 generation. A Co-IP for example would be able to demonstrate this along with KD of the identified SFs. From a drug discovery perspective, targeting the KMD6A protein would be more effective, possibly the TRP domain, which as discussed in previous chapters was important for protein-protein interaction.

Chapter 7. Discussion

The goal of this thesis was to validate if KMD6A was a viable target in CRPC for which there are currently no curative treatments (Del Re et al., 2019; Iguchi et al., 2019). The progression from CSPC to CRPC is driven by multiple mechanisms of treatment resistance, with the generation of alternatively spliced AR isoforms (termed androgen receptor variants) being one of the most prevalent and studied resistance mechanisms to date. AR-Vs continue to drive AR signalling due to harbouring fully functional transcriptional activation and DNA binding domains which maintains AR signalling in the presence of AR-targeting agents and allows for the continuation of PC growth and proliferation even in castrate conditions. AR-Vs are generally deemed 'undruggable' due to the loss of the LBD. Whilst AR-Vs still harbour the N-terminal and DNA-binding domain both of these are generally considered undruggable. The N-terminal domain is highly intrinsically disordered making structure-based drug design difficult (Ji et al., 2023). The DBD across the class 1 nuclear receptor family exhibits high structural similarity which makes targeting specific receptors DRB domain almost impossible (Frigo et al., 2021; Weikum et al., 2018). Due to these challenges, it was hypothesised that targeting splicing factors which regulated the synthesis of ARVs may be a more therapeutically viable option. Trans-acting elements are proteins which regulate splicing decisions (discussed in the introduction section 1.5.2), however more recently changes to the epigenetic landscape and the proteins (such as KDM6A) which cause these effects, have been shown as additional regulators of AS (Gimeno-Valiente et al., 2022; Luco et al., 2010, 2011). Increased generation of AR-V7 for example can be driven by KDM3A recruiting splicing components to CE3 (Fan et al., 2018). his work hypothesised that by inhibiting KDM6A there was the potential to interfere with splicing in the vicinity of CE3 which would prevent the generation of AR-V7.

Across both patient samples and prostate cancer cell line models, KDM6A expression was shown to correlate to that of AR-V7 and AR-FL. It was also validated that KDM6A was more highly expressed in models of CRPC than in benign and CSPC models **(Figure 4.4).** Interestingly, this same pattern was seen in patient clinical data **(Figure 4.1)** and demonstrated that *KDM6A* amplification was a common genetic alteration specifically in CRPC (**Figure 4.1).** Overexpression of *KDM6A* in a range of PC models leads to increased

expression of AR isoforms as well as the AR-target gene *PSA* **(Figure 4.7-4.11)**; with the KDM6A wild-type plasmid appearing to cause the greatest of changes. Whilst transient transfection of both KDM6A Wt and Mut KDM6A plasmid led to similar elevated levels of KDM6A, the Mut plasmid had minimal effects in changing the expression of AR isoforms for all PC models profiled. This implicated that the catalytic activity KDM6A may have been important for changes in AR isoform expression however this would need validating in the future with cell lines stably over-expressing KDM6A plasmid. Rescue experiments whereby cells were treated with GSK-J4 after KDM6A OE showed a clear reduction in AR-V7 expression however this data was not shown as only the KDM6A Wt plasmid was used. Interestingly, patient data revealed that rates of *KDM6A* alterations were higher than genes well known to play a role in PC, such as *SPOP* and BRCA2 (Dai et al., 2017; Messina et al., 2020; Nakazawa et al., 2022). By combining both *in vitro* and in silico data, the potential importance of KMD6A in CRPC was validated and provided sound reasoning to further investigate.

Diminishing KMD6A activity via siRNA-mediated KD or catalytic inhibition using GSK-J4 appeared to have a robust effect on reducing the proliferation and expression of AR isoforms in multiple PC cell line models **(Figure 5.1-5.5).** Consistent with the KDM6A overexpression studies, it appeared that the CWR22Rv1 cells were most sensitive to KMD6A inhibition. According to the Cell Model Passport data set (van der Meer et al., 2019), the CWR22Rv1 cell line harbours a loss of function mutations in *KMT2C.* Given that it is documented that KMT2C is essential for the stability of KDM6A (Rickels et al., 2020; Seehawer et al., 2024), one could speculate that the increased sensitivity shown by these cells is a result of *KMT2C* mutation. It should be noted, however, that a reduction in AR isoform expression and proliferation was seen in other CRPC models including LNCaP95 cells and the novel VCaP-EnzaR model generated during this project.

A key question throughout this work was whether KMD6A elicited the effect seen through its demethylase activity or by catalytic-independent mechanisms, such as enabling protein-protein interaction, as is the case of several histone demethylases, which have been shown to regulate processes such as AR activity, alternative splicing and PC metabolomics (Fan et al., 2018; Metzler et al., 2023b; Sehrawat et al., 2018; Z. Yang et al.,

2020). To address this question, and to gain a better overall understanding of the global effect of KMD6A inhibition in PC cell lines, RNA-Seq was conducted in cells after KDM6A KD or GSK-J4 treatment. The GSK-J4 experimental arm allowed us to identify genes and pathways which were regulated by KMD6A catalytic activity, whilst KD of KDM6A serves to reveal genes and pathways regulated by both catalytic and non-catalytic activities of the protein. As discussed in Chapter 5, whilst the specificity of GSK-J4 had been brought into question, the concentration used in the RNA sequencing experiments was below that to affect other HDM families. Whilst KDM6A KD resulted in considerably more significantly differentially-expressed genes compared to GSK-J4 treatment, this does not mean KDM6A regulated genes predominately through non-catalytic ways. Factors such as off-target effects of siRNA treatment and insufficient GSK-J4 concentration may also have skewed the data. In addition, it could be argued that a low number of significant gene alterations following GSK-J4 is a positive outcome as it shows the inhibitor has a low off-target effect whilst also making it easier to determine KDM6A-regulated genes and pathways essential in CRPC. Given that the focus of this thesis was to investigate the role of KMD6A in splicing it was initially disappointing to see that neither KD nor GSK-J4 treatments caused a significant change to the spliceosome pathway. Although as alluded to in the text, if KMD6A was specifically regulating splicing decisions around only the CE3, then it is plausible that the global spliceosome pathways may not be affected and essentially this change becomes masked by more significantly altered pathways. By running DEGs against a list of spliceosome-related genes generated by Sharp et al. (Sharp et al., 2019), we were able to determine that indeed in response to both KDM6A KD or GSK-J4 treatment there were changes to specific splicing-related genes such as SF3B and HNRNPA1. As shown by Fan et al, HDMs can act as anchors to recruit spliceosome components to CE3 to influence splicing decisions (Fan et al., 2018). Future work to assess a direct interaction between KDM6A and the spliceosome protein mentioned above would be useful in exploring a possible mechanism of KMD6A regulating AS of CE3 into mature AR-V7 transcripts.

RNA-Seq analysis also revealed that other than splicing, inhibition of KDM6A regulated other processes which makes it an attractive target in CRPC. One example validated in this study is the reduction in Oxidative Phosphorylation after KDM6A inhibition. In PC, AR signalling can drive cellular proliferation through the activation of oxidative

phosphorylation making it an attractive target in the disease (Audet-Walsh et al., 2017; Bader & McGuire, 2020). It is unclear whether the reduction in oxidative phosphorylation in this work is induced through a reduction in AR signalling or via changes in the epigenetic and chromatin landscape around genes involved in OXPHOS. Previous work in the AR-negative PC3 cell line demonstrated that KDM6A inhibition also resulted in the downregulation of the OXPHOS pathways (Chianese et al., 2022). This would suggest that changes seen in these may be independent of the downregulation of AR following KMD6A inhibition.

The RNA-Seq data was also useful to validate the relationship between AR and KDM6A. Within this thesis, a physical interaction whereby AR is bound to the specific regions of the KDM6A promoter was described. This likely led to the correlation in the expression of KDM6A and AR seen throughout this work. An experiment that would have been additionally informative would have been a co-immunoprecipitation between the AR and KDM6A, which could have further validated the interaction of both proteins. This has previously been done in VCaP lysates where AR was shown to interact directly with KMD6A (Grasso et al., 2012). It is worth reiterating the fact that several other HDMs (KDM3A, KDM5B, KDM7A) have been shown to regulate AR activity or act as AR co-activators (K. Lee et al., 2018; Xiang, Zhu, Han, Ye, et al., 2007; Yamane et al., 2006a). In these studies, HDMs can both directly interact with the AR protein or bind to AR target genes leading to their activation through changing the epigenetic landscape. The RNA-seq data revealed a reduction in the Hallmark “Androgen Response’ and several AR and AR-V7 regulated genes following KDM6A KD or GSK-J4 treatment, although the greater effects were seen in KMD6A KD cells. Whilst the effect of GSK-J4 on AR target gene expression may not have been as robust as anticipated, the work to examine if KDM6A inhibition could influence enzalutamide resistance provided some promising results. From early in the work, it was clear that KDM6A was overexpressed in CRPC patients and other studies had alluded to KMD6A being specifically essential in enzalutamide resistance (Grasso et al., 2012; Haldrup et al., 2023). Results from this work demonstrated a robust synergist effect of enzalutamide and GSK-J4 combination in CW22Rv1 cells and it would be interesting to further explore this work in vivo. It is possible that the in vivo work from this study, with GSK-J4 treatment alone, was hindered by ineffective drug uptake and drug concentrations

which were too low. It was interesting to see that other groups with similar dosing schedules in the CW22Rv1 cells had also concluded similar findings in single drug studies (Pecci et al., 2024). Pecci et al did recommend the use of GSK-J4 in combination with anti-androgens as they suggested that GSK-J4 treatment rendered tumours more sensitive to these by altering pathways essential for CRPC. Consistent with studies of other HDMs, such as that by Duan et al (Duan et al., 2022), KMD6A likely induces the re-sensitivity to enzalutamide through multiple mechanisms. This includes inhibition of AR activity, possible inhibition of splicing events required for AR-V7 generation and inhibiting expression of pathways such as *TNFα* and *IL2/Stat5* which are well documented to be upregulated in CRPC patients (Hawley et al., 2024; Lee et al., 2018; Sha et al., 2015. Regarding splicing changes, it should be noted that the ChIP data from this work appeared to show no changes in KDM6A or H3K27me3 around CE3 following GSK-J4 treatment. This would suggest that the effect of GSK-J4 is not through inhibiting splicing around CE3, although further investigation on the expression of splicing factors following GSK-J4 treatment may dispute this.

A key question in this work was to better understand how KMD6A itself was potentially influencing splicing to drive the generation of AR-V7 expression. As stated earlier, KDM6A is upregulated in CRPC and AR-V7+ tumours implicating its importance in AR-V7 generation. As literature demonstrated that histone demethylase could influence splicing decisions by acting as a splicing factor anchor or altering the rate of RNA polymerase elongation **(Figure 6.2),** bespoke assays were developed to assess if KMD6A could alter splicing via one of these two mechanisms. Data from this thesis implicated that KMD6A was more likely to affect splicing via the chromatin-adapter models (splicing factor anchor) as opposed to affecting the rate of RNA polymerase. This conclusion is drawn from two key findings; firstly, KMD6A accumulates around the CE3 in conditions which drive high expression of AR-V7 however levels of H3K27me3 are not reduced **(Figure 6.1).** This suggests that whilst KDM6A is important to alter the splicing of CE3, the demethylase activity of it is not. Secondly, the DRD assay reveals that in the same experimental set-up, accumulation of KDM6A did not alter the RNA polymerase elongation rate **(Figure 6.3).** As mentioned throughout the thesis, KDM3A has been shown to alter alternative splicing of the CE3 in this manner (Fan et al., 2018) and therefore it is plausible that KMD6A elicits a

similar effect. To further validate this, further experiments would be required. The generation of both KDM6A wild-type and mutant stable cell lines would allow the determination of the importance of demethylase activity in the splicing of CE3 and the generation of AR-V7. Alternatively, the generation of a KMD6A KO cell line followed by rescue with transfection of either KMD6A wild-type or mutant plasmid would allow for similar investigation. One of the fundamental questions that remain, to validate that KMD6A acts as an anchor, is what splicing factors it brings to the CE3. This could be addressed with co-immunoprecipitation assays to pull down KDM6A and subsequently analyse splicing factors within the KDM6A interactome. Additional RNA-immunoprecipitation assays could then be undertaken to establish if these splicing factors interact with CE3 of AR-V7 transcripts. Subsequent expression analysis of these proteins across in-house and patient-derived RNA-seq data-sets (TCGA and SU2C, for example) can indicate if they have a role to play in the generation of pathogenic AR transcripts.

As mentioned in the introduction, inhibition of splicing factors has yet to yield positive results in cancer treatment. A Phase I trial targeting the SF3B splicing complex, for example, was stopped due to high toxicity and poor efficacy (Bradley & Anczuków, 2023). SF3B is a core spliceosome protein active at all splicing junctions, both constitutively and alternatively where it forms part of the U2 snRNP (Yamauchi et al., 2022). Targeting such proteins, which are essential for all splicing, is unlikely to provide any therapeutic benefit due to a lack of specificity to pathophysiological splicing events and hence a negligible therapeutic window. Previously, however, KDM4B was shown to interact with SF3B and targeting of this histone demethylase opposed to SF3B appeared to be effective in reducing the expression of AR-V7. It is worth noting, however, that this was also in pre-clinical models of CRPC. Histone demethylase themselves are difficult to target in a clinical setting due to the high degree of similarity of the JmjC domain which is present in all but the KDM1 family of demethylase enzymes. This was recently highlighted in a review by Das et al., which indicated that currently there are only two inhibitors against HDMs in clinical trials (Das et al., 2023). TACH101 and caffeic acid are pan KDM4 and KDM4C inhibitors, respectively, which have shown some benefits in patients with gastrointestinal, colorectal and oesophageal cancer. Interestingly, caffeic acid is also an inhibitor of KMD6A which brings into question its specificity and therefore potential effectiveness in a clinical

setting (Jia et al., 2020). As the data of this thesis alludes to, a PROTAC approach to diminish KDM6A may be a more viable option given that KDM6A demonstrated involvement in transcriptional and splicing regulation that was independent of its catalytic function. It is likely, however, that efforts would focus on PROTACS directly targeting the AR itself given the decades of evidence on the role of AR in PC initiation and progression. Recently, ARV-110, an AR targeting PROTAC entered Phase II of clinical trial in patients with CRPC with promising results in patients who had relapsed after conventional ADT treatment (Gao et al., 2022a).

To conclude this work, there is some evidence that KDM6A may be a target in CRPC, for which there are no curative treatments. Inhibition of KDM6A has many beneficial effects by affecting genes and pathways which are essential in CRPC. There is some preliminary work in this thesis that suggests an interaction between AR and KDM6A but more work is required to validate this. KDM6A also appeared to have a role in regulating PC metabolomics. Regarding the original aim of this work, to identify if KDM6A had a role in the splicing of CE3, any involvement KDM6A does have in this process is independent of its catalytic function. Is it likely that KDM6A acts through the chromatin adapter models and future experiments mentioned in this discussion could confirm this.

References

AACR Project GENIE: Powering Precision Medicine through an International Consortium. (2017). *Cancer Discov*, *7*(8), 818–831. https://doi.org/10.1158/2159-8290.Cd-17-0151

Abeshouse, A., Ahn, J., Akbani, R., Ally, A., Amin, S., Andry, C. D., Annala, M., Aprikian, A., Armenia, J., Arora, A., Auman, J. T., Balasundaram, M., Balu, S., Barbieri, C. E., Bauer, T., Benz, C. C., Bergeron, A., Beroukhim, R., Berrios, M., … Zmuda, E. (2015). The Molecular Taxonomy of Primary Prostate Cancer. *Cell*, *163*(4), 1011–1025. https://doi.org/10.1016/j.cell.2015.10.025

Abida, W., Cyrta, J., Heller, G., Prandi, D., Armenia, J., Coleman, I., Cieslik, M., Benelli, M., Robinson, D., Van Allen, E. M., Sboner, A., Fedrizzi, T., Mosquera, J. M., Robinson, B. D., De Sarkar, N., Kunju, L. P., Tomlins, S., Wu, Y. M., Nava Rodrigues, D., … Sawyers, C. L. (2019). Genomic correlates of clinical outcome in advanced prostate cancer. *Proc Natl Acad Sci U S A*, *116*(23), 11428–11436. https://doi.org/10.1073/pnas.1902651116

Aggarwal, R., Starodub, A. N., Koh, B. D., Xing, G., Armstrong, A. J., & Carducci, M. A. (2022). Phase Ib Study of the BET Inhibitor GS-5829 as Monotherapy and Combined with Enzalutamide in Patients with Metastatic Castration-Resistant Prostate Cancer. *Clinical Cancer Research*, *28*(18), 3979–3989. https://doi.org/10.1158/1078-0432.CCR-22-0175

Agirre, E., Oldfield, A. J., Bellora, N., Segelle, A., & Luco, R. F. (2021). Splicing-associated chromatin signatures: a combinatorial and position-dependent role for histone marks in splicing definition. *Nature Communications*, *12*(1), 682. https://doi.org/10.1038/s41467-021-20979-x

Ahmed, H. U., El-Shater Bosaily, A., Brown, L. C., Gabe, R., Kaplan, R., Parmar, M. K., Collaco-Moraes, Y., Ward, K., Hindley, R. G., Freeman, A., Kirkham, A. P., Oldroyd, R., Parker, C., & Emberton, M. (2017). Diagnostic accuracy of multi-parametric MRI and TRUS biopsy in prostate cancer (PROMIS): a paired validating confirmatory study. *Lancet*, *389*(10071), 815–822. https://doi.org/10.1016/s0140-6736(16)32401-1

Akaza, H., Hinotsu, S., Usami, M., Arai, Y., Kanetake, H., Naito, S., Hirao, Y., & Study Group for the Combined Androgen Blockade Therapy of Prostate, C. (2009). Combined androgen blockade with bicalutamide for advanced prostate cancer: long-term follow-up of a phase 3, double-blind, randomized study for survival. *Cancer*, *115*(15), 3437–3445. https://doi.org/10.1002/cncr.24395

Ali Zaidi, S. S., Fatima, F., Ali Zaidi, S. A., Zhou, D., Deng, W., & Liu, S. (2023). Engineering siRNA therapeutics: challenges and strategies. *Journal of Nanobiotechnology*, *21*(1), 381. https://doi.org/10.1186/s12951-023-02147-z

Alshaer, W., Zureigat, H., Al Karaki, A., Al-Kadash, A., Gharaibeh, L., Hatmal, M. M., Aljabali, A. A. A., & Awidi, A. (2021). siRNA: Mechanism of action, challenges, and therapeutic approaches. *European Journal of Pharmacology*, *905*, 174178. https://doi.org/https://doi.org/10.1016/j.ejphar.2021.174178

Andrews, S. (2010). *FastQC: a quality control tool for high throughput sequence data.*

Antonarakis, E. S., Chandhasin, C., Osbourne, E., Luo, J., Sadar, M. D., & Perabo, F. (2016). Targeting the N-Terminal Domain of the Androgen Receptor: A New Approach for

the Treatment of Advanced Prostate Cancer. *The Oncologist*, *21*(12), 1427–1435. https://doi.org/10.1634/theoncologist.2016-0161

Antonarakis, E. S., Lu, C., Wang, H., Luber, B., Nakazawa, M., Roeser, J. C., Chen, Y., Mohammad, T. A., Chen, Y., Fedor, H. L., Lotan, T. L., Zheng, Q., De Marzo, A. M., Isaacs, J. T., Isaacs, W. B., Nadal, R., Paller, C. J., Denmeade, S. R., Carducci, M. A., … Luo, J. (2014a). AR-V7 and Resistance to Enzalutamide and Abiraterone in Prostate Cancer. *New England Journal of Medicine*, *371*(11), 1028–1038. https://doi.org/10.1056/NEJMoa1315815

Antonarakis, E. S., Lu, C., Wang, H., Luber, B., Nakazawa, M., Roeser, J. C., Chen, Y., Mohammad, T. A., Chen, Y., Fedor, H. L., Lotan, T. L., Zheng, Q., De Marzo, A. M., Isaacs, J. T., Isaacs, W. B., Nadal, R., Paller, C. J., Denmeade, S. R., Carducci, M. A., … Luo, J. (2014b). AR-V7 and resistance to enzalutamide and abiraterone in prostate cancer. *N Engl J Med*, *371*(11), 1028–1038. https://doi.org/10.1056/NEJMoa1315815

Armandari, I., Hamid, A. R., Verhaegh, G., & Schalken, J. (2014). Intratumoral steroidogenesis in castration-resistant prostate cancer: a target for therapy. *Prostate Int*, *2*(3), 105–113. https://doi.org/10.12954/PI.14063

Armstrong, L. (2014). *Epigenetics* (1st.). New York : Garland Science.

Asberry, A. M., Liu, S., Nam, H. S., Deng, X., Wan, J., & Hu, C.-D. (2022). Reprogramming landscape highlighted by dynamic transcriptomes in therapy-induced neuroendocrine differentiation. *Computational and Structural Biotechnology Journal*, *20*, 5873–5885. https://doi.org/10.1016/j.csbj.2022.10.031

Audet-Walsh, É., Yee, T., McGuirk, S., Vernier, M., Ouellet, C., St-Pierre, J., & Giguère, V. (2017). Androgen-Dependent Repression of ERRγ Reprograms Metabolism in Prostate Cancer. *Cancer Research*, *77*(2), 378–389. https://doi.org/10.1158/0008-5472.CAN-16-1204

Bader, D. A., & McGuire, S. E. (2020). Tumour metabolism and its unique properties in prostate adenocarcinoma. *Nature Reviews Urology*, *17*(4), 214–231. https://doi.org/10.1038/s41585-020-0288-x

Bae, T. H., Sung, K. W., Pham, T. M., Najy, A. J., Zamiri, A., Jang, H., Mun, S. R., Kim, S., Kwon, H. K., Son, Y. S., Shi, D., Kregel, S., Heath, E. I., Cher, M. L., Kwon, Y. T., & Kim, H.-R. C. (2025). An Autophagy-Targeting Chimera Induces Degradation of Androgen Receptor Mutants and AR-v7 in Castration-Resistant Prostate Cancer. *Cancer Research*, *85*(2), 342–359. https://doi.org/10.1158/0008-5472.CAN-24-0591

Balk, S. P., & Knudsen, K. E. (2008). AR, the cell cycle, and prostate cancer. *Nucl Recept Signal*, *6*, e001. https://doi.org/10.1621/nrs.06001

Bancroft, E. K., Page, E. C., Brook, M. N., Thomas, S., Taylor, N., Pope, J., McHugh, J., Jones, A.-B., Karlsson, Q., & Merson, S. (2021). A prospective prostate cancer screening programme for men with pathogenic variants in mismatch repair genes (IMPACT): initial results from an international prospective study. *The Lancet Oncology*, *22*(11), 1618–1631.

Bandau, S., Alvarez, V., Jiang, H., Graff, S., Sundaramoorthy, R., Gierlinski, M., Toman, M., Owen-Hughes, T., Sidoli, S., Lamond, A., & Alabert, C. (2024). RNA polymerase II promotes the organization of chromatin following DNA replication. *EMBO Reports*, *25*(3), 1387–1414. https://doi.org/10.1038/s44319-024-00085-x

Bansal, D., Reimers, M. A., Knoche, E. M., & Pachynski, R. K. (2021). Immunotherapy and immunotherapy combinations in metastatic castration-resistant prostate cancer. *Cancers*, *13*(2), 334.

Barber, L., Gerke, T., Markt, S. C., Peisch, S. F., Wilson, K. M., Ahearn, T., Giovannucci, E., Parmigiani, G., & Mucci, L. A. (2018). Family History of Breast or Prostate Cancer and Prostate Cancer Risk. *Clin Cancer Res*, *24*(23), 5910–5917. https://doi.org/10.1158/1078-0432.CCR-18-0370

Barfeld, S. J., Urbanucci, A., Itkonen, H. M., Fazli, L., Hicks, J. L., Thiede, B., Rennie, P. S., Yegnasubramanian, S., DeMarzo, A. M., & Mills, I. G. (2017). c-Myc Antagonises the Transcriptional Activity of the Androgen Receptor in Prostate Cancer Affecting Key Gene Networks. *EBioMedicine*, *18*, 83–93. https://doi.org/10.1016/j.ebiom.2017.04.006

Beebe-Dimmer, J. L., Hathcock, M., Yee, C., Okoth, L. A., Ewing, C. M., Isaacs, W. B., Cooney, K. A., & Thibodeau, S. N. (2015). The HOXB13 G84E Mutation Is Associated with an Increased Risk for Prostate Cancer and Other Malignancies. *Cancer Epidemiology, Biomarkers & Prevention*, *24*(9), 1366–1372. https://doi.org/10.1158/1055-9965.Epi-15-0247

Beier, A. K., Puhr, M., Stope, M. B., Thomas, C., & Erb, H. H. H. (2022). Metabolic changes during prostate cancer development and progression. *J Cancer Res Clin Oncol*. https://doi.org/10.1007/s00432-022-04371-w

Bennett, N. C., Gardiner, R. A., Hooper, J. D., Johnson, D. W., & Gobe, G. C. (2010). Molecular cell biology of androgen receptor signalling. *Int J Biochem Cell Biol*, *42*(6), 813–827. https://doi.org/10.1016/j.biocel.2009.11.013

Ben-Shlomo, Y., Evans, S., Ibrahim, F., Patel, B., Anson, K., Chinegwundoh, F., Corbishley, C., Dorling, D., Thomas, B., Gillatt, D., Kirby, R., Muir, G., Nargund, V., Popert, R., Metcalfe, C., Persad, R., & group, P. study. (2008). The risk of prostate cancer amongst black men in the United Kingdom: the PROCESS cohort study. *Eur Urol*, *53*(1), 99–105. https://doi.org/10.1016/j.eururo.2007.02.047

Bergengren, O., Pekala, K. R., Matsoukas, K., Fainberg, J., Mungovan, S. F., Bratt, O., Bray, F., Brawley, O., Luckenbaugh, A. N., Mucci, L., Morgan, T. M., & Carlsson, S. V. (2023). 2022 Update on Prostate Cancer Epidemiology and Risk Factors—A Systematic Review. *European Urology*, *84*(2), 191–206. https://doi.org/https://doi.org/10.1016/j.eururo.2023.04.021

Biagini, T., Petrizzelli, F., Bianco, S. D., Liorni, N., Napoli, A., Castellana, S., Luigi Vescovi, A., Carella, M., Caputo, V., & Mazza, T. (2022). KDM6A missense variants hamper H3 histone demethylation in lung squamous cell carcinoma. *Computational and Structural Biotechnology Journal*, *20*, 3151–3160. https://doi.org/https://doi.org/10.1016/j.csbj.2022.06.041

Bianchini, D., Omlin, A., Pezaro, C., Lorente, D., Ferraldeschi, R., Mukherji, D., Crespo, M., Figueiredo, I., Miranda, S., Riisnaes, R., Zivi, A., Buchbinder, A., Rathkopf, D. E., Attard, G., Scher, H. I., de Bono, J., & Danila, D. C. (2013). First-in-human Phase I study of EZN-4176, a locked nucleic acid antisense oligonucleotide to exon 4 of the androgen receptor mRNA in patients with castration-resistant prostate cancer. *British Journal of Cancer*, *109*(10), 2579–2586. https://doi.org/10.1038/bjc.2013.619

Bjorkman, M., Ostling, P., Harma, V., Virtanen, J., Mpindi, J. P., Rantala, J., Mirtti, T., Vesterinen, T., Lundin, M., Sankila, A., Rannikko, A., Kaivanto, E., Kohonen, P.,

Kallioniemi, O., & Nees, M. (2012). Systematic knockdown of epigenetic enzymes identifies a novel histone demethylase PHF8 overexpressed in prostate cancer with an impact on cell proliferation, migration and invasion. *Oncogene*, *31*(29), 3444–3456. https://doi.org/10.1038/onc.2011.512

Bonnal, S. C., Lopez-Oreja, I., & Valcarcel, J. (2020). Roles and mechanisms of alternative splicing in cancer - implications for care. *Nat Rev Clin Oncol*, *17*(8), 457–474. https://doi.org/10.1038/s41571-020-0350-x

Bornes, L., Belthier, G., & van Rheenen, J. (2021). Epithelial-to-Mesenchymal Transition in the Light of Plasticity and Hybrid E/M States. *J Clin Med*, *10*(11). https://doi.org/10.3390/jcm10112403

Boysen, G., Barbieri, C. E., Prandi, D., Blattner, M., Chae, S.-S., Dahija, A., Nataraj, S., Huang, D., Marotz, C., Xu, L., Huang, J., Lecca, P., Chhangawala, S., Liu, D., Zhou, P., Sboner, A., de Bono, J. S., Demichelis, F., Houvras, Y., & Rubin, M. A. (2015). SPOP mutation leads to genomic instability in prostate cancer. *Elife*, *4*, e09207. https://doi.org/10.7554/eLife.09207

Bradley, R. K., & Anczuków, O. (2023). RNA splicing dysregulation and the hallmarks of cancer. *Nature Reviews Cancer*, *23*(3), 135–155. https://doi.org/10.1038/s41568-022-00541-7

Bramsen, J. B., Pakula, M. M., Hansen, T. B., Bus, C., Langkjær, N., Odadzic, D., Smicius, R., Wengel, S. L., Chattopadhyaya, J., Engels, J. W., Herdewijn, P., Wengel, J., & Kjems, J. (2010). A screen of chemical modifications identifies position-specific modification by UNA to most potently reduce siRNA off-target effects. *Nucleic Acids Research*, *38*(17), 5761–5773. https://doi.org/10.1093/nar/gkq341

Bratt, O., Drevin, L., Akre, O., Garmo, H., & Stattin, P. (2016). Family history and probability of prostate cancer, differentiated by risk category: a nationwide population-based study. *Journal of the National Cancer Institute*, *108*(10), djw110.

Briganti, A., Suardi, N., Gallina, A., Abdollah, F., Novara, G., Ficarra, V., & Montorsi, F. (2014). Predicting the risk of bone metastasis in prostate cancer. *Cancer Treat Rev*, *40*(1), 3–11. https://doi.org/10.1016/j.ctrv.2013.07.001

Brodsky, A. S., Meyer, C. A., Swinburne, I. A., Hall, G., Keenan, B. J., Liu, X. S., Fox, E. A., & Silver, P. A. (2005). Genomic mapping of RNA polymerase II reveals sites of co-transcriptional regulation in human cells. *Genome Biology*, *6*(8), R64. https://doi.org/10.1186/gb-2005-6-8-r64

Brook, M. N., Ní Raghallaigh, H., Govindasami, K., Dadaev, T., Rageevakumar, R., Keating, D., Hussain, N., Osborne, A., Lophatananon, A., Muir, K. R., Kote-Jarai, Z., & Eeles, R. A. (2023). Family History of Prostate Cancer and Survival Outcomes in the UK Genetic Prostate Cancer Study. *European Urology*, *83*(3), 257–266. https://doi.org/https://doi.org/10.1016/j.eururo.2022.11.019

Butcher, H. L., Kennette, W. A., Collins, O., Zalups, R. K., & Koropatnick, J. (2004). Metallothionein Mediates the Level and Activity of Nuclear Factor KB in Murine Fibroblasts. *Journal of Pharmacology and Experimental Therapeutics*, *310*(2), 589–598. https://doi.org/10.1124/jpet.104.066126

Cai, C., He, H. H., Chen, S., Coleman, I., Wang, H., Fang, Z., Chen, S., Nelson, P. S., Liu, X. S., Brown, M., & Balk, S. P. (2011). Androgen receptor gene expression in prostate cancer is directly suppressed by the androgen receptor through recruitment of lysine-specific demethylase 1. *Cancer Cell*, *20*(4), 457–471. https://doi.org/10.1016/j.ccr.2011.09.001

Caines, J. K., Barnes, D. A., & Berry, M. D. (2022). The Use of Seahorse XF Assays to Interrogate Real-Time Energy Metabolism in Cancer Cell Lines. *Methods Mol Biol*, *2508*, 225–234. https://doi.org/10.1007/978-1-0716-2376-3_17

Campioni, G., Pasquale, V., Busti, S., Ducci, G., Sacco, E., & Vanoni, M. (2022a). An Optimized Workflow for the Analysis of Metabolic Fluxes in Cancer Spheroids Using Seahorse Technology. *Cells*, *11*(5), 866. https://doi.org/10.3390/cells11050866

Campioni, G., Pasquale, V., Busti, S., Ducci, G., Sacco, E., & Vanoni, M. (2022b). An Optimized Workflow for the Analysis of Metabolic Fluxes in Cancer Spheroids Using Seahorse Technology. *Cells*, *11*(5), 866. https://doi.org/10.3390/cells11050866

Cancer Genome Atlas Research, N. (2015). The Molecular Taxonomy of Primary Prostate Cancer. *Cell*, *163*(4), 1011–1025. https://doi.org/10.1016/j.cell.2015.10.025

Cancer Research UK. (2019). *Prostate Cancer Statistics*. Cancer Research UK. https://www.cancerresearchuk.org/health-professional/cancer-statistics-for-the-uk#heading-Four

Cao, Z., Shi, X., Tian, F., Fang, Y., Wu, J. B., Mrdenovic, S., Nian, X., Ji, J., Xu, H., Kong, C., Xu, Y., Chen, X., Huang, Y., Wei, X., Yu, Y., Yang, B., Chung, L. W. K., & Wang, F. (2021). KDM6B is an androgen regulated gene and plays oncogenic roles by demethylating H3K27me3 at cyclin D1 promoter in prostate cancer. *Cell Death Dis*, *12*(1), 2. https://doi.org/10.1038/s41419-020-03354-4

Carlsson, S. V, & Vickers, A. J. (2020). Screening for Prostate Cancer. *Med Clin North Am*, *104*(6), 1051–1062. https://doi.org/10.1016/j.mcna.2020.08.007

Carvalho, F. L. F., Marchionni, L., Gupta, A., Kummangal, B. A., Schaeffer, E. M., Ross, A. E., & Berman, D. M. (2015). HES6 promotes prostate cancer aggressiveness independently of Notch signalling. *Journal of Cellular and Molecular Medicine*, *19*(7), 1624–1636. https://doi.org/https://doi.org/10.1111/jcmm.12537

Cato, L., de Tribolet-Hardy, J., Lee, I., Rottenberg, J. T., Coleman, I., Melchers, D., Houtman, R., Xiao, T., Li, W., Uo, T., Sun, S., Kuznik, N. C., Goppert, B., Ozgun, F., van Royen, M. E., Houtsmuller, A. B., Vadhi, R., Rao, P. K., Li, L., … Brown, M. (2019). ARv7 Represses Tumor-Suppressor Genes in Castration-Resistant Prostate Cancer. *Cancer Cell*, *35*(3), 401-413 e6. https://doi.org/10.1016/j.ccell.2019.01.008

Cerami, E., Gao, J., Dogrusoz, U., Gross, B. E., Sumer, S. O., Aksoy, B. A., Jacobsen, A., Byrne, C. J., Heuer, M. L., Larsson, E., Antipin, Y., Reva, B., Goldberg, A. P., Sander, C., & Schultz, N. (2012). The cBio cancer genomics portal: an open platform for exploring multidimensional cancer genomics data. *Cancer Discov*, *2*(5), 401–404. https://doi.org/10.1158/2159-8290.Cd-12-0095

Cervantes-Arias, A., Pang, L. Y., & Argyle, D. J. (2013). Epithelial-mesenchymal transition as a fundamental mechanism underlying the cancer phenotype. *Veterinary and Comparative Oncology*, *11*(3), 169–184. https://doi.org/https://doi.org/10.1111/j.1476-5829.2011.00313.x

Chakraborty, A. A., Laukka, T., Myllykoski, M., Ringel, A. E., Booker, M. A., Tolstorukov, M. Y., Meng, Y. J., Meier, S. R., Jennings, R. B., Creech, A. L., Herbert, Z. T., McBrayer, S. K., Olenchock, B. A., Jaffe, J. D., Haigis, M. C., Beroukhim, R., Signoretti, S., Koivunen, P., & Kaelin, W. G. (2019). Histone demethylase KDM6A directly senses oxygen to control chromatin and cell fate. *Science*, *363*(6432), 1217–1222. https://doi.org/10.1126/science.aaw1026

Chakravarty, D., Gao, J., Phillips, S., Kundra, R., Zhang, H., Wang, J., Rudolph, J. E., Yaeger, R., Soumerai, T., Nissan, M. H., Chang, M. T., Chandarlapaty, S., Traina, T. A., Paik, P.

K., Ho, A. L., Hantash, F. M., Grupe, A., Baxi, S. S., Callahan, M. K., … Schultz, N. (2017). OncoKB: A Precision Oncology Knowledge Base. *JCO Precision Oncology*, *1*, 1–16. https://doi.org/10.1200/po.17.00011

Chan, S. C., Li, Y., & Dehm, S. M. (2012). Androgen receptor splice variants activate androgen receptor target genes and support aberrant prostate cancer cell growth independent of canonical androgen receptor nuclear localization signal. *J Biol Chem*, *287*(23), 19736–19749. https://doi.org/10.1074/jbc.M112.352930

Chandrasekar, T., Yang, J. C., Gao, A. C., & Evans, C. P. (2015). Mechanisms of resistance in castration-resistant prostate cancer (CRPC). *Transl Androl Urol*, *4*(3), 365–380. https://doi.org/10.3978/j.issn.2223-4683.2015.05.02

Chang, S., Yim, S., & Park, H. (2019a). The cancer driver genes IDH1/2, JARID1C/ KDM5C, and UTX/ KDM6A: crosstalk between histone demethylation and hypoxic reprogramming in cancer metabolism. *Experimental & Molecular Medicine*, *51*(6), 1–17. https://doi.org/10.1038/s12276-019-0230-6

Chang, S., Yim, S., & Park, H. (2019b). The cancer driver genes IDH1/2, JARID1C/ KDM5C, and UTX/ KDM6A: crosstalk between histone demethylation and hypoxic reprogramming in cancer metabolism. *Experimental & Molecular Medicine*, *51*(6), 1–17. https://doi.org/10.1038/s12276-019-0230-6

Chen, D., Tang, J.-X., Li, B., Hou, L., Wang, X., & Kang, L. (2018). CRISPR/Cas9-mediated genome editing induces exon skipping by complete or stochastic altering splicing in the migratory locust. *BMC Biotechnology*, *18*(1), 60. https://doi.org/10.1186/s12896-018-0465-7

Chen, L.-J., Xu, X.-Y., Zhong, X.-D., Liu, Y.-J., Zhu, M.-H., Tao, F., Li, C.-Y., She, Q.-S., Yang, G.-J., & Chen, J. (2023). The role of lysine-specific demethylase 6A (KDM6A) in tumorigenesis and its therapeutic potentials in cancer therapy. *Bioorganic Chemistry*, *133*, 106409. https://doi.org/https://doi.org/10.1016/j.bioorg.2023.106409

Chen, M., & Manley, J. L. (2009). Mechanisms of alternative splicing regulation: insights from molecular and genomics approaches. *Nat Rev Mol Cell Biol*, *10*(11), 741–754. https://doi.org/10.1038/nrm2777

Chen, Z. Y., Chen, H., Qiu, T., Weng, X. D., Guo, J., Wang, L., & Liu, X. H. (2016). Effects of cisplatin on the LSD1-mediated invasion and metastasis of prostate cancer cells. *Mol Med Rep*, *14*(3), 2511–2517. https://doi.org/10.3892/mmr.2016.5571

Cherian, M. (2003). Metallothioneins in human tumors and potential roles in carcinogenesis. *Mutation Research/Fundamental and Molecular Mechanisms of Mutagenesis*, *533*(1–2), 201–209. https://doi.org/10.1016/j.mrfmmm.2003.07.013

Chianese, U., Papulino, C., Passaro, E., Evers, T. M., Babaei, M., Toraldo, A., De Marchi, T., Nimeus, E., Carafa, V., Nicoletti, M. M., Del Gaudio, N., Iaccarino, N., Randazzo, A., Rotili, D., Mai, A., Cappabianca, S., Mashaghi, A., Ciardiello, F., Altucci, L., & Benedetti, R. (2022). Histone lysine demethylase inhibition reprograms prostate cancer metabolism and mechanics. *Mol Metab*, *64*, 101561. https://doi.org/10.1016/j.molmet.2022.101561

Chianese, U., Papulino, C., Passaro, E., Evers, T. M. J., Babaei, M., Toraldo, A., De Marchi, T., Niméus, E., Carafa, V., & Nicoletti, M. M. (2022). Histone lysine demethylase inhibition reprograms prostate cancer metabolism and mechanics. *Molecular Metabolism*, *64*, 101561.

Chianese, U., Papulino, C., Passaro, E., Evers, T. M. J., Babaei, M., Toraldo, A., De Marchi, T., Niméus, E., Carafa, V., Nicoletti, M. M., Del Gaudio, N., Iaccarino, N., Randazzo, A., Rotili, D., Mai, A., Cappabianca, S., Mashaghi, A., Ciardiello, F., Altucci, L., & Benedetti, R. (2022). Histone lysine demethylase inhibition reprograms prostate cancer metabolism and mechanics. *Molecular Metabolism*, *64*, 101561. https://doi.org/https://doi.org/10.1016/j.molmet.2022.101561

Choi, H., Park, J., Park, M., Won, H., Joo, H., Lee, C. H., Lee, J., & Kong, G. (2015). UTX inhibits EMT-induced breast CSC properties by epigenetic repression of EMT genes in cooperation with LSD 1 and HDAC 1. *EMBO Reports*, *16*(10), 1288–1298.

Chong, Z. X., Yeap, S. K., & Ho, W. Y. (2021). Transfection types, methods and strategies: a technical review. *PeerJ*, *9*, e11165. https://doi.org/10.7717/peerj.11165

Choudhury, A. D., Xie, W., Tewari, A., Miyamoto, D. T., Kochupurakkal, B., Ellis, L., Bandel, M., Leisner, C., Shapiro, G., D'Andrea, A. D., Allen, E. M. Van, Freedman, M., Taplin, M.-E., & Beltran, H. (2022). A phase Ia/Ib study of talazoparib in combination with tazemetostat in metastatic castration-resistant prostate cancer (mCRPC). *Journal of Clinical Oncology*, *40*(6_suppl), TPS195–TPS195. https://doi.org/10.1200/JCO.2022.40.6_suppl.TPS195

Chu, J. H., Yu, S., Hayward, S. W., & Chan, F. L. (2009). Development of a three-dimensional culture model of prostatic epithelial cells and its use for the study of epithelial-mesenchymal transition and inhibition of PI3K pathway in prostate cancer. *The Prostate*, *69*(4), 428–442. https://doi.org/https://doi.org/10.1002/pros.20897

Claessens, F., Denayer, S., Van Tilborgh, N., Kerkhofs, S., Helsen, C., & Haelens, A. (2008). Diverse roles of androgen receptor (AR) domains in AR-mediated signaling. *Nucl Recept Signal*, *6*, e008. https://doi.org/10.1621/nrs.06008

Clarke, N., Wiechno, P., Alekseev, B., Sala, N., Jones, R., Kocak, I., Chiuri, V. E., Jassem, J., Fléchon, A., & Redfern, C. (2018). Olaparib combined with abiraterone in patients with metastatic castration-resistant prostate cancer: a randomised, double-blind, placebo-controlled, phase 2 trial. *The Lancet Oncology*, *19*(7), 975–986.

Coffey, K., & Robson, C. N. (2012). Regulation of the androgen receptor by post-translational modifications. *Journal of Endocrinology*, *215*(2), 221–237. https://doi.org/10.1530/joe-12-0238

Conteduca, V., Mosca, A., Brighi, N., de Giorgi, U., & Rescigno, P. (2021). New Prognostic Biomarkers in Metastatic Castration-Resistant Prostate Cancer. *Cells*, *10*(1), 193. https://www.mdpi.com/2073-4409/10/1/193

Conteduca, V., Wetterskog, D., Sharabiani, M. T. A., Grande, E., Fernandez-Perez, M. P., Jayaram, A., Salvi, S., Castellano, D., Romanel, A., & Lolli, C. (2017). Androgen receptor gene status in plasma DNA associates with worse outcome on enzalutamide or abiraterone for castration-resistant prostate cancer: a multi-institution correlative biomarker study. *Annals of Oncology*, *28*(7), 1508–1516.

Conti, D. V, Darst, B. F., Moss, L. C., Saunders, E. J., Sheng, X., Chou, A., Schumacher, F. R., Olama, A. A. Al, Benlloch, S., Dadaev, T., Brook, M. N., Sahimi, A., Hoffmann, T. J., Takahashi, A., Matsuda, K., Momozawa, Y., Fujita, M., Muir, K., Lophatananon, A., … Haiman, C. A. (2021). Trans-ancestry genome-wide association meta-analysis of prostate cancer identifies new susceptibility loci and informs genetic risk prediction. *Nature Genetics*, *53*(1), 65–75. https://doi.org/10.1038/s41588-020-00748-0

Conti, D. V, Wang, K., Sheng, X., Bensen, J. T., Hazelett, D. J., Cook, M. B., Ingles, S. A., Kittles, R. A., Strom, S. S., Rybicki, B. A., Nemesure, B., Isaacs, W. B., Stanford, J. L.,

Zheng, W., Sanderson, M., John, E. M., Park, J. Y., Xu, J., Stevens, V. L., … Consortium, P. E. (2017). Two Novel Susceptibility Loci for Prostate Cancer in Men of African Ancestry. *J Natl Cancer Inst*, *109*(8). https://doi.org/10.1093/jnci/djx084

Cowley, G. S., Weir, B. A., Vazquez, F., Tamayo, P., Scott, J. A., Rusin, S., East-Seletsky, A., Ali, L. D., Gerath, W. F., Pantel, S. E., Lizotte, P. H., Jiang, G., Hsiao, J., Tsherniak, A., Dwinell, E., Aoyama, S., Okamoto, M., Harrington, W., Gelfand, E., … Hahn, W. C. (2014). Parallel genome-scale loss of function screens in 216 cancer cell lines for the identification of context-specific genetic dependencies. *Sci Data*, *1*, 140035. https://doi.org/10.1038/sdata.2014.35

Crea, F., Sun, L., Mai, A., Chiang, Y. T., Farrar, W. L., Danesi, R., & Helgason, C. D. (2012). The emerging role of histone lysine demethylases in prostate cancer. *Molecular Cancer*, *11*(1), 52. https://doi.org/10.1186/1476-4598-11-52

Crissman, H. A., & Steinkamp, J. A. (1973). Rapid, simultaneous measurement of DNA, protein, and cell volume in single cells from large mammalian cell populations. *The Journal of Cell Biology*, *59*(3), 766.

Crowley, F., Sterpi, M., Buckley, C., Margetich, L., Handa, S., & Dovey, Z. (2021). A Review of the Pathophysiological Mechanisms Underlying Castration-resistant Prostate Cancer. *Research and Reports in Urology*, *13*(null), 457–472. https://doi.org/10.2147/RRU.S264722

Cui, S. Z., Lei, Z. Y., Guan, T. P., Fan, L. L., Li, Y. Q., Geng, X. Y., Fu, D. X., Jiang, H. W., & Xu, S. H. (2020). Targeting USP1-dependent KDM4A protein stability as a potential prostate cancer therapy. *Cancer Sci*, *111*(5), 1567–1581. https://doi.org/10.1111/cas.14375

Culig, Z., & Santer, F. R. (2014). Androgen receptor signaling in prostate cancer. *Cancer Metastasis Rev*, *33*(2–3), 413–427. https://doi.org/10.1007/s10555-013-9474-0

Dai, X., Gan, W., Li, X., Wang, S., Zhang, W., Huang, L., Liu, S., Zhong, Q., Guo, J., Zhang, J., Chen, T., Shimizu, K., Beca, F., Blattner, M., Vasudevan, D., Buckley, D. L., Qi, J., Buser, L., Liu, P., … Wei, W. (2017). Prostate cancer–associated SPOP mutations confer resistance to BET inhibitors through stabilization of BRD4. *Nature Medicine*, *23*(9), 1063–1071. https://doi.org/10.1038/nm.4378

Dana, H., Chalbatani, G. M., Mahmoodzadeh, H., Karimloo, R., Rezaiean, O., Moradzadeh, A., Mehmandoost, N., Moazzen, F., Mazraeh, A., Marmari, V., Ebrahimi, M., Rashno, M. M., Abadi, S. J., & Gharagouzlo, E. (2017). Molecular Mechanisms and Biological Functions of siRNA. *Int J Biomed Sci*, *13*(2), 48–57.

Daniels, V. A., Luo, J., Paller, C. J., & Kanayama, M. (2024). Therapeutic Approaches to Targeting Androgen Receptor Splice Variants. *Cells*, *13*(1), 104. https://doi.org/10.3390/cells13010104

Das, N. D., Niwa, H., & Umehara, T. (2023). Chemical Inhibitors Targeting the Histone Lysine Demethylase Families with Potential for Drug Discovery. *Epigenomes*, *7*(1), 7. https://doi.org/10.3390/epigenomes7010007

Davey, R. A., & Grossmann, M. (2016). Androgen Receptor Structure, Function and Biology: From Bench to Bedside. *Clin Biochem Rev*, *37*(1), 3–15. https://www.ncbi.nlm.nih.gov/pubmed/27057074

Davis, I. D., Martin, A. J., Stockler, M. R., Begbie, S., Chi, K. N., Chowdhury, S., Coskinas, X., Frydenberg, M., Hague, W. E., Horvath, L. G., Joshua, A. M., Lawrence, N. J., Marx, G., McCaffrey, J., McDermott, R., McJannett, M., North, S. A., Parnis, F., Parulekar, W., … Prostate Cancer Trials, G. (2019). Enzalutamide with Standard First-

Line Therapy in Metastatic Prostate Cancer. *N Engl J Med*, *381*(2), 121–131. https://doi.org/10.1056/NEJMoa1903835

De Bono, J. S., Cojocaru, E., Plummer, E. R., Knurowski, T., Clegg, K., Ashby, F., Pegg, N., West, W., & Brooks, A. N. (2019). An open label phase I/IIa study to evaluate the safety and efficacy of CCS1477 as monotherapy and in combination in patients with advanced solid/metastatic tumors. *Journal of Clinical Oncology*, *37*(15_suppl), TPS5089–TPS5089. https://doi.org/10.1200/JCO.2019.37.15_suppl.TPS5089

De Bono, J. S., Cook, N., Yu, E. Y., Lara, P. "Lucky" N., Wang, J. S., Yamasaki, Y., Yamamiya, I., Gao, P., Calleja, E. M., & Rathkopf, D. E. (2021). First-in-human study of TAS3681, an oral androgen receptor (AR) antagonist with AR and AR splice variant (AR-SV) downregulation activity, in patients (pts) with metastatic castration-resistant prostate cancer (mCRPC) refractory to abiraterone (ABI) and/or enzalutamide (ENZ) and chemotherapy (CT). *Journal of Clinical Oncology*, *39*(15_suppl), 5031–5031. https://doi.org/10.1200/JCO.2021.39.15_suppl.5031

de Bono, J. S., Logothetis, C. J., Molina, A., Fizazi, K., North, S., Chu, L., Chi, K. N., Jones, R. J., Goodman Jr., O. B., Saad, F., Staffurth, J. N., Mainwaring, P., Harland, S., Flaig, T. W., Hutson, T. E., Cheng, T., Patterson, H., Hainsworth, J. D., Ryan, C. J., … Investigators, C.-A.-. (2011). Abiraterone and increased survival in metastatic prostate cancer. *N Engl J Med*, *364*(21), 1995–2005. https://doi.org/10.1056/NEJMoa1014618

Dehm, S. M., Schmidt, L. J., Heemers, H. V, Vessella, R. L., & Tindall, D. J. (2008). Splicing of a novel androgen receptor exon generates a constitutively active androgen receptor that mediates prostate cancer therapy resistance. *Cancer Res*, *68*(13), 5469–5477. https://doi.org/10.1158/0008-5472.CAN-08-0594

Dehm, S. M., & Tindall, D. J. (2007). Androgen receptor structural and functional elements: role and regulation in prostate cancer. *Mol Endocrinol*, *21*(12), 2855–2863. https://doi.org/10.1210/me.2007-0223

Del Re, M., Crucitta, S., Sbrana, A., Rofi, E., Paolieri, F., Gianfilippo, G., Galli, L., Falcone, A., Morganti, R., Porta, C., Efstathiou, E., van Schaik, R., Jenster, G., & Danesi, R. (2019). Androgen receptor (AR) splice variant 7 and full-length AR expression is associated with clinical outcome: a translational study in patients with castrate-resistant prostate cancer. *BJU International*, *124*(4), 693–700. https://doi.org/https://doi.org/10.1111/bju.14792

Di Blasi, R., Marbiah, M. M., Siciliano, V., Polizzi, K., & Ceroni, F. (2021). A call for caution in analysing mammalian co-transfection experiments and implications of resource competition in data misinterpretation. *Nature Communications*, *12*(1), 2545. https://doi.org/10.1038/s41467-021-22795-9

Dobin, A., Davis, C. A., Schlesinger, F., Drenkow, J., Zaleski, C., Jha, S., Batut, P., Chaisson, M., & Gingeras, T. R. (2013). STAR: ultrafast universal RNA-seq aligner. *Bioinformatics*, *29*(1), 15–21. https://doi.org/10.1093/bioinformatics/bts635

Dong, C., Zhang, H., Xu, C., Arrowsmith, C. H., & Min, J. (2014). Structure and function of dioxygenases in histone demethylation and DNA/RNA demethylation. *IUCrJ*, *1*(6), 540–549.

D'Oto, A., Tian, Q. W., Davidoff, A. M., & Yang, J. (2016). Histone demethylases and their roles in cancer epigenetics. *J Med Oncol Ther*, *1*(2), 34–40.

Du, C., Lv, C., Feng, Y., & Yu, S. (2020). Activation of the KDM5A/miRNA-495/YTHDF2/m6A-MOB3B axis facilitates prostate cancer progression. *J Exp Clin Cancer Res*, *39*(1), 223. https://doi.org/10.1186/s13046-020-01735-3

Duan, L., Chen, Y. A., Liang, Y., Chen, Z., Lu, J., Fang, Y., Cao, J., Lu, J., Zhao, H., Pong, R. C., Hernandez, E., Kapur, P., Tran, T. A. T., Smith, T., Martinez, E. D., Ahn, J. M., Hsieh, J. T., Luo, J. H., & Liu, Z. P. (2022). Therapeutic targeting of histone lysine demethylase KDM4B blocks the growth of castration-resistant prostate cancer. *Biomed Pharmacother*, *158*, 114077. https://doi.org/10.1016/j.biopha.2022.114077

Duan, L., Chen, Z., Lu, J., Liang, Y., Wang, M., Roggero, C. M., Zhang, Q. J., Gao, J., Fang, Y., Cao, J., Lu, J., Zhao, H., Dang, A., Pong, R. C., Hernandez, E., Chang, C. M., Hoang, D. T., Ahn, J. M., Xiao, G., … Liu, Z. P. (2019). Histone lysine demethylase KDM4B regulates the alternative splicing of the androgen receptor in response to androgen deprivation. *Nucleic Acids Res*, *47*(22), 11623–11636. https://doi.org/10.1093/nar/gkz1004

Dujardin, G., Lafaille, C., de la Mata, M., Marasco, L. E., Muñoz, M. J., Le Jossic-Corcos, C., Corcos, L., & Kornblihtt, A. R. (2014). How slow RNA polymerase II elongation favors alternative exon skipping. *Molecular Cell*, *54*(4), 683–690.

Duval, K., Grover, H., Han, L. H., Mou, Y., Pegoraro, A. F., Fredberg, J., & Chen, Z. (2017). Modeling Physiological Events in 2D vs. 3D Cell Culture. *Physiology (Bethesda)*, *32*(4), 266–277. https://doi.org/10.1152/physiol.00036.2016

Dvinge, H. (2018). Regulation of alternative mRNA splicing: old players and new perspectives. *FEBS Letters*, *592*(17), 2987–3006. https://doi.org/https://doi.org/10.1002/1873-3468.13119

Edwards, J., Krishna, N. S., Grigor, K. M., & Bartlett, J. M. (2003). Androgen receptor gene amplification and protein expression in hormone refractory prostate cancer. *Br J Cancer*, *89*(3), 552–556. https://doi.org/10.1038/sj.bjc.6601127

Einstein, D. J., Choudhury, A. D., Saylor, P. J., Patterson, J. C., Croucher, P., Ridinger, M., Erlander, M. G., Yaffe, M. B., & Bubley, G. (2022). A phase 2 study of onvansertib in combination with abiraterone and prednisone in patients with metastatic castration-resistant prostate cancer (mCRPC). *Journal of Clinical Oncology*, *40*(6_suppl), TPS219–TPS219. https://doi.org/10.1200/JCO.2022.40.6_suppl.TPS219

Eisermann, K., & Fraizer, G. (2017). The Androgen Receptor and VEGF: Mechanisms of Androgen-Regulated Angiogenesis in Prostate Cancer. *Cancers (Basel)*, *9*(4). https://doi.org/10.3390/cancers9040032

Erb, H. H. H., Bodenbender, J., Handle, F., Diehl, T., Donix, L., Tsaur, I., Gleave, M., Haferkamp, A., Huber, J., Fuessel, S., Juengel, E., Culig, Z., & Thomas, C. (2020). Assessment of STAT5 as a potential therapy target in enzalutamide-resistant prostate cancer. *PLOS ONE*, *15*(8), e0237248. https://doi.org/10.1371/journal.pone.0237248

Estebanez-Perpina, E., Bevan, C. L., & McEwan, I. J. (2021). Eighty Years of Targeting Androgen Receptor Activity in Prostate Cancer: The Fight Goes on. *Cancers (Basel)*, *13*(3). https://doi.org/10.3390/cancers13030509

Ewels, P., Magnusson, M., Lundin, S., & Käller, M. (2016). MultiQC: summarize analysis results for multiple tools and samples in a single report. *Bioinformatics*, *32*(19), 3047–3048. https://doi.org/10.1093/bioinformatics/btw354

Ewing, C. M., Ray, A. M., Lange, E. M., Zuhlke, K. A., Robbins, C. M., Tembe, W. D., Wiley, K. E., Isaacs, S. D., Johng, D., Wang, Y., Bizon, C., Yan, G., Gielzak, M., Partin, A. W.,

Shanmugam, V., Izatt, T., Sinari, S., Craig, D. W., Zheng, S. L., … Cooney, K. A. (2012). Germline Mutations in HOXB13 and Prostate-Cancer Risk. *New England Journal of Medicine*, *366*(2), 141–149. https://doi.org/10.1056/NEJMoa1110000

Fadul, S. M., Arshad, A., & Mehmood, R. (2023). CRISPR-Based Epigenome Editing: Mechanisms and Applications. *Epigenomics*, *15*(21), 1137–1155. https://doi.org/10.2217/epi-2023-0281

Fan, L., Zhang, F., Xu, S., Cui, X., Hussain, A., Fazli, L., Gleave, M., Dong, X., & Qi, J. (2018). Histone demethylase JMJD1A promotes alternative splicing of AR variant 7 (AR-V7) in prostate cancer cells. *Proc Natl Acad Sci U S A*, *115*(20), E4584–E4593. https://doi.org/10.1073/pnas.1802415115

Feehley, T., O'Donnell, C. W., Mendlein, J., Karande, M., & McCauley, T. (2023). Drugging the epigenome in the age of precision medicine. *Clin Epigenetics*, *15*(1), 6. https://doi.org/10.1186/s13148-022-01419-z

Ferre, P., & Foufelle, F. (2007). SREBP-1c transcription factor and lipid homeostasis: clinical perspective. *Horm Res*, *68*(2), 72–82. https://doi.org/10.1159/000100426

Fizazi, K., Piulats, J. M., Reaume, M. N., Ostler, P., McDermott, R., Gingerich, J. R., Pintus, E., Sridhar, S. S., Bambury, R. M., Emmenegger, U., Lindberg, H., Morris, D., Nolè, F., Staffurth, J., Redfern, C., Sáez, M. I., Abida, W., Daugaard, G., Heidenreich, A., … Bryce, A. H. (2023). Rucaparib or Physician's Choice in Metastatic Prostate Cancer. *New England Journal of Medicine*, *388*(8), 719–732. https://doi.org/10.1056/NEJMoa2214676

Forma, E., Krzeslak, A., Wilkosz, J., Jozwiak, P., Szymczyk, A., Rozanski, W., & Brys, M. (2012). Metallothionein 2A genetic polymorphisms and risk of prostate cancer in a Polish population. *Cancer Genetics*, *205*(9), 432–435. https://doi.org/10.1016/j.cancergen.2012.05.005

Fotouhi, O., Nizamuddin, S., Falk, S., Schilling, O., Knüchel-Clarke, R., Biniossek, M. L., & Timmers, H. T. M. (2023). Alternative mRNA Splicing Controls the Functions of the Histone H3K27 Demethylase UTX/KDM6A. *Cancers*, *15*(12), 3117. https://www.mdpi.com/2072-6694/15/12/3117

Fournier, P. G., Juarez, P., Jiang, G., Clines, G. A., Niewolna, M., Kim, H. S., Walton, H. W., Peng, X. H., Liu, Y., Mohammad, K. S., Wells, C. D., Chirgwin, J. M., & Guise, T. A. (2015). The TGF-beta Signaling Regulator PMEPA1 Suppresses Prostate Cancer Metastases to Bone. *Cancer Cell*, *27*(6), 809–821. https://doi.org/10.1016/j.ccell.2015.04.009

Francies, H. E., Barthorpe, A., McLaren-Douglas, A., Barendt, W. J., & Garnett, M. J. (2019). Drug Sensitivity Assays of Human Cancer Organoid Cultures. In K. Turksen (Ed.), *Organoids: Stem Cells, Structure, and Function* (pp. 339–351). Springer New York. https://doi.org/10.1007/7651_2016_10

Frigo, D. E., Bondesson, M., & Williams, C. (2021). Nuclear receptors: from molecular mechanisms to therapeutics. *Essays in Biochemistry*, *65*(6), 847–856. https://doi.org/10.1042/EBC20210020

Fu, Y., Sander, J. D., Reyon, D., Cascio, V. M., & Joung, J. K. (2014). Improving CRISPR-Cas nuclease specificity using truncated guide RNAs. *Nature Biotechnology*, *32*(3), 279–284. https://doi.org/10.1038/nbt.2808

Gallipoli, P., & Huntly, B. J. P. (2019). Histone modifiers are oxygen sensors. *Science*, *363*(6432), 1148–1149. https://doi.org/10.1126/science.aaw8373

Gandaglia, G., Leni, R., Bray, F., Fleshner, N., Freedland, S. J., Kibel, A., Stattin, P., Van Poppel, H., & La Vecchia, C. (2021). Epidemiology and Prevention of Prostate Cancer. *European Urology Oncology*, *4*(6), 877–892. https://doi.org/https://doi.org/10.1016/j.euo.2021.09.006

Gao, X., Burris III, H. A., Vuky, J., Dreicer, R., Sartor, A. O., Sternberg, C. N., Percent, I. J., Hussain, M. H. A., Rezazadeh Kalebasty, A., Shen, J., Heath, E. I., Abesada-Terk, G., Gandhi, S. G., McKean, M., Lu, H., Berghorn, E., Gedrich, R., Chirnomas, S. D., Vogelzang, N. J., & Petrylak, D. P. (2022a). Phase 1/2 study of ARV-110, an androgen receptor (AR) PROTAC degrader, in metastatic castration-resistant prostate cancer (mCRPC). *Journal of Clinical Oncology*, *40*(6_suppl), 17–17. https://doi.org/10.1200/JCO.2022.40.6_suppl.017

Gao, X., Burris III, H. A., Vuky, J., Dreicer, R., Sartor, A. O., Sternberg, C. N., Percent, I. J., Hussain, M. H. A., Rezazadeh Kalebasty, A., Shen, J., Heath, E. I., Abesada-Terk, G., Gandhi, S. G., McKean, M., Lu, H., Berghorn, E., Gedrich, R., Chirnomas, S. D., Vogelzang, N. J., & Petrylak, D. P. (2022b). Phase 1/2 study of ARV-110, an androgen receptor (AR) PROTAC degrader, in metastatic castration-resistant prostate cancer (mCRPC). *Journal of Clinical Oncology*, *40*(6_suppl), 17–17. https://doi.org/10.1200/JCO.2022.40.6_suppl.017

Garje, R., Chennamadhavuni, A., Mott, S. L., Chambers, I. M., Gellhaus, P., Zakharia, Y., & Brown, J. A. (2020). Utilization and Outcomes of Surgical Castration in Comparison to Medical Castration in Metastatic Prostate Cancer. *Clinical Genitourinary Cancer*, *18*(2), e157–e166. https://doi.org/https://doi.org/10.1016/j.clgc.2019.09.020

Garvey, B., Turkbey, B., Truong, H., Bernardo, M., Periaswamy, S., & Choyke, P. L. (2014). Clinical value of prostate segmentation and volume determination on MRI in benign prostatic hyperplasia. *Diagn Interv Radiol*, *20*(3), 229–233. https://doi.org/10.5152/dir.2014.13322

Gažová, I., Lengeling, A., & Summers, K. M. (2019). Lysine demethylases KDM6A and UTY: The X and Y of histone demethylation. *Molecular Genetics and Metabolism*, *127*(1), 31–44. https://doi.org/https://doi.org/10.1016/j.ymgme.2019.04.012

Giancotti, F. G., & Ruoslahti, E. (1999). Integrin Signaling. *Science*, *285*(5430), 1028–1033. https://doi.org/10.1126/science.285.5430.1028

Gimeno-Valiente, F., Lopez-Rodas, G., Castillo, J., & Franco, L. (2022). Alternative Splicing, Epigenetic Modifications and Cancer: A Dangerous Triangle, or a Hopeful One? *Cancers (Basel)*, *14*(3). https://doi.org/10.3390/cancers14030560

Gioeli, D., & Paschal, B. M. (2012). Post-translational modification of the androgen receptor. *Molecular and Cellular Endocrinology*, *352*(1), 70–78. https://doi.org/https://doi.org/10.1016/j.mce.2011.07.004

Gnanapragasam, V. J., Bratt, O., Muir, K., Lee, L. S., Huang, H. H., Stattin, P., & Lophatananon, A. (2018). The Cambridge Prognostic Groups for improved prediction of disease mortality at diagnosis in primary non-metastatic prostate cancer: a validation study. *BMC Medicine*, *16*, 1–10.

Goda, S., Isagawa, T., Chikaoka, Y., Kawamura, T., & Aburatani, H. (2013). Control of histone H3 lysine 9 (H3K9) methylation state via cooperative two-step demethylation by Jumonji domain containing 1A (JMJD1A) homodimer. *Journal of Biological Chemistry*, *288*(52), 36948–36956.

Goel, S., Bhatia, V., Biswas, T., & Ateeq, B. (2022). Epigenetic reprogramming during prostate cancer progression: A perspective from development. *Seminars in Cancer*

Biology, *83*, 136–151. https://doi.org/https://doi.org/10.1016/j.semcancer.2021.01.009

Gorodetska, I., Kozeretska, I., & Dubrovska, A. (2019). BRCA Genes: The Role in Genome Stability, Cancer Stemness and Therapy Resistance. *J Cancer*, *10*(9), 2109–2127. https://doi.org/10.7150/jca.30410

Gozdecka, M., Meduri, E., Mazan, M., Tzelepis, K., Dudek, M., Knights, A. J., Pardo, M., Yu, L., Choudhary, J. S., & Metzakopian, E. (2018). UTX-mediated enhancer and chromatin remodeling suppresses myeloid leukemogenesis through noncatalytic inverse regulation of ETS and GATA programs. *Nature Genetics*, *50*(6), 883–894.

Grasso, C. S., Wu, Y. M., Robinson, D. R., Cao, X., Dhanasekaran, S. M., Khan, A. P., Quist, M. J., Jing, X., Lonigro, R. J., Brenner, J. C., Asangani, I. A., Ateeq, B., Chun, S. Y., Siddiqui, J., Sam, L., Anstett, M., Mehra, R., Prensner, J. R., Palanisamy, N., … Tomlins, S. A. (2012). The mutational landscape of lethal castration-resistant prostate cancer. *Nature*, *487*(7406), 239–243. https://doi.org/10.1038/nature11125

Graveley, B. R. (2001). Alternative splicing: increasing diversity in the proteomic world. *Trends Genet*, *17*(2), 100–107. https://doi.org/10.1016/s0168-9525(00)02176-4

Groth, D., Hartmann, S., Klie, S., & Selbig, J. (2013). Principal components analysis. *Methods Mol Biol*, *930*, 527–547. https://doi.org/10.1007/978-1-62703-059-5_22

Gu, X., Ma, Y., Liu, Y., & Wan, Q. (2021a). Measurement of mitochondrial respiration in adherent cells by Seahorse XF96 Cell Mito Stress Test. *STAR Protoc*, *2*(1), 100245. https://doi.org/10.1016/j.xpro.2020.100245

Gu, X., Ma, Y., Liu, Y., & Wan, Q. (2021b). Measurement of mitochondrial respiration in adherent cells by Seahorse XF96 Cell Mito Stress Test. *STAR Protocols*, *2*(1), 100245. https://doi.org/10.1016/j.xpro.2020.100245

GUMULEC, J., MASARIK, M., KRIZKOVA, S., HLAVNA, M., BABULA, P., HRABEC, R., ROVNY, A., MASARIKOVA, M., SOCHOR, J., ADAM, V., ECKSCHLAGER, T., & KIZEK, R. (2012). Evaluation ofalpha-methylacyl-CoA racemase, metallothionein and prostate specific antigen as prostate cancer prognostic markers. *Neoplasma*, *59*(02), 191–201. https://doi.org/10.4149/neo_2012_025

Guo, H., Wu, Y., Nouri, M., Spisak, S., Russo, J. W., Sowalsky, A. G., Pomerantz, M. M., Wei, Z., Korthauer, K., Seo, J. H., Wang, L., Arai, S., Freedman, M. L., He, H. H., Chen, S., & Balk, S. P. (2021). Androgen receptor and MYC equilibration centralizes on developmental super-enhancer. *Nat Commun*, *12*(1), 7308. https://doi.org/10.1038/s41467-021-27077-y

Guo, X.-X., Xia, H.-R., Hou, H.-M., Liu, M., & Wang, J.-Y. (2021). Comparison of Oncological Outcomes Between Radical Prostatectomy and Radiotherapy by Type of Radiotherapy in Elderly Prostate Cancer Patients. *Frontiers in Oncology*, *11*. https://doi.org/10.3389/fonc.2021.708373

Hagberg Thulin, M., Nilsson, M. E., Thulin, P., Ceraline, J., Ohlsson, C., Damber, J. E., & Welen, K. (2016). Osteoblasts promote castration-resistant prostate cancer by altering intratumoral steroidogenesis. *Mol Cell Endocrinol*, *422*, 182–191. https://doi.org/10.1016/j.mce.2015.11.013

Haile, S., & Sadar, M. D. (2011). Androgen receptor and its splice variants in prostate cancer. *Cellular and Molecular Life Sciences : CMLS*, *68*(24), 3971–3981. https://doi.org/10.1007/s00018-011-0766-7

Haldrup, J., Weiss, S., Schmidt, L., & Sorensen, K. D. (2023). Investigation of enzalutamide, docetaxel, and cabazitaxel resistance in the castration resistant

prostate cancer cell line C4 using genome-wide CRISPR/Cas9 screening. *Sci Rep*, *13*(1), 9043. https://doi.org/10.1038/s41598-023-35950-7

Hamdy, F. C., Donovan, J. L., Lane, J. A., Metcalfe, C., Davis, M., Turner, E. L., Martin, R. M., Young, G. J., Walsh, E. I., Bryant, R. J., Bollina, P., Doble, A., Doherty, A., Gillatt, D., Gnanapragasam, V., Hughes, O., Kockelbergh, R., Kynaston, H., Paul, A., … Neal, D. E. (2023). Fifteen-Year Outcomes after Monitoring, Surgery, or Radiotherapy for Prostate Cancer. *New England Journal of Medicine*, *388*(17), 1547–1558. https://doi.org/10.1056/NEJMoa2214122

Hamid, A., Kusuma Putra, H. W., Sari, N. P., Diana, P., Sesari, S. S., Novita, E., Gultom, F. L., Saraswati, M., Tanurahardja, B., Asmarinah, Umbas, R., & Mochtar, C. A. (2020). Early upregulation of AR and steroidogenesis enzyme expression after 3 months of androgen-deprivation therapy. *BMC Urol*, *20*(1), 71. https://doi.org/10.1186/s12894-020-00627-0

Han, S., Udeshi, N. D., Deerinck, T. J., Svinkina, T., Ellisman, M. H., Carr, S. a, & Ting, A. Y. (2018). *Associated with mtDNA in Living Cells*. *24*(3), 404–414. https://doi.org/10.1016/j.chembiol.2017.02.002.Proximity

Hansen, K. D., Brenner, S. E., & Dudoit, S. (2010). Biases in Illumina transcriptome sequencing caused by random hexamer priming. *Nucleic Acids Res*, *38*(12), e131. https://doi.org/10.1093/nar/gkq224

Hashizume, R., Andor, N., Ihara, Y., Lerner, R., Gan, H., Chen, X., Fang, D., Huang, X., Tom, M. W., & Ngo, V. (2014). Pharmacologic inhibition of histone demethylation as a therapy for pediatric brainstem glioma. *Nature Medicine*, *20*(12), 1394–1396.

Hawley, J. E., Owens, L., Cheng, H. H., Grivas, P., Hsieh, A. C., Khan, H. M., Montgomery, R. B., Raychaudhuri, R., Schweizer, M. T., Sunkara, R., Yezefski, T., Nelson, P., & Yu, E. Y. (2024). TRAMP study: A phase 2 trial of tumor necrosis factor-α blockade and AR inhibition in men with CRPC. *Journal of Clinical Oncology*, *42*(16_suppl), TPS5117–TPS5117. https://doi.org/10.1200/JCO.2024.42.16_suppl.TPS5117

Hay, C. W., & McEwan, I. J. (2012). The impact of point mutations in the human androgen receptor: classification of mutations on the basis of transcriptional activity. *PLoS One*, *7*(3), e32514. https://doi.org/10.1371/journal.pone.0032514

Hayashi, N., Osaka, K., Muraoka, K., Hasumi, H., Makiyama, K., Kondo, K., Nakaigawa, N., Yao, M., Mukai, Y., Sugiura, M., Takano, S., Ito, E., Kaizu, H., Koike, I., Hata, M., Taguri, M., Miyoshi, Y., Izumi, K., Kawahara, T., & Uemura, H. (2020). Outcomes of treatment for localized prostate cancer in a single institution: comparison of radical prostatectomy and radiation therapy by propensity score matching analysis. *World Journal of Urology*, *38*(10), 2477–2484. https://doi.org/10.1007/s00345-019-03056-3

Heinemann, B., Nielsen, J. M., Hudlebusch, H. R., Lees, M. J., Larsen, D. V., Boesen, T., Labelle, M., Gerlach, L.-O., Birk, P., & Helin, K. (2014). Inhibition of demethylases by GSK-J1/J4. *Nature*, *514*(7520), E1–E2. https://doi.org/10.1038/nature13688

Hill, B. G., Benavides, G. A., Lancaster, J. R., Ballinger, S., Dell'Italia, L., Zhang, J., & Darley-Usmar, V. M. (2012). Integration of cellular bioenergetics with mitochondrial quality control and autophagy. *Bchm*, *393*(12), 1485–1512. https://doi.org/10.1515/hsz-2012-0198

Hille, C., Gorges, T. M., Riethdorf, S., Mazel, M., Steuber, T., Amsberg, G. V, König, F., Peine, S., Alix-Panabières, C., & Pantel, K. (2019). Detection of Androgen Receptor Variant 7 (ARV7) mRNA Levels in EpCAM-Enriched CTC Fractions for Monitoring

Response to Androgen Targeting Therapies in Prostate Cancer. *Cells*, *8*(9). https://doi.org/10.3390/cells8091067

Hofman, M. S., Emmett, L., Sandhu, S., Iravani, A., Joshua, A. M., Goh, J. C., Pattison, D. A., Tan, T. H., Kirkwood, I. D., & Ng, S. (2021). [177Lu] Lu-PSMA-617 versus cabazitaxel in patients with metastatic castration-resistant prostate cancer (TheraP): a randomised, open-label, phase 2 trial. *The Lancet*, *397*(10276), 797–804.

Holt, M. E., Mittendorf, K. F., LeNoue-Newton, M., Jain, N. M., Anderson, I., Lovly, C. M., Osterman, T., Micheel, C., & Levy, M. (2021). My Cancer Genome: Coevolution of Precision Oncology and a Molecular Oncology Knowledgebase. *JCO Clinical Cancer Informatics*, *5*, 995–1004. https://doi.org/10.1200/CCI.21.00084

Hong, B.-J., Park, W.-Y., Kim, H.-R., Moon, J. W., Lee, H. Y., Park, J. H., Kim, S.-K., Oh, Y., Roe, J.-S., & Kim, M.-Y. (2019). Oncogenic KRAS Sensitizes Lung Adenocarcinoma to GSK-J4–Induced Metabolic and Oxidative Stress. *Cancer Research*, *79*(22), 5849–5859. https://doi.org/10.1158/0008-5472.CAN-18-3511

Hong, S., Cho, Y.-W., Yu, L.-R., Yu, H., Veenstra, T. D., & Ge, K. (2007). Identification of JmjC domain-containing UTX and JMJD3 as histone H3 lysine 27 demethylases. *Proceedings of the National Academy of Sciences*, *104*(47), 18439–18444. https://doi.org/10.1073/pnas.0707292104

Hong, Z., Wu, G., Xiang, Z. D., Xu, C. D., Huang, S. S., Li, C., Shi, L., & Wu, D. L. (2019). KDM5C is transcriptionally regulated by BRD4 and promotes castration-resistance prostate cancer cell proliferation by repressing PTEN. *Biomed Pharmacother*, *114*, 108793. https://doi.org/10.1016/j.biopha.2019.108793

Hricak, H., & Scardino, P. T. (2009). *Prostate cancer*. Cambridge : Cambridge University Press.

Hu, R., Dunn, T. A., Wei, S., Isharwal, S., Veltri, R. W., Humphreys, E., Han, M., Partin, A. W., Vessella, R. L., Isaacs, W. B., Bova, G. S., & Luo, J. (2009). Ligand-Independent Androgen Receptor Variants Derived from Splicing of Cryptic Exons Signify Hormone-Refractory Prostate Cancer. *Cancer Research*, *69*(1), 16–22. https://doi.org/10.1158/0008-5472.CAN-08-2764

Hua, C., Chen, J., Li, S., Zhou, J., Fu, J., Sun, W., & Wang, W. (2021a). KDM6 Demethylases and Their Roles in Human Cancers. *Frontiers in Oncology*, *11*. https://doi.org/10.3389/fonc.2021.779918

Hua, C., Chen, J., Li, S., Zhou, J., Fu, J., Sun, W., & Wang, W. (2021b). KDM6 Demethylases and Their Roles in Human Cancers. *Frontiers in Oncology*, *11*. https://doi.org/10.3389/fonc.2021.779918

Huang, C.-C. F., Lingadahalli, S., Morova, T., Ozturan, D., Hu, E., Yu, I. P. L., Linder, S., Hoogstraat, M., Stelloo, S., Sar, F., van der Poel, H., Altintas, U. B., Saffarzadeh, M., Le Bihan, S., McConeghy, B., Gokbayrak, B., Feng, F. Y., Gleave, M. E., Bergman, A. M., … Lack, N. A. (2021). Functional mapping of androgen receptor enhancer activity. *Genome Biology*, *22*(1), 149. https://doi.org/10.1186/s13059-021-02339-6

Huelga, S. C., Vu, A. Q., Arnold, J. D., Liang, T. Y., Liu, P. P., Yan, B. Y., Donohue, J. P., Shiue, L., Hoon, S., Brenner, S., Ares Jr., M., & Yeo, G. W. (2012). Integrative genome-wide analysis reveals cooperative regulation of alternative splicing by hnRNP proteins. *Cell Rep*, *1*(2), 167–178. https://doi.org/10.1016/j.celrep.2012.02.001

Huggins, C., & Hodges, C. V. (1941). Studies on prostatic cancer. *Cancer Res*, *1*(4), 293–297.

Hum, N. R., Sebastian, A., Gilmore, S. F., He, W., Martin, K. A., Hinckley, A., Dubbin, K. R., Moya, M. L., Wheeler, E. K., Coleman, M. A., & Loots, G. G. (2020). Comparative Molecular Analysis of Cancer Behavior Cultured In Vitro, In Vivo, and Ex Vivo. *Cancers (Basel)*, *12*(3). https://doi.org/10.3390/cancers12030690

Hung, C.-L., Liu, H.-H., Fu, C.-W., Yeh, H.-H., Hu, T.-L., Kuo, Z.-K., Lin, Y.-C., Jhang, M.-R., Hwang, C.-S., Hsu, H.-C., Kung, H.-J., & Wang, L.-Y. (2023). Targeting androgen receptor and the variants by an orally bioavailable Proteolysis Targeting Chimeras compound in castration resistant prostate cancer. *EBioMedicine*, *90*, 104500. https://doi.org/10.1016/j.ebiom.2023.104500

Ianevski, A., Giri, A. K., & Aittokallio, T. (2022). SynergyFinder 3.0: an interactive analysis and consensus interpretation of multi-drug synergies across multiple samples. *Nucleic Acids Res*, *50*(W1), W739–W743. https://doi.org/10.1093/nar/gkac382

Ianevski, A., He, L., Aittokallio, T., & Tang, J. (2017). SynergyFinder: a web application for analyzing drug combination dose–response matrix data. *Bioinformatics*, *33*(15), 2413–2415. https://doi.org/10.1093/bioinformatics/btx162

Iguchi, T., Tamada, S., Kato, M., Yasuda, S., Yamasaki, T., & Nakatani, T. (2019). Enzalutamide versus flutamide for castration-resistant prostate cancer after combined androgen blockade therapy with bicalutamide: study protocol for a multicenter randomized phase II trial (the OCUU-CRPC study). *BMC Cancer*, *19*(1), 339. https://doi.org/10.1186/s12885-019-5526-3

Ip, J. Y., Schmidt, D., Pan, Q., Ramani, A. K., Fraser, A. G., Odom, D. T., & Blencowe, B. J. (2011). Global impact of RNA polymerase II elongation inhibition on alternative splicing regulation. *Genome Research*, *21*(3), 390–401. https://doi.org/10.1101/gr.111070.110

Ito, Y., & Sadar, M. D. (2018). Enzalutamide and blocking androgen receptor in advanced prostate cancer: lessons learnt from the history of drug development of antiandrogens. *Res Rep Urol*, *10*, 23–32. https://doi.org/10.2147/RRU.S157116

James, N. D., Pirrie, S. J., Pope, A. M., Barton, D., Andronis, L., Goranitis, I., Collins, S., Daunton, A., McLaren, D., O'Sullivan, J., Parker, C., Porfiri, E., Staffurth, J., Stanley, A., Wylie, J., Beesley, S., Birtle, A., Brown, J., Chakraborti, P., … Billingham, L. J. (2016). Clinical Outcomes and Survival Following Treatment of Metastatic Castrate-Refractory Prostate Cancer With Docetaxel Alone or With Strontium-89, Zoledronic Acid, or Both: The TRAPEZE Randomized Clinical Trial. *JAMA Oncol*, *2*(4), 493–499. https://doi.org/10.1001/jamaoncol.2015.5570

Ji, Y., Zhang, R., Han, X., & Zhou, J. (2023). Targeting the N-terminal domain of the androgen receptor: The effective approach in therapy of CRPC. *European Journal of Medicinal Chemistry*, *247*, 115077. https://doi.org/10.1016/j.ejmech.2022.115077

Jia, R., Mi, Y., Yuan, X., Kong, D., Li, W., Li, R., Wang, B., Zhu, Y., Kong, J., Ma, Z., Li, N., Mi, Q., & Gao, S. (2020). GASC1-Adapted Neoadjuvant Chemotherapy for Resectable Esophageal Squamous Cell Carcinoma: A Prospective Clinical Biomarker Trial. *Journal of Oncology*, *2020*, 1–8. https://doi.org/10.1155/2020/1607860

Jin, B., Zhu, J., Pan, T., Yang, Y., Liang, L., Zhou, Y., Zhang, T., Teng, Y., Wang, Z., Wang, X., Tian, Q., Guo, B., Li, H., & Chen, T. (2023). *MEN1* is a regulator of alternative splicing and prevents R-loop-induced genome instability through suppression of RNA polymerase II elongation. *Nucleic Acids Research*, *51*(15), 7951–7971. https://doi.org/10.1093/nar/gkad548

Kamba, T., Kamoto, T., Maruo, S., Kikuchi, T., Shimizu, Y., Namiki, S., Fujimoto, K., Kawanishi, H., Sato, F., Narita, S., Satoh, T., Saito, H., Sugimoto, M., Teishima, J., Masumori, N., Egawa, S., Sakai, H., Okada, Y., Terachi, T., & Ogawa, O. (2017). A phase III multicenter, randomized, controlled study of combined androgen blockade with versus without zoledronic acid in prostate cancer patients with metastatic bone disease: results of the ZAPCA trial. *Int J Clin Oncol*, *22*(1), 166–173. https://doi.org/10.1007/s10147-016-1037-2

Kanayama, M., Lu, C., Luo, J., & Antonarakis, E. S. (2021). AR Splicing Variants and Resistance to AR Targeting Agents. *Cancers*, *13*(11). https://doi.org/10.3390/cancers13112563

Kaneko, S., & Li, X. (2018). X chromosome protects against bladder cancer in females via a KDM6A-dependent epigenetic mechanism. *Science Advances*, *4*(6), eaar5598.

Kang, M. K., Mehrazarin, S., Park, N.-H., & Wang, C.-Y. (2017). Epigenetic gene regulation by histone demethylases: emerging role in oncogenesis and inflammation. *Oral Diseases*, *23*(6), 709–720. https://doi.org/https://doi.org/10.1111/odi.12569

Karantanos, T., Corn, P. G., & Thompson, T. C. (2013). Prostate cancer progression after androgen deprivation therapy: mechanisms of castrate resistance and novel therapeutic approaches. *Oncogene*, *32*(49), 5501–5511. https://doi.org/10.1038/onc.2013.206

Kargbo, R. B. (2019). *PROTAC-mediated degradation of KRAS protein for anticancer therapeutics* (Vol. 11, Issue 1, pp. 5–6). ACS Publications.

Karlson, C. K. S., Mohd-Noor, S. N., Nolte, N., & Tan, B. C. (2021). CRISPR/dCas9-Based Systems: Mechanisms and Applications in Plant Sciences. *Plants*, *10*(10), 2055. https://doi.org/10.3390/plants10102055

Kempe, H., Schwabe, A., Crémazy, F., Verschure, P. J., & Bruggeman, F. J. (2015). The volumes and transcript counts of single cells reveal concentration homeostasis and capture biological noise. *Molecular Biology of the Cell*, *26*(4), 797–804.

Khan, H. M., & Cheng, H. H. (2022). Germline genetics of prostate cancer. *The Prostate*, *82*(S1), S3–S12. https://doi.org/https://doi.org/10.1002/pros.24340

Kim, J., Lee, H., Yi, S.-J., & Kim, K. (2022). Gene regulation by histone-modifying enzymes under hypoxic conditions: a focus on histone methylation and acetylation. *Experimental & Molecular Medicine*, *54*(7), 878–889. https://doi.org/10.1038/s12276-022-00812-1

Kim, T. D., Shin, S., & Janknecht, R. (2008). Repression of Smad3 activity by histone demethylase SMCX/JARID1C. *Biochem Biophys Res Commun*, *366*(2), 563–567. https://doi.org/10.1016/j.bbrc.2007.12.013

Kittler, R., Surendranath, V., Heninger, A.-K., Slabicki, M., Theis, M., Putz, G., Franke, K., Caldarelli, A., Grabner, H., Kozak, K., Wagner, J., Rees, E., Korn, B., Frenzel, C., Sachse, C., Sönnichsen, B., Guo, J., Schelter, J., Burchard, J., … Buchholz, F. (2007). Genome-wide resources of endoribonuclease-prepared short interfering RNAs for specific loss-of-function studies. *Nature Methods*, *4*(4), 337–344. https://doi.org/10.1038/nmeth1025

Kluth, L. A., Shariat, S. F., Kratzik, C., Tagawa, S., Sonpavde, G., Rieken, M., Scherr, D. S., & Pummer, K. (2014). The hypothalamic-pituitary-gonadal axis and prostate cancer: implications for androgen deprivation therapy. *World J Urol*, *32*(3), 669–676. https://doi.org/10.1007/s00345-013-1157-5

Knuuttila, M., Mehmood, A., Huhtaniemi, R., Yatkin, E., Hakkinen, M. R., Oksala, R., Laajala, T. D., Ryberg, H., Handelsman, D. J., Aittokallio, T., Auriola, S., Ohlsson, C., Laiho, A., Elo, L. L., Sipila, P., Makela, S. I., & Poutanen, M. (2018). Antiandrogens Reduce Intratumoral Androgen Concentrations and Induce Androgen Receptor Expression in Castration-Resistant Prostate Cancer Xenografts. *Am J Pathol*, *188*(1), 216–228. https://doi.org/10.1016/j.ajpath.2017.08.036

Ko, C. J., Hsu, T. W., Wu, S. R., Lan, S. W., Hsiao, T. F., Lin, H. Y., Lin, H. H., Tu, H. F., Lee, C. F., Huang, C. C., Chen, M. M., Hsiao, P. W., Huang, H. P., & Lee, M. S. (2020). Inhibition of TMPRSS2 by HAI-2 reduces prostate cancer cell invasion and metastasis. *Oncogene*, *39*(37), 5950–5963. https://doi.org/10.1038/s41388-020-01413-w

Koch, J., Lang, A., Whongsiri, P., Schulz, W. A., Hoffmann, M. J., & Greife, A. (2021). KDM6A mutations promote acute cytoplasmic DNA release, DNA damage response and mitosis defects. *BMC Molecular and Cell Biology*, *22*(1), 54. https://doi.org/10.1186/s12860-021-00394-2

Kohli, M., Ho, Y., Hillman, D. W., Van Etten, J. L., Henzler, C., Yang, R., Sperger, J. M., Li, Y., Tseng, E., Hon, T., Clark, T., Tan, W., Carlson, R. E., Wang, L., Sicotte, H., Thai, H., Jimenez, R., Huang, H., Vedell, P. T., … Dehm, S. M. (2017). Androgen Receptor Variant AR-V9 Is Coexpressed with AR-V7 in Prostate Cancer Metastases and Predicts Abiraterone Resistance. *Clin Cancer Res*, *23*(16), 4704–4715. https://doi.org/10.1158/1078-0432.CCR-17-0017

Koryakina, Y., Knudsen, K. E., & Gioeli, D. (2015). Cell-cycle-dependent regulation of androgen receptor function. *Endocr Relat Cancer*, *22*(2), 249–264. https://doi.org/10.1530/erc-14-0549

Kounatidou, E., Nakjang, S., McCracken, S. R. C., Dehm, S. M., Robson, C. N., Jones, D., & Gaughan, L. (2019). A novel CRISPR-engineered prostate cancer cell line defines the AR-V transcriptome and identifies PARP inhibitor sensitivities. *Nucleic Acids Res*, *47*(11), 5634–5647. https://doi.org/10.1093/nar/gkz286

Kregel, S., Chen, J. L., Tom, W., Krishnan, V., Kach, J., Brechka, H., Fessenden, T. B., Isikbay, M., Paner, G. P., Szmulewitz, R. Z., & Vander Griend, D. J. (2016). Acquired resistance to the second-generation androgen receptor antagonist enzalutamide in castration-resistant prostate cancer. *Oncotarget*, *7*(18), 26259–26274. https://doi.org/10.18632/oncotarget.8456

Krossa, I., Strub, T., Martel, A., Nahon-Esteve, S., Lassalle, S., Hofman, P., Baillif, S., Ballotti, R., & Bertolotto, C. (2022). Recent advances in understanding the role of HES6 in cancers. *Theranostics*, *12*(9), 4374–4385. https://doi.org/10.7150/thno.72966

Kruidenier, L., Chung, C., Cheng, Z., Liddle, J., Che, K., Joberty, G., Bantscheff, M., Bountra, C., Bridges, A., Diallo, H., Eberhard, D., Hutchinson, S., Jones, E., Katso, R., Leveridge, M., Mander, P. K., Mosley, J., Ramirez-Molina, C., Rowland, P., … Wilson, D. M. (2012). A selective jumonji H3K27 demethylase inhibitor modulates the proinflammatory macrophage response. *Nature*, *488*(7411), 404–408. https://doi.org/10.1038/nature11262

Labbé, R. M., Holowatyj, A., & Yang, Z.-Q. (2014). Histone lysine demethylase (KDM) subfamily 4: structures, functions and therapeutic potential. *American Journal of Translational Research*, *6*(1), 1.

Laccetti, A. L., Chatta, G. S., Iannotti, N., Kyriakopoulos, C., Villaluna, K., Le Moigne, R., & Cesano, A. (2023). Phase 1/2 study of EPI-7386 in combination with enzalutamide (enz) compared with enz alone in subjects with metastatic castration-resistant prostate cancer (mCRPC). *Journal of Clinical Oncology*, *41*(6_suppl), 179–179. https://doi.org/10.1200/JCO.2023.41.6_suppl.179

Lallous, N., Volik, S. V, Awrey, S., Leblanc, E., Tse, R., Murillo, J., Singh, K., Azad, A. A., Wyatt, A. W., LeBihan, S., Chi, K. N., Gleave, M. E., Rennie, P. S., Collins, C. C., & Cherkasov, A. (2016). Functional analysis of androgen receptor mutations that confer anti-androgen resistance identified in circulating cell-free DNA from prostate cancer patients. *Genome Biol*, *17*, 10. https://doi.org/10.1186/s13059-015-0864-1

Lalonde, S., Stone, O. A., Lessard, S., Lavertu, A., Desjardins, J., Beaudoin, M., Rivas, M., Stainier, D. Y. R., & Lettre, G. (2017). Frameshift indels introduced by genome editing can lead to in-frame exon skipping. *PLoS One*, *12*(6), e0178700. https://doi.org/10.1371/journal.pone.0178700

Lan, J., Wei, G., Liu, J., Yang, F., Sun, R., & Lu, H. (2022). Chemotherapy-induced adenosine A2B receptor expression mediates epigenetic regulation of pluripotency factors and promotes breast cancer stemness. *Theranostics*, *12*(6), 2598.

Lang, A., Whongsiri, P., Yilmaz, M., Lautwein, T., Petzsch, P., Greife, A., Günes, C., Köhrer, K., Niegisch, G., & Hoffmann, M. (2020). Knockdown of UTX/KDM6A enriches precursor cell populations in urothelial cell cultures and cell lines. *Cancers*, *12*(4), 1023.

Lee, D. K., & Chang, C. (2003). Expression and Degradation of Androgen Receptor: Mechanism and Clinical Implication. *The Journal of Clinical Endocrinology & Metabolism*, *88*(9), 4043–4054. https://doi.org/10.1210/jc.2003-030261

Lee, K., Hong, S., Kang, M., Jeong, C. W., Ku, J. H., Kim, H., & Kwak, C. (2018). Histone demethylase KDM7A controls androgen receptor activity and tumor growth in prostate cancer. *International Journal of Cancer*, *143*(11), 2849–2861. https://doi.org/10.1002/ijc.31843

Lee, M. G., Villa, R., Trojer, P., Norman, J., Yan, K.-P., Reinberg, D., Di Croce, L., & Shiekhattar, R. (2007). Demethylation of H3K27 regulates polycomb recruitment and H2A ubiquitination. *Science*, *318*(5849), 447–450.

Lee, S. H., Kim, O., Kim, H. J., Hwangbo, C., & Lee, J. H. (2021). Epigenetic regulation of TGF-beta-induced EMT by JMJD3/KDM6B histone H3K27 demethylase. *Oncogenesis*, *10*(2), 17. https://doi.org/10.1038/s41389-021-00307-0

Lee, Y.-C., Lin, S.-C., Yu, G., Zhu, M., Song, J. H., Rivera, K., Pappin, D. J., Logothetis, C. J., Panaretakis, T., Wang, G., Yu-Lee, L.-Y., & Lin, S.-H. (2022). Prostate tumor-induced stromal reprogramming generates Tenascin C that promotes prostate cancer metastasis through YAP/TAZ inhibition. *Oncogene*, *41*(6), 757–769. https://doi.org/10.1038/s41388-021-02131-7

Lelong, E. I. J., Khelifi, G., Adjibade, P., Joncas, F.-H., Grenier St-Sauveur, V., Paquette, V., Gris, T., Zoubeidi, A., Audet-Walsh, E., Lambert, J.-P., Toren, P., Mazroui, R., & Hussein, S. M. I. (2022). Prostate cancer resistance leads to a global deregulation of translation factors and unconventional translation. *NAR Cancer*, *4*(4). https://doi.org/10.1093/narcan/zcac034

Lemster, A. L., Sievers, E., Pasternack, H., Lazar-Karsten, P., Klumper, N., Sailer, V., Offermann, A., Bragelmann, J., Perner, S., & Kirfel, J. (2022). Histone Demethylase

KDM5C Drives Prostate Cancer Progression by Promoting EMT. *Cancers (Basel)*, *14*(8). https://doi.org/10.3390/cancers14081894

Leng, X., Wang, J., An, N., Wang, X., Sun, Y., & Chen, Z. (2020). Histone 3 lysine-27 demethylase KDM6A coordinates with KMT2B to play an oncogenic role in NSCLC by regulating H3K4me3. *Oncogene*, *39*(41), 6468–6479.

Ler, L. D., Ghosh, S., Chai, X., Thike, A. A., Heng, H. L., Siew, E. Y., Dey, S., Koh, L. K., Lim, J. Q., & Lim, W. K. (2017). Loss of tumor suppressor KDM6A amplifies PRC2-regulated transcriptional repression in bladder cancer and can be targeted through inhibition of EZH2. *Science Translational Medicine*, *9*(378), eaai8312.

Leung, J. K., Tam, T., Wang, J., & Sadar, M. D. (2021). Isolation and characterization of castration-resistant prostate cancer LNCaP95 clones. *Hum Cell*, *34*(1), 211–218. https://doi.org/10.1007/s13577-020-00435-6

Lev Maor, G., Yearim, A., & Ast, G. (2015). The alternative role of DNA methylation in splicing regulation. *Trends Genet*, *31*(5), 274–280. https://doi.org/10.1016/j.tig.2015.03.002

Li, G., Kanagasabai, T., Lu, W., Zou, M. R., Zhang, S. M., Celada, S. I., Izban, M. G., Liu, Q., Lu, T., Ballard, B. R., Zhou, X., Adunyah, S. E., Matusik, R. J., Yan, Q., & Chen, Z. (2020). KDM5B Is Essential for the Hyperactivation of PI3K/AKT Signaling in Prostate Tumorigenesis. *Cancer Res*, *80*(21), 4633–4643. https://doi.org/10.1158/0008-5472.CAN-20-0505

Li, H., Lan, J., Wang, G., Guo, K., Han, C., Li, X., Hu, J., Cao, Z., & Luo, X. (2020). KDM4B facilitates colorectal cancer growth and glucose metabolism by stimulating TRAF6-mediated AKT activation. *J Exp Clin Cancer Res*, *39*(1), 12. https://doi.org/10.1186/s13046-020-1522-3

Li, H., Wang, X., Zhai, M., Xu, C., & Chen, X. (2024a). Exploration of the influence of GOLGA8B on prostate cancer progression and the resistance of castration-resistant prostate cancer to cabazitaxel. *Discover Oncology*, *15*(1), 152. https://doi.org/10.1007/s12672-024-00973-7

Li, H., Wang, X., Zhai, M., Xu, C., & Chen, X. (2024b). Exploration of the influence of GOLGA8B on prostate cancer progression and the resistance of castration-resistant prostate cancer to cabazitaxel. *Discover Oncology*, *15*(1), 152. https://doi.org/10.1007/s12672-024-00973-7

Li, J., & Al-Azzawi, F. (2009). Mechanism of androgen receptor action. *Maturitas*, *63*(2), 142–148. https://doi.org/10.1016/j.maturitas.2009.03.008

Li, N., Dhar, S. S., Chen, T. Y., Kan, P. Y., Wei, Y., Kim, J. H., Chan, C. H., Lin, H. K., Hung, M. C., & Lee, M. G. (2016). JARID1D Is a Suppressor and Prognostic Marker of Prostate Cancer Invasion and Metastasis. *Cancer Res*, *76*(4), 831–843. https://doi.org/10.1158/0008-5472.CAN-15-0906

Li, Y., Cooper, B. H., Liu, Y., Wu, D., Zhang, X., Rohs, R., & Qin, P. Z. (2023). CRISPR-Cas9 Activities with Truncated 16-Nucleotide RNA Guides Are Tuned by Target Duplex Stability Beyond the RNA/DNA Hybrid. *Biochemistry*, *62*(17), 2541–2548. https://doi.org/10.1021/acs.biochem.3c00250

Li, Y., Yang, R., Henzler, C. M., Ho, Y., Passow, C., Auch, B., Carreira, S., Nava Rodrigues, D., Bertan, C., Hwang, T. H., Quigley, D. A., Dang, H. X., Morrissey, C., Fraser, M., Plymate, S. R., Maher, C. A., Feng, F. Y., de Bono, J. S., & Dehm, S. M. (2020). Diverse *AR* Gene Rearrangements Mediate Resistance to Androgen Receptor Inhibitors in

Metastatic Prostate Cancer. *Clinical Cancer Research*, *26*(8), 1965–1976. https://doi.org/10.1158/1078-0432.CCR-19-3023

Li, Z., Bishop, A. C., Alyamani, M., Garcia, J. A., Dreicer, R., Bunch, D., Liu, J., Upadhyay, S. K., Auchus, R. J., & Sharifi, N. (2015). Conversion of abiraterone to D4A drives anti-tumour activity in prostate cancer. *Nature*, *523*(7560), 347–351. https://doi.org/10.1038/nature14406

Liao, Y., Smyth, G. K., & Shi, W. (2013). featureCounts: an efficient general purpose program for assigning sequence reads to genomic features. *Bioinformatics*, *30*(7), 923–930. https://doi.org/10.1093/bioinformatics/btt656

Lin, C. Y., Wang, B. J., Chen, B. C., Tseng, J. C., Jiang, S. S., Tsai, K. K., Shen, Y. Y., Yuh, C. H., Sie, Z. L., Wang, W. C., Kung, H. J., & Chuu, C. P. (2019). Histone Demethylase KDM4C Stimulates the Proliferation of Prostate Cancer Cells via Activation of AKT and c-Myc. *Cancers (Basel)*, *11*(11). https://doi.org/10.3390/cancers11111785

Lin, C. Y., Wang, B. J., Fu, Y. K., Huo, C., Wang, Y. P., Chen, B. C., Liu, W. Y., Tseng, J. C., Jiang, S. S., Sie, Z. L., Tsai, K. K., Yuh, C. H., Wang, W. C., Kung, H. J., & Chuu, C. P. (2022). Inhibition of KDM4C/c-Myc/LDHA signalling axis suppresses prostate cancer metastasis via interference of glycolytic metabolism. *Clin Transl Med*, *12*(3), e764. https://doi.org/10.1002/ctm2.764

Linja, M. J., Savinainen, K. J., Saramäki, O. R., Tammela, T. L., Vessella, R. L., & Visakorpi, T. (2001). Amplification and overexpression of androgen receptor gene in hormone-refractory prostate cancer. *Cancer Res*, *61*(9), 3550–3555.

Liu, C., Armstrong, C., Zhu, Y., Lou, W., & Gao, A. C. (2016). Niclosamide enhances abiraterone treatment via inhibition of androgen receptor variants in castration resistant prostate cancer. *Oncotarget*, *7*(22), 32210–32220. https://doi.org/10.18632/oncotarget.8493

Liu, L. L., Xie, N., Sun, S., Plymate, S., Mostaghel, E., & Dong, X. (2014). Mechanisms of the androgen receptor splicing in prostate cancer cells. *Oncogene*, *33*(24), 3140–3150. https://doi.org/10.1038/onc.2013.284

Liu, Q., Pang, J., Wang, L. A., Huang, Z., Xu, J., Yang, X., Xie, Q., Huang, Y., Tang, T., Tong, D., Liu, G., Wang, L., Zhang, D., Ma, Q., Xiao, H., Lan, W., Qin, J., & Jiang, J. (2021). Histone demethylase PHF8 drives neuroendocrine prostate cancer progression by epigenetically upregulating FOXA2. *J Pathol*, *253*(1), 106–118. https://doi.org/10.1002/path.5557

Liu, Q., Tong, D., Liu, G., Xu, J., Do, K., Geary, K., Zhang, D., Zhang, J., Zhang, Y., Li, Y., Bi, G., Lan, W., & Jiang, J. (2017). Metformin reverses prostate cancer resistance to enzalutamide by targeting TGF-β1/STAT3 axis-regulated EMT. *Cell Death & Disease*, *8*(8), e3007–e3007. https://doi.org/10.1038/cddis.2017.417

Liu, Y. F., Fu, S. Q., Yan, Y. C., Gong, B. B., Xie, W. J., Yang, X. R., Sun, T., & Ma, M. (2021). Progress in Clinical Research on Gonadotropin-Releasing Hormone Receptor Antagonists for the Treatment of Prostate Cancer. *Drug Des Devel Ther*, *15*, 639–649. https://doi.org/10.2147/DDDT.S291369

Liu, Z., Hu, M., Yang, Y., Du, C., Zhou, H., Liu, C., Chen, Y., Fan, L., Ma, H., Gong, Y., & Xie, Y. (2022). An overview of PROTACs: a promising drug discovery paradigm. *Mol Biomed*, *3*(1), 46. https://doi.org/10.1186/s43556-022-00112-0

Llombart, V., & Mansour, M. R. (2022). Therapeutic targeting of “undruggable” MYC. *EBioMedicine*, *75*, 103756. https://doi.org/10.1016/j.ebiom.2021.103756

Lomas, D. J., & Ahmed, H. U. (2020). All change in the prostate cancer diagnostic pathway. *Nature Reviews Clinical Oncology*, *17*(6), 372–381. https://doi.org/10.1038/s41571-020-0332-z

Lonergan, P. E., & Tindall, D. J. (2011). Androgen receptor signaling in prostate cancer development and progression. *J Carcinog*, *10*, 20. https://doi.org/10.4103/1477-3163.83937

Love, M. I., Huber, W., & Anders, S. (2014). Moderated estimation of fold change and dispersion for RNA-seq data with DESeq2. *Genome Biology*, *15*(12), 550. https://doi.org/10.1186/s13059-014-0550-8

Lu, C., & Luo, J. (2013). Decoding the androgen receptor splice variants. *Translational Andrology and Urology*, *2*(3), 178–186. https://doi.org/10.3978/j.issn.2223-4683.2013.09.08

Lu, H., Xie, Y., Tran, L., Lan, J., Yang, Y., Murugan, N. L., Wang, R., Wang, Y. J., & Semenza, G. L. (2020a). Chemotherapy-induced S100A10 recruits KDM6A to facilitate OCT4-mediated breast cancer stemness. *The Journal of Clinical Investigation*, *130*(9), 4607–4623.

Lu, H., Xie, Y., Tran, L., Lan, J., Yang, Y., Murugan, N. L., Wang, R., Wang, Y. J., & Semenza, G. L. (2020b). Chemotherapy-induced S100A10 recruits KDM6A to facilitate OCT4-mediated breast cancer stemness. *J Clin Invest*, *130*(9), 4607–4623. https://doi.org/10.1172/JCI138577

Lu, J., Lonergan, P. E., Nacusi, L. P., Wang, L., Schmidt, L. J., Sun, Z., Van der Steen, T., Boorjian, S. A., Kosari, F., Vasmatzis, G., Klee, G. G., Balk, S. P., Huang, H., Wang, C., & Tindall, D. J. (2015). The Cistrome and Gene Signature of Androgen Receptor Splice Variants in Castration Resistant Prostate Cancer Cells. *Journal of Urology*, *193*(2), 690–698. https://doi.org/10.1016/j.juro.2014.08.043

Lu, X., Gao, J., Zhang, Y., Zhao, T., Cai, H., & Zhang, T. (2018). CTEN induces epithelial-mesenchymal transition (EMT) and metastasis in non small cell lung cancer cells. *PLoS One*, *13*(7), e0198823. https://doi.org/10.1371/journal.pone.0198823

Lu, X., Wan, F., Zhang, H., Shi, G., & Ye, D. (2016). ITGA2B and ITGA8 are predictive of prognosis in clear cell renal cell carcinoma patients. *Tumor Biology*, *37*(1), 253–262. https://doi.org/10.1007/s13277-015-3792-5

Lu, Y.-C., Huang, C.-Y., Cheng, C.-H., Huang, K.-H., Lu, Y.-C., Chow, P.-M., Chang, Y.-K., Pu, Y.-S., Chen, C.-H., Lu, S.-L., Lan, K.-H., Jaw, F.-S., Chen, P.-L., & Hong, J.-H. (2022). Propensity score matching analysis comparing radical prostatectomy and radiotherapy with androgen deprivation therapy in locally advanced prostate cancer. *Scientific Reports*, *12*(1), 12480. https://doi.org/10.1038/s41598-022-16700-7

Luco, R. F., Allo, M., Schor, I. E., Kornblihtt, A. R., & Misteli, T. (2011). Epigenetics in alternative pre-mRNA splicing. *Cell*, *144*(1), 16–26. https://doi.org/10.1016/j.cell.2010.11.056

Luco, R. F., & Misteli, T. (2011). More than a splicing code: integrating the role of RNA, chromatin and non-coding RNA in alternative splicing regulation. *Curr Opin Genet Dev*, *21*(4), 366–372. https://doi.org/10.1016/j.gde.2011.03.004

Luco, R. F., Pan, Q., Tominaga, K., Blencowe, B. J., Pereira-Smith, O. M., & Misteli, T. (2010). Regulation of alternative splicing by histone modifications. *Science*, *327*(5968), 996–1000. https://doi.org/10.1126/science.1184208

Luna Velez, M. V., Paulino da Silva Filho, O., Verhaegh, G. W., van Hooij, O., El Boujnouni, N., Brock, R., & Schalken, J. A. (2022). Delivery of antisense oligonucleotides for splice-correction of androgen receptor pre-mRNA in castration-resistant prostate cancer models using cell-penetrating peptides. *The Prostate*, *82*(6), 657–665. https://doi.org/10.1002/pros.24309

Luo, J., Attard, G., Balk, S. P., Bevan, C., Burnstein, K., Cato, L., Cherkasov, A., De Bono, J. S., Dong, Y., Gao, A. C., Gleave, M., Heemers, H., Kanayama, M., Kittler, R., Lang, J. M., Lee, R. J., Logothetis, C. J., Matusik, R., Plymate, S., … Raj, G. V. (2018). Role of Androgen Receptor Variants in Prostate Cancer: Report from the 2017 Mission Androgen Receptor Variants Meeting. *European Urology*, *73*(5), 715–723. https://doi.org/10.1016/j.eururo.2017.11.038

Lynch, J. R., Salik, B., Connerty, P., Vick, B., Leung, H., Pijning, A., Jeremias, I., Spiekermann, K., Trahair, T., Liu, T., Haber, M., Norris, M. D., Woo, A. J., Hogg, P., Wang, J., & Wang, J. Y. (2019). JMJD1C-mediated metabolic dysregulation contributes to HOXA9-dependent leukemogenesis. *Leukemia*, *33*(6), 1400–1410. https://doi.org/10.1038/s41375-018-0354-z

MA, D., ZHOU, Z., YANG, B., HE, Q., ZHANG, Q., & ZHANG, X.-H. (2015). Association of molecular biomarkers expression with biochemical recurrence in prostate cancer through tissue microarray immunostaining. *Oncology Letters*, *10*(4), 2185–2191. https://doi.org/10.3892/ol.2015.3556

Maeda, T., Murata, M., Chiba, H., Takasawa, A., Tanaka, S., Kojima, T., Masumori, N., Tsukamoto, T., & Sawada, N. (2012). Claudin-4-targeted therapy using Clostridium perfringens enterotoxin for prostate cancer. *The Prostate*, *72*(4), 351–360. https://doi.org/https://doi.org/10.1002/pros.21436

Mandl, A., Markowski, M. C., Carducci, M. A., & Antonarakis, E. S. (2023). Role of bromodomain and extraterminal (BET) proteins in prostate cancer. *Expert Opinion on Investigational Drugs*, *32*(3), 213–228. https://doi.org/10.1080/13543784.2023.2186851

Maranto, C., Udhane, V., Jia, J., Verma, R., Müller-Newen, G., LaViolette, P. S., Pereckas, M., Sabharwal, L., Terhune, S., Pattabiraman, N., Njar, V. C. O., Imig, J. D., Wang, L., & Nevalainen, M. T. (2020). Prospects for Clinical Development of Stat5 Inhibitor IST5-002: High Transcriptomic Specificity in Prostate Cancer and Low Toxicity In Vivo. *Cancers*, *12*(11), 3412. https://doi.org/10.3390/cancers12113412

Marasco, L. E., Dujardin, G., Sousa-Luís, R., Liu, Y. H., Stigliano, J. N., Nomakuchi, T., Proudfoot, N. J., Krainer, A. R., & Kornblihtt, A. R. (2022). Counteracting chromatin effects of a splicing-correcting antisense oligonucleotide improves its therapeutic efficacy in spinal muscular atrophy. *Cell*, *185*(12), 2057-2070. e15.

Marino, F., Totaro, A., Gandi, C., Bientinesi, R., Moretto, S., Gavi, F., Pierconti, F., Iacovelli, R., Bassi, P., & Sacco, E. (2023). Germline mutations in prostate cancer: a systematic review of the evidence for personalized medicine. *Prostate Cancer and Prostatic Diseases*, *26*(4), 655–664. https://doi.org/10.1038/s41391-022-00609-3

Markolovic, S., Leissing, T. M., Chowdhury, R., Wilkins, S. E., Lu, X., & Schofield, C. J. (2016). Structure–function relationships of human JmjC oxygenases—demethylases versus hydroxylases. *Current Opinion in Structural Biology*, *41*, 62–72.

Marques, R. B., van Weerden, W. M., Erkens-Schulze, S., de Ridder, C. M., Bangma, C. H., Trapman, J., & Jenster, G. (2006). The human PC346 xenograft and cell line panel: a

model system for prostate cancer progression. *Eur Urol*, *49*(2), 245–257. https://doi.org/10.1016/j.eururo.2005.12.035

Martins, T., Ukoumunne, O. C., Banks, J., Raine, R., & Hamilton, W. (2015). Ethnic differences in patients' preferences for prostate cancer investigation: a vignette-based survey in primary care. *British Journal of General Practice*, *65*(632), e161–e170. https://doi.org/10.3399/bjgp15X683965

Marx, A., Schumann, A., Höflmayer, D., Bady, E., Hube-Magg, C., Möller, K., Tsourlakis, M. C., Steurer, S., Büscheck, F., Eichenauer, T., Clauditz, T. S., Graefen, M., Simon, R., Sauter, G., Izbicki, J. R., Huland, H., Heinzer, H., Haese, A., Schlomm, T., … Polonski, A. (2020). Up regulation of the Hippo signalling effector YAP1 is linked to early biochemical recurrence in prostate cancers. *Scientific Reports*, *10*(1), 8916. https://doi.org/10.1038/s41598-020-65772-w

Masarik, M., Gumulec, J., Hlavna, M., Sztalmachova, M., Babula, P., Raudenska, M., Pavkova-Goldbergova, M., Cernei, N., Sochor, J., Zitka, O., Ruttkay-Nedecky, B., Krizkova, S., Adam, V., & Kizek, R. (2012). Monitoring of the prostate tumour cells redox state and real-time proliferation by novel biophysical techniques and fluorescent staining. *Integrative Biology*, *4*(6), 672–684. https://doi.org/10.1039/c2ib00157h

Mateo, J., Carreira, S., Sandhu, S., Miranda, S., Mossop, H., Perez-Lopez, R., Nava Rodrigues, D., Robinson, D., Omlin, A., Tunariu, N., Boysen, G., Porta, N., Flohr, P., Gillman, A., Figueiredo, I., Paulding, C., Seed, G., Jain, S., Ralph, C., … de Bono, J. S. (2015). DNA-Repair Defects and Olaparib in Metastatic Prostate Cancer. *New England Journal of Medicine*, *373*(18), 1697–1708. https://doi.org/10.1056/NEJMoa1506859

Mateo, J., Porta, N., Bianchini, D., McGovern, U., Elliott, T., Jones, R., Syndikus, I., Ralph, C., Jain, S., Varughese, M., Parikh, O., Crabb, S., Robinson, A., McLaren, D., Birtle, A., Tanguay, J., Miranda, S., Figueiredo, I., Seed, G., … de Bono, J. S. (2020). Olaparib in patients with metastatic castration-resistant prostate cancer with DNA repair gene aberrations (TOPARP-B): a multicentre, open-label, randomised, phase 2 trial. *Lancet Oncol*, *21*(1), 162–174. https://doi.org/10.1016/s1470-2045(19)30684-9

Mateo, J., Seed, G., Bertan, C., Rescigno, P., Dolling, D., Figueiredo, I., Miranda, S., Nava Rodrigues, D., Gurel, B., Clarke, M., Atkin, M., Chandler, R., Messina, C., Sumanasuriya, S., Bianchini, D., Barrero, M., Petermolo, A., Zafeiriou, Z., Fontes, M., … de Bono, J. S. (2020). Genomics of lethal prostate cancer at diagnosis and castration resistance. *J Clin Invest*, *130*(4), 1743–1751. https://doi.org/10.1172/JCI132031

Maxwell, P. J., McKechnie, M., Armstrong, C. W., Manley, J. M., Ong, C. W., Worthington, J., Mills, I. G., Longley, D. B., Quigley, J. P., Zoubeidi, A., de Bono, J. S., Deryugina, E., LaBonte, M. J., & Waugh, D. J. J. (2022). Attenuating Adaptive VEGF-A and IL8 Signaling Restores Durable Tumor Control in AR Antagonist–Treated Prostate Cancers. *Molecular Cancer Research*, *20*(6), 841–853. https://doi.org/10.1158/1541-7786.MCR-21-0780

McManus, C. J., & Graveley, B. R. (2011). RNA structure and the mechanisms of alternative splicing. *Curr Opin Genet Dev*, *21*(4), 373–379. https://doi.org/10.1016/j.gde.2011.04.001

McNeal, J. E. (1981). The zonal anatomy of the prostate. *Prostate*, *2*(1), 35–49. https://doi.org/10.1002/pros.2990020105

Melnyk, J. E., Steri, V., Nguyen, H. G., Hwang, Y. C., Gordan, J. D., Hann, B., Feng, F. Y., & Shokat, K. M. (2022). Targeting a splicing-mediated drug resistance mechanism in prostate cancer by inhibiting transcriptional regulation by PKCβ1. *Oncogene*, *41*(11), 1536–1549. https://doi.org/10.1038/s41388-022-02179-z

Merson, S., Yang, Z. H., Brewer, D., Olmos, D., Eichholz, A., McCarthy, F., Fisher, G., Kovacs, G., Berney, D. M., Foster, C. S., Moller, H., Scardino, P., Cuzick, J., Cooper, C. S., Clark, J. P., & Transatlantic Prostate, G. (2014). Focal amplification of the androgen receptor gene in hormone-naive human prostate cancer. *Br J Cancer*, *110*(6), 1655–1662. https://doi.org/10.1038/bjc.2014.13

Mertens-Walker, I., Fernandini, B. C., Maharaj, M. S., Rockstroh, A., Nelson, C. C., Herington, A. C., & Stephenson, S.-A. (2015). The tumour-promoting receptor tyrosine kinase, EphB4, regulates expression of Integrin-β8 in prostate cancer cells. *BMC Cancer*, *15*(1), 164. https://doi.org/10.1186/s12885-015-1164-6

Messina, C., Cattrini, C., Soldato, D., Vallome, G., Caffo, O., Castro, E., Olmos, D., Boccardo, F., & Zanardi, E. (2020). BRCA Mutations in Prostate Cancer: Prognostic and Predictive Implications. *J Oncol*, *2020*, 4986365. https://doi.org/10.1155/2020/4986365

Messner, E. A., Steele, T. M., Tsamouri, M. M., Hejazi, N., Gao, A. C., Mudryj, M., & Ghosh, P. M. (2020). The Androgen Receptor in Prostate Cancer: Effect of Structure, Ligands and Spliced Variants on Therapy. *Biomedicines*, *8*(10). https://doi.org/10.3390/biomedicines8100422

Metzler, V. M., de Brot, S., Haigh, D. B., Woodcock, C. L., Lothion-Roy, J., Harris, A. E., Nilsson, E. M., Ntekim, A., Persson, J. L., Robinson, B. D., Khani, F., Laursen, K. B., Gudas, L. J., Toss, M. S., Madhusudan, S., Rakha, E., Heery, D. M., Rutland, C. S., Mongan, N. P., & Jeyapalan, J. N. (2023a). The KDM5B and KDM1A lysine demethylases cooperate in regulating androgen receptor expression and signalling in prostate cancer. *Front Cell Dev Biol*, *11*, 1116424. https://doi.org/10.3389/fcell.2023.1116424

Metzler, V. M., de Brot, S., Haigh, D. B., Woodcock, C. L., Lothion-Roy, J., Harris, A. E., Nilsson, E. M., Ntekim, A., Persson, J. L., Robinson, B. D., Khani, F., Laursen, K. B., Gudas, L. J., Toss, M. S., Madhusudan, S., Rakha, E., Heery, D. M., Rutland, C. S., Mongan, N. P., & Jeyapalan, J. N. (2023b). The KDM5B and KDM1A lysine demethylases cooperate in regulating androgen receptor expression and signalling in prostate cancer. *Frontiers in Cell and Developmental Biology*, *11*. https://doi.org/10.3389/fcell.2023.1116424

Michealraj, K. A., Kumar, S. A., Kim, L. J. Y., Cavalli, F. M. G., Przelicki, D., Wojcik, J. B., Delaidelli, A., Bajic, A., Saulnier, O., MacLeod, G., Vellanki, R. N., Vladoiu, M. C., Guilhamon, P., Ong, W., Lee, J. J. Y., Jiang, Y., Holgado, B. L., Rasnitsyn, A., Malik, A. A., … Taylor, M. D. (2020). Metabolic Regulation of the Epigenome Drives Lethal Infantile Ependymoma. *Cell*, *181*(6), 1329-1345 e24. https://doi.org/10.1016/j.cell.2020.04.047

Miller, K. J., Henry, I., Maylin, Z., Smith, C., Arunachalam, E., Pandha, H., & Asim, M. (2023). A compendium of Androgen Receptor Variant 7 target genes and their role in Castration Resistant Prostate Cancer. *Front Oncol*, *13*, 1129140. https://doi.org/10.3389/fonc.2023.1129140

Minshall, N., & Git, A. (2020). Enzyme-and gene-specific biases in reverse transcription of RNA raise concerns for evaluating gene expression. *Scientific Reports*, *10*(1), 8151.

Mishra, P., Kiebish, M. A., Cullen, J., Srinivasan, A., Patterson, A., Sarangarajan, R., Narain, N. R., & Dobi, A. (2019a). Genomic alterations of Tenascin C in highly aggressive prostate cancer: a meta-analysis. *Genes & Cancer*, *10*(5–6), 150–159. https://doi.org/10.18632/genesandcancer.196

Mishra, P., Kiebish, M. A., Cullen, J., Srinivasan, A., Patterson, A., Sarangarajan, R., Narain, N. R., & Dobi, A. (2019b). Genomic alterations of Tenascin C in highly aggressive prostate cancer: a meta-analysis. *Genes & Cancer*, *10*(5–6), 150–159. https://doi.org/10.18632/genesandcancer.196

Miyahira, A. K., & Soule, H. R. (2022). The 28th Annual Prostate Cancer Foundation Scientific Retreat report. *Prostate*, *82*(14), 1346–1377. https://doi.org/10.1002/pros.24409

Moe, A., & Hayne, D. (2020). Transrectal ultrasound biopsy of the prostate: does it still have a role in prostate cancer diagnosis? *Transl Androl Urol*, *9*(6), 3018–3024. https://doi.org/10.21037/tau.2019.09.37

Mohler, M. L., Sikdar, A., Ponnusamy, S., Hwang, D. J., He, Y., Miller, D. D., & Narayanan, R. (2021). An Overview of Next-Generation Androgen Receptor-Targeted Therapeutics in Development for the Treatment of Prostate Cancer. *Int J Mol Sci*, *22*(4). https://doi.org/10.3390/ijms22042124

Moigne, R. Le, Banuelos, C. A., Mawji, N. R., Tam, T., Wang, J., Jian, K., Andersen, R. J., Cesano, A., Sadar, M. D., Zhou, H. J., & Virsik, P. (2019). EPI-7386 is a novel N-terminal domain androgen receptor inhibitor for the treatment of prostate cancer. *Annals of Oncology*, *30*, v189–v190. https://doi.org/10.1093/annonc/mdz244.065

Moll, J. M., Teubel, W. J., Erkens, S. E., Jozefzoon-Agai, A., Dits, N. F., van Rijswijk, A., Jenster, G. W., & van Weerden, W. M. (2022). Cell Line Characteristics Predict Subsequent Resistance to Androgen Receptor-Targeted Agents (ARTA) in Preclinical Models of Prostate Cancer. *Frontiers in Oncology*, *12*. https://doi.org/10.3389/fonc.2022.877613

Morales Torres, C., Laugesen, A., & Helin, K. (2013). Utx is required for proper induction of ectoderm and mesoderm during differentiation of embryonic stem cells. *PLoS One*, *8*(4), e60020.

Morata-Tarifa, C., Jiménez, G., García, M. A., Entrena, J. M., Griñán-Lisón, C., Aguilera, M., Picon-Ruiz, M., & Marchal, J. A. (2016). Low adherent cancer cell subpopulations are enriched in tumorigenic and metastatic epithelial-to-mesenchymal transition-induced cancer stem-like cells. *Scientific Reports*, *6*(1), 18772. https://doi.org/10.1038/srep18772

Morozov, V. M., Li, Y., Clowers, M. M., & Ishov, A. M. (2017). Inhibitor of H3K27 demethylase JMJD3/UTX GSK-J4 is a potential therapeutic option for castration resistant prostate cancer. *Oncotarget*, *8*(37), 62131–62142. https://doi.org/10.18632/oncotarget.19100

Mu, H., Xiang, L., Li, S., Rao, D., Wang, S., & Yu, K. (2019). MiR-10a functions as a tumor suppressor in prostate cancer via targeting KDM4A. *J Cell Biochem*, *120*(4), 4987–4997. https://doi.org/10.1002/jcb.27774

Nadiminty, N., & Gao, A. C. (2012). Mechanisms of persistent activation of the androgen receptor in CRPC: recent advances and future perspectives. *World J Urol*, *30*(3), 287–295. https://doi.org/10.1007/s00345-011-0771-3

Nadiminty, N., Tummala, R., Liu, C., Lou, W., Evans, C. P., & Gao, A. C. (2015). NF-kappaB2/p52:c-Myc:hnRNPA1 Pathway Regulates Expression of Androgen Receptor

Splice Variants and Enzalutamide Sensitivity in Prostate Cancer. *Mol Cancer Ther*, *14*(8), 1884–1895. https://doi.org/10.1158/1535-7163.MCT-14-1057

Nakazawa, M., Fang, M., Marshall, H. C., Lotan, T. L., Isaacsson Velho, P., & Antonarakis, E. S. (2022). Clinical and genomic features of SPOP-mutant prostate cancer. *Prostate*, *82*(2), 260–268. https://doi.org/10.1002/pros.24269

Nauseef, J. T., & Henry, M. D. (2011). Epithelial-to-mesenchymal transition in prostate cancer: paradigm or puzzle? *Nat Rev Urol*, *8*(8), 428–439. https://doi.org/10.1038/nrurol.2011.85

Ni, W.-D., Yang, Z.-T., Cui, C.-A., Cui, Y., Fang, L.-Y., & Xuan, Y.-H. (2017). Tenascin-C is a potential cancer-associated fibroblasts marker and predicts poor prognosis in prostate cancer. *Biochemical and Biophysical Research Communications*, *486*(3), 607–612. https://doi.org/10.1016/j.bbrc.2017.03.021

NICE. (2019). *Prostate Cancer; diagnosis and management*. https://www.nice.org.uk/guidance/ng131/chapter/Recommendations#people-having-hormone-therapy

Nicolosi, P., Ledet, E., Yang, S., Michalski, S., Freschi, B., O'Leary, E., Esplin, E. D., Nussbaum, R. L., & Sartor, O. (2019). Prevalence of Germline Variants in Prostate Cancer and Implications for Current Genetic Testing Guidelines. *JAMA Oncol*, *5*(4), 523–528. https://doi.org/10.1001/jamaoncol.2018.6760

Niepel, M., Hafner, M., Chung, M., & Sorger, P. K. (2017). Measuring Cancer Drug Sensitivity and Resistance in Cultured Cells. *Curr Protoc Chem Biol*, *9*(2), 55–74. https://doi.org/10.1002/cpch.21

Norris, J. D., Chang, C.-Y., Wittmann, B. M., Kunder, R. S., Cui, H., Fan, D., Joseph, J. D., & McDonnell, D. P. (2009). The homeodomain protein HOXB13 regulates the cellular response to androgens. *Molecular Cell*, *36*(3), 405–416.

Ntziachristos, P., Tsirigos, A., Welstead, G. G., Trimarchi, T., Bakogianni, S., Xu, L., Loizou, E., Holmfeldt, L., Strikoudis, A., & King, B. (2014). Contrasting roles of histone 3 lysine 27 demethylases in acute lymphoblastic leukaemia. *Nature*, *514*(7523), 513–517.

Nuhn, P., De Bono, J. S., Fizazi, K., Freedland, S. J., Grilli, M., Kantoff, P. W., Sonpavde, G., Sternberg, C. N., Yegnasubramanian, S., & Antonarakis, E. S. (2019). Update on systemic prostate cancer therapies: management of metastatic castration-resistant prostate cancer in the era of precision oncology. *European Urology*, *75*(1), 88–99.

Oyola, M. G., & Handa, R. J. (2017). Hypothalamic-pituitary-adrenal and hypothalamic-pituitary-gonadal axes: sex differences in regulation of stress responsivity. *Stress*, *20*(5), 476–494. https://doi.org/10.1080/10253890.2017.1369523

Özden-Yılmaz, G., Savas, B., Bursalı, A., Eray, A., Arıbaş, A., Senturk, S., Karaca, E., Karakülah, G., & Erkek-Ozhan, S. (2023). Differential Occupancy and Regulatory Interactions of KDM6A in Bladder Cell Lines. *Cells*, *12*(6), 836. https://www.mdpi.com/2073-4409/12/6/836

Paolicchi, E., Crea, F., Farrar, W. L., Green, J. E., & Danesi, R. (2013). Histone lysine demethylases in breast cancer. *Critical Reviews in Oncology/Hematology*, *86*(2), 97–103.

Parekh, S., Ziegenhain, C., Vieth, B., Enard, W., & Hellmann, I. (2016). The impact of amplification on differential expression analyses by RNA-seq. *Scientific Reports*, *6*(1), 25533. https://doi.org/10.1038/srep25533

Parikh, M., Liu, C., Wu, C.-Y., Evans, C. P., Dall'Era, M., Robles, D., Lara, P. N., Agarwal, N., Gao, A. C., & Pan, C.-X. (2021). Phase Ib trial of reformulated niclosamide with abiraterone/prednisone in men with castration-resistant prostate cancer. *Scientific Reports*, *11*(1), 6377. https://doi.org/10.1038/s41598-021-85969-x

Park, J. W., Lee, J. K., Phillips, J. W., Huang, P., Cheng, D., Huang, J., & Witte, O. N. (2016). Prostate epithelial cell of origin determines cancer differentiation state in an organoid transformation assay. *Proc Natl Acad Sci U S A*, *113*(16), 4482–4487. https://doi.org/10.1073/pnas.1603645113

Paro, R. (2021). *Introduction to epigenetics* (U. Grossniklaus, R. Santoro, & A. Wutz, Eds.). Springer Nature.

Parsons, B. D., Schindler, A., Evans, D. H., & Foley, E. (2009). A Direct Phenotypic Comparison of siRNA Pools and Multiple Individual Duplexes in a Functional Assay. *PLoS ONE*, *4*(12), e8471. https://doi.org/10.1371/journal.pone.0008471

Paschalis, A., Sharp, A., Welti, J. C., Neeb, A., Raj, G. V, Luo, J., Plymate, S. R., & de Bono, J. S. (2018). Alternative splicing in prostate cancer. *Nat Rev Clin Oncol*, *15*(11), 663–675. https://doi.org/10.1038/s41571-018-0085-0

Paschalis, A., Welti, J., Neeb, A. J., Yuan, W., Figueiredo, I., Pereira, R., Ferreira, A., Riisnaes, R., Rodrigues, D. N., Jimenez-Vacas, J. M., Kim, S., Uo, T., Micco, P. D., Tumber, A., Islam, M. S., Moesser, M. A., Abboud, M., Kawamura, A., Gurel, B., … Team, S. U. C. P. C. F. I. P. C. D. (2021). JMJD6 Is a Druggable Oxygenase That Regulates AR-V7 Expression in Prostate Cancer. *Cancer Res*, *81*(4), 1087–1100. https://doi.org/10.1158/0008-5472.CAN-20-1807

Patel, R. A., Sayar, E., Coleman, I., Roudier, M. P., Hanratty, B., Low, J.-Y., Jaiswal, N., Ajkunic, A., Dumpit, R., Ercan, C., Salama, N., O'Brien, V. P., Isaacs, W. B., Epstein, J. I., De Marzo, A. M., Trock, B. J., Luo, J., Brennen, W. N., Tretiakova, M., … Haffner, M. C. (2024). Characterization of HOXB13 expression patterns in localized and metastatic castration-resistant prostate cancer. *The Journal of Pathology*, *262*(1), 105–120. https://doi.org/https://doi.org/10.1002/path.6216

Pchelintsev, N. A., Adams, P. D., & Nelson, D. M. (2016). Critical Parameters for Efficient Sonication and Improved Chromatin Immunoprecipitation of High Molecular Weight Proteins. *PLOS ONE*, *11*(1), e0148023. https://doi.org/10.1371/journal.pone.0148023

Pecci, V., Troisi, F., Aiello, A., De Martino, S., Carlino, A., Fiorentino, V., Ripoli, C., Rotili, D., Pierconti, F., Martini, M., Porru, M., Pinto, F., Mai, A., Bassi, P. F., Grassi, C., Gaetano, C., Pontecorvi, A., Strigari, L., Farsetti, A., & Nanni, S. (2024). Targeting of H19/cell adhesion molecules circuitry by GSK-J4 epidrug inhibits metastatic progression in prostate cancer. *Cancer Cell International*, *24*(1), 56. https://doi.org/10.1186/s12935-024-03231-6

Perez-Cornago, A., Appleby, P. N., Pischon, T., Tsilidis, K. K., Tjønneland, A., Olsen, A., Overvad, K., Kaaks, R., Kühn, T., Boeing, H., Steffen, A., Trichopoulou, A., Lagiou, P., Kritikou, M., Krogh, V., Palli, D., Sacerdote, C., Tumino, R., Bueno-de-Mesquita, H. B., … Travis, R. C. (2017). Tall height and obesity are associated with an increased risk of aggressive prostate cancer: results from the EPIC cohort study. *BMC Medicine*, *15*(1), 115. https://doi.org/10.1186/s12916-017-0876-7

Pfeiffer, M. J., Smit, F. P., Sedelaar, J. P., & Schalken, J. A. (2011). Steroidogenic enzymes and stem cell markers are upregulated during androgen deprivation in prostate cancer. *Mol Med*, *17*(7–8), 657–664. https://doi.org/10.2119/molmed.2010.00143

Pilka, E. S., James, T., & Lisztwan, J. H. (2015). Structural definitions of Jumonji family demethylase selectivity. *Drug Discovery Today*, *20*(6), 743–749. https://doi.org/https://doi.org/10.1016/j.drudis.2014.12.013

Plitzko, B., & Loesgen, S. (2018). Measurement of Oxygen Consumption Rate (OCR) and Extracellular Acidification Rate (ECAR) in Culture Cells for Assessment of the Energy Metabolism. *BIO-PROTOCOL*, *8*(10). https://doi.org/10.21769/BioProtoc.2850

Pomerantz, M. M., Qiu, X., Zhu, Y., Takeda, D. Y., Pan, W., Baca, S. C., Gusev, A., Korthauer, K. D., Severson, T. M., Ha, G., Viswanathan, S. R., Seo, J. H., Nguyen, H. M., Zhang, B., Pasaniuc, B., Giambartolomei, C., Alaiwi, S. A., Bell, C. A., O'Connor, E. P., … Freedman, M. L. (2020). Prostate cancer reactivates developmental epigenomic programs during metastatic progression. *Nat Genet*, *52*(8), 790–799. https://doi.org/10.1038/s41588-020-0664-8

Qiu, L., Meng, Y., Wang, L., Gunewardena, S., Liu, S., Han, J., & Krieg, A. J. (2021). Histone lysine demethylase 4B regulates general and unique gene expression signatures in hypoxic cancer cells. *MedComm (2020)*, *2*(3), 414–429. https://doi.org/10.1002/mco2.85

Qu, F., Gu, Y., Xue, M., He, M., Zhou, F., Wang, G., & Peng, Y. (2021). Impact of therapy on cancer metabolism in high-risk localized prostate cancer treated with neoadjuvant docetaxel and androgen deprivation therapy. *Prostate*, *81*(9), 560–571. https://doi.org/10.1002/pros.24134

Ragavi, R., Muthukumaran, P., Nandagopal, S., Ahirwar, D. K., Tomo, S., Misra, S., Guerriero, G., & Shukla, K. K. (2023). Epigenetics regulation of prostate cancer: Biomarker and therapeutic potential. *Urol Oncol*. https://doi.org/10.1016/j.urolonc.2023.03.005

Raina, K., Eastman, K. J., Yu, X., Forbes, C. D., Jones, K. M., Mousseau, J. J., Li, H., Kayser-Bricker, K. J., & Crews, C. M. (2023). An oral androgen receptor RIPTAC for prostate cancer. *Journal of Clinical Oncology*, *41*(6_suppl), 184–184. https://doi.org/10.1200/JCO.2023.41.6_suppl.184

Ramos-Montoya, A., Lamb, A. D., Russell, R., Carroll, T., Jurmeister, S., Galeano-Dalmau, N., Massie, C. E., Boren, J., Bon, H., Theodorou, V., Vias, M., Shaw, G. L., Sharma, N. L., Ross-Adams, H., Scott, H. E., Vowler, S. L., Howat, W. J., Warren, A. Y., Wooster, R. F., … Neal, D. E. (2014). HES6 drives a critical AR transcriptional programme to induce castration‐resistant prostate cancer through activation of an E2F1‐mediated cell cycle network. *EMBO Molecular Medicine*, *6*(5), 651–661. https://doi.org/https://doi.org/10.1002/emmm.201303581

Rao, D. S., Hyun, T. S., Kumar, P. D., Mizukami, I. F., Rubin, M. A., Lucas, P. C., Sanda, M. G., & Ross, T. S. (2002). Huntingtin-interacting protein 1 is overexpressed in prostate and colon cancer and is critical for cellular survival. *Journal of Clinical Investigation*, *110*(3), 351–360. https://doi.org/10.1172/JCI15529

Read, A., & Schröder, M. (2021). The Unfolded Protein Response: An Overview. *Biology (Basel)*, *10*(5). https://doi.org/10.3390/biology10050384

Ribatti, D., Tamma, R., & Annese, T. (2020). Epithelial-Mesenchymal Transition in Cancer: A Historical Overview. *Transl Oncol*, *13*(6), 100773. https://doi.org/10.1016/j.tranon.2020.100773

Rick, F. G., Block, N. L., & Schally, A. V. (2013). Agonists of luteinizing hormone-releasing hormone in prostate cancer. *Expert Opinion on Pharmacotherapy*, *14*(16), 2237–2247. https://doi.org/10.1517/14656566.2013.834328

Rickels, R., Wang, L., Iwanaszko, M., Ozark, P. A., Morgan, M. A., Piunti, A., Khalatyan, N., Soliman, S. H. A., Rendleman, E. J., Savas, J. N., Smith, E. R., & Shilatifard, A. (2020). A small UTX stabilization domain of Trr is conserved within mammalian MLL3-4/COMPASS and is sufficient to rescue loss of viability in null animals. *Genes & Development*, *34*(21–22), 1493–1502. https://doi.org/10.1101/gad.339762.120

Ritch, C., & Cookson, M. (2018). Recent trends in the management of advanced prostate cancer. *F1000Research*, *7*.

Rivera-Izquierdo, M., Pérez de Rojas, J., Martínez-Ruiz, V., Pérez-Gómez, B., Sánchez, M.-J., Khan, K. S., & Jiménez-Moleón, J. J. (2021). Obesity as a Risk Factor for Prostate Cancer Mortality: A Systematic Review and Dose-Response Meta-Analysis of 280,199 Patients. *Cancers*, *13*(16), 4169. https://www.mdpi.com/2072-6694/13/16/4169

Riviere, P., Kumar, A., Luterstein, E., Vitzthum, L. K., Nalawade, V., Sarkar, R. R., Bryant, A. K., Einck, J. P., Mundt, A. J., Murphy, J. D., & Rose, B. S. (2020). Tobacco smoking and death from prostate cancer in US veterans. *Prostate Cancer and Prostatic Diseases*, *23*(2), 252–259. https://doi.org/10.1038/s41391-019-0178-6

Robinson, D. R., Wu, Y.-M., Lonigro, R. J., Vats, P., Cobain, E., Everett, J., Cao, X., Rabban, E., Kumar-Sinha, C., Raymond, V., Schuetze, S., Alva, A., Siddiqui, J., Chugh, R., Worden, F., Zalupski, M. M., Innis, J., Mody, R. J., Tomlins, S. A., … Chinnaiyan, A. M. (2017). Integrative clinical genomics of metastatic cancer. *Nature*, *548*(7667), 297–303. https://doi.org/10.1038/nature23306

Robinson, D., Van Allen, E. M., Wu, Y. M., Schultz, N., Lonigro, R. J., Mosquera, J. M., Montgomery, B., Taplin, M. E., Pritchard, C. C., Attard, G., Beltran, H., Abida, W., Bradley, R. K., Vinson, J., Cao, X., Vats, P., Kunju, L. P., Hussain, M., Feng, F. Y., … Chinnaiyan, A. M. (2015). Integrative clinical genomics of advanced prostate cancer. *Cell*, *161*(5), 1215–1228. https://doi.org/10.1016/j.cell.2015.05.001

Robinson, M. D., McCarthy, D. J., & Smyth, G. K. (2010). edgeR: a Bioconductor package for differential expression analysis of digital gene expression data. *Bioinformatics (Oxford, England)*, *26*(1), 139–140. https://doi.org/10.1093/bioinformatics/btp616

Roggero, C. M., Jin, L., Cao, S., Sonavane, R., Kopplin, N. G., Ta, H. Q., Ekoue, D. N., Witwer, M., Ma, S., Liu, H., Ma, T., Gioeli, D., Raj, G. V, & Dong, Y. (2021). A detailed characterization of stepwise activation of the androgen receptor variant 7 in prostate cancer cells. *Oncogene*, *40*(6), 1106–1117. https://doi.org/10.1038/s41388-020-01585-5

Romani, M., Daga, A., Forlani, A., Pistillo, M. P., & Banelli, B. (2019). Targeting of histone demethylases KDM5A and KDM6B inhibits the proliferation of temozolomide-resistant glioblastoma cells. *Cancers*, *11*(6), 878.

Ruttkay-Nedecky, B., Nejdl, L., Gumulec, J., Zitka, O., Masarik, M., Eckschlager, T., Stiborova, M., Adam, V., & Kizek, R. (2013). The Role of Metallothionein in Oxidative Stress. *International Journal of Molecular Sciences*, *14*(3), 6044–6066. https://doi.org/10.3390/ijms14036044

Saad, F., Bögemann, M., Suzuki, K., & Shore, N. (2021). Treatment of nonmetastatic castration-resistant prostate cancer: focus on second-generation androgen receptor inhibitors. *Prostate Cancer and Prostatic Diseases*, *24*(2), 323–334. https://doi.org/10.1038/s41391-020-00310-3

Sainathan, S., Paul, S., Ramalingam, S., Baranda, J., Anant, S., & Dhar, A. (2015). Histone demethylases in cancer. *Current Pharmacology Reports*, *1*, 234–244.

Salamero, O., Somervaille, T. C. P., Molero, A., Acuña-Cruz, E., Pérez-Simón, J., Coll, R., Arnan Sangerman, M., Merchan, B., Perez, A., Cano, I., Rodríguez-Veiga, R., Gutierrez, S., Buesa, C., Bosch, F., & Montesinos, P. (2021). Iadademstat in Combination with Azacitidine Generates Robust and Long Lasting Responses in AML Patients (ALICE Trial). *Blood*, *138*, 3376. https://doi.org/https://doi.org/10.1182/blood-2021-152183

Saporita, A. J., Zhang, Q., Navai, N., Dincer, Z., Hahn, J., Cai, X., & Wang, Z. (2003). Identification and Characterization of a Ligand-regulated Nuclear Export Signal in Androgen Receptor. *Journal of Biological Chemistry*, *278*(43), 41998–42005. https://doi.org/10.1074/jbc.M302460200

Sarac, H., Morova, T., Pires, E., McCullagh, J., Kaplan, A., Cingoz, A., Bagci-Onder, T., Onder, T., Kawamura, A., & Lack, N. A. (2020). Systematic characterization of chromatin modifying enzymes identifies KDM3B as a critical regulator in castration resistant prostate cancer. *Oncogene*, *39*(10), 2187–2201. https://doi.org/10.1038/s41388-019-1116-8

Sarah, L., & Fujimori, D. G. (2023). Recent developments in catalysis and inhibition of the Jumonji histone demethylases. *Current Opinion in Structural Biology*, *83*, 102707. https://doi.org/10.1016/j.sbi.2023.102707

Sardesai, S. D., Thomas, A., Gallagher, C., Lynce, F., Ottaviano, Y. L., Ballinger, T. J., Schneider, B. P., Storniolo, A. M., Bauchle, A., & Althouse, S. K. (2021). Inhibiting fatty acid synthase with omeprazole to improve efficacy of neoadjuvant chemotherapy in patients with operable TNBC. *Clinical Cancer Research*, *27*(21), 5810–5817.

Sartor, O., de Bono, J., Chi, K. N., Fizazi, K., Herrmann, K., Rahbar, K., Tagawa, S. T., Nordquist, L. T., Vaishampayan, N., El-Haddad, G., Park, C. H., Beer, T. M., Armour, A., Pérez-Contreras, W. J., DeSilvio, M., Kpamegan, E., Gericke, G., Messmann, R. A., Morris, M. J., & Krause, B. J. (2021). Lutetium-177–PSMA-617 for Metastatic Castration-Resistant Prostate Cancer. *New England Journal of Medicine*, *385*(12), 1091–1103. https://doi.org/10.1056/NEJMoa2107322

Sartor, O., & de Bono, J. S. (2018). Metastatic Prostate Cancer. *New England Journal of Medicine*, *378*(7), 645–657. https://doi.org/10.1056/NEJMra1701695

Schalken, J., & Fitzpatrick, J. M. (2016). Enzalutamide: targeting the androgen signalling pathway in metastatic castration-resistant prostate cancer. *BJU Int*, *117*(2), 215–225. https://doi.org/10.1111/bju.13123

Scher, H. I., Graf, R. P., Schreiber, N. A., Jayaram, A., Winquist, E., McLaughlin, B., Lu, D., Fleisher, M., Orr, S., Lowes, L., Anderson, A., Wang, Y., Dittamore, R., Allan, A. L., Attard, G., & Heller, G. (2018). Assessment of the Validity of Nuclear-Localized Androgen Receptor Splice Variant 7 in Circulating Tumor Cells as a Predictive Biomarker for Castration-Resistant Prostate Cancer. *JAMA Oncol*, *4*(9), 1179–1186. https://doi.org/10.1001/jamaoncol.2018.1621

Schor, I. E., Rascovan, N., Pelisch, F., Alló, M., & Kornblihtt, A. R. (2009). Neuronal cell depolarization induces intragenic chromatin modifications affecting NCAM alternative splicing. *Proceedings of the National Academy of Sciences*, *106*(11), 4325–4330.

Schulz, W. A., Lang, A., Koch, J., & Greife, A. (2019). The histone demethylase UTX/KDM6A in cancer: Progress and puzzles. *International Journal of Cancer*, *145*(3), 614–620. https://doi.org/https://doi.org/10.1002/ijc.32116

Schweizer, M. T., & Antonarakis, E. S. (2012). Abiraterone and other novel androgen-directed strategies for the treatment of prostate cancer: a new era of hormonal therapies is born. *Ther Adv Urol*, *4*(4), 167–178. https://doi.org/10.1177/1756287212452196

Seehawer, M., Li, Z., Nishida, J., Foidart, P., Reiter, A. H., Rojas-Jimenez, E., Goyette, M.-A., Yan, P., Raval, S., Munoz Gomez, M., Cejas, P., Long, H. W., Papanastasiou, M., & Polyak, K. (2024). Loss of Kmt2c or Kmt2d drives brain metastasis via KDM6A-dependent upregulation of MMP3. *Nature Cell Biology*, *26*(7), 1165–1175. https://doi.org/10.1038/s41556-024-01446-3

Segelle, A., Nunez-Alvarez, Y., Oldfield, A. J., Webb, K. M., Voigt, P., & Luco, R. F. (2022). Histone marks regulate the epithelial-to-mesenchymal transition via alternative splicing. *Cell Rep*, *38*(7), 110357. https://doi.org/10.1016/j.celrep.2022.110357

Sehrawat, A., Gao, L., Wang, Y., Bankhead 3rd, A., McWeeney, S. K., King, C. J., Schwartzman, J., Urrutia, J., Bisson, W. H., Coleman, D. J., Joshi, S. K., Kim, D. H., Sampson, D. A., Weinmann, S., Kallakury, B. V. S., Berry, D. L., Haque, R., Van Den Eeden, S. K., Sharma, S., … Alumkal, J. J. (2018). LSD1 activates a lethal prostate cancer gene network independently of its demethylase function. *Proc Natl Acad Sci U S A*, *115*(18), E4179–E4188. https://doi.org/10.1073/pnas.1719168115

Sengoku, T., & Yokoyama, S. (2011). Structural basis for histone H3 Lys 27 demethylation by UTX/KDM6A. *Genes & Development*, *25*(21), 2266–2277. https://doi.org/10.1101/gad.172296.111

Severson, T. M., Zhu, Y., Prekovic, S., Schuurman, K., Nguyen, H. M., Brown, L. G., Hakkola, S., Kim, Y., Kneppers, J., Linder, S., Stelloo, S., Lieftink, C., van der Heijden, M., Nykter, M., van der Noort, V., Sanders, J., Morris, B., Jenster, G., van Leenders, G. J., … Bergman, A. M. (2023). *Enhancer profiling identifies epigenetic markers of endocrine resistance and reveals therapeutic options for metastatic castration-resistant prostate cancer patients*. https://doi.org/10.1101/2023.02.24.23286403

Severson, T., Qiu, X., Alshalalfa, M., Sjostrom, M., Quigley, D., Bergman, A., Long, H., Feng, F., Freedman, M. L., Zwart, W., & Pomerantz, M. M. (2022). Androgen receptor reprogramming demarcates prognostic, context-dependent gene sets in primary and metastatic prostate cancer. *Clin Epigenetics*, *14*(1), 60. https://doi.org/10.1186/s13148-022-01278-8

Sha, K., Yeh, S., Chang, C., Nastiuk, K. L., & Krolewski, J. J. (2015). TNF signaling mediates an enzalutamide-induced metastatic phenotype of prostate cancer and microenvironment cell co-cultures. *Oncotarget*, *6*(28), 25726–25740. https://doi.org/10.18632/oncotarget.4535

Shao, J. B., Gao, Z. M., Huang, W. Y., & Lu, Z. B. (2017). The mechanism of epithelial-mesenchymal transition induced by TGF-β1 in neuroblastoma cells. *Int J Oncol*, *50*(5), 1623–1633. https://doi.org/10.3892/ijo.2017.3954

Sharma, M., Gupta, S., Dhole, B., & Kumar, A. (2017). The Prostate Gland. In A. Kumar & M. Sharma (Eds.), *Basics of Human Andrology: A Textbook* (pp. 17–35). Springer Singapore. https://doi.org/10.1007/978-981-10-3695-8_2

Sharp, A., Coleman, I., Yuan, W., Sprenger, C., Dolling, D., Rodrigues, D. N., Russo, J. W., Figueiredo, I., Bertan, C., Seed, G., Riisnaes, R., Uo, T., Neeb, A., Welti, J., Morrissey, C., Carreira, S., Luo, J., Nelson, P. S., Balk, S. P., … Plymate, S. R. (2019). Androgen receptor splice variant-7 expression emerges with castration resistance in prostate cancer. *J Clin Invest*, *129*(1), 192–208. https://doi.org/10.1172/jci122819

Shi, B., Li, W., Song, Y., Wang, Z., Ju, R., Ulman, A., Hu, J., Palomba, F., Zhao, Y., Le, J. P., Jarrard, W., Dimoff, D., Digman, M. A., Gratton, E., Zang, C., & Jiang, H. (2021). UTX condensation underlies its tumour-suppressive activity. *Nature*, *597*(7878), 726–731. https://doi.org/10.1038/s41586-021-03903-7

Shim, M., Bang, W. J., Oh, C. Y., Lee, Y. S., & Cho, J. S. (2019). Effectiveness of three different luteinizing hormone-releasing hormone agonists in the chemical castration of patients with prostate cancer: Goserelin versus triptorelin versus leuprolide. *Icu*, *60*(4), 244–250. https://doi.org/10.4111/icu.2019.60.4.244

Shin, S., & Janknecht, R. (2007). Activation of androgen receptor by histone demethylases JMJD2A and JMJD2D. *Biochemical and Biophysical Research Communications*, *359*(3), 742–746.

Shiota, M., Fujimoto, N., Matsumoto, T., Tsukahara, S., Nagakawa, S., Ueda, S., Ushijima, M., Kashiwagi, E., Takeuchi, A., Inokuchi, J., Uchiumi, T., & Eto, M. (2021). Differential Impact of TGFB1 Variation by Metastatic Status in Androgen-Deprivation Therapy for Prostate Cancer. *Front Oncol*, *11*, 697955. https://doi.org/10.3389/fonc.2021.697955

Shore, N. D., Abrahamsson, P. A., Anderson, J., Crawford, E. D., & Lange, P. (2013). New considerations for ADT in advanced prostate cancer and the emerging role of GnRH antagonists. *Prostate Cancer Prostatic Dis*, *16*(1), 7–15. https://doi.org/10.1038/pcan.2012.25

Shpargel, K. B., Starmer, J., Wang, C., Ge, K., & Magnuson, T. (2017). UTX-guided neural crest function underlies craniofacial features of Kabuki syndrome. *Proceedings of the National Academy of Sciences*, *114*(43), E9046–E9055.

Singh, J., & Padgett, R. A. (2009). Rates of in situ transcription and splicing in large human genes. *Nat Struct Mol Biol*, *16*(11), 1128–1133. https://doi.org/10.1038/nsmb.1666

Smith, D. J., Jaggi, M., Zhang, W., Galich, A., Du, C., Sterrett, S. P., Smith, L. M., & Balaji, K. C. (2006). Metallothioneins and resistance to cisplatin and radiation in prostate cancer. *Urology*, *67*(6), 1341–1347. https://doi.org/10.1016/j.urology.2005.12.032

Sobhani, N., Neeli, P. K., D'Angelo, A., Pittacolo, M., Sirico, M., Galli, I. C., Roviello, G., & Nesi, G. (2021). AR-V7 in Metastatic Prostate Cancer: A Strategy beyond Redemption. *Int J Mol Sci*, *22*(11). https://doi.org/10.3390/ijms22115515

Song, H., Weinstein, H. N. W., Allegakoen, P., Wadsworth, M. H., Xie, J., Yang, H., Castro, E. A., Lu, K. L., Stohr, B. A., Feng, F. Y., Carroll, P. R., Wang, B., Cooperberg, M. R., Shalek, A. K., & Huang, F. W. (2022). Single-cell analysis of human primary prostate cancer reveals the heterogeneity of tumor-associated epithelial cell states. *Nature Communications*, *13*(1), 141. https://doi.org/10.1038/s41467-021-27322-4

Sreedharan, S. P., Kumar, A., & Giridhar, P. (2018). Primer design and amplification efficiencies are crucial for reliability of quantitative PCR studies of caffeine biosynthetic N-methyltransferases in coffee. *3 Biotech*, *8*(11), 467. https://doi.org/10.1007/s13205-018-1487-5

Staal, J., & Beyaert, R. (2018). Inflammation and NF-κB Signaling in Prostate Cancer: Mechanisms and Clinical Implications. *Cells*, *7*(9), 122. https://www.mdpi.com/2073-4409/7/9/122

Stadler, M., Scherzer, M., Walter, S., Holzner, S., Pudelko, K., Riedl, A., Unger, C., Kramer, N., Weil, B., Neesen, J., Hengstschläger, M., & Dolznig, H. (2018). Exclusion from spheroid formation identifies loss of essential cell-cell adhesion molecules in colon

cancer cells. *Scientific Reports*, *8*(1), 1151. https://doi.org/10.1038/s41598-018-19384-0

Stein, M., Lin, H., Jeyamohan, C., Dvorzhinski, D., Gounder, M., Bray, K., Eddy, S., Goodin, S., White, E., & Dipaola, R. S. (2010). Targeting tumor metabolism with 2-deoxyglucose in patients with castrate-resistant prostate cancer and advanced malignancies. *Prostate*, *70*(13), 1388–1394. https://doi.org/10.1002/pros.21172

Steinberg, M. (2009). Degarelix: A gonadotropin-releasing hormone antagonist for the management of prostate cancer. *Clinical Therapeutics*, *31*, 2312–2331. https://doi.org/https://doi.org/10.1016/j.clinthera.2009.11.009

Sterling, J., Menezes, S. V, Abbassi, R. H., & Munoz, L. (2021). Histone lysine demethylases and their functions in cancer. *International Journal of Cancer*, *148*(10), 2375–2388. https://doi.org/https://doi.org/10.1002/ijc.33375

Su, W., Han, H. H., Wang, Y., Zhang, B., Zhou, B., Cheng, Y., Rumandla, A., Gurrapu, S., Chakraborty, G., Su, J., Yang, G., Liang, X., Wang, G., Rosen, N., Scher, H. I., Ouerfelli, O., & Giancotti, F. G. (2019). The Polycomb Repressor Complex 1 Drives Double-Negative Prostate Cancer Metastasis by Coordinating Stemness and Immune Suppression. *Cancer Cell*, *36*(2), 139-155 e10. https://doi.org/10.1016/j.ccell.2019.06.009

Subramanian, A., Tamayo, P., Mootha, V. K., Mukherjee, S., Ebert, B. L., Gillette, M. A., Paulovich, A., Pomeroy, S. L., Golub, T. R., Lander, E. S., & Mesirov, J. P. (2005). Gene set enrichment analysis: A knowledge-based approach for interpreting genome-wide expression profiles. *Proceedings of the National Academy of Sciences*, *102*(43), 15545–15550. https://doi.org/doi:10.1073/pnas.0506580102

Suehnholz, S. P., Nissan, M. H., Zhang, H., Kundra, R., Nandakumar, S., Lu, C., Carrero, S., Dhaneshwar, A., Fernandez, N., Xu, B. W., Arcila, M. E., Zehir, A., Syed, A., Brannon, A. R., Rudolph, J. E., Paraiso, E., Sabbatini, P. J., Levine, R. L., Dogan, A., … Chakravarty, D. (2024). Quantifying the Expanding Landscape of Clinical Actionability for Patients with Cancer. *Cancer Discovery*, *14*(1), 49–65. https://doi.org/10.1158/2159-8290.Cd-23-0467

Sugiura, M., Sato, H., Okabe, A., Fukuyo, M., Mano, Y., Shinohara, K. I., Rahmutulla, B., Higuchi, K., Maimaiti, M., Kanesaka, M., Imamura, Y., Furihata, T., Sakamoto, S., Komiya, A., Anzai, N., Kanai, Y., Luo, J., Ichikawa, T., & Kaneda, A. (2021). Identification of AR-V7 downstream genes commonly targeted by AR/AR-V7 and specifically targeted by AR-V7 in castration resistant prostate cancer. *Transl Oncol*, *14*(1), 100915. https://doi.org/10.1016/j.tranon.2020.100915

Sun, M., Choueiri, T. K., Hamnvik, O.-P. R., Preston, M. A., De Velasco, G., Jiang, W., Loeb, S., Nguyen, P. L., & Trinh, Q.-D. (2016). Comparison of Gonadotropin-Releasing Hormone Agonists and Orchiectomy: Effects of Androgen-Deprivation Therapy. *JAMA Oncology*, *2*(4), 500–507. https://doi.org/10.1001/jamaoncol.2015.4917

Sun, S., Sprenger, C. C., Vessella, R. L., Haugk, K., Soriano, K., Mostaghel, E. A., Page, S. T., Coleman, I. M., Nguyen, H. M., Sun, H., Nelson, P. S., & Plymate, S. R. (2010). Castration resistance in human prostate cancer is conferred by a frequently occurring androgen receptor splice variant. *J Clin Invest*, *120*(8), 2715–2730. https://doi.org/10.1172/JCI41824

Tagawa, S. T., Antonarakis, E. S., Gjyrezi, A., Galletti, G., Kim, S., Worroll, D., Stewart, J., Zaher, A., Szatrowski, T. P., Ballman, K. V, Kita, K., Tasaki, S., Bai, Y., Portella, L., Kirby, B. J., Saad, F., Eisenberger, M. A., Nanus, D. M., & Giannakakou, P. (2019). Expression

of AR-V7 and ARv(567es) in Circulating Tumor Cells Correlates with Outcomes to Taxane Therapy in Men with Metastatic Prostate Cancer Treated in TAXYNERGY. *Clin Cancer Res*, *25*(6), 1880–1888. https://doi.org/10.1158/1078-0432.CCR-18-0320

Taheri, M., Safarzadeh, A., Hussen, B. M., Ghafouri-Fard, S., & Baniahmad, A. (2022). LncRNA/miRNA/mRNA Network Introduces Novel Biomarkers in Prostate Cancer. *Cells*, *11*(23), 3776. https://doi.org/10.3390/cells11233776

Tan, M. H., Li, J., Xu, H. E., Melcher, K., & Yong, E. L. (2015). Androgen receptor: structure, role in prostate cancer and drug discovery. *Acta Pharmacol Sin*, *36*(1), 3–23. https://doi.org/10.1038/aps.2014.18

Tang, B., Qi, G., Tang, F., Yuan, S., Wang, Z., Liang, X., Li, B., Yu, S., Liu, J., Huang, Q., Wei, Y., Zhai, R., Lei, B., Yu, H., Jiao, X., & He, S. (2015). JARID1B promotes metastasis and epithelial-mesenchymal transition via PTEN/AKT signaling in hepatocellular carcinoma cells. *Oncotarget*, *6*(14), 12723–12739. https://doi.org/10.18632/oncotarget.3713

Tang, D. E., Dai, Y., He, J. X., Lin, L. W., Leng, Q. X., Geng, X. Y., Fu, D. X., Jiang, H. W., & Xu, S. H. (2020). Targeting the KDM4B-AR-c-Myc axis promotes sensitivity to androgen receptor-targeted therapy in advanced prostate cancer. *J Pathol*, *252*(2), 101–113. https://doi.org/10.1002/path.5495

Tang, D. E., He, J. X., Dai, Y., Zhou, H. F., Zhang, C., Leng, Q. X., Geng, X., Fu, D., Jiang, H. W., Sun, R., & Xu, S. H. (2021). Targeting KDM6A suppresses SREBP1c-dependent lipid metabolism and prostate tumorigenesis. *Cancer Res*. https://doi.org/10.1158/0008-5472.CAN-21-1825

Tang, D., He, J., Dai, Y., Geng, X., Leng, Q., Jiang, H., Sun, R., & Xu, S. (2022). Targeting KDM1B-dependent miR-215-AR-AGR2-axis promotes sensitivity to enzalutamide-resistant prostate cancer. *Cancer Gene Ther*, *29*(5), 543–557. https://doi.org/10.1038/s41417-021-00332-6

Taplin, M.-E., Antonarakis, E. S., Ferrante, K. J., Horgan, K., Blumenstein, B., Saad, F., Luo, J., & de Bono, J. S. (2019). Androgen Receptor Modulation Optimized for Response—Splice Variant: A Phase 3, Randomized Trial of Galeterone Versus Enzalutamide in Androgen Receptor Splice Variant-7–expressing Metastatic Castration-resistant Prostate Cancer. *European Urology*, *76*(6), 843–851. https://doi.org/10.1016/j.eururo.2019.08.034

Teo, M. Y., Rathkopf, D. E., & Kantoff, P. (2019). Treatment of advanced prostate cancer. *Annual Review of Medicine*, *70*, 479–499.

Tepper, C. G., Boucher, D. L., Ryan, P. E., Ma, A. H., Xia, L., Lee, L. F., Pretlow, T. G., & Kung, H. J. (2002). Characterization of a novel androgen receptor mutation in a relapsed CWR22 prostate cancer xenograft and cell line. *Cancer Res*, *62*(22), 6606–6614. https://www.ncbi.nlm.nih.gov/pubmed/12438256

Thomas, E., Thankan, R. S., Purushottamachar, P., Weber, D. J., & Njar, V. C. O. (2023). Targeted Degradation of Androgen Receptor by VNPP433-3β in Castration-Resistant Prostate Cancer Cells Implicates Interaction with E3 Ligase MDM2 Resulting in Ubiquitin-Proteasomal Degradation. *Cancers*, *15*(4), 1198. https://doi.org/10.3390/cancers15041198

Thomas, R., Jerome, J. M., Dang, T. D., Souto, E. P., Mallam, J. N., & Rowley, D. R. (2022a). Androgen receptor variant-7 regulation by tenascin-c induced src activation. *Cell Communication and Signaling*, *20*(1), 119. https://doi.org/10.1186/s12964-022-00925-0

Thomas, R., Jerome, J. M., Dang, T. D., Souto, E. P., Mallam, J. N., & Rowley, D. R. (2022b). Androgen receptor variant-7 regulation by tenascin-c induced src activation. *Cell Communication and Signaling*, *20*(1), 119. https://doi.org/10.1186/s12964-022-00925-0

Thomas, R., Jerome, J. M., Dang, T. D., Souto, E. P., Mallam, J. N., & Rowley, D. R. (2022c). Androgen receptor variant-7 regulation by tenascin-c induced src activation. *Cell Communication and Signaling*, *20*(1), 119. https://doi.org/10.1186/s12964-022-00925-0

Thompson, R. (2013). Hear me now: The uncomfortable reality of prostate cancer in Black African-Caribbean Men. *BME Cancer Communities*.

Tomlins, S. A., Mehra, R., Rhodes, D. R., Cao, X., Wang, L., Dhanasekaran, S. M., Kalyana-Sundaram, S., Wei, J. T., Rubin, M. A., Pienta, K. J., Shah, R. B., & Chinnaiyan, A. M. (2007). Integrative molecular concept modeling of prostate cancer progression. *Nat Genet*, *39*(1), 41–51. https://doi.org/10.1038/ng1935

Tong, D. (2021). The role of JMJD6/U2AF65/AR-V7 axis in castration-resistant prostate cancer progression. *Cancer Cell Int*, *21*(1), 45. https://doi.org/10.1186/s12935-020-01739-1

Tran, N., Broun, A., & Ge, K. (2020). Lysine Demethylase KDM6A in Differentiation, Development, and Cancer. *Molecular and Cellular Biology*, *40*(20), e00341-20. https://doi.org/10.1128/MCB.00341-20

Travison, T. G., Vesper, H. W., Orwoll, E., Wu, F., Kaufman, J. M., Wang, Y., Lapauw, B., Fiers, T., Matsumoto, A. M., & Bhasin, S. (2017). Harmonized Reference Ranges for Circulating Testosterone Levels in Men of Four Cohort Studies in the United States and Europe. *The Journal of Clinical Endocrinology & Metabolism*, *102*(4), 1161–1173. https://doi.org/10.1210/jc.2016-2935

Tsui, C., Inouye, C., Levy, M., Lu, A., Florens, L., Washburn, M. P., & Tjian, R. (2018). dCas9-targeted locus-specific protein isolation method identifies histone gene regulators. *Proc Natl Acad Sci U S A*, *115*(12), E2734–E2741. https://doi.org/10.1073/pnas.1718844115

Uttley, L., Whyte, S., Gomersall, T., Ren, S., Wong, R., Chambers, D., & Tappenden, P. (2017). Degarelix for Treating Advanced Hormone-Dependent Prostate Cancer: An Evidence Review Group Perspective of a NICE Single Technology Appraisal. *PharmacoEconomics*, *35*(7), 717–726. https://doi.org/10.1007/s40273-016-0481-1

Valentín López, J. C., Lange, C. A., & Dehm, S. M. (2024). Androgen receptor and estrogen receptor variants in prostate and breast cancers. *The Journal of Steroid Biochemistry and Molecular Biology*, *241*, 106522. https://doi.org/10.1016/j.jsbmb.2024.106522

Van der Steen, T., Tindall, D. J., & Huang, H. (2013). Posttranslational Modification of the Androgen Receptor in Prostate Cancer. *International Journal of Molecular Sciences*, *14*(7), 14833–14859. https://www.mdpi.com/1422-0067/14/7/14833

Van Hemelryk, A., Mout, L., Erkens-Schulze, S., French, P. J., van Weerden, W. M., & van Royen, M. E. (2021). Modeling Prostate Cancer Treatment Responses in the Organoid Era: 3D Environment Impacts Drug Testing. *Biomolecules*, *11*(11). https://doi.org/10.3390/biom11111572

Vander Ark, A., Cao, J., & Li, X. (2018a). Mechanisms and Approaches for Overcoming Enzalutamide Resistance in Prostate Cancer. *Frontiers in Oncology*, *8*. https://doi.org/10.3389/fonc.2018.00180

Vander Ark, A., Cao, J., & Li, X. (2018b). Mechanisms and Approaches for Overcoming Enzalutamide Resistance in Prostate Cancer. *Frontiers in Oncology*, *8*. https://doi.org/10.3389/fonc.2018.00180

van der Meer, D., Barthorpe, S., Yang, W., Lightfoot, H., Hall, C., Gilbert, J., Francies, H. E., & Garnett, M. J. (2019). Cell Model Passports—a hub for clinical, genetic and functional datasets of preclinical cancer models. *Nucleic Acids Research*, *47*(D1), D923–D929. https://doi.org/10.1093/nar/gky872

Vellky, J. E., & Ricke, W. A. (2020). Development and prevalence of castration-resistant prostate cancer subtypes. *Neoplasia*, *22*(11), 566–575. https://doi.org/https://doi.org/10.1016/j.neo.2020.09.002

Veloso, A., Kirkconnell, K. S., Magnuson, B., Biewen, B., Paulsen, M. T., Wilson, T. E., & Ljungman, M. (2014). Rate of elongation by RNA polymerase II is associated with specific gene features and epigenetic modifications. *Genome Res*, *24*(6), 896–905. https://doi.org/10.1101/gr.171405.113

Vidal, A. C., Oyekunle, T., Howard, L. E., De Hoedt, A. M., Kane, C. J., Terris, M. K., Cooperberg, M. R., Amling, C. L., Klaassen, Z., Freedland, S. J., & Aronson, W. J. (2020). Obesity, race, and long-term prostate cancer outcomes. *Cancer*, *126*(16), 3733–3741. https://doi.org/https://doi.org/10.1002/cncr.32906

Vietri, M. T., D'Elia, G., Caliendo, G., Resse, M., Casamassimi, A., Passariello, L., Albanese, L., Cioffi, M., & Molinari, A. M. (2021). Hereditary Prostate Cancer: Genes Related, Target Therapy and Prevention. *International Journal of Molecular Sciences*, *22*(7), 3753. https://www.mdpi.com/1422-0067/22/7/3753

Wach, S., Taubert, H., & Cronauer, M. (2020). Role of androgen receptor splice variants, their clinical relevance and treatment options. *World Journal of Urology*, *38*(3), 647–656. https://doi.org/10.1007/s00345-018-02619-0

Wadosky, K. M., & Koochekpour, S. (2017). Androgen receptor splice variants and prostate cancer: From bench to bedside. *Oncotarget*, *8*(11), 18550–18576. https://doi.org/10.18632/oncotarget.14537

Wahl, M. C., Will, C. L., & Luhrmann, R. (2009). The spliceosome: design principles of a dynamic RNP machine. *Cell*, *136*(4), 701–718. https://doi.org/10.1016/j.cell.2009.02.009

Walker, L. E. (2023). The novel siRNA inclisiran and population health management. *Prescriber*, *34*(1), 33–35. https://doi.org/https://doi.org/10.1002/psb.2037

Waltering, K. K., Urbanucci, A., & Visakorpi, T. (2012). Androgen receptor (AR) aberrations in castration-resistant prostate cancer. *Mol Cell Endocrinol*, *360*(1–2), 38–43. https://doi.org/10.1016/j.mce.2011.12.019

Wan, W., Peng, K., Li, M., Qin, L., Tong, Z., Yan, J., Shen, B., & Yu, C. (2017). Histone demethylase JMJD1A promotes urinary bladder cancer progression by enhancing glycolysis through coactivation of hypoxia inducible factor 1alpha. *Oncogene*, *36*(27), 3868–3877. https://doi.org/10.1038/onc.2017.13

Wang, B.-R., Chen, Y.-A., Kao, W.-H., Lai, C.-H., Lin, H., & Hsieh, J.-T. (2022). Developing New Treatment Options for Castration-Resistant Prostate Cancer and Recurrent Disease. *Biomedicines*, *10*(8), 1872. https://www.mdpi.com/2227-9059/10/8/1872

Wang, C., Lee, J.-E., Cho, Y.-W., Xiao, Y., Jin, Q., Liu, C., & Ge, K. (2012). UTX regulates mesoderm differentiation of embryonic stem cells independent of H3K27 demethylase activity. *Proceedings of the National Academy of Sciences*, *109*(38), 15324–15329. https://doi.org/10.1073/pnas.1204166109

Wang, C.-Y., Cusack, J. C., Liu, R., & Baldwin, A. S. (1999). Control of inducible chemoresistance: Enhanced anti-tumor therapy through increased apoptosis by inhibition of NF-κB. *Nature Medicine*, *5*(4), 412–417. https://doi.org/10.1038/7410

Wang, H. J., Pochampalli, M., Wang, L. Y., Zou, J. X., Li, P. S., Hsu, S. C., Wang, B. J., Huang, S. H., Yang, P., Yang, J. C., Chu, C. Y., Hsieh, C. L., Sung, S. Y., Li, C. F., Tepper, C. G., Ann, D. K., Gao, A. C., Evans, C. P., Izumiya, Y., … Kung, H. J. (2019). KDM8/JMJD5 as a dual coactivator of AR and PKM2 integrates AR/EZH2 network and tumor metabolism in CRPC. *Oncogene*, *38*(1), 17–32. https://doi.org/10.1038/s41388-018-0414-x

Wang, I., Song, L., Wang, B. Y., Rezazadeh Kalebasty, A., Uchio, E., & Zi, X. (2022). Prostate cancer immunotherapy: a review of recent advancements with novel treatment methods and efficacy. *Am J Clin Exp Urol*, *10*(4), 210–233.

Wang, L., Lu, B., He, M., Wang, Y., Wang, Z., & Du, L. (2022). Prostate Cancer Incidence and Mortality: Global Status and Temporal Trends in 89 Countries From 2000 to 2019. *Frontiers in Public Health*, *10*. https://doi.org/10.3389/fpubh.2022.811044

Wang, M., Liu, X., Jiang, G., Chen, H., Guo, J., & Weng, X. (2015). Relationship between LSD1 expression and E-cadherin expression in prostate cancer. *Int Urol Nephrol*, *47*(3), 485–490. https://doi.org/10.1007/s11255-015-0915-2

Wang, X., Xu, Z., Tian, Z., Zhang, X., Xu, D., Li, Q., Zhang, J., & Wang, T. (2017). The EF-1α promoter maintains high-level transgene expression from episomal vectors in transfected CHO-K1 cells. *Journal of Cellular and Molecular Medicine*, *21*(11), 3044–3054. https://doi.org/10.1111/jcmm.13216

Wang, Y., Liu, J., Huang, B. O., Xu, Y. M., Li, J., Huang, L. F., Lin, J., Zhang, J., Min, Q. H., Yang, W. M., & Wang, X. Z. (2015). Mechanism of alternative splicing and its regulation. *Biomed Rep*, *3*(2), 152–158. https://doi.org/10.3892/br.2014.407

Wang, Z., & Burge, C. B. (2008). Splicing regulation: from a parts list of regulatory elements to an integrated splicing code. *RNA*, *14*(5), 802–813. https://doi.org/10.1261/rna.876308

Wang, Z., Tang, F., Qi, G., Yuan, S., Zhang, G., Tang, B., & He, S. (2015). KDM5B is overexpressed in gastric cancer and is required for gastric cancer cell proliferation and metastasis. *Am J Cancer Res*, *5*(1), 87–100. https://www.ncbi.nlm.nih.gov/pubmed/25628922

Watanabe, S., Shimada, S., Akiyama, Y., Ishikawa, Y., Ogura, T., Ogawa, K., Ono, H., Mitsunori, Y., Ban, D., & Kudo, A. (2019). Loss of KDM6A characterizes a poor prognostic subtype of human pancreatic cancer and potentiates HDAC inhibitor lethality. *International Journal of Cancer*, *145*(1), 192–205.

Weikum, E. R., Liu, X., & Ortlund, E. A. (2018). The nuclear receptor superfamily: A structural perspective. *Protein Science*, *27*(11), 1876–1892. https://doi.org/10.1002/pro.3496

Weinstein, J. N., Collisson, E. A., Mills, G. B., Shaw, K. R., Ozenberger, B. A., Ellrott, K., Shmulevich, I., Sander, C., & Stuart, J. M. (2013). The cancer genome atlas pan-cancer analysis project. *Nature Genetics*, *45*(10), 1113–1120.

Welti, J., Sharp, A., Brooks, N., Yuan, W., McNair, C., Chand, S. N., Pal, A., Figueiredo, I., Riisnaes, R., Gurel, B., Rekowski, J., Bogdan, D., West, W., Young, B., Raja, M., Prosser, A., Lane, J., Thomson, S., Worthington, J., … de Bono, J. S. (2021). Targeting the p300/CBP Axis in Lethal Prostate Cancer. *Cancer Discovery*, *11*(5), 1118–1137. https://doi.org/10.1158/2159-8290.CD-20-0751

Wissmann, M., Yin, N., Muller, J. M., Greschik, H., Fodor, B. D., Jenuwein, T., Vogler, C., Schneider, R., Gunther, T., Buettner, R., Metzger, E., & Schule, R. (2007). Cooperative demethylation by JMJD2C and LSD1 promotes androgen receptor-dependent gene expression. *Nat Cell Biol*, *9*(3), 347–353. https://doi.org/10.1038/ncb1546

Wu, M. J., Chen, C. J., Lin, T. Y., Liu, Y. Y., Tseng, L. L., Cheng, M. L., Chuu, C. P., Tsai, H. K., Kuo, W. L., Kung, H. J., & Wang, W. C. (2021). Targeting KDM4B that coactivates c-Myc-regulated metabolism to suppress tumor growth in castration-resistant prostate cancer. *Theranostics*, *11*(16), 7779–7796. https://doi.org/10.7150/thno.58729

Xiang, Y., Zhu, Z., Han, G., Lin, H., Xu, L., & Chen, C. D. (2007). JMJD3 is a histone H3K27 demethylase. *Cell Res*, *17*(10), 850–857. https://doi.org/10.1038/cr.2007.83

Xiang, Y., Zhu, Z., Han, G., Ye, X., Xu, B., Peng, Z., Ma, Y., Yu, Y., Lin, H., Chen, A. P., & Chen, C. D. (2007). JARID1B is a histone H3 lysine 4 demethylase up-regulated in prostate cancer. *Proceedings of the National Academy of Sciences*, *104*(49), 19226–19231. https://doi.org/10.1073/pnas.0700735104

Xie, G., Liu, X., Zhang, Y., Li, W., Liu, S., Chen, Z., Xu, B., Yang, J., He, L., & Zhang, Z. (2017). UTX promotes hormonally responsive breast carcinogenesis through feed-forward transcription regulation with estrogen receptor. *Oncogene*, *36*(39), 5497–5511.

Xie, N., Zhou, Y., Sun, Q., & Tang, B. (2018). Novel Epigenetic Techniques Provided by the CRISPR/Cas9 System. *Stem Cells International*, *2018*, 1–12. https://doi.org/10.1155/2018/7834175

Xu, Y., Zhao, W., Olson, S. D., Prabhakara, K. S., & Zhou, X. (2018). Alternative splicing links histone modifications to stem cell fate decision. *Genome Biology*, *19*(1), 133. https://doi.org/10.1186/s13059-018-1512-3

Xue, L., Yu, X., Zhao, L., Garrett, A., Wu, D., & Liu, H. Y. (2024). Targeted Delivery of AR-V7 siRNA with Bivalent PSMA Aptamers Effectively Suppresses the Growth of Enzalutamide-Resistant Prostate Cancer. *Molecular Pharmaceutics*, *21*(11), 5749–5760. https://doi.org/10.1021/acs.molpharmaceut.4c00743

Xue, S., Lam, Y. M., He, Z., Zheng, Y., Li, L., Zhang, Y., Li, C., Mbadhi, M. N., Zheng, L., Cheng, Z., Liu, Y., Wang, X., Chan, L. C., Ng, R. K., & Zhang, J. (2020). Histone lysine demethylase KDM5B maintains chronic myeloid leukemia via multiple epigenetic actions. *Experimental Hematology*, *82*, 53–65. https://doi.org/10.1016/j.exphem.2020.01.006

Yamane, K., Toumazou, C., Tsukada, Y., Erdjument-Bromage, H., Tempst, P., Wong, J., & Zhang, Y. (2006a). JHDM2A, a JmjC-Containing H3K9 Demethylase, Facilitates Transcription Activation by Androgen Receptor. *Cell*, *125*(3), 483–495. https://doi.org/10.1016/j.cell.2006.03.027

Yamane, K., Toumazou, C., Tsukada, Y., Erdjument-Bromage, H., Tempst, P., Wong, J., & Zhang, Y. (2006b). JHDM2A, a JmjC-containing H3K9 demethylase, facilitates transcription activation by androgen receptor. *Cell*, *125*(3), 483–495.

Yamauchi, H., Nishimura, K., & Yoshimi, A. (2022). Aberrant RNA splicing and therapeutic opportunities in cancers. *Cancer Science*, *113*(2), 373–381. https://doi.org/10.1111/cas.15213

Yan, N., Xu, L., Wu, X., Zhang, L., Fei, X., Cao, Y., & Zhang, F. (2017). GSKJ4, an H3K27me3 demethylase inhibitor, effectively suppresses the breast cancer stem cells. *Experimental Cell Research*, *359*(2), 405–414. https://doi.org/https://doi.org/10.1016/j.yexcr.2017.08.024

Yan, Q. (2023). *Targeting Lysine Demethylases in Cancer and Other Human Diseases* (1st ed. 2023..). Cham : Springer International Publishing : Imprint: Springer.

Yang, J., AlTahan, A. M., Hu, D., Wang, Y., Cheng, P. H., Morton, C. L., Qu, C., Nathwani, A. C., Shohet, J. M., Fotsis, T., Koster, J., Versteeg, R., Okada, H., Harris, A. L., & Davidoff, A. M. (2015). The role of histone demethylase KDM4B in Myc signaling in neuroblastoma. *J Natl Cancer Inst*, *107*(6), djv080. https://doi.org/10.1093/jnci/djv080

Yang, Z., Xu, J., Fang, D., & Ke, J. (2020). Analysis of key genes reveal lysine demethylase 5B promotes prostate cancer progression. *Oncology Letters*. https://doi.org/10.3892/ol.2020.11923

Yi, Z., Wei, S., Jin, L., Jeyarajan, S., Yang, J., Gu, Y., Kim, H. S., Schechter, S., Lu, S., & Paulsen, M. T. (2022). KDM6A regulates cell plasticity and pancreatic cancer progression by noncanonical activin pathway. *Cellular and Molecular Gastroenterology and Hepatology*, *13*(2), 643–667.

Yoshihama, Y., LaBella, K. A., Kim, E., Bertolet, L., Colic, M., Li, J., Shang, X., Wu, C. J., Spring, D. J., Wang, Y. A., Hart, T., & DePinho, R. A. (2021). AR-negative prostate cancer is vulnerable to loss of JMJD1C demethylase. *Proc Natl Acad Sci U S A*, *118*(36). https://doi.org/10.1073/pnas.2026324118

Yu, E. Y., Massard, C., Retz, M., Tafreshi, A., Carles Galceran, J., Hammerer, P., Fong, P. C. C., Shore, N. D., Joshua, A., & Linch, M. D. (2019). *Keynote-365 cohort a: pembrolizumab (pembro) plus olaparib in docetaxel-pretreated patients (pts) with metastatic castrate-resistant prostate cancer (mCRPC)*. American Society of Clinical Oncology.

Yu, W., Huang, W., Yang, Y., Qiu, R., Zeng, Y., Hou, Y., Sun, G., Shi, H., Leng, S., & Feng, D. (2019). GATA3 recruits UTX for gene transcriptional activation to suppress metastasis of breast cancer. *Cell Death & Disease*, *10*(11), 832.

Yu, X., Yi, P., Hamilton, R. A., Shen, H., Chen, M., Foulds, C. E., Mancini, M. A., Ludtke, S. J., Wang, Z., & O'Malley, B. W. (2020). Structural Insights of Transcriptionally Active, Full-Length Androgen Receptor Coactivator Complexes. *Mol Cell*, *79*(5), 812-823 e4. https://doi.org/10.1016/j.molcel.2020.06.031

Zacharopoulou, N., Tsapara, A., Kallergi, G., Schmid, E., Tsichlis, P. N., Kampranis, S. C., & Stournaras, C. (2018). The epigenetic factor KDM2B regulates cell adhesion, small rho GTPases, actin cytoskeleton and migration in prostate cancer cells. *Biochim Biophys Acta Mol Cell Res*, *1865*(4), 587–597. https://doi.org/10.1016/j.bbamcr.2018.01.009

Zhan, Y., Zhang, G., Wang, X., Qi, Y., Bai, S., Li, D., Ma, T., Sartor, O., Flemington, E. K., Zhang, H., Lee, P., & Dong, Y. (2017). Interplay between Cytoplasmic and Nuclear Androgen Receptor Splice Variants Mediates Castration Resistance. *Molecular Cancer Research*, *15*(1), 59–68. https://doi.org/10.1158/1541-7786.MCR-16-0236

Zhang, C., Wu, S., Song, R., & Liu, C. (2021). Long noncoding RNA NR2F1-AS1 promotes the malignancy of non-small cell lung cancer via sponging microRNA-493-5p and thereby increasing ITGB1 expression. *Aging*, *13*(5), 7660–7675. https://doi.org/10.18632/aging.103564

Zhang, D., Zhao, S., Li, X., Kirk, J. S., & Tang, D. G. (2018). Prostate Luminal Progenitor Cells in Development and Cancer. *Trends Cancer*, *4*(11), 769–783. https://doi.org/10.1016/j.trecan.2018.09.003

Zhang, J., Jing, L., Li, M., He, L., & Guo, Z. (2019). Regulation of histone arginine methylation/demethylation by methylase and demethylase (Review). *Mol Med Rep*, *19*(5), 3963–3971. https://doi.org/10.3892/mmr.2019.10111

Zhang, J., Ying, Y., Li, M., Wang, M., Huang, X., Jia, M., Zeng, J., Ma, C., Zhang, Y., & Li, C. (2020). Targeted inhibition of KDM6 histone demethylases eradicates tumor-initiating cells via enhancer reprogramming in colorectal cancer. *Theranostics*, *10*(22), 10016.

Zhang, Z., Wang, X., Kim, M., He, D., Wang, C., Fong, K. W., & Liu, X. (2023). Downregulation of EZH2 inhibits epithelial-mesenchymal transition in enzalutamide-resistant prostate cancer. *Prostate*, *83*(15), 1458–1469. https://doi.org/10.1002/pros.24602

Zhang, Z., Zhou, N., Huang, J., Ho, T. T., Zhu, Z., Qiu, Z., Zhou, X., Bai, C., Wu, F., Xu, M., & Mo, Y. Y. (2016). Regulation of androgen receptor splice variant AR3 by PCGEM1. *Oncotarget*, *7*(13), 15481–15491. https://doi.org/10.18632/oncotarget.7139

Zhao, L., Zhao, J., Zhong, K., Tong, A., & Jia, D. (2022). Targeted protein degradation: mechanisms, strategies and application. *Signal Transduction and Targeted Therapy*, *7*(1), 113. https://doi.org/10.1038/s41392-022-00966-4

Zhao, Y., Wang, L., Ren, S., Wang, L., Blackburn, P. R., McNulty, M. S., Gao, X., Qiao, M., Vessella, R. L., Kohli, M., Zhang, J., Karnes, R. J., Tindall, D. J., Kim, Y., MacLeod, R., Ekker, S. C., Kang, T., Sun, Y., & Huang, H. (2016). Activation of P-TEFb by Androgen Receptor-Regulated Enhancer RNAs in Castration-Resistant Prostate Cancer. *Cell Reports*, *15*(3), 599–610. https://doi.org/10.1016/j.celrep.2016.03.038

Zheng, R., Wan, C., Mei, S., Qin, Q., Wu, Q., Sun, H., Chen, C.-H., Brown, M., Zhang, X., Meyer, C. A., & Liu, X. S. (2018). Cistrome Data Browser: expanded datasets and new tools for gene regulatory analysis. *Nucleic Acids Research*, *47*(D1), D729–D735. https://doi.org/10.1093/nar/gky1094

Zhu, M. L., Horbinski, C. M., Garzotto, M., Qian, D. Z., Beer, T. M., & Kyprianou, N. (2010). Tubulin-targeting chemotherapy impairs androgen receptor activity in prostate cancer. *Cancer Res*, *70*(20), 7992–8002. https://doi.org/10.1158/0008-5472.CAN-10-0585

Zhu, Y., & Luo, J. (2020). Regulation of androgen receptor variants in prostate cancer. *Asian J Urol*, *7*(3), 251–257. https://doi.org/10.1016/j.ajur.2020.01.001

Zurowska, A., Peksa, R., Bienkowski, M., Skrobisz, K., Sowa, M., Matuszewski, M., Biernat, W., & Szurowska, E. (2023). Prostate Cancer and Its Mimics-A Pictorial Review. *Cancers (Basel)*, *15*(14). https://doi.org/10.3390/cancers15143682